PRODUCTION OF ALCOHOLS VIA SYNGAS FERMENTATION USING *ALKALIBACULUM BACCHI* MONOCULTURE AND A MIXED CULTURE

By

KAN LIU

Bachelor of Science in Pharmaceutical Engineering
Tianjin University of Science & Technology
Tianjin, China
2006

Master of Science in Fermentation Engineering
Tianjin University of Science & Technology
Tianjin, China
2009

Submitted to the Faculty of the
Graduate College of the
Oklahoma State University
in partial fulfillment of
the requirements for
the Degree of
DOCTOR OF PHILOSOPHY
December, 2013

PRODUCTION OF ALCOHOLS VIA SYNGAS FERMENTATION USING *ALKALIBACULUM BACCHI* MONOCULTURE AND A MIXED CULTURE

Dissertation Approved:

Dr. Hasan K. Atiyeh

Dissertation Adviser

Dr. Babu Z. Fathepure

Dr. Raymond L. Huhnke

Dr. Mark R. Wilkins

ACKNOWLEDGEMENTS

I appreciate my advisor Dr. Hasan Atiyeh giving me the opportunity to study in the United States and obtain my Ph.D. at Oklahoma State University. During the four years study, he gave me a lot of encouragements and guidance on my Ph.D. project, making me grow up quickly and become more professional in the way to think, to perform and to present. The experience and knowledge I learned from him will be a precious treasure for my future career. I also acknowledge the financial support for this project from USDA-NIFA 2010-34447-20772, Oklahoma NSF EPSCoR, Oklahoma Bioenergy Center and the Oklahoma Agricultural Experiment Station.

I also appreciate Dr. Raymond Huhnke for guidance on my Ph.D. project, presentations and papers. Also, I am very grateful to Dr. Mark Wilkins's help and support for designing my experiments, reviewing my papers, presentations and providing valuable suggestions, especially giving me a precious opportunity to visit Washington D.C. to present the Biowin*ol* project at 2012 National Sustainable Design Expo, which greatly increased my experience to explain the technology to different people. In addition, I thank my committee member Dr. Babu Fathepure who provided great support and encouragement for my whole education at OSU.

I specially thank Dr. Ralph Tanner who provided the *Alkalibaculum bacchi* strains and gave valuable suggestions for my research. Also, I appreciate Dr. Ralph Tanner and

Dr. Bradley Stevenson who helped me to identify the strains in the mixed culture used in this research via the 16s rRNA test and provided a solid information for my paper and dissertation.

I am very lucky to have wonderful lab colleagues during the Ph.D. life. Firstly, I would like to thank Prasanth Maddipati who trained me all research related equipment and techniques from scratch. Also, I thank Dr. Marthah De Lorme and Dr. Jennine Terrill for their help and training when I was a new comer to the lab. I show my great gratitude to the Research Engineer, Dr. John Randy Philips, for his help when I had research problems and gave me valuable advice on my project. I also thank Jie Gao and Research Engineer Oscar Pardo Planas's help. I specially thank lab manager, Mark Gilstrap, who was always helpful to resolve issues with GC, HPLC, lab operation and safety.

For the four years lab work and life at OSU, I highly appreciate my colleagues and friends Naveen Pessani, Karthikeyan Ramachandriya, Michael Muller, Mamatha Devarapalli. You gave me a great time not only in academics but also in my life. I enjoyed the every moment with you at OSU.

Finally, I want to show my deepest appreciation to my parents' wholehearted support, love and expectation.

Name: KAN LIU

Date of Degree: DECEMBER, 2013

Title of Study: PRODUCTION OF ALCOHOLS VIA SYNGAS FERMENTATION USING *ALKALIBACULUM BACCHI* MONOCULTURE AND A MIXED CULTURE

Major Field: BIOSYSTEMS AND AGRICULTURAL ENGINEERING

Abstract: Gasification-syngas fermentation is a hybrid conversion technology. In this process, feedstocks such as biomass or municipal solid waste are gasified to syngas (CO, H_2 and CO_2), which is then converted into biofuels and chemicals using biocatalysts. Recently isolated *Alkalibaculum bacchi* strains $CP11^T$, CP13 and CP15 were found to convert CO and H_2 into ethanol and acetic acid at initial pH 8.0. Bottle fermentations showed that CP15 was the most promising strain for ethanol production because of its higher growth and ethanol production rates and yield than $CP11^T$ and CP13. The cost of CP15 medium was reduced by 27% by removing TAPS buffer and replacing yeast extract (YE), minerals and vitamins with corn steep liquor (CSL). The use of CSL resulted in a twofold increase in ethanol production in bottle fermentations. Fermentations were scaled up to 3-L and 7-L fermentors in semi-continuous and continuous modes with and without cell recycle. Results of the continuous syngas fermentation with cell recycle showed a maximum of 5.5 g/L cell mass concentration at a dilution rate of 0.033 h^{-1} in the YE medium. Cell mass and ethanol concentrations were 2.2 g/L and 6.5 g/L, respectively, at a dilution rate of 0.011 h^{-1}. When CSL medium was used in continuous syngas fermentation, the maximum produced concentrations of ethanol, n-propanol and n-butanol were 8 g/L, 6 g/L and 1 g/L, respectively. n-Propanol and n-butanol were not typical products of strain CP15. A 16S rRNA gene-based survey revealed a mixed culture in the fermentor dominated by *A. bacchi* strain CP15 (56%) and *Clostridium propionicum* (34%). The mixed culture presents an opportunity for higher alcohols production from syngas. Semi-continuous fermentations in a 3-L fermentor with the mixed culture and CSL medium resulted in a twofold more total alcohol production than in the YE medium. The synergy between strain CP15 and *C. propionicum* in the mixed culture in bottle fermentations resulted in 50% higher efficiency in converting propionic acid, butyric acid and hexanoic acid to their respective alcohol.

TABLE OF CONTENTS

Chapter Page

CHAPTER I INTRODUCTION 1

CHAPTER II LITERATURE REVIEW 9

2.1 Biofuels development 9
2.2 Routes for lignocellulosic biomass conversion to biofuels 11
2.2.1 Biochemical platform 11
2.2.2 Thermochemical platform 13
2.3 Conversion of syngas to advanced biofuels 15
2.3.1 Fischer-Tropsch process 15
2.3.2 Syngas fermentation 16
2.3.2.1 Comparison of syngas fermentation to FT process for biofuels production 16
2.3.2.2 Acetogens 17
2.3.2.3 Metabolism and bioenergetics 20
2.3.2.3.1 Metabolism 20
2.3.2.3.2 Bioenergetics 23
2.3.2.4 Syngas fermentation operation 26
2.3.2.4.1 Mass transfer 26
2.3.2.4.2 Medium composition 31
2.3.2.4.3 Fermentation pH 34
2.3.2.4.4 Redox potential 35
2.3.2.4.5 Syngas compositions and impurities 35
2.3.2.4.6 Substrates concentration 38
2.3.2.4.7 Mixed culture fermentation 39
2.3.2.4.8 Fermentation mode 39
2.4 Commercialization 40
2.5 References 44

CHAPTER III OBJECTIVES 59

CHAPTER IV FERMENTATIVE PRODUCTION OF ETHANOL FROM SYNGAS USING NOVEL MODERATELY ALKALIPHILIC STRAINS OF *ALKALIBACULUM BACCHI* 61

4.1 Introduction 62
4.2 Materials and methods 65

Chapter Page

4.2.1 Microorganisms and fermentation medium 65
4.2.2 Syngas composition 65
4.2.3 Fermentation runs 66
4.2.4 Analytical procedures 67
4.2.4.1 Cell concentration 67
4.2.4.2 Solvent analysis 67
4.2.4.3 Gas analysis 68
4.2.5 Statistical analysis and calculations 68
4.3 Results and discussion 68
4.3.1 Cell growth and pH profiles 69
4.3.2 Products formation 74
4.3.3 Gas utilization 78
4.4 Conclusions 82
4.5 References 82

CHAPTER V MASS TRANSFER ANALYSIS OF A 7-L BIOFLO 415 FERMENTOR 88

5.1 Introduction 90
5.2 Material and methods 92
5.2.1 Fermentor configuration and operating conditions 92
5.2.2 Calculations 96
5.2.2.1 Overall volumetric mass transfer coefficient 96
5.2.2.2 Volumetric flow rate at various headspace pressures 96
5.2.2.3 Power consumption 97
5.2.2.4 Mass Transfer Model of a 7-L Bioflo 415 Fermentor 99
5.2.2.5 Statistical analysis 100
5.3 Results and discussion 101
5.3.1 Mass transfer characteristics in 7-L Bioflo 415 fermentor 101
5.3.2 Effect of headspace backmixing k_La/V_L for O_2 104
5.3.3 Predictions of the k_La/V_L values for O_2, CO, H_2 and CO_2 108
5.4 Conclusions 111
5.5 References 112

CHAPTER VI CONTINUOUS SYNGAS FERMENTATION FOR THE PRODUCTION OF ETHANOL, N-PROPANOL AND N-BUTANOL 115

6.1 Introduction 115
6.2 Materials and methods 118
6.2.1 Microorganisms 118
6.2.2 Effect of medium composition 119
6.2.3 Continuous syngas fermentation in a 7-L fermentor 120
6.2.4 16S rRNA analysis for continuous fermentation culture 123
6.2.5 Analytical procedures 125

Chapter Page

6.2.5.1 Cell mass and product concentrations and gas analysis 125
6.2.5.2 Statistical analysis and estimation of kinetic parameters 126
6.3 Results and discussion 127
6.3.1 Effect of medium composition 127
6.3.2 Continuous fermentation in a 7-L fermentor 131
6.3.2.1 Fermentation in yeast extract medium 131
6.3.2.2 Fermentation in yeast extract free medium 137
6.3.2.3 Fermentation in CSL medium 138
6.4 Conclusions 147
6.5 References 147

CHAPTER VII MIXED CULTURE SYNGAS FERMENTATION AND CONVERSION OF CARBOXYLIC ACIDS INTO ALCOHOLS 152

7.1 Introduction 152
7.2 Materials and methods 155
7.2.1 Microorganisms 155
7.2.2 Semi-continuous fermentation in a 3-L fermentor using mixed culture 155
7.2.3 Conversion of carboxylic acids into alcohols in bottle fermentations 156
7.2.4 Analytical procedures 157
7.2.4.1 Cell mass, acid and solvent concentrations and gas analysis 157
7.2.4.2 Statistical analysis and kinetic parameters calculation 158
7.3 Results and discussion 160
7.3.1 Semi-continuous fermentation in a 3-L fermentor using mixed culture 160
7.3.1.1 Cell growth and pH profiles 160
7.3.1.2 Products formation 165
7.3.1.3 Gas utilization and carbon balance 168
7.3.2 Conversion of carboxylic acids into alcohols in 250-mL bottles 169
7.3.2.1 Effect of carboxylic acids on cell growth 169
7.3.2.2 Products formation 173
7.3.2.3 Gas utilization and carbon balance 180
7.4 Conclusions 180
7.5 References 180

CHAPTER VIII CONCLUSIONS AND FUTURE WORK 186

8.1 Conclusions 186
8.2 Future work 188

APPENDICES 190

APPENDIX A EFFECT OF MEDIUM COMPOSITION 190

A1 Cell growth and pH profiles 190

Chapter Page

A2 Products formation 192
A3 Gas utilization 195
A4 References 196

APPENDIX B CONVERSION OF CARBOXYLIC ACIDS INTO ALCOHOLS IN BOTTLE FERMENTATIONS 198

B1 pH profiles 198
B3 Gas consumption and production profiles 200

APPENDIX C 204

C1 EFFECT OF SWITCHGRASS DERIVED PRODUCER GAS ON *ALKALIBACULUM BACCHI* STRAIN CP11^T FERMENTATION 204

C1.1 Background 204
C1.2 Growth and product profiles 205
C1.3 Gas consumption profiles 206
C1.4 Conclusions 207
C1.5 References 208

C2 EFFECT OF $NAHCO_3$ ON *ALKALIBACULUM BACCHI* STRAIN CP11^T SYNGAS FERMENTATION 210

C2.1 Background 210
C2.2 Growth and pH profiles 211
C2.3 Products formation 211
C2.4 Conclusions 213
C2.5 References 213

APPENDIX D FED-BATCH FERMENTATION USING *A. BACCHI* STRAIN CP15 IN A 7-L FERMENTOR 216

D1 Background 216
D2 Growth, pH and product profiles 217
D2.1 Phase a, standard yeast extract medium fermentation 217
D2.2 Phase b, added concentrated nutrients and boost agitation from 150 rpm to 300 rpm 219
D2.3 Phases c and d, added concentrated trace metals and vitamins solution 221
D2.4 Phases e and f, added concentrated minerals solution 221
D2.5 Phase g, added yeast extract 222
D3 Conclusions 222
D4 References 222

Chapter Page

APPENDIX E EFFECT OF ADDED ETHANOL ON STRAIN CP15 ABILITY TO FERMENT SYNGAS 224

E1 Background 224
E2 Growth and products profiles with N_2 headspace and 1.2 g/L ethanol 225
E3 Growth and products profiles with syngas headspace and 1.2 g/L ethanol 227
E4 Growth and products profiles with syngas headspace and 12.1 g/L ethanol 229
E5 Conclusions 231
E6 References 231

APPENDIX F EFFECT OF TEMPERATURE ON STRAIN CP15 ABILITY TO FERMENT SYNGAS 233

F1 Background 233
F2 Fermentation with Syngas I 234
F3 Fermentation with Syngas II 236
F4 Conclusions 238
F5 References 238

APPENDIX G SEMI-CONTINUOUS SYNGAS FERMENTATION USING A MIXED CULTURE OF STRAIN CP15 AND *CLOSTRIDIUM PROPIONICUM* WITHOUT PH CONTROL 239

G1 Background 239
G2 Growth and products profiles 239
G3 Gas consumption profiles 243
G4 Conclusions 243
G5 References 244

APPENDIX H SAS PROGRAM USED TO DETERMINE THE STATISTICAL DIFFERENCES AMONG TREATMENTS 245

H1 SAS code 245
H2 Output 246

APPENDIX I 249

LIST OF TABLES

Table Page

Table 2.1 Reactions during gasification process..... 14

Table 2.2 Characteristics and end products of strains used in syngas fermentation..... 19

Table 2.3 Theoretical reactions for ethanol and acetic acid formation from CO and H_2. 25

Table 2.4 Effects of minerals and trace metals on acetyl-CoA pathway..... 33

Table 2.5 Syngas compositions from gasifying various feedstocks 37

Table 2.6 Syngas fermentation operation modes. 42

Table 3.1 Molar compositions of various syngas mixtures used in this study. 60

Table 4.1 Fermentation parameters of *Alkalibaculum bacchi* strains CP11^T, CP13 and CP15 with various gas mixtures 72

Table 5.1 Estimated $(k_L a/V_L)_i /(k_L a/V_L)_{O2}$ for CO, CO_2 and H_2 at 37 ℃ in water. 100

Table 5.2 Backmixing effect on $k_L a/V_L$ for O_2 at various air pressures in the headspace..... 106

Table 5.3 Effect of headspace pressures on backmixing in the 7-L Bioflo 415 fermentor with the 3 L working volume and air flow rate of 600 sccm and 900 rpm 107

Table 6.1 Carbon to ethanol and acetic acid conversion efficiencies from syngas with various H_2:CO ratios..... 117

Table 6.2 Compositions of four media formulations used in bottle fermentations 120

Table Page

Table 6.3 Maximum cell mass and final ethanol concentrations, CO and H_2 utilization and cost of the four media used during syngas fermentation by *A. bacchi* CP15 in bottle fermentations 130

Table 6.4 Fermentation parameters during continuous syngas fermentation in 7-L fermentor at various operating conditions 143

Table 7.1 Kinetic parameters in the YE and CSL media in the 3-L fermentor with the mixed culture 164

Table 7.2 Possible reactions for ethanol conversion to n-propanol and propionic acid and their standard Gibbs free energy 167

Table 7.3 Syngas fermentation parameters during the conversion of carboxylic acids into alcohols in 250-mL bottle fermentors 172

Table I1 Compositions of trace metal, vitamin and mineral stock solutions 249

LIST OF FIGURES

Figure Page

Fig. 1.1 U.S. energy production by energy source between 2000 and 2011 2

Fig. 4.1 (a) Cell mass and (b) pH profiles of *Alkalibaculum bacchi* strains..... 71

Fig. 4.2 (a) Acetic acid and (b) ethanol profiles using *Alkalibaculum bacchi* strains 75

Fig. 4.3 Cumulative (a) CO and (b) H_2 utilized and (c) CO_2 produced using *Alkalibaculum bacchi* strains 80

Fig. 5.1 The 7-L Bioflo 415 fermentor with the 3 L and 5.6 L working volumes and impellers configuration 93

Fig. 5.2 Bioflo 415 fermentor setup used 94

Fig. 5.3 Overall mass transfer coefficient for O_2 in air water system under the same standard flow rate 90 sccm, 150 sccm and 600 sccm with headspace pressure 101 kPa, 150 kPa and 240 kPa in 3 L and 5.6 L working volume..... 102

Fig. 5.4 Experimental and predicted kLa/VL values for O_2 with 3 L and 5.6 L working volumes in the 7 L Bioflo 415 fermentor at flow rates between 40 mL/min to 630 mL/min and 37 ℃ and various agitation speeds 110

Fig. 5.5 Experimental and predicted k_La/V_L values for O_2 at flow rates between 40 mL/min to 630 mL/min and 37 ℃, agitation speeds range from 150 rpm to 900 rpm in the 3 L and 5.6 L working volumes..... 111

Fig. 6.2 (A) Growth and products profiles (B) Specific gas uptake profiles during continuous syngas fermentation in YE medium with cell recycle..... 132

Fig. 6.3 (A) Growth and products profiles (B) Specific gas uptake profiles during continuous syngas fermentation in YE-free medium with cell recycle 138

Figure Page

Fig. 6.4 (A) Growth and products profiles (B) Specific gas uptake profiles during continuous syngas fermentation in 20 g/L CSL medium with cell recycle. 140

Fig. 6.5 n-propanol, n-butanol, propionic acid and butyric acid profiles during continuous syngas fermentation in 20 g/L CSL medium with cell recycle 141

Fig. 6.6 Fermentation profiles in YE medium at various dilution rates at pH 7.0 using Syngas III (A) products profiles, (B) gas uptake profiles. 144

Fig. 7.1 Semi-continuous fermentation profiles in 3-L fermentor using the mixed culture in YE medium and CSL medium; (A) pH and cell mass concentration; (B) acetic acid and ethanol 162

Fig. 7.2 Semi-continuous fermentation profiles in 3-L fermentor using the mixed culture in YE medium and CSL medium; (A) n-propanol and propionic acid; (B) butanol and butyric acid 163

Fig.7.3 Semi-continuous fermentation in 3-L fermentor using the mixed culture in YE medium and in CSL medium cumulative CO and H_2 consumption. 168

Fig. 7.4 Cell mass concentration profiles during syngas bottle fermentations with the addition of various carboxylic acids (A) monoculture of strain CP15 and (B) mixed culture 171

Fig. 7.5 Ethanol profiles during syngas bottle fermentations with the addition of various carboxylic acids (A) monoculture of CP15 and (B) mixed culture..... 174

Fig. 7.6 Acetic acid profiles during syngas bottle fermentations with the addition of various carboxylic acids (A) monoculture of CP15 and (B) mixed culture..... 175

Fig. 7.7 Carboxylic acids and their respective alcohols profiles during syngas bottle fermentations using the monoculture of CP15 and mixed culture for treatments (A) propionic acid (B) lactic acid 178

Fig. 7.8 Carboxylic acids and their respective alcohols profiles during syngas bottle fermentations using the monoculture of CP15 and mixed culture for treatments (A) butyric acid (B) hexanoic acid 179

Fig. A1 Cell growth profiles in standard YE medium; YE medium with 3X minerals; 20 g/L CSL medium ; 50 g/L CSL medium 191

Figure Page

Fig. A2 pH profiles in standard YE medium; YE medium with 3X minerals; 20 g/L CSL medium ; 50 g/L CSL medium 192

Fig. A3 Acetic acid profiles in standard YE medium; YE medium with 3X minerals; 20 g/L CSL; 50 g/L CSL..... 194

Fig. A4 Ethanol profiles in standard YE medium; YE medium with 3X minerals; 20 g/L CSL medium; 50 g/L CSL medium 194

Fig. A5 Cumulative CO consumption profiles in standard YE medium; YE medium with 3X minerals; 20 g/L CSL medium; 50 g/L CSL medium..... 195

Fig. A6 Cumulative H_2 consumption profiles in standard YE medium; YE medium with 3X minerals; 20 g/L CSL medium; 50 g/L CSL medium..... 196

Fig. B1 pH profiles during syngas fermentation in 250-mL bottles with the addition of various carboxylic acids (A) strain CP15 monoculture (B) mixed culture .. 199

Fig. B2 Cumulative CO consumption profiles during syngas fermentation in 250-mL bottles with the addition of various carboxylic acids (A) strain CP15 monoculture (B) mixed culture..... 201

Fig. B3 Cumulative H_2 consumption profiles during syngas fermentation in 250-mL bottles with the addition of various carboxylic acids (A) strain CP15 monoculture (B) mixed culture..... 202

Fig. B4 Cumulative CO_2 production profiles during syngas fermentation in 250-mL bottles with the addition of various carboxylic acids (A) strain CP15 monoculture (B) mixed culture..... 203

Fig. C1 Growth and products profiles of *A. bacchi* strain $CP11^T$ in producer gas bottle fermentation..... 206

Fig. C2 Gas consumption and production profiles of *A. bacchi* strain $CP11^T$ in producer gas bottle fermentation..... 207

Fig. C3 Growth and pH profiles of *A. bacchi* strain $CP11^T$ at various $NaHCO_3$ concentrations 212

Fig. C4 Acetic acid profiles of *A. bacchi* strain $CP11^T$ at various $NaHCO_3$ concentrations. 212

Figure Page

Fig. C5 Ethanol profiles of *A. bacchi* strain CP11^T at various $NaHCO_3$ concentrations 213

Fig. D1 Growth and products profiles in 7-L Bioflo 415 fermentor with strain CP15... 218

Fig. D2 Cumulative CO and H_2 consumption and CO_2 production profiles in 7-L Bioflo 415 fermentor with strain CP15..... 219

Fig. E1 Growth and products profiles during growth of strain CP15 on 1.2 g/L ethanol with N_2 headspace in bottle fermentation 226

Fig. E2 Gas production profiles during growth of strain CP15 on 1.2 g/L ethanol with N_2 headspace in bottle fermentation 226

Fig. E3 Growth and products profiles during growth of strain CP15 on 1.2 g/L ethanol with Syngas I in bottle fermentation 228

Fig. E4 Gas consumption and production profiles during growth of strain CP15 on 1.2 g/L ethanol with Syngas I in bottle fermentation..... 228

Fig. E5 Growth and products profiles during growth of strain CP15 on 12.1 g/L ethanol with Syngas I in bottle fermentation 230

Fig. E6 Gas consumption and production profiles during growth of strain CP15 on 12.1 g/L ethanol with Syngas I in bottle fermentation..... 230

Fig. F1 Growth and products profile of strain CP15 at 45 ℃ followed by 37 ℃ with Syngas I in bottle fermentation 235

Fig. F2 Gas consumption and production profiles of strain CP15 at 45 ℃ followed by 37 ℃ with Syngas I in bottle fermentation..... 236

Fig. F3 Growth and products profile of strain CP15 at 45 ℃ followed by 37 ℃ with Syngas II in bottle fermentation..... 237

Fig. F4 Gas consumption profile of strain CP15 at 45 ℃ followed by 37 ℃ with Syngas II in bottle fermentation..... 237

Fig. G1 Growth and pH profiles of the mixed culture in semi-continuous fermentation in 3-L Bioflo 110 fermentor without pH control..... 241

Fig. G2 Ethanol and acetic acid profiles of the mixed culture in semi-continuous fermentation in 3-L Bioflo 110 fermentor without pH control..... 241

Figure Page

Fig. G3 Propanol and propionic acid profiles of the mixed culture in semi-continuous fermentation in 3-L Bioflo 110 fermentor without pH control..... 242

Fig. G4 Butanol and butyric acid profiles of the mixed culture in semi-continuous fermentation in 3-L Bioflo 110 fermentor without pH control..... 242

Fig. G5 Cumulative CO and H_2 consumption and CO_2 production profiles using mixed culture in semi-continuous fermentation in 3-L Bioflo 110 fermentation without pH control..... 243

CHAPTER I

INTRODUCTION

Fossil fuels such as crude oil, natural gas and coal are unsustainable energy sources, which have been broadly used in the production of transportation fuels and chemicals (Henstra et al., 2007). The U.S. energy production from petroleum, natural gas and coal accounts for 80% of the total energy production between year 2000 to 2011 as shown in Fig. 1 (DOE, 2011). It was predicted that the reserves of petroleum and natural gas will be depleted in less than 40 years and 60 years, respectively (Vasudevan et al., 2010). In addition, the environmental pollution from coal burning and difficulties in natural gas transportation make it hard to rely on these fossil resources as a major energy supply in the future (Tirado-Acevedo et al., 2010). From Fig. 1.1, the percentage of renewable energy produced in the U.S. was increased from 7% in 2001 to 12% in 2011. The 5% increase in renewable energy production indicates the growing interest in this type of energy in the U.S.. Renewable energy from biomass accounted for 49% of the total renewable energy production in 2011 (DOE, 2011).

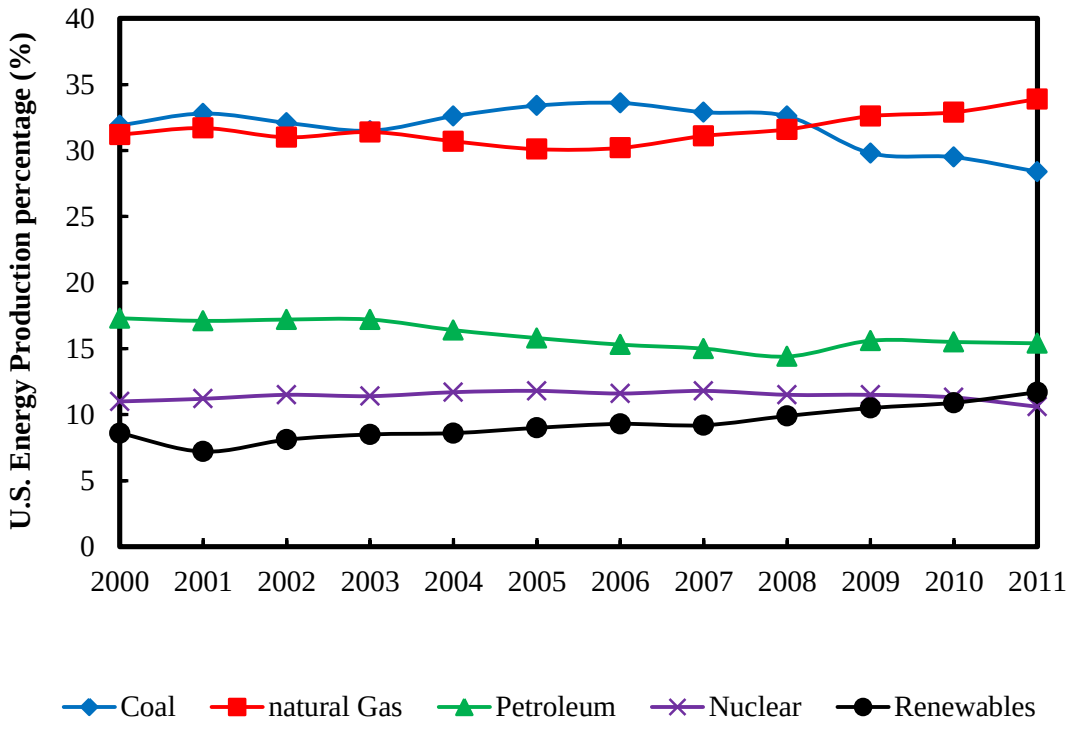

Fig. 1.1 U.S. energy production by energy source between 2000 and 2011 (DOE, 2011).

Bioethanol produced from food commodities is called first generation biofuel (Tyner, 2010). The production of first generation bioethanol is led by the U.S. and Brazil using maize and sugarcane, respectively (Tyner, 2010). However, it was argued that the amount of corn for first generation bioethanol production in the U.S. could feed 330 million people in the world (Love, 2010) and therefore, biofuels production from non-food sources should be pursued.

To reduce dependency on fossil fuels, the U.S. government enacted the Energy Policy Act in 2005 and the Energy Independence and Security Act (EISA) in 2007 (Winters, 2011). The EISA mandates for the production of biofuels from lignocellulosic biomass, also called advanced biofuels (Winters, 2011). Advanced biofuels are expected

to reduce 60% of greenhouse gas (GHG) emission from gasoline, compared to corn ethanol with 20% reduction of GHG emission from gasoline (Winters, 2011). Thus, lignocellulosic biofuels have advantages in reducing GHG emission and decreasing reliance on food resources for fuels (Demirbas, 2011). According to the United States Department of Agriculture, a fuel derived from renewable biomass, but not from corn starch, is defined as advanced fuel (USDA, 2013). The advanced biofuels include (USDA, 2013):

- Cellulose, hemicelluloses and lignin (lignocellulose) derived biofuels
- Sugar and starch but not corn starch derived biofuels
- Biofuels derived from wastes such as crops, vegetables, animals, food and yard wastes
- Biodiesel from vegetable oil and animal fat
- Biogas derived from renewable biomass organic matter
- Butanol or other alcohols derived from renewable biomass organic matter

In the past several years, more attention was given to ethanol. However, the hygroscopic and corrosive characteristics of ethanol create an incompatibility problem with current fuel infrastructure (Atsumi et al., 2008). Currently, E10 gasoline (90% gasoline is blended with 10% ethanol) has been used in the U.S. market, but ethanol must be carried separately by truck instead of gasoline pipeline, thus increasing the fuel transportation cost (Tyner, 2010). Higher alcohols with more than two carbon atoms have less water affinity (except for three carbon alcohols) and higher energy density than ethanol, which have been proposed as candidates for gasoline replacement (Atsumi et al., 2008). Also, higher alcohols such as propanol, butanol, isopentanol and n-hexanol have

been considered as candidates for "drop-in" biofuels (Simmons, 2011). "Drop-in" biofuels are similar to gasoline, jet fuel or biodiesel and can be directly "dropped" in the current fuel systems.

There are two main platforms for conversion of lignocellulosic biomass into biofuels, namely the biochemical and thermochemical platforms (Henstra et al., 2007; Tirado-Acevedo et al., 2010). The biochemical platform includes (1) biomass pretreatment to break or loosen the lignocellulosic structure, (2) enzymatic hydrolysis of pretreated biomass to obtain sugars, and (3) fermentation of sugars (Munasinghe and Khanal, 2010). However, the efficiency of enzymatic hydrolysis was lowered by the presence of lignin and hemicellulose that negatively affect cellulase accessibility to cellulose (Rajagopalan et al., 2002). The thermochemical platform includes gasification and pyrolysis technologies to convert lignocellulosic biomass into synthesis gas (syngas) and bio-oil, respectively (Atsumi et al., 2008; Henstra et al., 2007). Biofuels can be produced from syngas in two ways: (1) Fischer-Tropsch process (FT) via chemical catalysts and (2) fermentation via biocatalysts in a process called syngas fermentation (Huhnke et al., 2010; Kenealy and Waselefsky, 1985; Liu et al., 2012; Phillips et al., 1994). Biofuels from bio-oil are produced after upgrading and processing to hydrocarbon (Xiu and Shahbazi, 2012).

Gasification–syngas fermentation is an emerging hybrid technology for biofuel production. Gasification converts nearly all of the components from biomass into syngas, which primarily contains CO, H_2 and CO_2. This is followed by fermentation of syngas into ethanol and other products using acetogenic microorganisms such as *Clostridium ljungdahlii, Clostridium carboxidivorans, Clostridium autoethanogenum, Eubacterium*

limosum, *Clostridium ragsdalei* and *Alkalibaculum bacchi* (Wilkins and Atiyeh, 2011). Compared to the FT process with chemical catalysts, syngas fermentation has the advantage of high specificity to substrate, operation at low temperature and pressure, and high tolerance to toxic gases (Henstra et al., 2007; Munasinghe and Khanal, 2010).

Most syngas fermentation strains grow at optimal pH between 5.8 to 7.0 and few strains can grow on syngas with pH above 7.5 (Munasinghe and Khanal, 2010). Novel *Alkalibaculum bacchi* strains $CP11^T$, CP13 and CP15 were isolated recently from livestock-impacted soil and found to convert syngas components CO, H_2 and CO_2 to acetic acid and ethanol (Allen et al., 2010). These strains are able to grow at initial pH 8.0 to 8.5 to produce ethanol, which is different from syngas fermenting strains that grow at initial pH below 7 and typically produce ethanol when the pH is below 5.0. The isolation and identification of *A. bacchi* strains were done by Dr. Ralph Tanner's group at the University of Oklahoma. Growth and product kinetics of these strains and their abilities to ferment syngas with various compositions have not been studied. These parameters are critical to evaluate the suitability of these strains for potential use in large-scale production of alcohols from syngas. The proposed research will explore the potential of *A. bacchi* strains for the production of advanced biofuels in fed-batch, semi-continuous and continuous syngas fermentations, including development of low cost media to support larger scale fermentation, characterization of the mass transfer and identifying operating conditions in fermentors in order to improve syngas conversion efficiency and products yield.

References

Abubackar, H.N., Veiga, M.C., Kennes, C., 2011. Biological conversion of carbon monoxide: rich syngas or waste gases to bioethanol. Biofuels, Bioprod. Biorefin. 5, 93-114.

Allen, T.D., Caldwell, M.E., Lawson, P.A., Huhnke, R.L., Tanner, R.S., 2010. *Alkalibaculum bacchi* gen. nov., sp. nov., a CO-oxidizing, ethanol-producing acetogen isolated from livestock-impacted soil. Int. J. Syst. Evol. Microbiol. 60, 2483-2489.

Atsumi, S., Hanai, T., Liao, J.C., 2008. Non-fermentative pathways for synthesis of branched-chain higher alcohols as biofuels. Nature 451, 86-89.

Chaudhari, S., Dalai, A., Bakhshi, N., 2003. Production of hydrogen and/or syngas (H_2+CO) via steam gasification of biomass-derived chars. Energy Fuels 17, 1062-1067.

Demirbas, A., 2007. Progress and recent trends in biofuels. Prog. Energ. Combust. 33, 1-18.

Demirbas, M.F., 2011. Biofuels from algae for sustainable development. Appl. Energ. 88, 3473-3480.

DOE. 2011. 2011 Renewable energy data book.

Henstra, A.M., Sipma, J., Rinzema, A., Stams, A.J.M., 2007. Microbiology of synthesis gas fermentation for biofuel production. Curr. Opin. Biotechnol. 18, 200-206.

Huhnke, R.L., Lewis, R.S., Tanner, R.S. 2010. Isolation and characterization of novel clostridial species. US Patent No. 7,704,723.

Kenealy, W.R., Waselefsky, D.M., 1985. Studies on the substrate range of Clostridium kluyveri; the use of propanol and succinate. Arch. Microbiol. 141, 187-194.

Liu, K., Atiyeh, H.K., Tanner, R.S., Wilkins, M.R., Huhnke, R.L., 2012. Fermentative production of ethanol from syngas using novel moderately alkaliphilic strains of *Alkalibaculum bacchi*. Bioresour. Technol. 104, 336-341.

Love, P., 2010. Fueling hunger? Biofuel grain "could feed 330 million". Accessed April 19, 2013. http://oecdinsights.org/2010/01/25/biofuel/.

Munasinghe, P.C., Khanal, S.K., 2010. Biomass-derived syngas fermentation into biofuels: Opportunities and challenges. Bioresour. Biotechnol. 101, 5013-5022.

Phillips, J., Clausen, E., Gaddy, J., 1994. Synthesis gas as substrate for the biological production of fuels and chemicals. Appl. Biochem. Biotechnol. 45-46, 145-157.

Rajagopalan, S., P. Datar, R., Lewis, R.S., 2002. Formation of ethanol from carbon monoxide via a new microbial catalyst. Biomass Bioenerg. 23, 487-493.

Simmons, B.A., 2011. Opportunities and challenges in advanced biofuel production: the importance of synthetic biology and combustion science. Biofuels 2, 5-7.

Tirado-Acevedo, O., Chinn, M.S., Grunden, A.M., 2010. Production of biofuels from synthesis gas using microbial catalysts. Adv. Appl. Microbiol. 70, 57-92.

Tyner, W.E., 2010. Policy Update: Why the push for drop-in biofuels? Biofuels 1, 813-814.

USDA, 2013. Advanced biofuel payment program-eligibility. Accessed June 06, 2013. http://www.rurdev.usda.gov/BCP_Biofuels_Eligibility.html.

Wilkins, M.R., Atiyeh, H.K., 2011. Microbial production of ethanol from carbon monoxide. Curr. Opin. Biotechnol. 22, 326-330.

Winters, P., 2011. Current status of cellulosic biofuel commercialization in the United States. Ind. Biotechnol. 7, 365-374.

Xiu, S., Shahbazi, A., 2012. Bio-oil production and upgrading research: A review. Renew. Sust. Energ. Rev. 16, 4406-4414.

CHAPTER II

LITERATURE REVIEW

2.1 Biofuels development

The decreasing reserves of fossil fuels and corresponding environmental issues related to GHG emissions drove the development of alternative renewable energy resources (Daniell et al., 2012). Governments have enacted policies and incentives to stimulate research and development (R&D) in alternative renewable energy (Liew et al., 2013). Renewable energy sources include wind, solar, geothermal, hydropower and biofuels (Painuly, 2001). There has been an average of 15% to 50% annual increase in renewable energy usage rate during 2005 to 2010, which accounts for an estimated 16.7% of total global energy production (Liew et al., 2013; REN21, 2013). The global investment in renewable energy increased from 161 billion US dollars in 2009 to 257 billion US dollars in 2011 and government's policies related to renewable energy increased from 57 to 72 during 2009 to 2011 (REN21, 2013).

Biofuels include solid fuels such as biochar, liquid fuels such as ethanol, butanol and biodiesel, and gaseous fuels such as synthesis gas (syngas), hydrogen and biogas

(Liew et al., 2013). Global annual bioethanol production increased from 19.3 billion gallons in 2009 to 22.8 billion gallons in 2011, and biodiesel production increased from 4.7 billion gallons in 2009 to 5.7 billion gallons in 2011 (REN21, 2013). In addition, the U.S. has mandated the consumption of 35 billion gallons of biofuels by 2022 and the EU is planning to make biofuels account for 10% of its members' liquid fuels market by 2020 (Daniell et al., 2012).

Two generations of biofuels have been extensively studied. The first generation of biofuels includes ethanol that is made from sugar and corn starch, and biodiesel that is made from vegetable oils and animal fats (Demirbas, 2009; Daniell et al., 2012). However, the significant increase in sugar and corn prices for biofuel production and deficiency of cropland for sugar and corn production created uncertainty for them as future sustainable and reliable resources. For example, there was an increase of 3.7 times in the world raw sugar price from US $216/ton in 2000 to US $795/ton in 2011 (Liew et al., 2013). In addition, the arguments on food security for crop-based biofuels have pointed out that the use of arable land for biofuels production could result in the shortage of food supply and increase in food price (Daniell et al., 2012). The second generation of biofuels are produced from lignocellulosic feedstock such as agricultural and forest residues, municipal solid wastes and energy grasses (Demirbas, 2009; Daniell et al., 2012; EPA, 2013). Undoubtedly, the second generation of biofuels will shed the lights on reducing the food security issues as well as lowering the feedstock price.

The third generation of biofuel refers to the biofuel produced from algae such as biodiesel (Demirbas, 2009; EPA, 2013). Also, fourth generation biofuel has been proposed by Demirbas (2011), which refers to manipulating metabolically engineered

crops to sequester more CO_2 in the atmosphere than the release of CO_2 from these crops' derived fuels. The advanced technologies in the fourth generation biofuels will include pyrolysis, gasification, solar energy to fuel, hydrocarbon production from biocatalysts and upgrading biodiesel and vegetable oil into renewable gasoline (Demirbas, 2009; Demirbas, 2011).

2.2 Routes for lignocellulosic biomass conversion to biofuels

Lignocellulosic biomass typically contains 14% to 70% cellulose, 9% to 22% hemicelluloses and 8% to 30% lignin on a dry basis (Tirado-Acevedo et al., 2010). The biochemical and thermochemical platforms are the two common platforms being studied to convert lignocellulosic biomass into biofuels.

2.2.1 Biochemical platform

In the biochemical platform, lignocellulosic biomass is converted into biofuels through pretreatment, hydrolysis and fermentation. In the pretreatment step, the complex structure of lignocellulosic feedstock is disrupted to increase the accessibility of cellulose and hemicellulose to enzymes. Pretreatment methods include physical, physico-chemical, chemical and biological pretreatment (Mosier et al., 2005; Talebnia et al., 2010). After pretreatment, cellulose and hemicellulose from pretreated biomass are hydrolyzed by enzymes to produce monosaccharides such as glucose, xylose, arabinose and mannose which are fermented by bacteria or yeasts to make biofuels (Öhgren et al., 2007). Various hydrolysis and fermentation schemes have been investigated for the production of biofuels from biomass such as separate hydrolysis and fermentation (SHF), simultaneous

saccharification and fermentation (SSF) and consolidated bioprocessing (CBP) (Öhgren et al., 2007; Olofsson et al., 2008; Linger and Darzins, 2013).

The advantages of SHF include separate operations for controlling hydrolysis and fermentation individually, avoiding undesirable interactions between different steps and allowing each step to be operated at their own optimized conditions such as pH and temperature (Cheng, 2010). However, high yields of end products, such as glucose and cellobiose in SHF inhibit enzymes, thereby decreasing the enzymes' conversion efficiency (Olofsson et al., 2008). Moreover, separate steps require transferring treated feedstock from one reactor to another reactor, increasing risk of contamination (Cheng, 2010).

In order to increase ethanol production and reduce enzyme inhibition, simultaneous saccharification and fermentation (SSF) can be used (Öhgren et al., 2007). There are several advantages of SSF such as (1) increase in hydrolysis rate due to simultaneous conversion of sugars that inhibit the enzymes to products, (2) low enzymes loading requirement, (3) high ethanol yield and concentration, (4) short process time, (5) and use of a single reactor, reducing the capital cost (Öhgren et al., 2007; Cheng, 2010). The drawbacks of SSF include: (1) enzyme inhibition by high concentration of ethanol and (2) use of non-optimal pH and temperature conditions for hydrolysis and fermentation (Olofsson et al., 2008; Cheng, 2010).

Consolidated bioprocessing (CBP) combines enzymatic hydrolysis and fermentation in a single step using microorganisms via monoculture or co-culture to produce biofuels (Linger and Darzins, 2013). The advantage of CBP is that it has the potential to reduce biofuel production cost by combining all biomass processing steps

into one step. However, this process requires metabolically engineered microorganisms to produce enzymes for delignification of biomass and hydrolysis of cellulose and hemicellulose to monosaccharides and then conversion of both C5 and C6 sugars to products (Lynd et al., 2005). Although CBP has the potential to reduce biofuels production cost, it is still in early stage of research (Lynd et al., 2005; Linger and Darzins, 2013).

2.2.2 Thermochemical platform

The thermochemical platform for biofuel production includes two main processes: pyrolysis and gasification. Pyrolysis is a process in which biomass is converted to bio-oil in the absence of oxygen with short vapor residence time, < 2 seconds, at 425 −500 ℃ (Mohan et al., 2006). The end products of fast pyrolysis are bio-oil (liquid intermediate for biofuels upon upgrading), solid char (solid biofuel) and noncondensable gases (Mohan et al., 2006).

Unlike pyrolysis, gasification is normally operated at temperatures between 600 ℃ to 1000 ℃ with oxidizing agents such as air, steam or oxygen (Griffin and Schultz, 2012). Gasification occurs with the use of less than the stoichiometric amount of oxygen needed for complete combustion to produce synthesis gas (syngas) containing mainly CO, CO_2 and H_2 (Foust et al., 2009; Tirado-Acevedo et al., 2010; Daniell et al., 2012; Griffin and Schultz, 2012). Syngas also contains minor contaminants such as carbonyl sulfide (COS), HCl, hydrogen cyanide (HCN), SO_x, NO_x, ammonia, tars, chars and hydrocarbons. Essentially, syngas is the gaseous biofuel. The gasification of biomass is typically a four step process: drying, pyrolysis, oxidation and reduction (Daniell et al.,

2012). The reactions during gasification are complex and affected by temperature, pressure, reactants concentration and gasifier type (Daniell et al., 2012). The key reactions of gasification are listed in Table 2.1.

Table 2.1 Reactions during gasification process (adapted from Daniell et al., 2012 and Tirado-Acevedo et al., 2010).

	Reactions	**Gibbs free energy**
Partial oxidation	$C+ 0.5\ O_2 \leftrightarrow CO$	$\Delta G^{o'}$= -151 kJ/mol
Complete oxidation	$C+ O_2 \leftrightarrow CO_2$	$\Delta G^{o'}$= -423 kJ/mol
water gas reaction	$C+ H_2O \leftrightarrow CO + H_2$	$\Delta G^{o'}$= -100 kJ/mol
Water gas-shift reaction	$CO + H_2O \leftrightarrow CO_2 + H_2$	$\Delta G^{o'}$= -20 kJ/mol
Methane formation	$CO + 3\ H_2 \leftrightarrow CH_4 + H_2O$	$\Delta G^{o'}$= -151 kJ/mol

Gasifier types include fixed bed and fluidized bed gasifiers (Tirado-Acevedo et al., 2010; Liew et al., 2013). Fixed bed design includes updraft and downdraft gasifers. Updraft gasifer (counter-current flow of biomass and oxidizing agent) requires simple construction, low cost, and high energy efficiency due to a lower energy requirement to cool gas leaving the gasifier (Tirado-Acevedo et al., 2010; Liew et al., 2013). However, gas cleanup is necessary for an updraft gasfier due to relatively high tars and hydrocarbons formation, which make it difficult for downstream processing such as Fischer-Tropsch (FT) process that requires clean syngas (Tirado-Acevedo et al., 2010). The downdraft gasifier (co-current flow of biomass and oxidizing agents) also has a simple design and low cost (Tirado-Acevedo et al., 2010; Liew et al., 2013). Compared to updraft gasifiers, downdraft gasifiers result in relatively low tars formation but requires

more external energy to cool gas leaving the gasifier (Tirado-Acevedo et al., 2010; Liew et al., 2013). The fluidized bed gasifier is the most common type of gasifiers and can reach up to 100% carbon conversion. However, a fluidized bed gasifier is more expensive to operate than other types of gasifier and ash in the biomass can cause a loss of fluidization (Tirado-Acevedo et al., 2010; Liew et al., 2013).

2.3 Conversion of syngas to advanced biofuels

2.3.1 Fischer-Tropsch process

Liquid biofuels can be obtained from syngas using Fischer-Tropsch (FT) process. FT process is a surface catalyzed polymerization process to produce hydrocarbons from monomers CH_x generated by hydrogenation of CO in the syngas (Iglesia, 1997). Metal catalysts such as C_O, Ru, Rh, and Fe have been used in FT process (Tirado-Acevedo et al., 2010). Liquid biofuels such as ethanol and butanol can be produced from FT process by the following reactions (Tirado-Acevedo et al., 2010):

$$2\ CO + 4\ H_2 \rightarrow C_2H_5OH + H_2O \quad (1)$$

$$4\ CO + 8\ H_2 \rightarrow C_4H_{10}OH + 3\ H_2O \quad (2)$$

FT process has been developed over 90 years and already been applied into large scale process for coal to liquid fuel conversion in South Africa (Tijmensen et al., 2002). This process is also recommended to use lignocellulosic biomass as feedstock to produce liquid fuels; however, no commercial plant is available (Tijmensen et al., 2002; Daniell et al., 2012).

2.3.2 Syngas fermentation

2.3.2.1 Comparison of syngas fermentation to FT process for biofuels production

Syngas fermentation is a part of the hybrid technology that incorporates gasification and fermentation to make ethanol, butanol and other products (Wilkins and Atiyeh, 2011; Daniell et al., 2012; Griffin and Schultz, 2012; Liew et al., 2013). Compared to FT process that converts syngas into fuels via chemical catalyst, the conversion of syngas via biocatalysts to biofuels has several advantages:

(1) Low operating temperature and pressure

Syngas fermentation is normally operated at ambient pressure, 101 kPa, and 37 ℃ to favor the microorganism growth condition (Munasinghe and Khanal, 2010; Tirado-Acevedo et al., 2010; Abubackar et al., 2011). However, FT process is normally operated at 200 ℃ to 400 ℃ and pressures up to 20 MPa (Tirado-Acevedo et al., 2010).

(2) High specificity to substrate

FT process catalysts have low specificity to convert syngas into target products, which was reported to only have 50% conversion efficiency compared to the syngas fermentation process (Datta et al., 2011). Also, FT process produced more byproducts than syngas fermentation (Daniell et al., 2012).

(3) Independent of H_2:CO ratio

Syngas fermentation utilizes different H_2:CO ratios generated from the gasifier (Wilkins and Atiyeh, 2011; Daniell et al., 2012; Liu et al., 2012). However, FT process requires a specific H_2:CO ratio usually about 2.15 (Dry, 2002). The strict H_2:CO ratio

requirements in FT process is a challenge to obtain by gasifying biomass (Daniell et al., 2012).

(4) High tolerance of toxic gas compared to chemical catalysts

The impurities in syngas generated during gasification include NH_3, H_2S, SO_x, COS, HCN and HCl (Van Steen and Claeys, 2008; Xu et al., 2011; Daniell et al., 2012). Syngas fermentation strain *Clostridium ljungdahlii* was reported to tolerate up to 5.2% H_2S (Klasson et al., 1993). No significant lag phase occurred for *Clostridium ragsdalei* when 150 mmol/L of NH_4OH was added to the medium, which simulated ammonia from syngas in the form of ammonium accumulated in the fermentation media (Xu et al., 2011). However, the impurities in FT process can poison the catalyst, e.g., sulfur can attach to the active site of cobalt and iron, resulting in irreversible poisoning to the catalysts (Tijmensen et al., 2002).

2.3.2.2 Acetogens

Acetogens are anaerobes that follow the acetyl-CoA pathway for the (1) reductive synthesis of the acetyl moiety of acetyl-CoA from CO_2, (2) conservation of energy, and (3) assimilation of CO_2 into cell mass (Drake et al., 2008). The earlier definition of acetogens was to form a sole reduced end product—acetic acid, and they are also called "homoacetogens" (Drake, 1994). However, these acetogens do not strictly follow homoacetogenetic process. Other products such as CO, H_2, ethanol and lactate are minor end products of these "homoacetogens", which depends on the growth conditions (Drake, 1994). Even though more than 100 species of acetogens were reported to produce acetic acid from acetyl-CoA, there were few strains that were able to synthesize other products

besides acetic acid (Köpke et al., 2011a). Currently, most studies with acetogens in syngas fermentation are focused on the production of acetic acid, ethanol, butanol and 2,3-butanediol (Klasson et al., 1992; Ahmed et al., 2006; Huhnke et al., 2010; Köpke et al., 2010; Köpke et al., 2011a; Ramachandriya et al., 2011; Tracy et al., 2011; Liu et al., 2012). Table 2.2 lists characteristics and end products of acetogens used in syngas fermentation.

Table 2.2 Characteristics and end products of strains used in syngas fermentation.

Strains	Growth temperature	Optimal growth pH	Gases used	Products	Reference
Clostridium ragsdalei P11	Mesophilic	6.3	CO, CO_2/H_2, $CO/CO_2/H_2$	Ethanol/butanol/ 2,3-butanediol/ acetic acid	(Huhnke et al., 2010; Köpke et al., 2011b; Wilkins and Atiyeh, 2011)
Clostridium carboxidivorans P7	Mesophilic	6.2	CO_2/H_2, $CO/CO_2/H_2$	Ethanol/butanol/ butyrate/ acetic acid	(Liou et al., 2005; Ahmed et al., 2006)
Clostridium ljungdahlii	Mesophilic	6.0	CO_2/H_2, $CO/CO_2/H_2$	Ethanol/2,3-butanediol/butanol/ butyrate/acetic acid	(Daniel et al., 1990; Phillips et al., 1994; Köpke et al., 2010)
Clostridium autoethanogenum	Mesophilic	5.8-6.0	CO, CO_2/H_2, $CO/CO_2/H_2$	Ethanol/2,3-butanediol/ acetic acid	(Daniel et al., 1990; Köpke et al., 2011b)
Butyribacterium methylotrophicum	Mesophilic	7.5	CO	Ethanol/ acetic acid / butanol/butyric acid	(Shen et al., 1999)
Eubacterium limosum KIST 612	Mesophilic	6.8	CO	Ethanol/ acetic acid	(Chang et al., 2001)
Moorella sp. HUC22-1	Thermophilic	6.3	H_2/CO_2	Ethanol/ acetic acid	(Sakai et al., 2004)
Clostridium coskatii	Mesophilic	5.8-6.5	$CO/CO_2/H_2$	Ethanol/ acetic acid	(Zahn and Saxena, 2011)
Alkalibaculum bacchi	Mesophilic	8.0-8.5	CO/CO_2, CO, H_2/CO_2	Ethanol/ acetic acid	Present study (Allen et al., 2010; Liu et al., 2012)

2.3.2.3 Metabolism and bioenergetics

2.3.2.3.1 Metabolism

The acetogens used in syngas fermentation follow the acetyl-CoA pathway, also called the Wood-Ljungdahl pathway (Ljungdhal, 1986; Wood et al., 1986; Drake et al., 2008; Köpke et al., 2010) (Fig. 2.1). In this pathway, CO or CO_2 is fixed to synthesize acetyl-CoA via two branches—methyl branch and carbonyl branch (Ljungdahl, 1986; Wood et al., 1986; Diekert and Wohlfarth, 1994; Köpke et al., 2010). In methyl branch, CO_2 is first reduced to formate via formate dehydrogenase (FDH) (Eq. 3). The electron donor for this reaction can be ferredoxin or pyridine nucleotides (NAD(P)H) (Diekert and Wohlfarth, 1994). Formate is then bound to tetrahydrofolate (H_4folate) into 10-formyl-H_4folate via formyl-H_4folate synthetase at the expense of ATP (Eq. 4). Next, dehydration of 10-formyl-H_4folate to 5,10-methenyl-H_4folate is catalyzed by methenyl-H_4folate cyclohydrolase (Eq. 5). 5,10-methenyl-H_4folate is further catalyzed by 5,10-methylene-H_4folate dehydrogenase to 5,10-methylene-H_4folate (Eq. 6). The electron donor of this reaction is NAD(P)H (Diekert and Wohlfarth, 1994). Then, 5,10-methylene-H_4folate is converted to 5-methyl-H_4folate via 5,10-methylene-H_4folate reductase (Eq.7). NADH or ferredoxin can be the electron donor for this reaction (Diekert and Wohlfarth, 1994). Finally, 5-methyl-H_4folate combines with corrinoid protein (E-[Co]) via methyl transferase to form methyl-E-[Co] (Eq. 8).

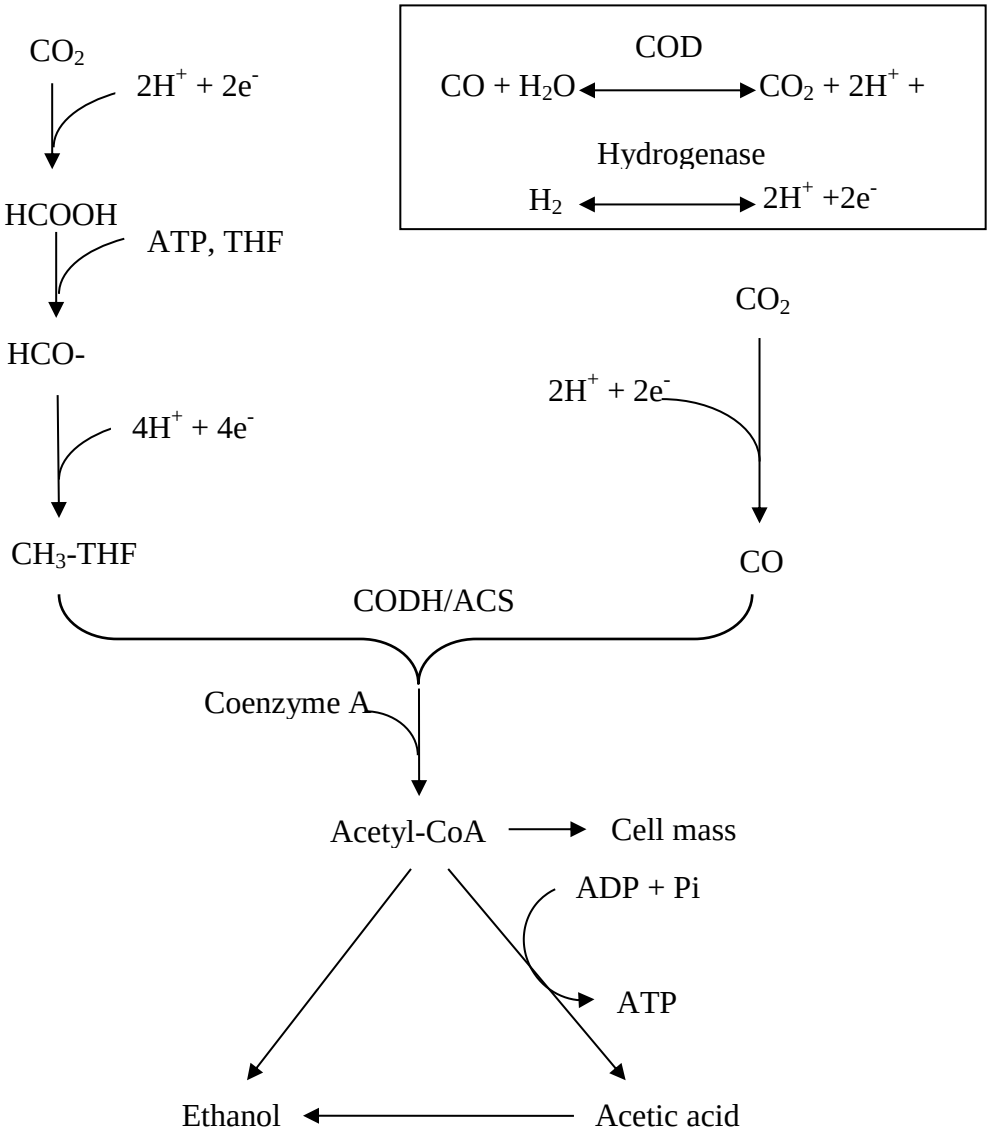

Fig. 2.1 Acetyl-CoA pathway for the production ethanol and acetic acid (adapted from Wilkins and Atiyeh, 2011); THF-tetrahydrofolate, ACS-acetyl CoA syngthase, CODH-carbon monoxide dehydrogenase.

$$CO_2 + 2[H] \rightarrow HCOO^- + H^+ \quad (3)$$

$$\text{Formate} + ATP + H_4\text{folate} \rightarrow \text{10-formyl-}H_4\text{folate} + ADP + Pi \quad (4)$$

$$\text{10-formyl-}H_4\text{folate} + H^+ \rightarrow \text{5,10-methenyl-}H_4\text{folate}^+ + H_2O \quad (5)$$

$$5,\ 10\text{-methly-}H_4\text{folate}^{+} + NAD(P)H \rightarrow 5,10\text{-methylene-}H_4\text{folate} + NAD(P)^{+} \quad (6)$$

$$5,\ 10\text{-methylene-}H_4\text{folate} + 2[H] \rightarrow 5\text{-methyl-}H_4\text{folate} \quad (7)$$

$$5\text{-methyl-}H_4\text{folate} + E\text{-}[Co] \rightarrow H_4\text{folate} + E\text{-}[Co]\text{-}CH_3 \quad (8)$$

The second branch of the acetyl-CoA pathway is called the carbonyl branch. In this branch, CO_2 is reduced to CO by carbon monoxide dehydrogenase/acetyl-CoA synthase complex (CODH/ACS) (Eq. 9) (Köpke et al., 2010; Tracy et al., 2011). Then, E-[Co]-CH_3 from methyl branch combines with CO and free coenzyme A (CoA) to synthesize acetyl-CoA via CODH/ACS complex (Eq. 10).

$$CO_2 + 2[H] \rightarrow CO + H_2O \quad (9)$$

$$E\text{-}[Co]\text{-}CH_3 + CO + CoA \rightarrow E\text{-}[Co] + \text{Acetyl-CoA} \quad (10)$$

In the reductive acetyl-CoA pathway, CO and H_2 from syngas are electron donors (Fig. 2.1). Electrons from CO are produced by CODH and electrons from H_2 are generated by hydrogenase (Wilkins and Atiyeh, 2011). Also, CO and CO_2 are carbon donors for the acetyl-CoA pathway (Wilkins and Atiyeh, 2011).

Three routes for ethanol formation from acetyl-CoA have been proposed:

(1) Route 1 (Köpke et al., 2011a): Acetyl-phosphate was formed from acetyl-CoA via phosphotransacetylase and then acetate kinase catalyzed acetyl-phosphate to acetate which generates ATP. Acetate was then reduced by aldehyde oxidoreductase to acetaldehyde which was further reduced by alcohol dehydrogenase to ethanol. This route was found in *C. ljungdahlii*.

(2) Route 2 (Köpke et al., 2011a): Acetyl-CoA was directly reduced to acetaldehyde by bifunctional enzyme acetaldehyde/ethanol dehydrogenase. Then acetaldehyde was reduced by alcohol dehydrogenase to ethanol. This route was also found in *C. ljungdahlii*.

(3) Route 3 (Reeves, 2010): Acetyl-CoA was directly reduced to ethanol by NADH, catalyzed by secondary alcohol dehydrogenase. Secondary alcohol dehydrogenase has been found in *C. ragsdalei* and *C. ljungdahlii*.

2.3.2.3.2 Bioenergetics

The driving force for the reductive acetyl-CoA pathway depends on the electron donors CO and H_2 (Fig. 2.1), which transfer their electrons via CODH and H_2ase to ferredoxin then to NAD(P)H and finally to ethanol (Köpke et al., 2010). In the acetyl-CoA pathway, one ATP is produced from acetic acid formation, which compensates for the one ATP consumed to form 10-formyl-H_4folate formation (Eq. 4). In other words, there is no net ATP production during acetate and ethanol formation based on substrate level phosphorylation (Köpke et al., 2011a; Liew et al., 2013). However, cell growth requires ATP to maintain cellular functions such as motility and nutrients uptake (Shuler and Fikret, 2002). Others postulated that the extra ATP to support cell function could be obtained from two ways due to no net ATP production based on substrate level phosphorylation: (1) electrochemical gradient of transmembrane via proton pump and sodium pump (2) Rnf complex (Müller et al., 2008; Köpke et al., 2010; Liew et al., 2013). The Rnf complex was originally found in *Rhodobacter capsulatus* and Rnf is the short name of *Rhodobacter* nitrogen fixation (Schmehl et al., 1993). In the study of *C. ljungdahlii*, the electrons from reduced ferredoxin were proposed to be transferred by Rnf

complex to reduce NAD^+ and generate NADH, simultaneously generating a proton gradient for ATP synthesis in *C. ljungdahlii* (Köpke et al., 2010).

The theoretically possible reactions for production of acetic acid and ethanol formation from CO, H_2 and CO_2 and the change in Gibbs free energy for each reaction are shown in Table 2.3 (Wilkins and Atiyeh, 2011; Daniell et al., 2012). Gibbs free energy shows that the reactions with only H_2 used as the reducing equivalent for the production of ethanol or acetic acid are less thermodynamically favorable than if only CO or both CO and H_2 are used. However, the carbon conversion efficiency increases with more H_2 involved in ethanol or acetic acid formation due to less CO serving as electron donor. The thermodynamics study on syngas fermentation reported CO was always the preferred electron donor compared to H_2, which was independent of pH, ionic strength, gas partial pressure and either electron carrier NADH or ferredoxin (Hu et al., 2011).

.

Table 2.3 Theoretical reactions for ethanol and acetic acid formation from CO and H_2.

	Ethanol Formation		Carbon conversion efficiency (%)	Ethanol yield from CO or CO_2 (mol/mol)
(1)	$6CO + 3H_2O \rightarrow C_2H_5OH + 4CO_2$	ΔG^o = -217.4 kJ/mol[a]	33.3	0.167
(2)	$3CO + 3H_2 \rightarrow C_2H_5OH + CO_2$	ΔG^o = -157.2 kJ/mol	66.7	0.333
(3)	$2CO + 4H_2 \rightarrow C_2H_5OH + H_2O$	ΔG^o = -137.1 kJ/mol	100.0	0.500
(4)	$6H_2 + 2CO_2 \rightarrow C_2H_5OH + 3H_2O$	ΔG^o = -97.0 kJ/mol[a]	100.0	0.500
	Acetic acid Formation		**Carbon conversion efficiency (%)**	**Acetic acid yield from CO or CO_2 (mol/mol)**
(5)	$4CO + 2H_2O \rightarrow CH_3COOH + 2CO_2$	ΔG^o =-154.6 kJ/mol[a]	50.0	0.250
(6)	$2CO + 2H_2 \rightarrow CH_3COOH$	ΔG^o =-114.5kJ/mol	100.0	0.500
(7)	$4H_2 + 2CO_2 \rightarrow CH_3COOH + 2H_2O$	ΔG^o =-74.3 kJ/mol[a]	100.0	0.500

[a] adapted from Ukpong et al., 2012.

2.3.2.4 Syngas fermentation operation

Syngas fermentation should be designed to allow the production of desired products at high yield and productivity and low cost. This requires resolving several technical challenges associated with syngas fermentation technology that include mass transfer limitation, high medium cost, low productivity and sensitivity to process parameters such as gas composition, pH and culture kinetics.

2.3.2.4.1 Mass transfer

Mass transfer of the sparingly soluble syngas components, CO and H_2, should match the kinetic requirements of the microorganism to ensure sustainable cells' activity and productivity. CO and H_2 have aqueous solubility of about 75% and 69%, respectively, compared to O_2 on a molar basis (Cooney, 1976; Incropera and DeWitt, 1985). Mass transfer limitation occurs when the rate of gas transfer in the fermentor does not match the maximum gas uptake rate by the microbe used (Shuler and Fikret, 2002). Similar to aerobic fermentation, the gas to liquid mass transfer is the rate-limiting step for syngas fermentation (Munasinghe and Khanal, 2010; Tirado-Acevedo et al., 2010; Wilkins and Atiyeh, 2011; Liew et al., 2013; Orgill et al., 2013). The low availability of the substrate gas for the microbe to utilize during syngas fermentation results in low cell concentration and low productivity (Vega et al., 1990).

There are three main phases for the transfer of gas from the headspace to the cells, namely bulk gas, liquid medium and cells (Klasson et al., 1992). The major mass transfer resistance is assumed to be at the gas-liquid interface, while mass transfer of the bulk gas phase is considered as instantaneous and the mass transfer resistance from liquid to cell is

neglected due to the large surface area of cells (Klasson et al., 1992). The rate of mass transfer is given by the following equation (Vega et al., 1990):

$$-\frac{1}{V_L}\frac{dN_S^G}{dt} = \frac{k_L a/V_L}{H}\left(P_S^G - P_S^L\right) \quad (11)$$

where: k_La/V_L is the overall volumetric mass transfer coefficient, H is Henry's law constant, N_S^G is mole of substrate gas transferred from the gas phase, a is gas liquid interfacial area, V_L is the liquid volume in the fermentor, P_S^G and P_S^L are the partial pressures of gaseous substrate in the gas and liquid phases, respectively.

Under mass transfer limitation condition, dissolved gaseous substrates in the liquid medium are considered to be utilized immediately. Thus, P_S^L is assumed to be zero (Vega et al., 1990). Thus, the Eq. 11 is modified to Eq. 12:

$$-\frac{1}{V_L}\frac{dN_S^G}{dt} = \frac{k_L a/V_L}{H} P_S^G \quad (12)$$

From Eq.12, it can be seen that the mass transfer rate depends on the volumetric mass transfer coefficient k_La/V_L and partial pressure of gaseous substrate in the gas phase P_S^G. The k_La/V_L depends on many factors including reactor type, reactor configuration, gas flow rate and agitation speed. The k_La/V_L is desired to be high to allow faster transfer rate of gaseous substrate into the cells. Among many of the reactors that can be used for syngas fermentation, the continuous stirred-tank reactor (CSTR) has been the most common type of fermentor used in syngas fermentation (Abubackar et al., 2011; Orgill et al., 2013). The CSTR has a simple design and easy to operate. However, the CSTR has disadvantages such as high power to volume ratio requirement due to high

agitation speed to obtain high k_La/V_L. This is still an issue to advance syngas fermentation to a viable commercial operation (Klasson et al., 1993; Bredwell et al., 1999; Orgill et al., 2013). Several studies reported on other types of fermentors such as bubble column, trickle-bed reactor (TBR) and membrane reactor (Munasinghe and Khanal, 2010; Orgill et al., 2013). Bubble column reactor is similar to a CSTR but it does not require mechanical agitation, thus lowering the energy cost. There are several important design parameters for bubble column reactors such as bubble size distribution, gas holdup, gas liquid interfacial area, mass transfer coefficient and heat transfer characteristics (Shah et al., 1982). However, the disadvantages of bubble column reactors include bubble coalescence, high pressure drop and backmixing of gaseous component due to the heterogeneous flow at high gas flow rates (Abubackar et al., 2011; Wilkins and Atiyeh, 2012).

TBRs can enhance gas liquid mass transfer by minimizing liquid resistance to mass transfer through a thin liquid film on the packing bed for gas contact (Orgill et al., 2013). However, an external pump is required to recirculate liquid back to the TBR, which adds to the energy input to the process (Orgill et al., 2013). Membrane reactors provide large area to volume ratio, thus enhancing gas liquid mass transfer efficiency. Different designs of membrane reactors for syngas fermentation have been included in patents by Coskata Inc. (Tsai et al., 2009; Tsai et al., 2009). In this type of reactor and depending on the membrane material of construction, cells can be immobilize within the membrane and directly contact syngas via larger membrane surface area (Tsai et al., 2009; Tsai et al., 2009). However, membrane reactors suffer from fouling problems (Liew et al., 2013).

Mass transfer rate was shown to be improved by increasing the driving force via increasing partial pressure of the gaseous substrates (Vega et al., 1990). However, the increase in the mass transfer by elevating CO partial pressure beyond the culture ability to use CO caused a negative effect on cell growth (Vega et al., 1990; Klasson et al., 1992). To overcome this problem, high cell mass concentration is required to match the high mass transfer rate of the gas (Vega et al., 1990; Munasinghe and Khanal, 2010; Orgill et al., 2013).

There are several methods to experimentally determine the mass transfer coefficient in a fermentor. One such method is the static method, which is based on gas mass balance calculation of the gas concentration in the liquid, inlet gas and outlet gas compositions and gas flow rates (Blanch and Clark, 1997). This method works in well-mixed gas and liquid phase, but a large reactor may not be well-mixed and cause an error of measurement (Blanch and Clark, 1997). Another method is the dynamic method, in which the change in oxygen concentration in the liquid phase is measured with time. Normally, a dissolved oxygen probe is utilized to record the % dissolved oxygen change in the liquid (Shuler and Fikret, 2002; Orgill et al., 2013). This method is simple and has been applied in small and larger scale fermentation (Blanch and Clark, 1997).

CO or H_2 mass transfer coefficients can be estimated from equations developed based on mass transfer theories such as two-film theory, boundary layer theory, penetration theory and surface renewal theory. The two-film theory assumes the fluid in each liquid and gas film is stagnant and mass transfer occurs by molecular diffusion (McCabe and Smith, 2005). However, this is not true for syngas fermentation under turbulent flow because turbulent eddies can penetrate the film (McCabe and Smith, 2005;

Jones, 2007). The boundary layer theory is similar to the two-film theory that assumes the mass transfer occurs in a thick boundary layer near a surface with laminar flow, but it does not apply to the situation when the boundary layer becomes turbulent (McCabe and Smith, 2005). The penetration theory and surface renewal theory are commonly accepted theory to model mass transfer between gas-liquid interface (Kawase et al., 1992). The penetration theory assumes an unsteady diffusion of gas into liquid across the gas-liquid interface in an exposure time (McCabe and Smith, 2005):

$$k_La/V_L=2(D/\pi\ t_e)^{1/2} \quad (13)$$

where D is diffusivity of gas and t_e is the exposure time. Similarly, surface renewal theory considers the liquid element at surface is randomly replaced by bulk liquid and the average mass transfer is expressed as (McCabe and Smith, 2005):

$$k_La/V_L=(D\ \cdot s)^{1/2} \quad (14)$$

where s is the fractional rate of surface renewal (the fraction of surface area renewed in unit time).

Mass transfer in syngas fermentation can be described with the penetration or surface renewal theories because turbulent gas flow is required to improve mass transfer (Jones, 2007). Thus, the ratio of k_La/V_L for each gas species such as O_2, CO, H_2 and CO_2 can be expressed as the ratio of their diffusivities to the half power based on Eq. 13 or Eq. 14:

$$\frac{(k_La/V_L)_i}{(k_La/V_L)_j}=\left(\frac{D_i}{D_j}\right)^{1/2} \quad (15)$$

where i, j represents each gas species and D is diffusivity of each gas species in the liquid.

2.3.2.4.2 Medium composition

Currently, most syngas fermentation media are not defined, due to the use of yeast extract or other complex nutrients (Younesi et al., 2005; Ahmed et al., 2006; Huhnke et al., 2010; Saxena and Tanner, 2010; Ramachandriya et al., 2011; Liu et al., 2012). Phillips and co-workers had successfully removed yeast extract from *C. ljungdahlii* medium and designed a defined medium based on *Escherichia coli* elemental cell composition (Phillips et al., 1993). In their study with defined medium, 48 g/L ethanol was produced after 560 h in continuous syngas fermentation with a cell recycle system. Coskata Inc., a company pursuing a commercial scale ethanol syngas fermentation biorefinery, has isolated a novel strain called *Clostridium coskatii* , which grows in defined medium and produced 20 g/L ethanol (Zahn and Saxena, 2011).

The concentrations of trace metals, minerals, vitamins and other nutrients in the fermentation medium affect the microorganism's growth and fermentation ability to convert syngas into products. Therefore, it is crucial to optimize the concentration of these nutrients towards directing the syngas components into increasing products titer and productivity for the viability of the syngas fermentation process. For example, when concentrations of Ni^{2+}, Zn^{2+}, SeO^{4-}, WO^{4-}, Fe^{2+} were optimized and Na^{+} and Cu^{2+} were removed from the standard growth medium for *C. ragsdalei*, ethanol production increased by four-fold (Saxena and Tanner, 2010). In addition, the minerals $Ca^{2+,}$ Mg^{2+}, K^{+}, NH_4^{+} in the *C. ragsdalei* medium were optimized to remove excessive amounts of

these minerals (Saxena and Tanner, 2012). Also, 20 g/L corn steep liquor (CSL) medium was found to have comparable ethanol concentration to yeast extract medium (Saxena and Tanner, 2012). Ethanol production was improved by limiting the concentration of calcium pantothenate, cobalt and Vitamin B_{12}, which was due to acetyl-CoA synthesis rate decrease and accumulation of NADH for more ethanol production (Gaddy et al., 2003; Kundiyana et al., 2011a). Table 2.4 summarizes the effect of selected minerals and trace metals on key enzymes in the acetyl-CoA pathway.

In addition to developing a defined medium with optimized nutrient concentrations, the medium should be inexpensive to support production at commercial level. According to several published studies on compositions of syngas fermentation media, the use of Good's buffer (MES and TAPS) in these media accounts for over 90% of the total medium cost (Ahmed et al., 2006; Babu et al., 2010; Huhnke et al., 2010; Panneerselvam et al., 2010; Maddipati et al., 2011; Ramachandriya et al., 2011; Liu et al., 2012). The cost of these media was over $6.00/L, which is too high for commercial production of ethanol. Other studies focused on the development of low cost medium using complex nutrients such as corn steep liquor (CSL) (Maddipati et al., 2011) and cotton seed extract (CSE) (Kundiyana et al., 2010) to replace yeast extract (YE). The industrial costs of CSL and CSE were $0.18 /kg and $0.98/kg, respectively, which were much lower than industrial yeast extract cost of $ 9.20 /kg (Kundiyana et al., 2010; Maddipati et al., 2011). The results from these studies showed improved ethanol production at least twofold compared to YE medium, indicating the potentials for CSL and CSE to be used as low cost nutrient replacements in syngas fermentation (Kundiyana et al., 2010; Maddipati et al., 2011).

Table 2.4 Effects of minerals and trace metals on acetyl-CoA pathway.

Chemicals	Function	Reference
Sodium	There is no net ATP produced from substrate level phosphorylation via Acetyl-CoA pathway. The ATP is proposed to generate from membrane gradient. Sodium is required for Na+-translocating ATPase for some strains such as *Acetobacterium woodii* or other extreme alkaliphilic bacteria	(Heise et al., 1991; Köpke et al., 2010; Pitryuk and Pusheva, 2001)
Calcium	Increase cell membrane stability and stabilize ATPase activity inhibited by ethanol; Required by CO dehydrogenase, disulfide reductase which activates CO dehydrogenase	(Ciesarova et al., 1996; Ingram,1986; Ljungdhal, 1986; Osman and Ingram, 1985)
Magnesium	Protect cell leakage induced from ethanol and restore metabolic activity	(Ciesarova et al., 1996; Osman and Ingram, 1985)
Ammonium	Preferred as an inorganic nitrogen source for cell growth; Formyl-H_4folate synthetase activator	(Ljungdhal, 1986; Saxena and Tanner, 2012)
Potassium	Formyl-H_4folate synthase activator	(Ljungdhal, 1986; Saxena and Tanner, 2010; Scopes, 1983)
Iron	Required by CO dehydrogenase, formate dehydrogenase, hydrogenase, alcohol dehydrogenase, Ferredoxin	(George and Chen, 1983; Ljungdhal, 1986; Saxena and Tanner, 2010)
Nickel	Required by CO dehydrogenase, hydrogenase, acetyl-CoA synthase,	(Ljungdhal, 1986; Saxena and Tanner, 2010)

Manganese	Required by phosphotransacetylase	(Ljungdhal, 1986)
Tungsten	Required by formate dehydrogenase	(Ljungdhal, 1986; Saxena and Tanner, 2010)
Molybdate	Required by formate dehydrogenase	(Saxena and Tanner, 2010)
Selenium	Required by formate dehydrogenase	(Saxena and Tanner, 2010)
Zinc	Required by CO dehydrogenase and CO dehydrogenase disulfide reductase, alcohol dehydrogenase	(Ljungdhal, 1986; Saxena and Tanner, 2010)
Cobalt	Required by corrinoid enzyme for synthesis methyl-group of acetyl-CoA	(Wood et al., 1986)
Sulfur	Required by hydrogenase and corrinoid enzyme for synthesis methyl-group of acetyl-CoA	(Albracht, 2003; Menon and Ragsdale, 1999)
Copper	Negative effect on acetyl-CoA synthase activity	(Saxena and Tanner, 2010)

2.3.2.4.3 Fermentation pH

The pH of the fermentation medium also plays an important role in regulating the carbon flow towards production ethanol instead of making more cell mass or acetic acid. The pH of the fermentation medium also affects the switch from acetogenesis to solventogenesis (Worden et al., 1991). *C. ragsdalei, Eubacterium limosum* (old name *Butyribacterium methylotrophicum*) and *C. carboxidivorans* were found to switch from acetogenesis to solventogenesis at a pH range 4.5 to 5.0 (Worden et al., 1991; Ahmed et al., 2006; Maddipati et al., 2011; Ramachandriya et al., 2011).

2.3.2.4.4 Redox potential

Redox potential plays a critical role for monitoring and controlling the fermentation process. It was observed that there was a decreasing trend in redox potential during the cell growth stage and an increasing trend during ethanol production stage by *C. ragsdalei* (Kundiyana et al., 2010; Maddipati et al., 2011). This indicates that cell growth could be associated with increasing NADH/NAD^+ ratio by decreasing redox potential. The thermodynamics of syngas fermentation using *C. ragsdalei* indicates that the redox potential affects ethanol production and more negative redox potential (at least below -200 mV, standard hydrogen electrode, SHE) would be more favorable for the reaction requiring NADH, which drives the reaction toward ethanol formation (Hu, 2010).

2.3.2.4.5 Syngas compositions and impurities

Syngas compositions change with feedstock, types of gasifier and gasification conditions used. The H_2:CO ratio can range from 0 to 2 as seen in Table 2.5. The H_2:CO ratios cover stoichiometric ratios required for ethanol and acetic acid production (Table 2.5). A H_2:CO ratio of 2 can be obtained from gasification of biomass using steam and pure oxygen (Turn et al., 1998) or dairy biomass (cow manure) using air (Gordillo and Annamalai,2010), which has the potential to meet the theoretical 100% carbon conversion during syngas fermentation.

Syngas was reported to contain several impurities such as tars, chars, ash, ethylene, ethane, acetylene, methane, NO_x, COS and SO_x (Datar et al. 2004; Ahmed et al., 2006; Xu et al., 2011). NO and acetylene were considered as inhibitors of hydrogenase, decreasing H_2 uptake during fermentation (Mohammadi et al., 2011). Also, tars in the producer gas were found to cause cell dormancy of *C. carboxidivorans* (Ahmed et al., 2006). H_2S up to 5.2 % (v/v) did not show significant inhibition on growth and gas uptake by *C. ljungdahlii* (Klasson et al., 1993). However, NH_3 was an inhibitor of alcohol dehydrogenase and hydrogenase, which was found in *C. ragsdalei* syngas fermentation (Xu et al., 2011). Thus, syngas cleanup is recommended and can be achieved by adding a 0.025 μm gas filter, gas scrubbers or cyclones (Liew et al., 2013).

Table 2.5 Syngas compositions from gasifying various feedstocks (adapted from Liew et al., 2013).

Source	%CO	%CO_2	%H_2	%N_2	%CH_4	%Others	Gasifier type	H_2/CO	Reference
Switchgrass[c]	14.7	16.5	4.4	56.8	4.2	3.4	Fluidized bed	0.3	(Datar et al., 2004)
Pine wood chips[b]	16.1	13.6	16.6	37.6	2.7	13.4	Fluidized bed	1.0	(Corella et al., 1998)
Willow[c]	9.4	17.1	7.2	60.5	3.3	2.5	Fluidized bed	0.8	(Van der Drift et al., 2001)
Cacao shells[c]	8.0	16.0	9	61.5	2.3	3.2	Fluidized bed	1.1	(Van der Drift et al., 2001)
Dairy biomass (cow manure)[c]	8.7	15.7	18.6	56.0	0.6	0.4	Updraft fixed bed	2.1	(Gordillo and Annamalai, 2010)
Demolition wood/ paper residue[c]	9.2	16.1	6.1	63.2	2.8	2.6	Fluidized bed	0.7	(Van der Drift et al., 2001)
Coal gasification[b,d]	67.0	4.0	24	1.0	0.02	4.0	Fluidized bed	0.36	(Subramani and Gangwal, 2008)
Steel mill	44.0	22.0	2.0	32.0	0.0	0.0	NA[a]	0.004	(Köpke et al., 2011b)

[a] Not applicable [b] steam was used; [c] air was gasifying agent; [d] oxygen was gasifying agent.

2.3.2.4.6 Substrates concentration

The substrates in syngas fermentation are mainly CO and H_2. However, CO was found to be a competitive inhibitor of hydrogenase (Albracht, 2003), which hinders the uptake of H_2 and decreases H_2 conversion efficiency. There were several studies on the effect of CO partial pressures on the activity of hydrogenase. A 97% decrease in the specific activity of hydrogenase was reported with an increase in CO partial pressure from 35 kPa (abs) to 202 kPa (abs) using *C. carboxidivorans* (Hurst and Lewis, 2010). When CO partial pressure increased from 35 kPa (abs) to 202 kPa (abs), cell mass and ethanol concentrations increased fourfold and ethanol production changed from non-growth associated to growth-associated using *C. carboxidivorans*, which was similar to a study on *C. ragsdalei* when CO partial pressure increased from 47 kPa (abs) to 95 kPa (abs), ethanol was growth-associated product (Hurst, 2005; Terrill et al., 2012). The hydrogenase activity of *C. ragsdalei* at initial partial pressures of CO and H_2 of 9 kPa and 77 kPa, respectively, was 90% lower than the activity of hydrogenase at initial pressures of CO and H_2 of 0 kPa (abs) and 77 kPa (abs), respectively (Skidmore, 2010). In addition, hydrogenase was least inhibited when syngas was made of 10% H_2,20% CO, 30% CO_2 and 40% N_2, compared to other syngas mixtures with H_2 (20% to 30%), CO (20% to 40%), 30% CO_2 and N_2 as balance (Terrill et al., 2012). H_2 was reported to be an inhibitor of hydrogenase when the partial pressure of H_2 was above 92 kPa (abs) (Arp and Burris, 1981).

2.3.2.4.7 Mixed culture fermentation

Most syngas fermentations studies report the use of a monoculture for biofuels production. No studies were found on syngas fermentation to liquid biofuels using mixed culture. Mixed culture fermentation was originated from waste treatment processing. It has the advantage of needing no sterilization, being highly adaptive to various waste sources, being flexible on substrates type and continuous operation (Kleerebezem and van Loosdrecht, 2007). Basically, biofuels such as methane, alcohols and biohydrogen were reported to be included in the end products of waste treatment (Kleerebezem and van Loosdrecht, 2007).

Syngas containing CO and H_2 has already been studied in waste treatment processing to transfer electrons from syngas to products. A mixed culture in anaerobic sludge that contained sulfate reducing bacteria, methanogenic archaea and homoacetogenic bacteria was reported to reduce sulfate into acetate or methane via feed CO and H_2 (Esposito et al., 2003; Sipma et al., 2004). Methane was produced from a mixed culture consisting of *Rhodospirillum rubrum*, *Methanobacterium formicicum* and *Methanosarcina barkeri* by converting CO, CO_2 and H_2 from syngas due to the synergistic effect of the three bacteria (Klasson et al., 1990).

2.3.2.4.8 Fermentation mode

Currently, three syngas fermentation modes are mostly studied in literature: fed-batch fermentation, continuous syngas flow and liquid batch (semi-continuous fermentation) and continuous fermentation with or without cell recycle. High ethanol concentrations above 10 g/L were mostly achieved in continuous syngas fermentation in

larger fermentor than small bottle fermentations as shown in Table 2.6. The highest reported ethanol concentration in syngas fermentation was 48 g/L in a CSTR that was operated in continuous mode with cell recycle (Phillips et al., 1993). Table 2.6 summarizes syngas fermentation studies in various fermentation modes and scale.

2.4 Commercialization

Three companies are pursuing commercial production of biofuels from syngas. INEOS Bio acquired Bioengineering Resources Inc. (BRI) and is building a plant to produce 8 million gallon of cellulosic ethanol per year (Liew et al., 2013) and announced in July 2013 that it started production at commercial scale (INEOS Bio, 2013).

Coskata Inc. licensed strains *C. ragsdalei* and *C. carboxidivorans* from Oklahoma State University and the University of Oklahoma (Lewis et al., 2007; Huhnke et al., 2010). Coskata Inc. also isolated and patented another strain, *C. coskatii* that produced 20 g/L ethanol (Zahn and Saxena, 2011).

LanzaTech is another syngas fermentation company that is headquartered in New Zealand. This company is collaborating with steel mill companies to ferment steel mill off gas, mainly containing CO, into ethanol. LanzaTech has opened branches in the US and China. Especially, they demonstrated a pilot scale plant of 100,000 gallon of ethanol production in Shanghai, China from a steel mill company called Baosteel Group. LanzaTech is planning to build a commercial plant in China with a capacity of 50 million gallons ethanol per year (Liew et al., 2013).

Syngas fermentation can be used to produce biobased products such as 2,3 butanediol, acetic acid, and butyric acid besides ethanol and butanol. 2,3-butanediol is a

high added value product as a precursor for methyl ethyl ketone, 1,3-butadiene synthesis (Köpke et al., 2011b). 2,3-butanediol is currently produced from petroleum and has a potential global market of 32 million tons per year equivalent to $43 billion (Köpke et al., 2011b). Acetic acid is currently produced by the vinegar industry via oxidation of ethanol using biocatalysts with a cost of $0.78/kg to $1.00/kg as well as petroleum derived process by carbonization of methanol to acetic acid with a cost of $0.33/kg to $0.78/kg (Rogers et al., 2013). The applications of butyric acid in current industrial processes are in cellulose acetate butyrate plastics, textile fiber, feather tanning, additives in soft drink and chewing gums, and pharmaceutical application (Zidwick et al., 2013). Due to numerous studies on biofuel production from lignocellulosic feedstock, the Department of Energy (DOE) has reported the target price of ethanol in both the biochemical platform and thermochemical platform. Since 2007 to 2012, the price of ethanol has been targeted to decrease from $2.52/gallon ($0.67/L) to $1.41/gallon ($0.37/L) for biochemical process and decrease from $3.35/gallon ($0.89/L) to $1.31/gallon ($0.35/L) for thermochemical process (DOE, 2011). The estimated ethanol price based on syngas fermentation was between $1.32/L to $1.68/L (Munasinghe and Khanal, 2010).

Table 2.6 Syngas fermentation operation modes.

Strains	Fermentation mode	Reactor type	Working volume	Headspace pressure, kPa (abs)	Gas composition	pH	Max. cell conc. g/L	Alcohols g/L	Duration	Reference
Clostridium ljungdahlii	Batch	Bottle reactor	50 mL	182	55% CO, 20% H_2, 10% CO_2, 15% Ar	4.0-6.0	1.15	Ethanol 0.55	120 h	(Younesi et al., 2005)
Clostridium ljungdahlii	Continuous gas flow and liquid batch	CSTR	250 mL	101	20% CO, 10% H_2, 20% CO_2, 50% N_2	6.8	0.56	Ethanol 0.23	44 h	(Cotter et al., 2009)
Clostridium ljungdahlii	Continuous fermentation	CSTR	2L	101	55% CO, 20% H_2, 10% CO_2, 15% Ar	6.8	2.1	Ethanol 6.5	792 h	(Mohammadi et al., 2012)
Clostridium ljungdahlii	Continuous fermentation with cell recycle	CSTR	N/A	101	55% CO, 20% H_2, 10% CO_2, 15% Ar	4.5	4	Ethanol 48	560 h	(Phillips et al., 1993)
Clostridium ljungdahlii	Continuous gas flow and liquid batch	Immobilized cell reactor (ICR) with fabric cells support medium	4.9 L	101	14% CO, 17% H_2, 4% CO_2, 65% N_2	5.1	0.018	Ethanol 2.74	N/A	(Gaddy, 2000)
Clostridium autoethanogenum	Batch	Bottle reactor	20 mL	202	60% CO and rest of gas contains CO_2 and N_2 but composition is not specified	4.74	N/A	Ethanol 0.26	60 h	(Guo et al., 2010)
Clostridium autoethanogenum	Continuous gas flow and liquid batch	CSTR	250 mL	202	20% CO, 10% H_2, 20% CO_2, 50% N_2	N/A	0.15	Ethanol <0.1	72 h	(Cotter et al., 2009)
Butyribacterium methylotrophicum	Continuous gas flow and liquid batch	CSTR	0.5 L	121	100% CO	6.0	0.55	Ethanol 0.16, butanol 0.08	400 h	(Grethlein et al., 1991)

Butyribacterium methylotrophicum	Continuous fermentation	CSTR	1.25 L	101	100% CO	6.0	0.29	Ethanol 0.06 butanol 0.08	216 h	(Grethlein et al., 1990)
Butyribacterium methylotrophicum	Continuous fermentation with cell recycle	CSTR	1.2 L	101	100% CO	5.5	4.55	Ethanol 0.33, butanol 2.7	N/A	(Grethlein et al., 1991)
Clostridium carboxidivorans	Continuous fermentation	Bubble column reactor	4 L	101	25% CO, 15% CO_2, 60% N_2	Initial 5.75 and then control at 5.2	0.35	Ethanol 0.35, butanol 0.08	408 h	(Lewis et al., 2007)
Clostridium carboxidivorans	Continuous fermentation	Bubble column reactor	2.8 L	135	25% CO, 15% CO_2, 60% N_2	5.3	N/A	Ethanol 0.56 butanol 0.08	720 h	(Rajagopalan et al., 2002)
Clostridium carboxidivorans	Continuous gas flow and liquid batch	CSTR	3.3 L	101	20% CO, 5% H_2, 15% CO_2, 60% N_2	Initial pH 5.7	0.30 g/L	Ethanol 2.81, butanol 0.53	264 h	(Ukpong et al., 2012)
Clostridium carboxidivorans	Continuous fermentation	CSTR	3 L	137	17% CO, 5% H_2, 15% CO_2, 63% N_2	Initial pH 5.85 and not allow pH below 5.25	0.22 g/L	Butanol 0.5	504 h	(Ahmed et al., 2006)
Clostridium ragsdalei	Batch	Bottle reactor	100 mL	238	20% CO, 5% H_2, 15% CO_2, 60% N_2	Initial pH 6.0	0.4 g/L	Ethanol 1.7, butanol 0.6	360 h	(Maddipati et al., 2011)
Clostridium ragsdalei	Batch	Bottle reactor	100 mL	238	20% CO, 5% H_2, 15% CO_2, 60% N_2	Initial pH 6.0	0.95 g/L	Ethanol 1.9	360 h	(Kundiyana et al., 2011b)
Clostridium ragsdalei	Batch	Bottle reactor,	50 mL	238	20% CO, 5% H_2, 15% CO_2, 60% N_2	Initial pH 6.0	0.63 g/L	Adding acetone with initial 2 g/L, ethanol 1.9, isopropanol 1.9 g/L	240 h	(Ramachandriya et al., 2011)
Clostridium ragsdalei	Continuous gas flow and liquid batch	CSTR	3.3 L	143	20% CO, 5% H_2, 15% CO_2, 60% N_2	Initial pH 6.0	0.74 g/L	Ethanol 9.6	360 h	(Maddipati et al., 2011)

2.5 References

Abubackar, H.N., Veiga, M.C., Kennes, C., 2011. Biological conversion of carbon monoxide: rich syngas or waste gases to bioethanol. Biofuels, Bioprod. Biorefin. 5, 93-114.

Ahmed, A., Cateni, B.G., Huhnke, R.L., Lewis, R.S., 2006. Effects of biomass-generated producer gas constituents on cell growth, product distribution and hydrogenase activity of *Clostridium carboxidivorans* $P7^T$. Biomass Bioenerg. 30, 665-672.

Albracht, S.P.J., 2003. Mechanism of hydrogen activation (Eds.), Biochemistry and physiology of anaerobic bacteria. Johnson, Springer-Verlag, New York.

Allen, T.D., Caldwell, M.E., Lawson, P.A., Huhnke, R.L., Tanner, R.S., 2010. *Alkalibaculum bacchi* gen. nov., sp. nov., a CO-oxidizing, ethanol-producing acetogen isolated from livestock-impacted soil. Int. J. Syst. Evol. Microbiol. 60, 2483-2489.

Arp, D.J., Burris, R.H., 1981. Kinetic mechanism of the hydrogen-oxidizing hydrogenase from soybean nodule bacteroids. Biochemistry 20, 2234-2240.

Babu, B.K., Atiyeh, H.K., Wilkins, M.R., Huhnke, R.L., 2010. Effect of the reducing agent dithiothreitol on ethanol and acetic acid production by *Clostridium* strain P11 using simulated biomass-based syngas. Biol. Eng. 3, 19-35.

Blanch, H.W., Clark, d.S., 1997. Biochemcial Engineering. Marcel Dekker, Inc, New York, pp.702.

Bredwell, M.D., Srivastava, P., Worden, R.M., 1999. Reactor design issues for synthesis-gas fermentations. Biotechnol. Prog. 15, 834-844.

Chang, I.S., Kim, B.H., Lovitt, R.W., Bang, J.S., 2001. Effect of CO partial pressure on cell-recycled continuous CO fermentation by *Eubacterium limosum* KIST612. Process Biochem. 37, 411-421.

Cheng, J., 2010. Biomass to renewable energy process. CRC Press, Boca Raton, pp.517.

Ciesarova, Z., Šmogrovičová, D., Dömény, Z., 1996. Enhancement of yeast ethanol tolerance by calcium and magnesium. Folia microbiol. 41, 485-488.

Cooney, D.O., 1976. Biomedical engineering principles. Marcel Dekker, New York, pp.352.

Corella, J., Orio, A., Aznar, P., 1998. Biomass gasification with air in fluidized bed: reforming of the gas composition with commercial steam reforming catalysts. Ind. Eng. Chem. Res. 37, 4617-4624.

Cotter, J.L., Chinn, M.S., Grunden, A.M., 2009. Influence of process parameters on growth of *Clostridium ljungdahlii* and *Clostridium autoethanogenum* on synthesis gas. Enzyme Microb. Technol. 44, 281-288.

Daniel, S.L., Hsu, T., Dean, S., Drake, H., 1990. Characterization of the H_2-and CO-dependent chemolithotrophic potentials of the acetogens *Clostridium thermoaceticum* and *Acetogenium kivui*. J. Bacteriol. 172, 4464-4471.

Daniell, J., Köpke, M., Simpson, S.D., 2012. Commercial Biomass Syngas Fermentation. Energies 5, 5372-5417.

Datar, R.P., Shenkman, R.M., Cateni, B.G., Huhnke, R.L., Lewis, R.S., 2004. Fermentation of biomass-generated producer gas to ethanol. Biotechnol. Bioeng. 86, 587-594.

Datta, R., Maher, M.A., Jones, C., Brinker, R.W., 2011. Ethanol—the primary renewable liquid fuel. J. Chem. Technol. Biotechnol. 86, 473-480.

Demirbas, M.F., 2011. Biofuels from algae for sustainable development. Appl. Energ. 88, 3473-3480.

Demirbas, M.F., 2009. Biorefineries for biofuel upgrading: a critical review. Appl. Energ. 86, S151-S161.

Diekert, C., Wohlfarth, G., 1994. Energetics of acetogenesis from C_1 units. in: Drake, H.L. (Eds.), Acetogenesis. Chapman & Hall, New York, pp. 157-179.

DOE. 2011. Biomass program multi-year program plan. Department of Energy.

Drake, H.L., 1994. Acetogenesis, acetogenesis bacteria, and the acetyl-CoA "Wood/Ljungdahl" pathway: Past and current perspectives. in: Drake, H.L. (Eds.), Acetogenesis. Chaman & Hall, London.

Drake, H.L., Gößner, A.S., Daniel, L.S., 2008. Old acetogens, new light. Ann. N. Y. Acad. Sci. 1125, 100-128.

Dry, M.E., 2002. The Fischer–Tropsch process: 1950–2000. Catal. today 71, 227-241.

EPA, 2013. Accessed June 13, 2013. http://www.epa.gov/ncea/biofuels/basicinfo.htm.

Esposito, G., Weijma, J., Pirozzi, F., Lens, P., 2003. Effect of the sludge retention time on H_2 utilization in a sulphate reducing gas-lift reactor. Process Biochem. 39, 491-498.

Foust, T.D., Aden, A., Dutta, A., Phillips, S., 2009. An economic and environmental comparison of a biochemical and a thermochemical lignocellulosic ethanol conversion processes. Cellulose 16, 547-565.

Gaddy, J.L. 2000. Biological production of ethanol from waste gases with *Clostridium ljungdahlii*. US patent 6136577.

Gaddy, J.L., Arora, D.K., Ko, C.-W., Phillips, J.R., Basu, R., Wikstrom, C.V., Clausen, E.C. 2003. Method for increasing the production of ethanol from microbial fermentation. US patent 2003/0211585 A1.

George, H.A., Chen, J.S., 1983. Acidic conditions are not obligatory for onset of butanol formation by *Clostridium beijerinckii* (synonym, *C. butylicum*). Appl. environ. microbiol. 46, 321-327.

Gordillo, G., Annamalai, K., 2010. Adiabatic fixed bed gasification of dairy biomass with air and steam. Fuel 89, 384-391.

Grethlein, A., Worden, R., Jain, M., Datta, R., 1990. Continuous production of mixed alcohols and acids from carbon monoxide. Appl. Biochem. Biotechnol. 24, 875-884.

Grethlein, A.J., Worden, R.M., Jain, M.K., Datta, R., 1991. Evidence for production of butanol from carbon monoxide by *Butyribacterium methylotrophicum*. J. Biosci. Bioeng. 72, 58-60.

Griffin, D.W., Schultz, M.A., 2012. Fuel and chemical products from biomass syngas: A comparison of gas fermentation to thermochemical conversion routes. Environ. Prog. Sustainable Energy 31, 219-224.

Guo, Y., Xu, J., Zhang, Y., Xu, H., Yuan, Z., Li, D., 2010. Medium optimization for ethanol production with Clostridium autoethanogenum with carbon monoxide as sole carbon source. Bioresour. Technol. 101, 8784-8789.

Heise, R., Reidlinger, J., Müller, V., Gottschalk, G., 1991. A sodium-stimulated ATP synthase in the acetogenic bacterium *Acetobacterium woodii*. FEBS Lett. 295, 119-122.

Hu, P. 2010. Thermodynamic, sulfide, redox potential, and pH effects on syngas fermentation. Ph.D. Dissertation. Brigham Young University, pp. 192.

Hu, P., Bowen, S.H., Lewis, R.S., 2011. A thermodynamic analysis of electron production during syngas fermentation. Bioresour. Technol. 102, 8071-8076.

Huhnke, R.L., Lewis, R.S., Tanner, R.S. 2010. Isolation and characterization of novel clostridial species. US Patent No. 7,704,723.

Hurst, K.M. 2005. Effects of carbon monoxide and yeast extract on growth, hydrogenase activity, and product formation of *Clostridium carboxidivorans* P7^{T}. M.S. Thesis. Oklahoma State University, pp. 86.

Hurst, K.M., Lewis, R.S., 2010. Carbon monoxide partial pressure effects on the metabolic process of syngas fermentation. Biochem. Eng. J. 48, 159-165.

Iglesia, E., 1997. Design, synthesis, and use of cobalt-based Fischer-Tropsch synthesis catalysts. Appl. Catal. A. 161, 59-78.

Incropera, F.P., DeWitt, D.P., 1985. Fundamentals of heat and mass transfer. Wiley, New York, pp.778.

INEOS Bio, 2013. Accessed July 31, 2013. http://www.ineos.com/en/businesses/INEOS-Bio/.

Ingram, L., 1986. Microbial tolerance to alcohols: role of the cell membrane. Trends Biotechnol. 4, 40-44.

Jones, S.T. 2007. Gas-liquid mass transfer in an external airlift loop reactor for syngas fermentation. Iowa State University, pp 173-192.

Kawase, Y., Halard, B., Moo-Young, M., 1992. Liquid-phase mass transfer coefficients in bioreactors. Biotechnol. Bioeng. 39, 1133-1140.

Klasson, K., Cowger, J., Ko, C., Vega, J., Clausen, E., Gaddy, J., 1990. Methane production from synthesis gas using a mixed culture of *R. rubrum* , *M. barkeri*, and *M. formicicum*. Appl. Biochem. Biotechnol. 24, 317-328.

Klasson, K.T., Ackerson, M.D., Clausen, E.C., Gaddy, J.L., 1992. Bioconversion of synthesis gas into liquid or gaseous fuels. Enzyme. Microb. Technol. 14, 602-608.

Klasson, K.T., Ackerson, M.D., Clausen, E.C., Gaddy, J.L., 1993. Biological conversion of coal and coal-derived synthesis gas. Fuel 72, 1673-1678.

Kleerebezem, R., van Loosdrecht, M., 2007. Mixed culture biotechnology for bioenergy production. Curr. Opin. Biotechnol. 18, 207-212.

Köpke, M., Held, C., Hujer, S., Liesegang, H., Wiezer, A., Wollherr, A., Ehrenreich, A., Liebl, W., Gottschalk, G., Dürre, P., 2010. *Clostridium ljungdahlii* represents a microbial production platform based on syngas. Proc. Natl. Acad. Sci. 107, 13087-13092.

Köpke, M., Mihalcea, C., Bromley, J.C., Simpson, S.D., 2011a. Fermentative production of ethanol from carbon monoxide. Curr. Opin. Biotechnol. 22, 320-325.

Köpke, M., Mihalcea, C., Liew, F., Tizard, J.H., Ali, M.S., Conolly, J.J., Al-Sinawi, B., Simpson, S.D., 2011b. 2,3-Butanediol production by acetogenic bacteria, an alternative route to chemical synthesis, using industrial waste gas. Appl. Environ. Microbiol. 77, 5467-5475.

Kundiyana, D.K., Huhnke, R.L., Maddipati, P., Atiyeh, H.K., Wilkins, M.R., 2010. Feasibility of incorporating cotton seed extract in *Clostridium* strain P11 fermentation medium during synthesis gas fermentation. Bioresour. Technol. 101, 9673-9680.

Kundiyana, D.K., Huhnke, R.L., Wilkins, M.R., 2011a. Effect of nutrient limitation and two-stage continuous fermentor design on productivities during "*Clostridium ragsdalei*" syngas fermentation. Bioresour. Technol. 102, 6058-6064.

Kundiyana, D.K., Wilkins, M.R., Maddipati, P., Huhnke, R.L., 2011b. Effect of temperature, pH and buffer presence on ethanol production from synthesis gas by "*Clostridium ragsdalei*". Bioresour. Biotechnol. 102, 5794-5799.

Lewis, R.S., Tanner, R.S., Huhnke, R.L. 2007. Indirect or direct fermentation of biomass to fuel alcohol. US 2007/0275447.

Liew, F.M., Köpke, M., Simpson, S.a.D., 2013. Gas fermentation for commercial biofuels production. in: Fang, Z. (Eds.), Liquid, gaseous and solid biofuels. InTech, pp. 125-173.

Linger, J.G., Darzins, A., 2013. Consolidated bioprocessing. in: Lee, J.W. (Eds.), Advanced biofuels and bioproducts. Springer New York, pp. 267-280.

Liou, J.S.C., Balkwill, D.L., Drake, G.R., Tanner, R.S., 2005. *Clostridium carboxidivorans* sp. nov., a solvent-producing *clostridium* isolated from an agricultural settling lagoon, and reclassification of the acetogen *Clostridium scatologenes* strain SL1 as *Clostridium drakei* sp. nov. Int. J. Syst. Evol. Microbiol. 55, 2085-2091.

Liu, K., Atiyeh, H.K., Tanner, R.S., Wilkins, M.R., Huhnke, R.L., 2012. Fermentative production of ethanol from syngas using novel moderately alkaliphilic strains of *Alkalibaculum bacchi*. Bioresour. Technol. 104, 336-341.

Ljungdahl, L.G., 1986. The autotrophic pathway of acetate synthesis in acetogenic bacteria. Annu. Rev. Microbiol. 40, 415-450.

Lynd, L.R., Zyl, W.H., McBride, J.E., Laser, M., 2005. Consolidated bioprocessing of cellulosic biomass: an update. Curr. Opin. Biotechnol. 16, 577.

Maddipati, P., Atiyeh, H.K., Bellmer, D.D., Huhnke, R.L., 2011. Ethanol production from syngas by *Clostridium* strain P11 using corn steep liquor as a nutrient replacement to yeast extract. Bioresour. Technol. 102, 6494-6501.

McCabe, W.L., Smith, J.C., 2005. Unit operations of chemcial engineering. 7th ed. Mcgraw-Hill Inc., New York, pp.1007.

Menon, S., Ragsdale, S.W., 1999. The Role of an Iron-Sulfur cluster in an enzymatic methylation reaction. J. Biol. Chem. 274, 11513-11518.

Mohammadi, M., Najafpour, G.D., Younesi, H., Lahijani, P., Uzir, M.H., Mohamed, A.R., 2011. Bioconversion of synthesis gas to second generation biofuels: A review. Renew. Sustain. Energy Rev. 15, 4255-4273.

Mohammadi, M., Younesi, H., Najafpour, G., Mohamed, A.R., 2012. Sustainable ethanol fermentation from synthesis gas by *Clostridium ljungdahlii* in a continuous stirred tank bioreactor. J. Chem. Technol. Biotechnol. 87, 837-843.

Mohan, D., Pittman, C.U., Steele, P.H., 2006. Pyrolysis of wood/biomass for bio-oil: a critical review. Energ. Fuels 20, 848-889.

Mosier, N., Wyman, C., Dale, B., Elander, R., Lee, Y., Holtzapple, M., Ladisch, M., 2005. Features of promising technologies for pretreatment of lignocellulosic biomass. Bioresour. Technol. 96, 673-686.

Müller, V., Imkamp, F., Biegel, E., Schmidt, S., Dilling, S., 2008. Discovery of a Ferredoxin: NAD^+-Oxidoreductase (Rnf) in *Acetobacterium woodii*. Ann. N. Y. Acad. Sci. 1125, 137-146.

Munasinghe, P.C., Khanal, S.K., 2010. Biomass-derived syngas fermentation into biofuels: Opportunities and challenges. Bioresour. Biotechnol. 101, 5013-5022.

Öhgren, K., Bura, R., Lesnicki, G., Saddler, J., Zacchi, G., 2007. A comparison between simultaneous saccharification and fermentation and separate hydrolysis and fermentation using steam-pretreated corn stover. Process Biochem. 42, 834-839.

Olofsson, K., Bertilsson, M., Lidén, G., 2008. A short review on SSF-an interesting process option for ethanol production from lignocellulosic feedstocks. Biotechnol. Biofuels 1, 1-14.

Orgill, J.J., Atiyeh, H.K., Devarapalli, M., Phillips, J.R., Lewis, R.S., Huhnke, R.L., 2013. A comparison of mass transfer coefficients between trickle-bed, hollow fiber membrane and stirred tank reactors. Bioresour. Technol. 133, 340-346.

Osman, Y.A., Ingram, L., 1985. Mechanism of ethanol inhibition of fermentation in *Zymomonas mobilis* CP4. J. Bacteriol. 164, 173-180.

Painuly, J.P., 2001. Barriers to renewable energy penetration; a framework for analysis. Renew. Energ. 24, 73-89.

Panneerselvam, A., Wilkins, M.R., DeLorme, M.J.M., Atiyeh, H.K., Huhnke, R.L., 2010. Effects of reducing agents on syngas fermentation by "*Clostridium ragsdalei* ". Biol. Eng. 2, 135-144.

Phillips, J., Clausen, E., Gaddy, J., 1994. Synthesis gas as substrate for the biological production of fuels and chemicals. Appl. Biochem. Biotechnol. 45-46, 145-157.

Phillips, J., Klasson, K., Clausen, E., Gaddy, J., 1993. Biological production of ethanol from coal synthesis gas. Appl. Biochem. Biotechnol. 39, 559-571.

Pitryuk, A.V., Pusheva, M.A., 2001. Different ionic specificities of ATP synthesis in extremely alkaliphilic sulfate-reducing and acetogenic bacteria. Microbiology 70, 398-402.

Rajagopalan, S., P. Datar, R., Lewis, R.S., 2002. Formation of ethanol from carbon monoxide via a new microbial catalyst. Biomass Bioenerg. 23, 487-493.

Ramachandriya, K.D., Wilkins, M.R., Delorme, M.J.M., Zhu, X., Kundiyana, D.K., Atiyeh, H.K., Huhnke, R.L., 2011. Reduction of acetone to isopropanol using producer gas fermenting microbes. Biotechnol. Bioeng. 108, 2330-2338.

Reeves, A. 2010. Recombinant microorganisms having modified production of alcohols and acids. US patent 2010/0151543.

REN21. 2013. Renewables 2012 global status report. Paris: REN21 Secretariat.

Rogers, P., Chen, J.S., Zidwick, M.J., 2013. Organic acid and solvent production: Acetic, lactic, gluconic, succinic, and polyhydroxyalkanoic acids. in: Rosenberg, E., DeLong, E.F., Lory, S., Stackebrandt, E., Thompson, F. (Eds.), The Prokaryotes. Springer, pp. 4-75.

Sakai, S., Nakashimada, Y., Yoshimoto, H., Watanabe, S., Okada, H., Nishio, N., 2004. Ethanol production from H_2 and CO_2 by a newly isolated thermophilic bacterium, *Moorella* sp. HUC22-1. Biotechnol. lett. 26, 1607-1612.

Saxena, J., Tanner, R., 2010. Effect of trace metals on ethanol production from synthesis gas by the ethanologenic acetogen, *Clostridium ragsdalei*. J. Ind. Microbiol. Biotechnol. 38, 513-521.

Saxena, J., Tanner, R., 2012. Optimization of a corn steep medium for production of ethanol from synthesis gas fermentation by *Clostridium ragsdalei*. World J. Microbiol. Biotechnol. 28, 1553-1561.

Schmehl, M., Jahn, A., Meyer zu Vilsendorf, A., Hennecke, S., Masepohl, B., Schuppler, M., Marxer, M., Oelze, J., Klipp, W., 1993. Identification of a new class of nitrogen fixation genes in *Rhodobacter capsalatus*: a putative membrane complex involved in electron transport to nitrogenase. Mol. Gen. Genet. 241, 602-615.

Scopes, R., 1983. An iron-activated alcohol dehydrogenase. FEBS Lett. 156, 303-306.

Shah, Y.T., Kelkar, B.G., Godbole, S.P., Deckwer, W.D., 1982. Design parameters estimations for bubble column reactors. AIChE J. 28, 353-379.

Shen, G.J., Shieh, J.S., Grethlein, A.J., Jain, M.K., Zeikus, J.G., 1999. Biochemical basis for carbon monoxide tolerance and butanol production by *Butyribacterium methylotrophicum*. Appl. Microbiol. Biotechnol. 51, 827-832.

Shuler, M.L., Fikret, K., 2002. Bioprocess Engineering: Basic concepts. Second ed. Prentice Hall, Englewood Cliffs, New Jersey, pp.576.

Sipma, J., Meulepas, R., Parshina, S., Stams, A., Lettinga, G., Lens, P., 2004. Effect of carbon monoxide, hydrogen and sulfate on thermophilic (55 C) hydrogenogenic carbon monoxide conversion in two anaerobic bioreactor sludges. Appl. Microbiol. Biotechnol. 64, 421-428.

Skidmore, B.E. 2010. Syngas Fermentation: Quantification of assay techniques, reaction kinetics, and pressure dependencies of the *Clostridial* P11 hydrogenase. M.S. Thesis. Brigham Young University, pp. 54.

Subramani, V., Gangwal, S.K., 2008. A review of recent literature to search for an efficient catalytic process for the conversion of syngas to ethanol. Energ. Fuels 22, 814-839.

Talebnia, F., Karakashev, D., Angelidaki, I., 2010. Production of bioethanol from wheat straw: an overview on pretreatment, hydrolysis and fermentation. Bioresour.Technol. 101, 4744-4753.

Terrill, J.B., Wilkins, M.R., DeLorme, M.J., Atiyeh, H.K., Lewis, R.S., 2012. Effect of energetic gas composition on hydrogenase activity and ethanol productin in syngas fermetnation by *clostridium ragsdalei*. Biol. Eng. Trans. 5, 87-98.

Tijmensen, M.J.A., Faaij, A.P.C., Hamelinck, C.N., van Hardeveld, M.R.M., 2002. Exploration of the possibilities for production of Fischer Tropsch liquids and power via biomass gasification. Biomass Bioenerg. 23, 129-152.

Tirado-Acevedo, O., Chinn, M.S., Grunden, A.M., 2010. Production of biofuels from synthesis gas using microbial catalysts. Adv. Appl. Microbiol. 70, 57-92.

Tracy, B.P., Jones, S.W., Fast, A.G., Indurthi, D.C., Papoutsakis, E.T., 2011. *Clostridia*: the importance of their exceptional substrate and metabolite diversity for biofuel and biorefinery applications. Curr. Opin. Biotechnol. 23, 364-381.

Tsai, S.p., Datta, R., Basu, R., Yoon, S.H. 2009 horizontal array bioreactor for conversion of syngas compoents to liquid products. US patent US2009/0215142.

Tsai, S.p., Datta, R., Basu, R., Yoon, S.H. 2009. Syngas conversion system using asymmetric membrane and anaerobic microorganism. US patent US2009/0215163 A1.

Turn, S., Kinoshita, C., Zhang, Z., Ishimura, D., Zhou, J., 1998. An experimental investigation of hydrogen production from biomass gasification. Int. J. Hydrogen Energy 23, 641-648.

Ukpong, M.N., Atiyeh, H.K., De Lorme, M.J.M., Liu, K., Zhu, X., Tanner, R.S., Wilkins, M.R., Stevenson, B.S., 2012. Physiological response of *Clostridium carboxidivorans* during conversion of synthesis gas to solvents in a gas-fed bioreactor. Biotechnol. Bioeng. 109, 2720-2728.

Van der Drift, A., Van Doorn, J., Vermeulen, J., 2001. Ten residual biomass fuels for circulating fluidized-bed gasification. Biomass Bioenerg. 20, 45-56.

Van Steen, E., Claeys, M., 2008. Fischer-Tropsch catalysts for the biomass to liquid (BTL) process. Chem. Eng. Technol. 31, 655-666.

Vega, J., Clausen, E., Gaddy, J., 1990. Design of bioreactors for coal synthesis gas fermentations. Resour. Conserv. Recyc. 3, 149-160.

Wilkins, M.R., Atiyeh, H.K., 2012. Fermentation. in: Dunford, N.T. (Eds.), Food and Industrial Bioproducts and Processing. Wiley-Blackwell, pp. 185-204.

Wilkins, M.R., Atiyeh, H.K., 2011. Microbial production of ethanol from carbon monoxide. Curr. Opin. Biotechnol. 22, 326-330.

Wood, H.G., Ragsdale, S.W., Pezacka, E., 1986. The acetyl-CoA pathway of autotrophic growth. FEMS Microbiol. Lett. 39, 345-362.

Worden, R.M., Grethlein, A.J., Jain, M.K., Datta, R., 1991. Production of butanol and ethanol from synthesis gas via fermentation. Fuel 70, 615-619.

Xu, D., Tree, D.R., Lewis, R.S., 2011. The effects of syngas impurities on syngas fermentation to liquid fuels. Biomass Bioenerg. 35, 2690-2696.

Younesi, H., Najafpour, G., Mohamed, A.R., 2005. Ethanol and acetate production from synthesis gas via fermentation processes using anaerobic bacterium, *Clostridium ljungdahlii*. Biochem. Eng. J. 27, 110-119.

Zahn, J.A., Saxena, J. 2011. Novel ethanologenic clostridium species, *Clostridium coskatii*. US patent 2011/0229947.

Zidwick, M.J., Chen, J.S., Rogers, P., 2013. Organic acid and solvent production: Propionic and butyric acids and ethanol. in: Rosenberg, E., DeLong, E.F., Lory, S., Stackebrandt, E., Thompson, F. (Eds.), The Prokaryotes. Springer, pp. 135-167.

CHAPTER III

OBJECTIVES

Alkalibaculum bacchi strains CP11^T, CP13 and CP15 were recently isolated and found to be able to convert syngas components CO and H_2 into ethanol and acetic acid. The fermentation kinetics for these novel microorganisms has not been studied. Thus, the objectives of this study include:

1. Study fermentation characteristics of *A. bacchi* strains CP11^T, CP13 and CP15 and determine the best candidate for ethanol production. Syngas I and Syngas II simulating switchgrass derived syngas and coal derived syngas, respectively, were used. The composition of Syngas I and Syngas II are shown in Table 3.1.
2. Examine the effect of working volume, agitation, flow rate, headspace pressure and backmixing on mass transfer characteristics of a 7-L fermentor using an air-water system to guide the production of ethanol during syngas fermentation.
3. Investigate low cost syngas fermentation media for ethanol production using Syngas I.

4. Examine the effects of different H_2:CO ratios, agitation, dilution rate and medium type on product concentration, productivity and yield and gas uptake and conversion efficiency during continuous syngas fermentation in a 7-L fermentor. Syngas III, Syngas IV and Syngas V with various gas compositions and H_2:CO ratios were used (Table 3.1).
5. Study mixed culture syngas fermentation for production of higher alcohols in bottle fermentors using Syngas II and in a 3-L fermentor using Syngas VI. Syngas VI was similar to Syngas II, which simulates coal derived syngas. However, Syngas VI contained 5% N_2 as an internal standard to help in the estimation of CO and H_2 consumption in the 3-L fermentor.

Table 3.1 Molar compositions of various syngas mixtures used in this study.

Syngas Type	**%H_2**	**%CO**	**%CO_2**	**%N_2**	**H_2:CO**
Syngas I	5.0	20.0	15.0	60.0	0.25
Syngas II	30.0	40.0	30.0	0.0	0.75
Syngas III	27.0	39.0	24.0	10.0	0.70
Syngas IV	43.0	20.0	25.0	12.0	2.00
Syngas V	60.0	28.0	12.0	0.0	2.00
Syngas VI	28.5	38.0	28.5	5.0	0.75

CHAPTER IV

FERMENTATIVE PRODUCTION OF ETHANOL FROM SYNGAS USING NOVEL MODERATELY ALKALIPHILIC STRAINS OF *ALKALIBACULUM BACCHI*

This chapter has been published in Bioresource Technology and appears in this dissertation with the journal's permission.

Liu, K., Atiyeh, H.K., Tanner, R.S., Wilkins, M.R., Huhnke, R.L. 2012. Fermentative production of ethanol from syngas using novel moderately alkaliphilic strains of *Alkalibaculum bacchi*. Bioresource Technology, 104, 336-341.

ABSTRACT

Ethanol production from syngas using three moderately alkaliphilic strains of a novel genus and species *Alkalibaculum bacchi* CP11^T, CP13 and CP15 was investigated in 250 ml bottle fermentations containing 100 ml of yeast extract medium at 37 °C and pH 8.0. Two commercial syngas mixtures (Syngas I: 20% CO, 15% CO_2, 5% H_2, 60% N_2) and (Syngas II: 40% CO, 30% CO_2, 30% H_2) were used. Syngas I and Syngas II represent gasified biomass and coal, respectively. The maximum ethanol concentration (1.7 g l^{-1}) and yield from CO (76%) were obtained with strain CP15 and Syngas II after 360 h. CP15 produced over twofold more ethanol with Syngas I compared to strains CP11^T and CP13. In addition, CP15 produced 18% and 71% more ethanol using Syngas II compared to strains CP11^T and CP13, respectively. These results show that CP15 is the most promising for ethanol production because of its higher growth and ethanol production rates and yield compared to CP11^T and CP13.

***Keywords*:** Moderately alkaliphilic bacterium; *Alkalibaculum bacchi*; syngas fermentation; ethanol; acetic acid.

4.1 Introduction

Ethanol production from lignocellulosic biomass feedstocks using gasification-fermentation is a relatively new technology. This technology combines gasifying nearly all of the components in biomass into synthesis gas, also called syngas, which primarily contains CO, H_2 and CO_2. This is followed by fermentation of syngas into ethanol and other products using acetogenic organisms. Compared to the Fischer-Tropsch process, which incorporates chemical catalysts to convert syngas to fuels, syngas fermentation has

the advantage of high specificity to substrate, operation at low temperature and pressure, and high tolerance of toxic gases (Henstra et al., 2007; Munasinghe and Khanal, 2010). In order not to cause irreversible poisoning of expensive catalyst used in Fischer-Tropsch process, the syngas should contain no ash and less than 10 ppb of either H_2S, carbonyl sulfide (COS) or HCl (Tijmensen et al., 2002). The tolerance of syngas fermentation to higher levels of toxic gases reduces the cost associated with gas cleaning required for Fischer-Tropsch process (Tijmensen et al., 2002).

Clostridium ljungdahlii (Klasson et al., 1993; Phillips et al., 1994), *Clostridium carboxidivorans* P7 (Ahmed et al., 2006) and "*Clostridium ragsdalei*", also called *Clostridium* strain P11 (Babu et al., 2010; Kundiyana et al., 2010; Panneerselvam et al., 2010; Saxena and Tanner, 2010; Maddipati et al., 2011), were reported to produce ethanol and acetic acid from syngas. These microorganisms utilize the reductive acetyl-CoA pathway for growth and production of acetic acid and ethanol from CO, H_2 and CO_2 (Wood et al., 1986; Phillips et al., 1994; Köpke et al., 2010) at pH range from 4.0 to 7.0. The overall stoichiometry for acetic acid and ethanol synthesis from CO, H_2 and CO_2 are (Vega et al., 1989):

$$4CO + 2H_2O \rightarrow CH_3COOH + 2CO_2 \quad (1)$$

$$4H_2 + 2CO_2 \rightarrow CH_3COOH + 2H_2O \quad (2)$$

$$6CO + 3H_2O \rightarrow C_2H_5OH + 4CO_2 \quad (3)$$

$$6H_2 + 2CO_2 \rightarrow C_2H_5OH + 3H_2O \quad (4)$$

One of the important factors in fermentor design is the material of construction,

which strongly affects the cost of the fermentor (Zhang, 2009). It is well-known that fermentations at low pH of 3 to 5 require bioreactors with costly construction materials such as stainless steel to reduce corrosion effects. Stainless steel is selected for industrial fermentors due to its high resistance to oxidation and corrosion, suitability for cleaning and sterilization, and much better durability than steel or lined vessels (Zhang, 2009). Fermentations close to neutral pH values reduce the risk of corrosion, increase the lifetime of the bioreactor and lower capital and maintenance costs (Shuler and Fikret, 2002). Several microorganisms were reported to utilize gas components such as CO, CO_2 and H_2 for growth at pH above 7. *Acetoanaerobium noterae* grew at an optimal pH between 7.6 and 7.8 and produced acetate using 80% H_2 and 20% CO_2 gas mixture (Sleat et al., 1985). *Clostridium aceticum* grew at pH 8.5 and produced acetate using 4% H_2, 78% CO and 18% Ar gas mixture (Sim et al., 2007). No ethanol production was reported with the previous two microorganisms. However, *Butyribacterium methylotrophicum* grew at initial pH 7.3 on pure CO or mixtures of CO:CO_2 or CO:CO_2:H_2 to produce 0.1 g l^{-1} ethanol in addition to acetate and butyrate (Shen et al., 1999). *Eubacterium limosum* KIST612 produced less than 0.1 g l^{-1} ethanol at pH 6.8 with continuous feeding of CO and cell recycle (Chang et al., 2001).

Recently, three strains of a novel genus and species *Alkalibaculum bacchi*, $CP11^T$, CP13 and CP15, were reported to grow at pH between 6.5 and 10.5 with optimal growth between pH 8.0 and 8.5, and to produce ethanol and acetate from H_2:CO_2 and CO:CO_2 mixtures (Allen et al., 2010). However, growth characteristics and fermentation kinetics of these strains were not investigated. To the best of our knowledge, no reports have been cited previously on other strains that can grow and convert syngas into ethanol at initial

pH above 7.5. The main objective of this study was to determine growth and product kinetics of *A. bacchi* strains CP11^T, CP13 and CP15 using syngas mixtures similar to producer gas generated from gasifying biomass and coal-derived syngas.

4.2 Materials and methods

4.2.1 Microorganisms and fermentation medium

Alkalibaculum bacchi strains CP11^T (=ATCC BAA-1772^T = DSM 22112^T), CP13 and CP15 are rod-shaped, gram-negative strains that were isolated from livestock-impacted soil. These strains were maintained on standard yeast extract medium and grew under strict anoxic conditions at 37 ℃ and pH between 8.0 and 8.5.

The fermentation medium used contained (per liter) 10 ml mineral solution (Tanner, 2007), 10 ml vitamin solution (Tanner, 2007), 10 ml trace metal solution (Tanner, 2007), 20 g N-[Tris(hydroxymethyl)methyl]-3-aminopropanesulfonic acid (TAPS), 1.0 g yeast extract (Difco Laboratories, Detroit, MI, USA), 5.0 g sodium bicarbonate, and 1.0 ml resazurin (1%) as a redox indicator. TAPS and sodium bicarbonate were used as buffers. The medium was reduced by the addition of 2.5 ml of 4% cysteine-sulfide. Except those mentioned above, all chemicals were purchased from Sigma Aldrich (St. Louis, MO, USA). The initial pH of the medium was adjusted to 8.0 using 2N KOH.

4.2.2 Syngas composition

Two commercial syngas mixtures obtained from Stillwater Steel and Supply Company (Stillwater, OK, USA) were used in this study. The first syngas (Syngas I) contained 20% CO, 15% CO_2, 5% H_2 and 60% N_2 by volume, which is similar to

producer gas generated from the Oklahoma State University gasification facility using switchgrass (Ahmed et al., 2006). The second syngas (Syngas II) contained 40% CO, 30% CO_2, and 30% H_2 by volume, which is similar to coal-derived syngas (Klasson et al., 1993).

4.2.3 Fermentation runs

Fed-batch fermentations were done in 250 ml serum bottles (Wheaton, NJ, USA) each containing 100 ml of medium. Inoculum of strains $CP11^T$, CP13 and CP15 were prepared by sub-culturing twice in order to reduce lag phase when cells were transferred to the fermentation serum bottles. In each sub-culture, 10% (v/v) of inoculum was transferred to fresh media when the optical density of the original culture was between 0.4 and 0.8. Syngas, as described above, was fed every 24 h to all bottles at 239 kPa and incubated at 37 ℃ on an orbital shaker (Innova 2100, New Brunswick Scientific, Edison, NJ, USA) with constant agitation of 150 rpm. The syngas was exchanged by flushing the headspace for 3 min with fresh syngas and then the bottlers were pressurized to 239 kPa. The syngas was exchanged with fresh syngas at 239 kPa every 24 h. Liquid samples (2 ml) were withdrawn every 24 h from the fermentation bottles under aseptic conditions to measure OD, pH and acetic acid and ethanol concentrations. Gas samples were withdrawn from the head space every 24 h to determine changes in gas composition during fermentation. Fermentations were run in triplicate for 360 h.

4.2.4 Analytical procedures

4.2.4.1 Cell concentration

Cell mass concentration was determined using a UV-Vis spectrophotometer (Cary 50 Bio, Varian Inc., Palo Alto, CA, USA) at 660 nm. Samples with OD values higher than 0.4 were diluted so that the OD was within the linear range of the calibration curves (cell mass for $CP11^T$, g l^{-1} = 0.369 × OD - 0.0073; cell mass for CP13, g l^{-1} = 0.367 × OD - 0.006; cell mass for CP15, g l^{-1} = 0.399 × OD - 0.0069). The pH was measured using a pH meter (Themo Orion, Beverly, MA, USA).

4.2.4.2 Solvent analysis

Liquid samples were centrifuged at 12,000 rpm for 10 min. The supernatant was filtered through 0.45 μm nylon membrane filters (VWR International, West Chester, PA, USA). Ethanol and acetic acid concentrations were analyzed using gas chromatography (GC) (Agilent 6890 N GC, Agilent Technologies, Wilmington, DE, USA) with a flame ionization detector (FID) and DB-FFAP capillary column (Agilent Technologies, Wilmington, DE, USA). Hydrogen was used as carrier gas at initial flow rate of 1.9 ml min^{-1} for 3 min and then the flow rate was increased to 4 ml min^{-1} with ramping rate of 0.5 ml min^{-2}. The inlet port temperature was kept at 200 ℃ with a split ratio 50:1. The initial oven temperature was set at 40 ℃ with a holding time of 1.5 min. It was then increased at a ramping rate of 40 ℃ min^{-1} to 235 ℃. The FID temperature was set at 250 ℃ with hydrogen and air flow rates of 40 ml min^{-1} and 450 ml min^{-1}, respectively.

4.2.4.3 Gas analysis

A volume of 100 µl of gas was injected in an Agilent 6890N GC (Agilent Technologies, Wilmington, DE, USA) with a thermal conductivity detector (TCD) and Carboxen 1010 PLOT capillary column (Supelco, Bellefonte, PA, USA). Argon was the carrier gas with an initial gas flow rate of 2 ml min^{-1} and holding time of 3.5 min. The flow rate was then increased to 2.5 ml min^{-1} at a ramping rate of 0.1 ml min^{-2}. The inlet port temperature was set at 200 ℃ with a split ratio 30:1. The initial oven temperature was set at 40 ℃ with a holding time of 3.5 min and it was then increased to 235 ℃ at a ramping rate of 40 ℃ min^{-1}. The TCD temperature was set at 230 ℃.

4.2.5 Statistical analysis and calculations

Analysis of variance (ANOVA) was determined using the GLM procedure of SAS Release 9.2 (Cary, NC). A Duncan's multiple range test (Duncan, 1955) at 95% confidence level was used to determine if statistical significant differences exist in pH, cell mass, ethanol and acetic acid, CO utilization, H_2 utilization and CO_2 production between the treatments with the three strains and two syngas mixtures used. The cell mass yield was calculated at maximum cell concentration and related CO consumed as follows:

$$\text{Cell mass yield} = \frac{\text{Maximum cell mass - Initial cell mass}}{\text{Moles of CO consumed}} \quad (5)$$

Ethanol yield from CO was calculated based on Eq. 3 as follows:

$$\text{Ethanol yield} = \frac{\dfrac{\text{Total moles of EtOH produced}}{\text{Total moles of CO consumed}}}{\dfrac{\text{1 mole EtOH produced}}{\text{6 moles of CO consumed}}} \times 100\% \quad (6)$$

The percentages of CO and H_2 utilization were calculated as follows:

$$\text{CO utilization, \%} = \frac{\text{Total moles of CO consumed}}{\text{Total moles of CO supplied}} \times 100\% \quad (7)$$

$$H_2 \text{ utilization, \%} = \frac{\text{Total moles of } H_2 \text{ consumed}}{\text{Total moles of } H_2 \text{ supplied}} \times 100\% \quad (8)$$

4.3 Results and discussion

4.3.1 Cell growth and pH profiles

The growth and pH profiles of *A. bacchi* strains CP11^T, CP13 and CP15 using two syngas mixtures are shown in Fig. 4.1. Cells of strains CP13 and CP15 were in the growth phase in the first 48 h with Syngas I (20% CO, 15% CO_2, 5% H_2 and 60% N_2) as shown in Fig. 4.1a. However, there was about 24 h of lag phase after which strain CP11^T started to grow until 144 h and attained a maximum cell mass concentration of 0.37 g l^{-1} with Syngas I. The cell mass concentration then decreased to 0.08 g l^{-1} at 360 h, which could be due to nutrients depletion from the medium. No stationary phase was observed with strain CP11^T. However, strains CP13 and CP15 entered a stationary phase after 96 h and 24 h, respectively. Minor changes in cell mass concentrations of CP13 were observed during the stationary phase until 360 h. More variability in cell mass concentrations was observed with strains CP11^T and CP15 than with CP13 with Syngas I.

The three strains were in the growth phase during the first 24 h with Syngas II (40% CO, 30% CO_2 and 30% H_2) as shown in Fig. 4.1a. Although strain CP15 had similar growth trends and a longer stationary phase than CP13, the maximum cell mass concentration obtained with CP15 was 0.21 g l^{-1} at 144 h. Cell mass yields were generally similar for each strain with both syngas mixtures (Table 4.1). However, the growth rates of $CP11^T$, CP13 and CP15 with Syngas II were higher than with Syngas I because Syngas II is richer with CO and H_2 required for growth and fermentation. The growth rates of CP15 with both syngas mixtures were higher compared to $CP11^T$ and CP13.

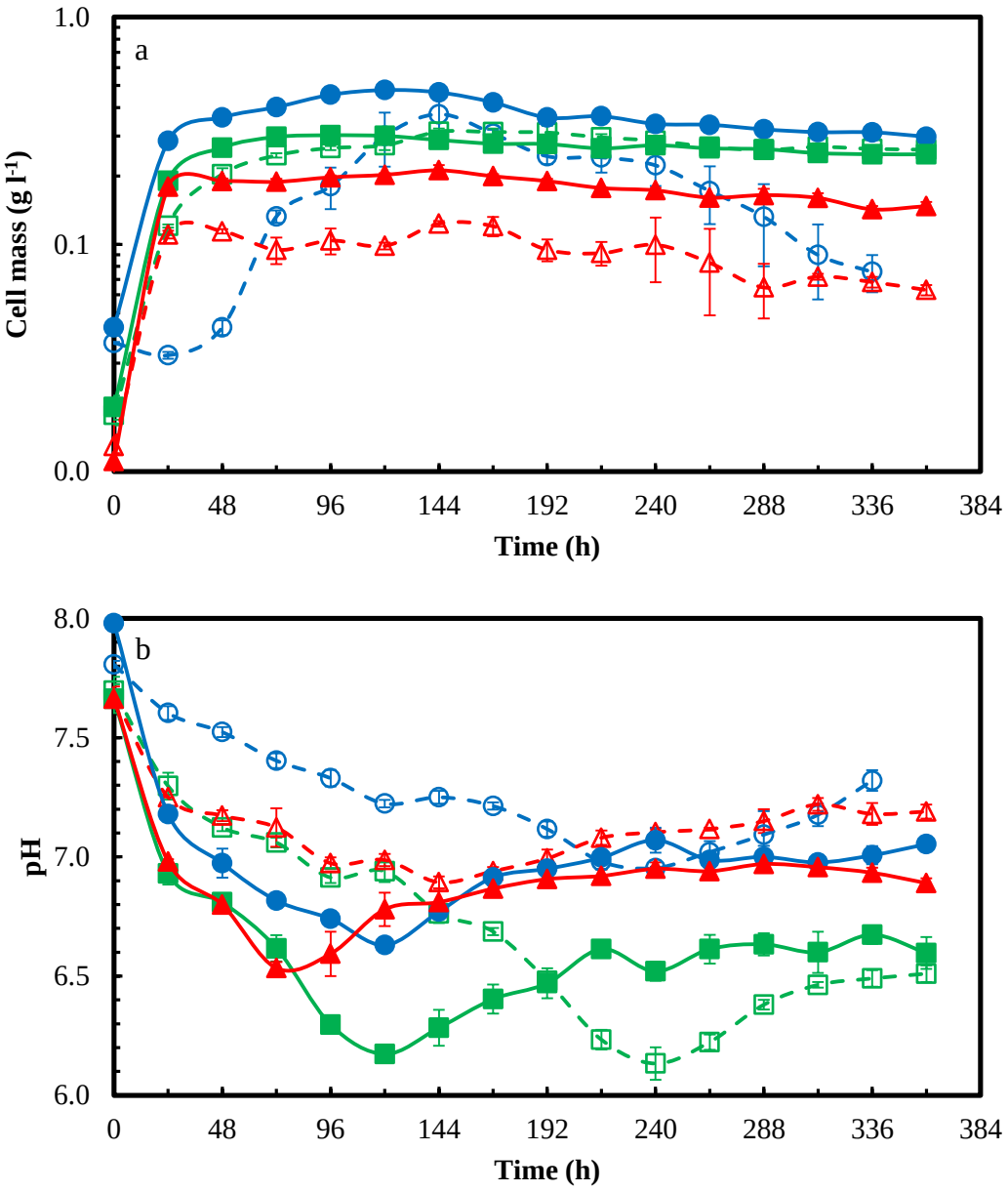

Fig. 4.1 (a) Cell mass and (b) pH profiles of *Alkalibaculum bacchi* strains (O) CP11^{T}, (□) CP13 and (Δ) CP15 using Syngas I (open symbol and dash line) and Syngas II (solid symbol and solid line). Error bars (n=3) not visible are smaller than the symbols.

Table 4.1 Fermentation parameters of *Alkalibaculum bacchi* strains CP11^T, CP13 and CP15 with various gas mixtures.

Strains	**CP11^T**	**CP13**	**CP15**	**CP11^T**	**CP13**	**CP15**
Fermentation parameters	Syngas I: $CO:CO_2:H_2:N_2$ 20:15:5:60 (%)			Syngas II: $CO:CO_2:H_2$ 40:30:30 (%)		
Growth rate, (h^{-1})	$0.03 \pm 0.00^{A,D}$	$0.05 \pm 0.00^{B,D}$	$0.09 \pm 0.01^{C,D}$	$0.08 \pm 0.00^{A,D}$	$0.10 \pm 0.01^{B,D}$	$0.12 \pm 0.00^{C,D}$
Cell mass yield from utilized CO[a], g mol^{-1}	3.15 ±1.06	1.98 ± 0.08	0.78 ± 0.03^{C}	1.89 ± 0.03^{A}	2.06 ± 0.10^{B}	0.80 ± 0.02^{C}
Ethanol yield from utilized CO[b], %	$27.66 \pm 1.25^{A,D}$	$19.64 \pm 3.08^{B,D}$	$65.09 \pm 0.79^{C,D}$	$53.04 \pm 2.92^{A,D}$	$39.30 \pm 7.37^{B,D}$	$75.71 \pm 1.47^{C,D}$
CO utilization[b], %	52.51 ± 2.15^{D}	51.35 ± 1.20^{D}	47.91 ± 3.86^{D}	28.30 ± 0.29^{D}	27.07 ± 0.22^{D}	$25.44 \pm 1.98^{C,D}$
H_2 utilization[b], %	30.64 ± 1.50^{D}	$34.17 \pm 6.77^{B,D}$	$14.07 \pm 4.81^{C,D}$	6.52 ± 0.51^{D}	7.82 ± 1.94^{D}	5.77 ± 2.78^{D}

[a] Values were calculated at maximum cell mass concentrations (Syngas I, CP11^T = 144 h, CP13 = 144 h, CP15 = 144 h; Syngas II, CP11^T = 120h, CP13 = 72h, CP15 = 144 h).

[b] Values were calculated at 360 h except for strain CP11^T with syngas I, which was calculated after 336 h.

[A] Values were significantly different for CP11^T and CP13 using the same syngas ($p < 0.05$).

[B] Values were significantly different for CP13 and CP15 using the same syngas ($p < 0.05$).

[C] Values were significantly different for CP11^T and CP15 using the same syngas ($p < 0.05$).

[D] Values were significantly different for the same strain with Syngas I and Syngas II ($p < 0.05$).

Strains CP11^{T}, CP13 and CP15 showed similar growth trends to "*C. ragsdalei"* strain P11 (Maddipati et al., 2011). However, the specific growth rate of CP15 (Table 4.1) was higher than reported for other acetogens such as "*C. ragsdalei"* strain P11 (0.06 h^{-1}) (Maddipati et al.,2011) and *C. ljungdahlii* (0.06 h^{-1}) (Phillips et al., 1994), respectively. The differences in the specific growth rates between *A. bacchi* strains and other microorganisms were related to the differences in media and gas compositions used. For example, the specific growth rate of "*C. ragsdalei"* strain P11 increased by 36% in 20 g l^{-1} corn steep liquor medium compared to 1 g l^{-1} yeast extract medium (Maddipati et al., 2011). In addition, the specific growth rate of "*C. ragsdalei"* strain P11 was improved after optimizing the concentrations of Ni^{2+}, Zn^{2+}, WO_4^{2-} and SeO_4^{2-} in the fermentation medium (Saxena and Tanner, 2010).

The initial pH values in media with the three strains and two syngas mixtures were between 7.7 and 8.0 (Fig. 4.1b). The pH decreased during growth and initial stationary phases, which was due to the production of acetic acid. The pH with strain CP13 decreased to lower levels than CP11^{T} and CP15 with both syngas mixtures due to more acetic acid production. The lowest pH was 6.1 with strain CP13 and both syngas mixtures. After the pH reached a minimum in all media, it increased due to a decrease in the concentration of acetic acid that was converted to ethanol (Fig. 4.2).

The statistical analysis indicated that the pH with strain CP13 was significantly lower than with CP11^{T} with both syngas mixtures ($p < 0.05$). There were only significant differences in the pH values with strains CP11^{T} and CP15 in the first 264 h with Syngas I and the first 120 h with Syngas II ($p < 0.05$). No significant differences were observed in pH with strains CP13 and CP15 in the first 144 h with Syngas I and the first 72 h with

Syngas II ($p > 0.05$). However, the pH with strain CP13 was significantly lower than with CP15 after 144 h with Syngas I and after 72 h with Syngas II ($p < 0.05$).

4.3.2 Products formation

A. bacchi strains CP11^T, CP13 and CP15 were able to grow at initial pH between 7.7 and 8.0 and converted modeled switchgrass-derived Syngas I and coal-derived Syngas II into acetic acid and ethanol (Fig. 4.2). Acetic acid and ethanol were produced during acetogenic and solventogenic phases, respectively. Medium pH is an important factor for switching from acetogenic phase to solventogenic phase. Strains CP11^T and CP15 switched to solventogenic phase and produced ethanol at pH 7.0 with Syngas I and at pH 6.5 with Syngas II (Figs. 4.1b and 4.2). However, ethanol production by CP13 started at pH 6.2. The differences in the pH at which the switch occurred can be correlated to the variation in growth rates with the two syngas mixtures (Table 4.1). For these moderately alkaliphilic strains, the switch occurred at pH range higher than acetogens that optimally grow at pH between 4.5 and 6.5. For example, "*C. ragsdalei"* strain P11 (Kundiyana et al., 2010; Maddipati et al., 2011), *B. methylotrophicum* (Worden et al., 1991) and *C. carboxidivorans* P7 (Ahmed et al., 2006) switched from acetogenic phase to solventogenic phase at pH 4.7, 4.5 and 5.3, respectively.

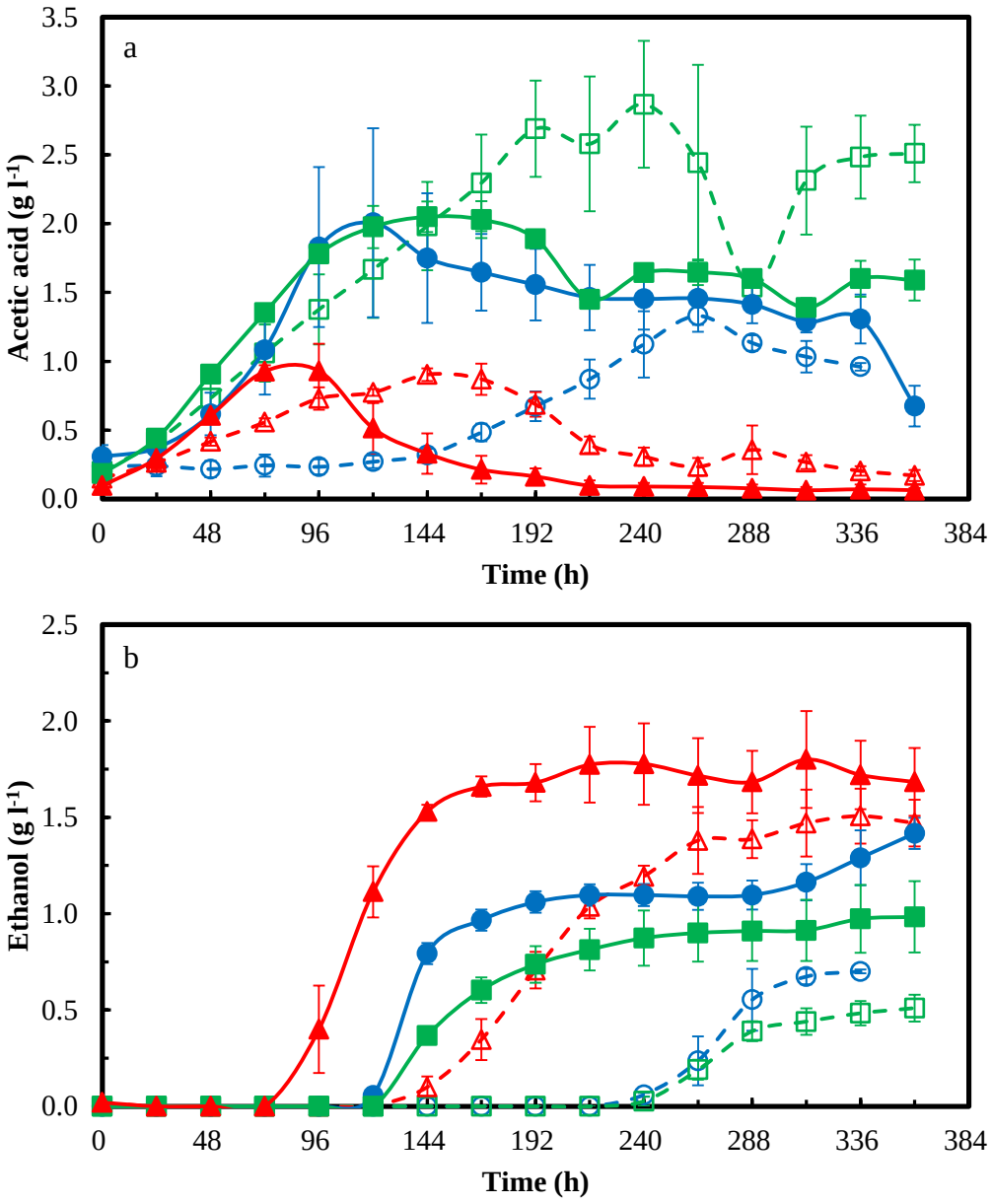

Fig. 4.2 (a) Acetic acid and (b) ethanol profiles using *Alkalibaculum bacchi* strains (O) CP11^{T}, (□) CP13 and (Δ) CP15 using Syngas I (open symbol and dash line) and Syngas II (solid symbol and solid line). Error bars (n=3) not visible are smaller than the symbols.

In the present study, strain CP13 produced the highest amount of acetic acid (2.9 g l^{-1}), of all strains using Syngas I (Fig. 4.2a). The maximum amount of acetic acid

(2.1 g l^{-1}) was produced at 144 h by CP13 using Syngas II, which was 28% lower than with Syngas I. Strain CP11^T produced 2.0 g l^{-1} acetic acid at 120 h with Syngas II, which was 51% higher than the maximum concentration obtained at 264 h with Syngas I. The difference between the maximum concentrations of acetic acid formed by strain CP15 with both syngas mixtures was insignificant ($p > 0.05$).

Strains CP11^T, CP13 and CP15 produced acetic acid mainly during cell growth and in early stationary phase (Figs. 4.1a and 4.2a). These strains partially consumed acetic acid during solventogenic phase to form ethanol (Fig. 4.2b). This was similar to "*C. ragsdalei"* strain P11 (Kundiyana et al., 2010; Maddipati et al., 2011). Unlike strains CP11^T and CP13, over 80% of the acetic acid formed by CP15 with both syngas mixtures was consumed after 360 h (Fig. 4.2a). More acetic acid conversion to ethanol by CP15 than by CP11^T and CP13 could indicate higher alcohol dehydrogenase (ADH) activity and accumulation of reduced ferredoxin required to convert acetate to acetaldehyde, which is then reduced to ethanol (Köpke et al., 2010).

In the present study, ethanol production with the three strains was non-growth associated and started when acetic acid concentrations in the fermentation media reached a maximum level (Fig. 4.2b). Ethanol production with all strains started over 48 h earlier using Syngas II than with Syngas I. Strains CP11^T, CP13 and CP15 produced 103%, 93% and 16% more ethanol, respectively, after 360 h using Syngas II compared to Syngas I. The difference in the amounts of ethanol formed by strain CP15 with the two syngas mixtures after 264 h was insignificant ($p > 0.05$). In addition, strain CP15 produced over twofold more ethanol compared to CP11^T and CP13 with Syngas I ($p < 0.05$). CP15 produced 18% ($p > 0.05$) and 71% ($p < 0.05$) more ethanol compared to CP11^T and

CP13, respectively, with Syngas II. Ethanol yields from CO with strains CP11^T, CP13 and CP15 using Syngas II were 92%, 100% and 16%, higher than with Syngas I, respectively (Table 4.1). Ethanol yields from CO obtained by strain CP15 with Syngas I and yeast extract medium were 12% higher than "*C. ragsdalei"* strain P11 (Maddipati et al., 2011). Strains CP11^T, CP13 and CP15 produced more ethanol with Syngas II compared to Syngas I, which indicates that higher CO content in Syngas II improved ethanol formation (Fig. 4.2b and Table 4.1). This was similar to a study with *C. carboxidivorans* P7 in which ethanol production was increased from trace amounts to 2 g l^{-1} with an increase in CO partial pressure from 35 kPa to 203 kPa (Hurst and Lewis, 2010).

Similar to other acetogens, the production of ethanol and acetic acid by *A. bacchi* strains CP11^T, CP13 and CP15 appears to follow the acetyl-CoA pathway (Wood et al., 1986; Ragsdale, 2004). It was suggested that *C. ljungdahlii* followed two routes to convert acetyl-CoA to ethanol (Köpke et al., 2010; Köpke et al., 2011). The first route involved the conversion of acetyl-CoA to acetate, which was then reduced to acetaldehyde with reduced ferredoxin and finally to ethanol via alcohol dehydrogenase (Köpke et al., 2010). The second route was through a direct conversion of acetyl-CoA to acetaldehyde via a bifunctional acetaldehyde/ethanol dehydrogenase, followed by reduction of acetaldehyde to ethanol (Köpke et al., 2010; Köpke et al., 2011). Although ethanol formation by strains CP11^T, CP13 and CP15 appears to follow the first route that involves the reduction of acetate to ethanol (Fig. 4.2), it could also be possible that the three strains directly convert acetyl-CoA to acetaldehyde and then reduce acetaldehyde to ethanol. Although the second route for ethanol formation does not produce ATP required

for cell growth (Köpke et al., 2010), there could be two electrochemical potentials to facilitate ATP synthesis from ATP synthase. One is based on H^+-translocating ATPase using the H^+ gradient between outside and inside cell membrane, which was reported in some alkaliphilic bacteria at extreme alkaliphilic conditions above pH 10 (Hicks et al., 2010). Another ATP source could be the sodium gradient used by Na^+-translocating ATPase, as the cells grow at a condition of proton deficiency (Pitryuk and Pusheva, 2001).

4.3.3 Gas utilization

Both CO and H_2 were utilized by the three strains for growth, acetic acid and ethanol production, while CO_2 was mainly produced during the fermentation process (Fig. 4.3). CO and H_2 serve as energy and electron sources for cell growth and product formation (Wilkins and Atiyeh, 2011). CO utilization started after inoculation by strains CP13 and CP15 using both syngas mixtures, and by $CP11^T$ with Syngas II (Fig. 4.3a). With $CP11^T$ and Syngas I, there was a lag phase of 48 h after which $CP11^T$ rapidly consumed CO. Strain $CP11^T$ utilized significantly less CO compared to CP13 and CP15 in the first 264 h and 240 h, respectively, with Syngas I ($p < 0.05$). The rate of CO utilization in the first 144 h by strains $CP11^T$, CP13 and CP15 with Syngas II were 80% higher than with Syngas I (Fig. 4.3a), which explains the higher growth rates observed with Syngas II (Table 4.1). CO utilization by the three strains substantially decreased after 288 h and 144 h with Syngas I and Syngas II, respectively (Fig. 4.3a). The differences in total amounts of CO utilized by the three strains with Syngas I after 360 h were insignificant ($p > 0.05$) as shown in Table 1. There were also insignificant differences between the total amounts of CO utilized after 360 h by strains $CP11^T$ and

CP13, and strains CP13 and CP15 with Syngas II ($p > 0.05$). The percentage of CO utilized by each strain with Syngas II was about 50% lower than with Syngas I (Table 4.1).

H_2 utilization by strain CP11^T was observed immediately with Syngas II, while H_2 utilization started after 72 h with Syngas I (Fig. 4.3b). Strains CP13 and CP15 utilized H_2 after 24 h with either Syngas I or Syngas II. H_2 utilization by the three strains was higher during acetic acid formation than during ethanol production (Fig. 4.2). When Syngas I was used, strain CP13 utilized significantly more H_2 between 24 h and 192 h and between 24 h and 360 h compared to CP11^T and CP15, respectively ($p < 0.05$). The differences between the amounts of H_2 utilized by strains CP11^T and CP13 with Syngas II after 48 h were insignificant ($p > 0.05$). However, strain CP11^T utilized significantly more H_2 with Syngas II compared to CP15 during the first 216 h ($p < 0.05$). The percentages of H_2 utilization by strains CP11^T, CP13 and CP15 with Syngas I were 31%, 34% and 14%, respectively (Table 4.1). However, the percentages of H_2 utilization with Syngas II were below 8% for all strains.

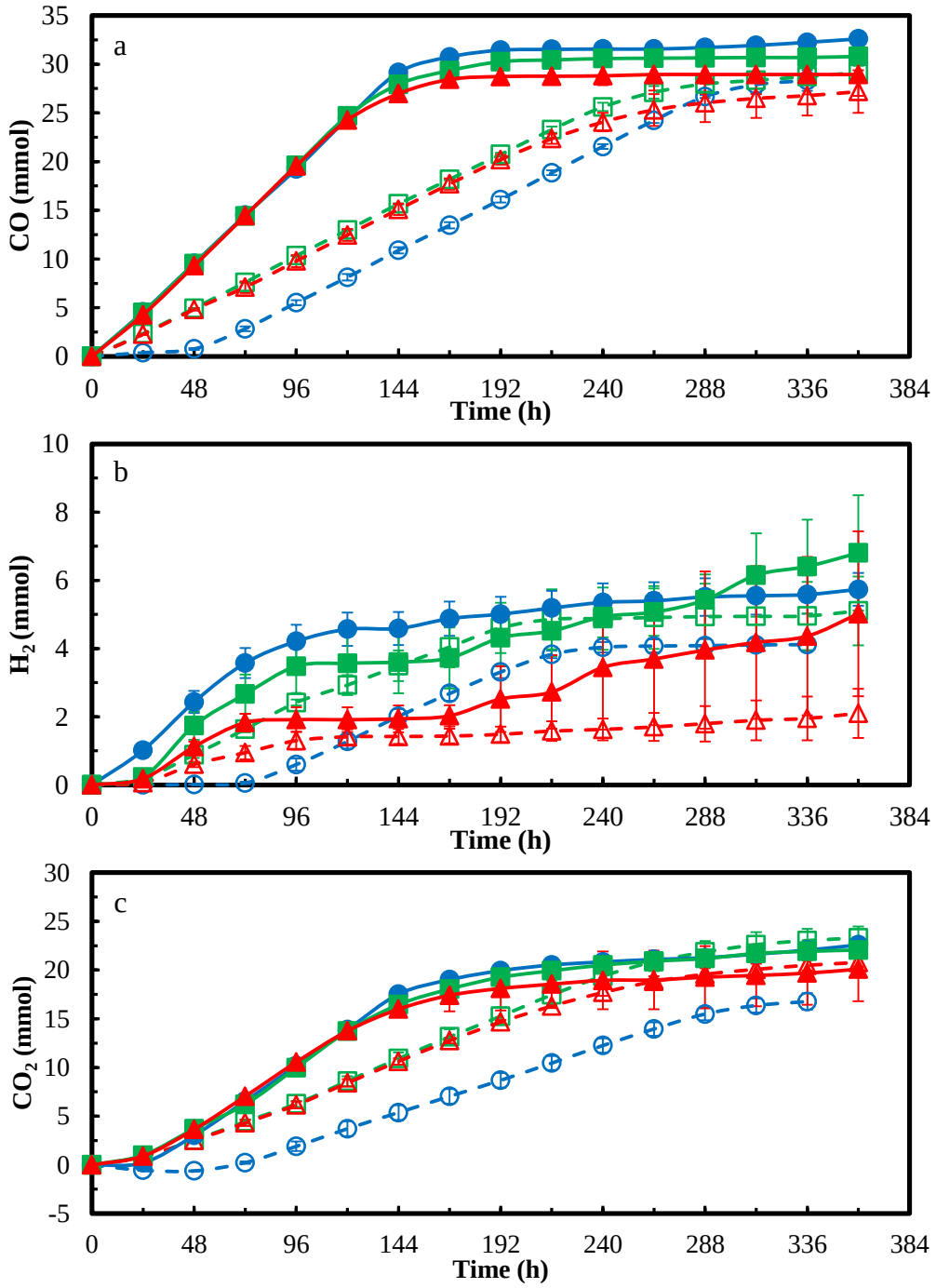

Fig. 4.3 Cumulative (a) CO and (b) H_2 utilized and (c) CO_2 produced using *Alkalibaculum bacchi* strains (O) CP11^T, (□) CP13 and (Δ) CP15 using Syngas I (open symbol and dash line) and Syngas II (solid symbol and solid line). Error bars (n=3) not visible are smaller than the symbols.

The lower H_2 utilization by the three strains with Syngas II could be due to the higher initial partial pressure of CO in Syngas II (96 kPa) compared to Syngas I (48 kPa), which inhibits hydrogenase (H_2ase) activity (Hurst, 2005). CO can reversibly or irreversibly inhibit H_2ase, depending on the type of H_2ase and microorganism (Evans and Pickett, 2003; De Lacey et al., 2007). A 97% decrease in the specific activity of H_2ase was reported with an increase in CO partial pressure from 35 kPa to 203 kPa with *C. carboxidivorans* P7 (Hurst, 2005). The H_2ase activity of "*C. ragsdalei"* strain P11 at initial partial pressures of CO and H_2 of 9 kPa and 77 kPa, respectively, was 90% lower than the original activity at initial pressures of CO and H_2 of 0 kPa and 77 kPa, respectively (Skidmore, 2010). In the present study, the initial partial pressures of H_2 with the three strains in Syngas I and Syngas II were 12 kPa and 72 kPa, respectively. These were below the level of 92 kPa that inhibits H_2ase activity (Arp and Burris, 1981) .

In the present study, strain CP15 produced the lowest cell mass concentration compared to $CP11^T$ and CP13 with both syngas mixtures (Fig. 4.1a), which also corresponded with its lowest H_2 utilization (Fig. 4.3b). This indicates that the H_2ase activity of strain CP15 was lower than for strains $CP11^T$ and CP13 during the growth stage, catalyzing less H_2 into the form of H^+. Thus, compared to $CP11^T$ and CP13, less H^+ catalyzed by CP15 may generate less proton gradient for ATP synthesis, reducing the electrochemical potentials for cell growth. However, the highest ethanol yield was obtained by strain CP15 using both syngas mixtures (Table 4.1), which indicates that ethanol yield may not be proportionally associated with cell mass concentration.

Strains $CP11^T$, CP13 and CP15 also produced CO_2 during fermentation with both syngas mixtures (Fig. 4.3c), which is similar to "*C. ragsdalei"* strain P11 (Maddipati et

al., 2011). Only slight CO_2 utilization was observed by strain CP11^T with Syngas I during the first 48 h of fermentation, which may have been due to CO_2 dissolving in the media. The CO_2 production rate in the first 144 h by the three strains using Syngas II was twofold higher than with Syngas I. Then, the rate of CO_2 production by the three strains substantially decreased. Strain CP11^T produced 27% more CO_2 using Syngas II compared to Syngas I after 336 h ($p < 0.05$). Although the total amounts of CO_2 production after 360 h by strain CP13 was significantly higher than CP11^T and CP15 with Syngas I ($p < 0.05$), there were no significant differences between the final amounts of CO_2 produced by the three strains with Syngas II ($p > 0.05$).

4.4 Conclusions

The three moderately alkaliphilic novel strains of *Alkalibaculum bacchi* CP11^T, CP13 and CP15 grew at initial pH between 7.7 and 8.0 and produced ethanol and acetic acid using Syngas I and Syngas II. However, CP15 is the most promising for ethanol production because it has higher growth and ethanol production rates and ethanol yield compared to CP11^T and CP13. Ethanol yields from CO by CP15 using Syngas I and Syngas II were 65% and 76%, respectively. It is expected that medium optimization and process development will further enhance CP15 cell growth and ethanol yield for a potential use in large-scale fermentation.

4.5 References

Ahmed, A., Cateni, B.G., Huhnke, R.L., Lewis, R.S., 2006. Effects of biomass-generated producer gas constituents on cell growth, product distribution and hydrogenase activity of *Clostridium carboxidivorans* P7^T. Biomass Bioenerg. 30, 665-672.

Allen, T.D., Caldwell, M.E., Lawson, P.A., Huhnke, R.L., Tanner, R.S., 2010. *Alkalibaculum bacchi* gen. nov., sp. nov., a CO-oxidizing, ethanol-producing acetogen isolated from livestock-impacted soil. Int. J. Syst. Evol. Microbiol. 60, 2483-2489.

Arp, D.J., Burris, R.H., 1981. Kinetic mechanism of the hydrogen-oxidizing hydrogenase from soybean nodule bacteroids. Biochemistry 20, 2234-2240.

Babu, B.K., Atiyeh, H.K., Wilkins, M.R., Huhnke, R.L., 2010. Effect of the reducing agent dithiothreitol on ethanol and acetic acid production by *Clostridium* strain P11 using simulated biomass-based syngas. Biol. Eng. 3, 19-35.

Chang, I.S., Kim, B.H., Lovitt, R.W., Bang, J.S., 2001. Effect of CO partial pressure on cell-recycled continuous CO fermentation by *Eubacterium limosum* KIST612. Process Biochem. 37, 411-421.

De Lacey, A.L., Fernandez, V.M., Rousset, M., Cammack, R., 2007. Activation and inactivation of hydrogenase function and the catalytic cycle: spectroelectrochemical studies. Chem. Rev. 107, 4304-4330.

Duncan, D.B., 1955. Multiple range and multiple F tests. Biometrics 11, 1-42.

Evans, D.J., Pickett, C.J., 2003. Chemistry and the hydrogenases. Chem. Soc. Rev. 32, 268-275.

Henstra, A.M., Sipma, J., Rinzema, A., Stams, A.J.M., 2007. Microbiology of synthesis gas fermentation for biofuel production. Curr. Opin. Biotechnol. 18, 200-206.

Hicks, D.B., Liu, J., Fujisawa, M., Krulwich, T.A., 2010. F1F0-ATP synthases of alkaliphilic bacteria: Lessons from their adaptations. Biochim. Biophys. Acta. Bioenerg. 1797, 1362-1377.

Hurst, K.M. 2005. Effects of carbon monoxide and yeast extract on growth, hydrogenase activity, and product formation of *Clostridium carboxidivorans* P7^{T}. M.S. Thesis. Oklahoma State University, pp. 86.

Hurst, K.M., Lewis, R.S., 2010. Carbon monoxide partial pressure effects on the metabolic process of syngas fermentation. Biochem. Eng. J. 48, 159-165.

Klasson, K.T., Ackerson, M.D., Clausen, E.C., Gaddy, J.L., 1993. Biological conversion of coal and coal-derived synthesis gas. Fuel 72, 1673-1678.

Köpke, M., Held, C., Hujer, S., Liesegang, H., Wiezer, A., Wollherr, A., Ehrenreich, A., Liebl, W., Gottschalk, G., Dürre, P., 2010. *Clostridium ljungdahlii* represents a microbial production platform based on syngas. Proc. Natl. Acad. Sci. 107, 13087-13092.

Köpke, M., Mihalcea, C., Bromley, J.C., Simpson, S.D., 2011. Fermentative production of ethanol from carbon monoxide. Curr. Opin. Biotechnol. 22, 320-325.

Kundiyana, D.K., Huhnke, R.L., Maddipati, P., Atiyeh, H.K., Wilkins, M.R., 2010. Feasibility of incorporating cotton seed extract in *Clostridium* strain P11 fermentation medium during synthesis gas fermentation. Bioresour. Technol. 101, 9673-9680.

Maddipati, P., Atiyeh, H.K., Bellmer, D.D., Huhnke, R.L., 2011. Ethanol production from syngas by *Clostridium* strain P11 using corn steep liquor as a nutrient replacement to yeast extract. Bioresour. Technol. 102, 6494-6501.

Munasinghe, P.C., Khanal, S.K., 2010. Biomass-derived syngas fermentation into biofuels: Opportunities and challenges. Bioresour. Biotechnol. 101, 5013-5022.

Panneerselvam, A., Wilkins, M.R., DeLorme, M.J.M., Atiyeh, H.K., Huhnke, R.L., 2010. Effects of reducing agents on syngas fermentation by "*Clostridium ragsdalei* ". Biol. Eng. 2, 135-144.

Phillips, J., Clausen, E., Gaddy, J., 1994. Synthesis gas as substrate for the biological production of fuels and chemicals. Appl. Biochem. Biotechnol. 45-46, 145-157.

Pitryuk, A.V., Pusheva, M.A., 2001. Different ionic specificities of ATP synthesis in extremely alkaliphilic sulfate-reducing and acetogenic bacteria. Microbiology 70, 398-402.

Ragsdale, S.W., 2004. Life with Carbon Monoxide. Crit. Rev. Biochem. Mol. Biol. 39, 165-195.

Saxena, J., Tanner, R., 2010. Effect of trace metals on ethanol production from synthesis gas by the ethanologenic acetogen, *Clostridium ragsdalei*. J. Ind. Microbiol. Biotechnol. 38, 513-521.

Shen, G.J., Shieh, J.S., Grethlein, A.J., Jain, M.K., Zeikus, J.G., 1999. Biochemical basis for carbon monoxide tolerance and butanol production by *Butyribacterium methylotrophicum*. Appl. Microbiol. Biotechnol. 51, 827-832.

Shuler, M.L., Fikret, K., 2002. Bioprocess Engineering: Basic concepts. Second ed. Prentice Hall, Englewood Cliffs, New Jersey, pp.576.

Sim, J.H., Kamaruddin, A.H., Long, W.S., Najafpour, G., 2007. *Clostridium aceticum*—A potential organism in catalyzing carbon monoxide to acetic acid: Application of response surface methodology. Enzyme Microb. Technol. 40, 1234-1243.

Skidmore, B.E. 2010. Syngas Fermentation: Quantification of assay techniques, reaction kinetics, and pressure dependencies of the *Clostridial* P11 hydrogenase. M.S. Thesis. Brigham Young University, pp. 54.

Sleat, R., Mah, R.A., Robinson, R., 1985. *Acetoanaerobium noterae* gen. nov., sp. nov.: an anaerobic bacterium that forms acetate from H_2 and CO_2. Int. J. Syst. Bacteriol. 35, 10-15.

Tanner, R.S., 2007. Cultivation of bacteria and fungi. in: Hurst CJ, Crawford AL, Mills AL, Garland JL, Stetzenbach LD, Lipson DA (Eds.), Manual of Environmental Microbiology. ASM Press, Washington D. C., pp. 69-78.

Tijmensen, M.J.A., Faaij, A.P.C., Hamelinck, C.N., van Hardeveld, M.R.M., 2002. Exploration of the possibilities for production of Fischer Tropsch liquids and power via biomass gasification. Biomass Bioenerg. 23, 129-152.

Vega, J.L., Antorrena, G.M., Clausen, E.C., Gaddy, J.L., 1989. Study of gaseous substrate fermentations: Carbon monoxide conversion to acetate. 2. Continuous culture. Biotechnol. Bioeng. 34, 785-793.

Wilkins, M.R., Atiyeh, H.K., 2011. Microbial production of ethanol from carbon monoxide. Curr. Opin. Biotechnol. 22, 326-330.

Wood, H.G., Ragsdale, S.W., Pezacka, E., 1986. The acetyl-CoA pathway of autotrophic growth. FEMS Microbiol. Lett. 39, 345-362.

Worden, R.M., Grethlein, A.J., Jain, M.K., Datta, R., 1991. Production of butanol and ethanol from synthesis gas via fermentation. Fuel 70, 615-619.

Zhang, H., 2009. Batch fermentation and fermentor design. in: Ingledew, W.M. (Eds.), The alcohol textbook. Nottingham University Press, pp. 229-257.

CHAPTER V

MASS TRANSFER ANALYSIS OF A 7-L BIOFLO 415 FERMENTOR

Nomenclature

a: Interfacial area (m^2)

α, β and c: Model parameters in Equation 11

A, B, C and E: Parameters in Equations 9 and 10

C_L: Bulk DO in the liquid (mol/m^3)

C_s : Saturated dissolved oxygen (DO) concentration (mol/m^3)

D: Diameter of impeller (m)

D_i and D_j: Diffusivities of gas species i and j in water (cm^2/s)

g: Gravitational acceleration (9.81 m/s^2)

h: Distance of microsparger from the surface of liquid (m)

N: Impeller rotational speed (s^{-1})

N_A: Aeration number (dimensionless)

N_{Fr}: Froude number (dimensionless)

N_p: Power number of single Rushton impeller or marine impeller (dimensionless)

$p_{headspace}$: Pressure in the headspace (kPa)

$p_{hydraulic\ pressure}$: Water pressure above the microsparger (kPa)

p_{total}: Total fermentor headspace pressure and hydraulic pressure (kPa)

P_g : Impeller power draw under gassed condition (W)

$P_{g,lower}$: Gassed power draw of single impeller mounted directly above microsparger (W)

$P_{g,upper}$: Gassed power draw for impellers not directly installed above microsparger (W)

P_u: Ungassed power draw of single impeller (W)

Q_g: Actual gas volumetric flow rate at actual conditions of pressure and temperature (m^3/s)

R: Ideal gas law constant (8.314 L kPa/mol K)

t : Time (h)

T: Diameter of tank (m)

T_{NIST}: NIST standard temperature, 293.15 K

v_g: Superficial gas velocity (m/s)

$V_{37\,℃}$: Volumetric flow rate of air in the fermentor at 37 ℃ (mL/min)

V_L: Liquid working volume (m^3)

V_{NIST} : Standard flow rate (m^3/min) at National Institute of Science and Technology (NIST) standard condition (20 ℃, 101.3 kPa) for thermal mass flow controller (MFC)

ρ_{air}: Air density at 20 ℃ (1.204 kg/m^3)

ρ_{water} : Water density at at 37 ℃ (993.25 kg/m^3)

μ: Dynamic viscosity of water at 37 ℃ (0.696×10^{-3} Pa s)

5.1 Introduction

Gasification-synthesis gas (syngas) fermentation is a hybrid conversion process, in which biomass feedstocks are first gasified into syngas (CO, H_2 and CO_2) which is then converted to liquid fuels and chemicals using microbial catalysts (Liu et al., 2012; Wilkins and Atiyeh, 2011). One bottleneck during syngas fermentation is gas mass transfer limitation due to the low solubility of the gaseous substrates CO and H_2 (Bredwell et al., 1999). Mass transfer limitations occur when cells have the capacity to process more gas than the bioreactor can supply. The resistance of gaseous substrate diffusion at the gas-liquid interface was recognized as the limiting step in syngas fermentation (Klasson et al., 1993; Munasinghe and Khanal, 2010). Gaseous substrate mass transfer limitation results in low cell concentration and low productivity, making it less economically feasible (Vega et al., 1989). Therefore, it is necessary to characterize

the mass transfer of the bioreactor used for syngas fermentation to better understand how to overcome mass transfer limitations of the gaseous substrates CO and H_2.

The mass transfer characteristics of several types of bioreactors such as continuous stirred tank reactor (CSTR), trickle bed reactor (TBR), hollow fiber membrane reactor (HFR), bubble column, packed bubble column and airlift reactor have been reported (Bredwell et al., 1999; Munasinghe and Khanal, 2010; Orgill et al., 2013). These studies estimated the volumetric mass transfer coefficient via an air-water system, or sparging syngas into medium with and without real syngas fermentation. HFR and TBR were reported to be more promising than CSTR in terms of providing a high volumetric mass transfer coefficient (k_La/V_L). However, each reactor when considered for syngas fermentation has its own advantages and disadvantages in terms of operation and scale up (Orgill et al., 2013). The HFR and TBR provided 4 to 9 times higher k_La/V_L than the CSTR. However, the CSTR, as a conventional reactor, has been more extensively studied and applied in industrial fermentation processes than the HFR and TBR (Bredwell et al., 1999; Orgill et al., 2013). In addition, the CSTR operation is simpler than other reactors and can provide good mixing capability and high mass transfer rates, but requires high power consumption. This becomes an issue for large reactors because it makes their operation less economically feasible due to power cost. Moreover, the HFR operation can suffer from membrane fouling, and the pump for liquid recirculation requires external power input (Liew et al., 2013; Orgill et al., 2013). The TBR increases gas and liquid contact on packing bed via forming a thin liquid film; however, an external pump is required to circulate the liquid to the TBR (Orgill et al., 2013). Issues related to scale up of various bioreactors for syngas fermentation have been

addressed recently (Munasinghe and Khanal, 2010; Abubackar et al., 2011; Orgill et al., 2013).

Most mass transfer studies in syngas fermentation using CSTR investigated operating parameters such as gas flow rate and agitation speed at a fixed working volume and one pressure in the headspace (Klasson et al., 1991; Younesi et al., 2008; Orgill et al., 2013). CO and H_2 solubility and driving force for mass transfer increase with elevating headspace CO and H_2 partial pressure (Klasson et al., 1993). The incorporation of various liquid working volumes and pressures will provide a more accurate description of mass transfer characteristics of the fermentor.

Typically, mass transfer characteristics of reactors are done using the dynamic method with air-water system due to simplicity of setup that only requires a dissolved oxygen probe (Shuler and Fikret, 2002).The objectives of this study were to experimentally investigate and model the overall volumetric mass transfer coefficient, k_La/V_L, for O_2 in an air-water system at various gas flow rates, headspace pressures, agitations and working volumes in a 7-L fermentor. Moreover, the k_La/V_L for syngas components CO, H_2 and CO_2 will be estimated from k_La/V_L for O_2 based on the penetration and surface renewal theory (Kawase et al., 1992; McCabe and Smith, 2005).

5.2 Material and methods

5.2.1 Fermentor configuration and operating conditions

A 7-L Bioflo 415 fermentor (New Brunswick Scientific Co., Edison, NJ, USA) was used. The fermentor is 14.6 cm in diameter and 41.9 cm in length (Fig. 5.1). The configuration of the 7-L fermentor followed the suggestions by Bakker et al. (1994). Four

baffles, 1.3 cm in width and 34.6 cm in length, were used to avoid liquid vortices. Two working volumes were examined with 3 L and 5.6 L of water at 43% and 80% of the total fermentor volume, respectively. The number of impellers mounted on the drive shaft was based on the ratio of gassed liquid level to the fermentor diameter (Bakker et al., 1994). Thus, two six-blade Rushton impellers were chosen with the 3 L working volume (Fig. 5.1). For the 5.6 L working volume, three impellers were used consisting of two six-blade Rushton impellers and one curved three-blade marine impeller pumping downward (Fig. 5.1). The downward marine impeller was chosen to increase the air retention time in the liquid and increase mass transfer area. The distance between all impellers was equal to the impeller diameter.

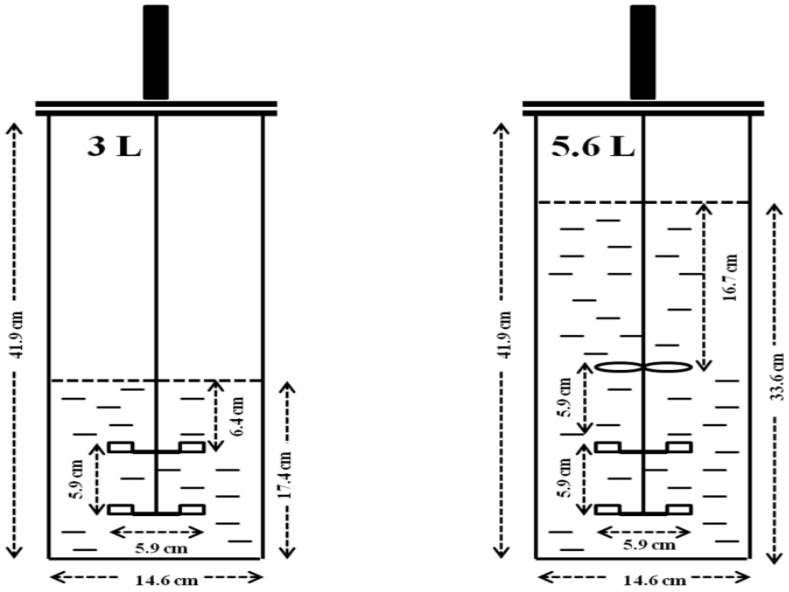

Fig. 5.1 The 7-L Bioflo 415 fermentor with the 3 L and 5.6 L working volumes and impellers configuration.

The fermentor setup used for the mass transfer study is shown in Fig. 5.2. Inlet N_2 or air (UHP/Zero grade, Stillwater steel Co., OK, USA) entered in the fermentor using a microsparger with 10-15 µm pore size (New Brunswick Scientific Co.). The inlet N_2 and air flow rates were controlled by two separate thermal mass flow controllers (MFC) (Burkert, Charlotte, NC, USA). Two 0.2 µm pore size gas filters (New Brunswick Scientific Co.) were used in the inlet and outlet gas lines. The fermentor temperature was controlled at 37 ℃ by a water heating jacket. A dissolved oxygen (DO) probe (Mettler Toledo, Columbus, OH, USA) was used to measure % DO saturation.

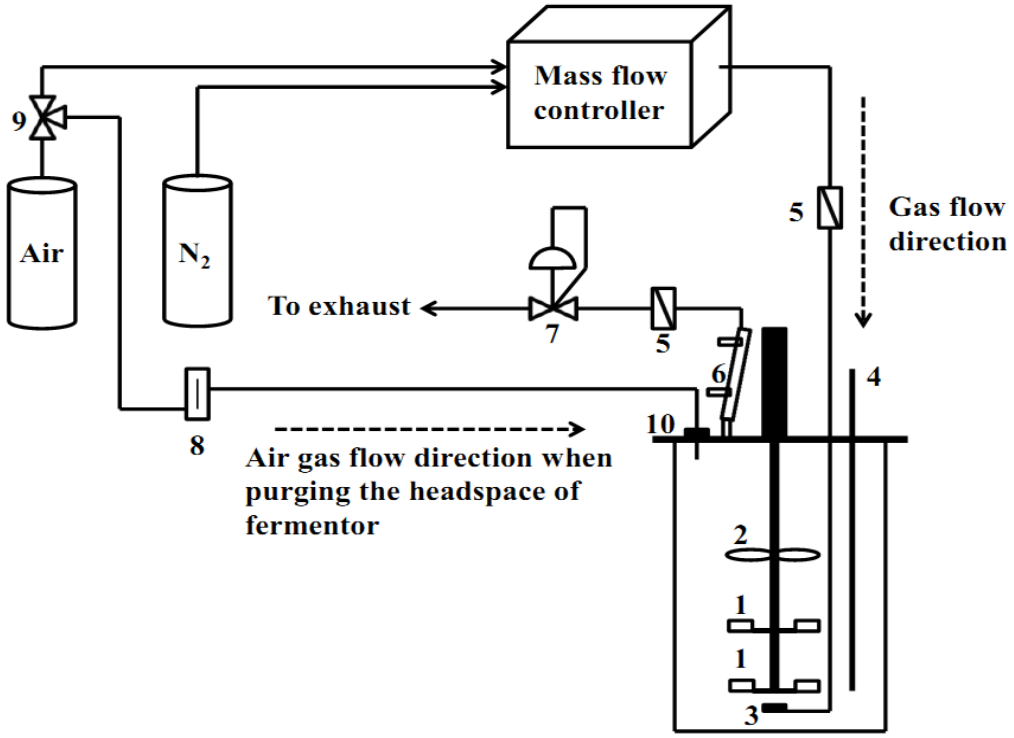

Fig. 5.2 Bioflo 415 fermentor setup used. (1) Rushton impellers, (2) marine impeller, (3) microsparger, (4) DO probe, (5) 0.2 µm gas filters, (6) condenser, (7) backpressure regulator, (8) rotameter, (9) two-way valve, and (10) headspace septum used with purging the headspace.

Before the beginning of the experiment, the fermentor was first filled with deionized (DI) water to the required working volume (3 L or 5.6 L). The temperature was set at 37 ℃ similar to syngas fermentation temperature. N_2 was then sparged into the fermentor at 1000 sccm (standard cubic centimeters, 20 ℃ and 101 kPa) to remove dissolved O_2 from the DI water with agitation speed set at 900 rpm and headspace pressure of 101 kPa (abs). The high N_2 flow rate and agitation speed were used to shorten the O_2 stripping time. The maximum pressure rating of the fermentor is 376 kPa (abs). Three headspace pressures were studied 101, 150 and 240 kPa. When % DO in the DI water was close to 0%, the headspace pressure was set at 150 or 240 kPa using a backpressure regulator in the experiments with pressurized headspace. Then, the N_2 flow rate and agitation speed were adjusted to the testing conditions. When the headspace pressure was stable at the required value, the N_2 flow was stopped and air flow was started immediately at the desired flow rate. Three standard air flow rates were tested at 90, 150, and 600 sccm. The agitation speeds examined were 150, 300, 450, 600, 750 and 900 rpm. The changes in the % DO in the DI water during aeration were recorded by the Biocommand software (New Brunswick Scientific Co.) for the estimation of k_La/V_L values. When the % DO in the water reached saturation, air flow was stopped. Experiments were performed in duplicates.

The effect of backmixing of gas from the headspace on mass transfer in the Bioflo 415 fermentor was also examined. The experiment started by first stripping out O_2 from the DI water with N_2 until the % DO was close to 0%. Then, N_2 flow and agitation were stopped. To replace the N_2 in the headspace, the headspace was flushed with air at 1000 mL/min for 2 min by inserting a needle into the fermentor headplate septum as shown in

Fig. 5.2. The pressure inside the fermentor was then set at the desired value of 101, 150 or 240 kPa using the backpressure regulator. Two agitation speeds were examined (150 and 900 rpm). Agitation was started immediately when the headspace pressure reached to the required value. During the backmixing experiment, no air was sparged in water inside the fermentor and the fermentor exhaust was completely closed by the backpressure regulator set to the hold pressure in the headspace (Fig. 5.2).

5.2.2 Calculations

5.2.2.1 Overall volumetric mass transfer coefficient

The overall volumetric mass transfer coefficient, k_La/V_L, was estimated by the following equation (Orgill et al., 2013; Shuler and Fikret, 2002):

$$\frac{k_La}{V_L} = -\frac{\ln(1-\frac{C_L}{C_S})}{t} \qquad (1)$$

where, C_s is the saturated DO concentration in the liquid (mol/m^3), C_L is the DO concentration in the bulk liquid (mol/m^3), V_L is the liquid working volume (m^3) and t is time (h). Because C_L/C_s is a ratio and the DO probe measures % DO in the liquid, C_L is replaced by % DO in the bulk liquid and C_S is replaced by saturated % DO (Orgill et al., 2013). The k_La/V_L value for O_2 was estimated from the slope of the ln (1- C_L/C_S) versus time.

5.2.2.2 Volumetric flow rate at various headspace pressures

The volumetric air flow rates at various pressures and 37 ℃ were calculated using Eq. 2 to Eq. 5 that included estimation of the pressure in the headspace and hydraulic

head of water above the microsparger (Munson et al., 2010):

$$n_{air} = \frac{\rho_{air} \cdot V_{NIST} \cdot 1000}{M_{air}} \quad (2)$$

$$p_{\text{hydraulic pressure}} = \frac{(\rho_{water} \cdot g \cdot h)}{1000} \quad (3)$$

$$p_{total} = p_{\text{headspace}} + p_{\text{hydraulic pressure}} \quad (4)$$

$$V_{37°C} = \left(\frac{n_{air} \cdot R \cdot T_{310.15K}}{P_{total}}\right) \times 1000 \quad (5)$$

where, ρ_{air} is air density at 20 ℃ (1.204 kg/m^3), M_{air} is air molecular weight 28.964 g/mol, V_{NIST} is standard flow rate (m^3/min) at National Institute of Science and Technology (NIST) standard condition (20 ℃, 101.3 kPa) obtained from the thermal mass flow controller (MFC), n_{air} is air mole flow rate from MFC (mol/min), T_{NIST}: NIST standard temperature, 293.15 K, $p_{\text{hydraulic pressure}}$ is the water pressure above the microsparger (kPa), ρ_{water} is the density of water at 37 ℃ (993.25 kg/m^3), g is gravitational acceleration (9.81 m/s^2), h is the distance between the microsparger and liquid surface (m), $p_{\text{headspace}}$ is the pressure of air in the headspace (kPa), p_{total} is the total pressure in the fermentor that include the headspace pressure and hydraulic pressure (kPa), $V_{37℃}$ is volumetric air flow rate in the fermentor at 37 ℃ (mL/min), R is the ideal gas constant (8.314 L·kPa/mol·K), $T_{310.15K}$ is the temperature at 37 ℃.

5.2.2.3 Power consumption

The impellers used were two six-blade Rushton impellers for the 3 L working volume, and one marine impeller plus two six-blade Rushton impellers for the 5.6 L

working volume. The marine impeller was estimated to have a power number at 40% of a single Rushton impeller (McCabe and Smith, 2005). The power number (N_p) of a single six-blade Rushton impeller was reported to be 5.5 by Bakker et al.(1994). Thus, the power number 2.2 was chosen for the marine impeller. The power consumption of impellers above amicrosparger was calculated using Eqs. 6 to 10 as suggested by Bakker et al.(1994):

$$N_A = \frac{Q_g}{ND^3} \tag{6}$$

$$N_{Fr} = \frac{N^2 \cdot D}{g} \tag{7}$$

$$P_u = N_p \cdot \rho_{water} \cdot N^3 \cdot D^5 \tag{8}$$

$$P_{g,lower} = P_u \cdot \left[1 - (B - A \cdot \mu) \cdot N_{Fr}^E \cdot \tanh(C \cdot N_A)\right] \tag{9}$$

$$P_{g,upper} = P_u \cdot [(1 - (A + B \cdot N_{Fr}) \cdot N_A^{C + 0.04\, N_{Fr}}] \tag{10}$$

where N_A is aeration number (dimensionless), N_{Fr} is Froude number (dimensionless), Q_g is volumetric flow rate at 37 ℃ (m^3/s), g is gravity acceleration (9.81 m/s^2), P_u is the ungassed power draw of single impeller (W), N_p is power number of single Rushton impeller or marine impeller (dimensionless), N is the impeller rotational speed (s^{-1}), D is the diameter of impeller (m), T is the tank diameter (m), $P_{g,lower}$ is gassed power draw of single impeller mounted directly above microsparger (W), μ is dynamic viscosity of water at 37 ℃ (0.696×10^{-3} Pa s), $P_{g,upper}$ is the power draw of upper impeller that are not mounted directly above a gas sparger (W), $A = 5.3 \exp[-5.4 \cdot (D/T)]$; $B = 0.47 \cdot (D/T)^{1.3}$; $C = 0.64 - 1.1 \cdot (D/T)$; $E = 0.25$.

For the second Rushton impeller and marine impellerabove the microsparger , the power drawn was calculated from Eq. 10 (Bakker et al., 1994). The total power consumption was the additive power consumption from each impeller mounted on the shaft.

5.2.2.4 Mass Transfer Model of a 7-L Bioflo 415 Fermentor

There are many studies reported in literature that described various correlations of the volumetric mass transfer coefficient, k_La/V_L, at different operating parameters. However, the most used correlation for k_La/V_L is expressed in terms of power input per unit volume and superficial gas velocity (Lee, 1992; Bakker et al., 1994; Blanch and Clark, 1997; Shuler and Fikret, 2002). The overall volumetric mass transfer coefficient typically follows the model below (Bakker et al., 1994):

$$\frac{k_La}{V_L} = c \cdot \left(\frac{P_g}{V_L}\right)^{\alpha} \cdot v_g^{\beta} \cdot 3600 \qquad (11)$$

where k_La/V_L is the overall volumetric mass transfer coefficient (h^{-1}), a is interfacial area (m^2), P_g is impeller power draw under gassed condition (W), α, β and c are model parameters, V_L is the liquid working volume (m^3), v_g is superficial gas velocity (m/s). The model parameters α, β and c in Eq. 11 were estimated based on volumetric flow rates at 37 ℃, agitation speeds, and working volumes used in this study. The least square approach and SOLVER function in EXCEL 2010 (Microsoft, Redmond, WA, USA) were used to estimate the model parameters α, β and c in Eq.11.

The k_La/V_L for H_2, CO and CO_2 were calculated from the measured k_La/V_L for O_2 using the penetration or surface renewal theory based on their diffusivities in the

fermentation broth. The k_La/V_L for gas species i can be calculated from k_La/V_L for gas species j using the following equation (Kawase et al., 1992; McCabe and Smith, 2005):

$$\frac{(k_La/V_L)_i}{(k_La/V_L)_j} = \left(\frac{D_i}{D_j}\right)^{1/2} \quad (12)$$

where D_i and D_j are the diffusivities of gas species i and j. In water, the diffusivities of CO, CO_2 and H_2 were 107 %, 90 %, and 212 %, respectively, of the O_2 diffusivity at 37 ℃ (Orgill et al., 2013). Thus, the ratios of $(k_L a/V_L)_i/(k_L a/V_L)_{O2}$ for CO, H_2 and CO_2 based on their diffusivities are given in Table 5.1.

Table 5.1 Estimated $(k_L a/V_L)_i/(k_L a/V_L)_{O2}$ for CO, CO_2 and H_2 at 37 ℃ in water.

Species	**O_2 (h^{-1})**	**CO (h^{-1})**	**H_2 (h^{-1})**	**CO_2 (h^{-1})**
$(k_L a/V_L)_i/(k_L a/V_L)_{O2}$	1	1.03	1.46	0.95

5.2.2.5 Statistical analysis

TTEST procedure was performed using SAS Release 9.3 (Cary, NC) to determine the statistical differences in the k_La/V_L values found for O_2 between when the headspace was flushed with air for 2 min and 12 min during the effect of backmixing study at 95% confidence level. Also, the statistical differences of the k_La/V_L values found for O_2 in the backmixing study with and without air flushing of the headspace were also determined by TTEST procedure using SAS.

5.3 Results and discussion

5.3.1 Mass transfer characteristics in 7-L Bioflo 415 fermentor

The effects of agitation speed, headspace pressure, and gas flow rate on the k_La/V_L for O_2 with the 3 L and 5.6 L working volumes in the air-water system are shown in Fig. 5.3. The k_La/V_L values for O_2 increased as agitation speed increased at fixed air standard flow rate, headspace pressure and working volume. Also, the mass transfer of O_2 to the DI water was improved with increasing air flow rate. The highest observed k_La/V_L for O_2 was 116.2 h^{-1} at 600 sccm, 900 rpm and 101 kPa with the 3 L working volume (Fig. 5.3). When the other operating conditions were the same, the k_La/V_L for O_2 in 3 L working volume was higher than in 5.6 L working volume at all agitation speeds except at 900 rpm. At 900 rpm, the k_La/V_L for O_2 was generally lower in the 3 L working volume than in the 5.6 L working volume at headspace pressures of 150 and 240 kPa and flow rates 90 and 150 sccm. The decrease in the k_La/V_L for O_2 was due to N_2 backmixing at these conditions.

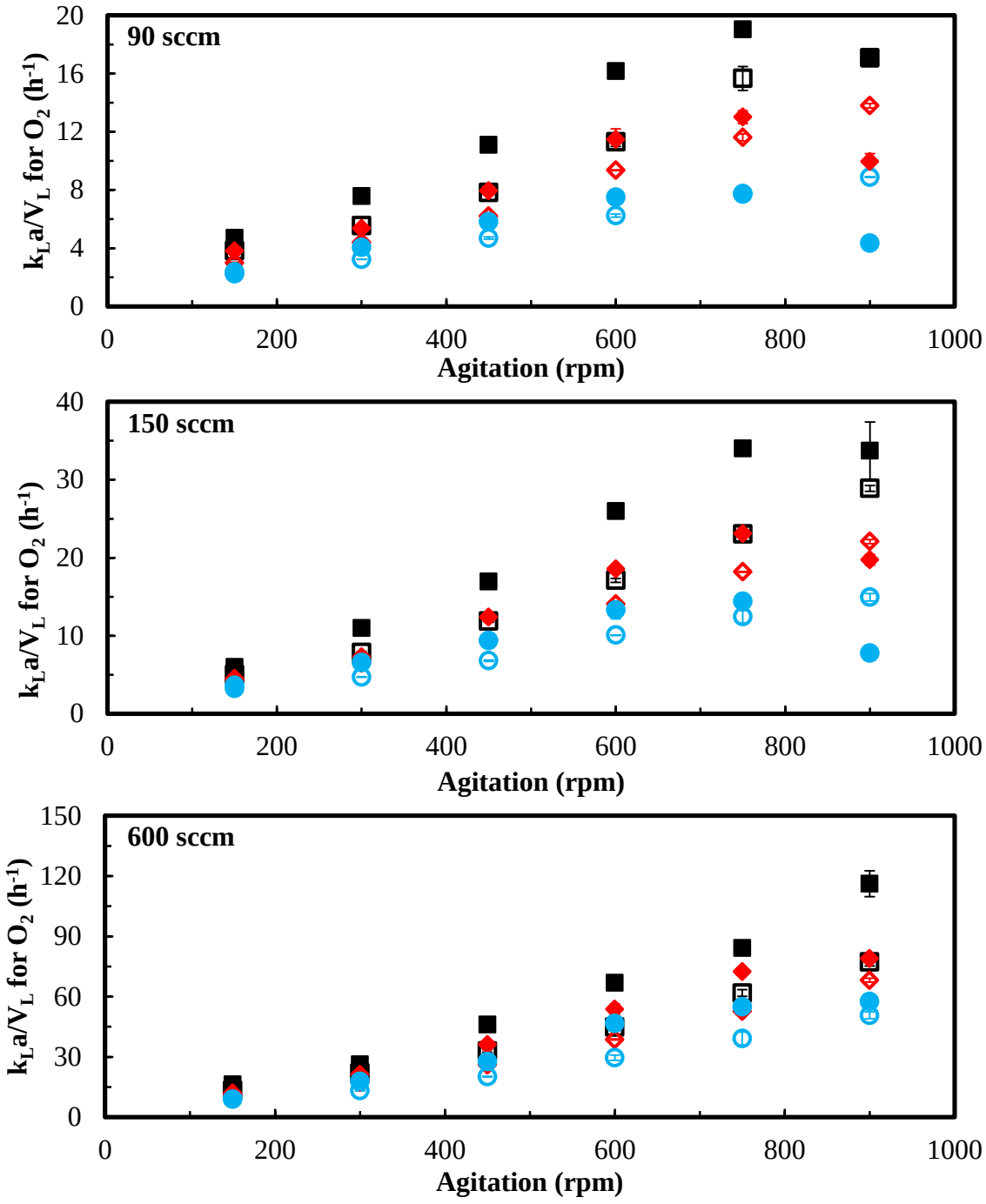

Fig. 5.3 Overall mass transfer coefficient for O_2 in air water system under the same standard flow rate 90 sccm, 150 sccm and 600 sccm with headspace pressure 101 kPa (■), 150 kPa (♦) and 240 kPa (●) in 3 L (solid symbol) and 5.6 L (open symbol) working volume.

It is important to investigate the effect of headspace pressure on the overall mass transfer coefficient during syngas fermentation, which would open opportunities to operate syngas fermentations at various pressures. The k_La/V_L for O_2 was the highest at the lowest headspace pressure of 101 kPa compared to 150 kPa and 240 kPa at the same agitation, standard air flow rate and working volume. Although the standard air flow rate controlled by the MFC and introduced into the fermentor does not change with the headspace pressure, the increase in the headspace pressure reduces the volumetric air flow rate in the fermentor and subsequently reduces the k_La/V_L values. The decrease in the volumetric air flow rate reduces the air superficial velocity, v_g (m/s), as calculated from Eq. 13, resulting in reducing the k_La/V_L.

$$v_g = \frac{V_{37°C}}{\pi\frac{D^2}{4}} \times 0.017 \times 10^{-6} \qquad (13)$$

The observed k_La/V_L values for O_2 with the 3 L working volume decreased when the agitation speed increased from 750 rpm to 900 rpm when the air flow rate was below 600 sccm (Fig. 5.3). However, the k_La/V_L values for O_2 with the 3 L working volume did not decrease when the agitation speed was increased from 750 rpm to 900 rpm with an air flow rate of 600 sccm. This phenomenon was not observed with the 5.6 L working volume. The decrease in mass transfer in the 3 L working volume was due to the severe backmixing of headspace N_2 into water that decreased O_2 mass transfer. There was 2.9 fold more available N_2 in the headspace with the 3 L working volume compared to the 5.6 L working volume, which stripped dissolved O_2 from water with the 3 L working volume. The total number of moles of N_2 in the headspace was 1.5 times and 2.4 times at headspace pressures of 150 kPa and 250 kPa, respectively, compared 101 kPa. The higher

the pressure in the headspace, the higher the backmixing severity, especially at low air flow rates. The k_La/V_L values for O_2 at air flow rate of 600 sccm, 900 rpm and 101 kPa in the 3 L working volume did not decrease, which was probably due to the high air flow rate that flushed out the headspace N_2 at a rate of least 4 times greater than at 90 sccm and 150 sccm. The k_La/V_L values for O_2 leveled off at 600 sccm with the headspace pressures of 150 kPa and 240 kPa when the agitation speeds were above 750 rpm with the 3 L working volume (Fig. 5.3). This was due to low volumetric air flow rate at headspace pressures above 101 kPa, which could not flush N_2 out of headspace as fast as at 101 kPa.

5.3.2 Effect of headspace backmixing k_La/V_L for O_2

The backmixing effects on mass transfer in the 7-L fermentor were evaluated at 150 rpm and 900 rpm for 3 L and 5.6 L working volumes under headspace air pressures 101, 150 and 240 kPa (Table 5.2). The fermentor headspace was purged with air at 1000 mL/min for 2 min. During the test, the inlet and outlet were completely closed and no air was sparged from the inlet. The backmixing effect on the k_La/V_L for O_2 with the 5.6 L working volume was small, and the k_La/V_L for O_2 was below 2 h^{-1} (Table 5.2). For the 3 L working volume at 150 rpm and 240 kPa, the backmixing was low which resulted in a k_La/V_L for O_2 of 1.3 h^{-1}. However, the k_La/V_L for O_2 was significantly increased from 0.7 h^{-1} to 67.3 h^{-1} when the agitation speed was increased from 150 rpm to 900 rpm at 101 kPa. Moreover, the k_La/V_L for O_2 increased 77% by boosting the headspace pressure from 101 kPa to 240 kPa in the 3 L working volume. This could explain the decrease in the k_La/V_L for O_2 at 900 rpm with low flow rates of 90 sccm and 150 sccm at 150 kPa and 240 kPa due to N_2 backmixing (Fig. 5.3).

In addition to the higher headspace volume with the 3 L working volume fermentor, the high k_La/V_L due to backmixing at 900 rpm was probably due to the impeller arrangement. The distance from the top impeller to the liquid surface was 6.4 cm in the 3 L working volume. However, there was 16.7 cm between the top impeller and the liquid surface in the 5.6 L working volume (Fig. 5.1). There was no vertex observed in the 5.6 L working volume at 900 rpm. However, a vortex was formed between the top impeller and water surface in the 3 L working volume, which contributed to backmixing.

In order to test if there was a difference of headspace air flushing time on k_La/V_L for O_2, the headspace in the bioreactor with 3 L working volume was flushed with air at 1000 mL/min for 12 min to compare with the 2 min flushing time. The results showed there was no statistical difference between the headspace flushing times (Table 5.2). Thus, 2 minutes were sufficient to flush the headspace with air to evaluate the backmixing effect.

Table 5.2 Backmixing effect on k_La/V_L for O_2 at various air pressures in the headspace.

	k_La/V_L for O_2 (h^{-1})					
Headspace pressure (kPa)	**101**		**150**		**240**	
Agitation (rpm)	150	900	150	900	150	900
3 L[a]	0.7 ±0.0	67.3 ±1.0[N]	0.8 ±0.0	92.0 ±3.5[N]	1.3 ±0.4	119.3 ±2.1[N]
3 L[b]	—[c]	67.0 ±0.2	—	88.2 ±0.3	—	122.3 ±1.4
5.6 L[a]	0.2 ±0.0	1.5 ±0.0	0.2 ±0.0	1.8 ±0.0	0.3 ±0.0	1.8 ±0.0

[a] Flush headspace for 2 min with air.
[b] Flush headspace for 12 min with air.
[c] Not determined.
[N] There was no statistical difference between 2 min and 12 min air flushing time in the headspace at 95% confidence level ($p > 0.05$).

The backmixing effect with the 5.6 L working volume was less than 2 h^{-1}. Therefore, the subsequent experiments on effect of backmixing were done with the 3 L working volume. In this set of experiments, the headspace was flushed with air before air was sparged through the fermentor inlet sparger to evaluate if the backmixing of air affects the k_La/V_L for O_2 in the 3 L working volume at 600 sccm and 900 rpm and various headspace pressures (Table 5.3).

There was at least a 20% increase in k_La/V_L for O_2 when the headspace was flushed with air before flowing air into the bioreactor compared to N_2 the headspace. The k_La/V_L values for O_2 were 32% and 50% lower at 150 kPa and 240 kPa, respectively, than at 101 kPa when the headspace was not initially flushed with air (Table 5.3). However,

when the headspace was flushed with air, the k_La/V_L values for O_2 were 16% and 41% lower at 150 kPa and 240 kPa, respectively, than at 101 kPa.

Table 5.3 Effect of headspace pressures on backmixing in the 7-L Bioflo 415 fermentor with the 3 L working volume and air flow rate of 600 sccm and 900 rpm.

Headspace pressure, kPa	101	150	240
Actual volumetric flow rate at 37 ℃, mL/min	628	428	270
k_La/V_L without flushing headspace with air, h^{-1}	116.2 ± 6.4	79.0 ±0.1	57.7 ±0.5
k_La/V_L with headspace flushing with air[a], h^{-1}	139.8 ±5.4	116.8 ±5.7[Y]	82.6 ±1.4[Y]
% improve in k_La/V_L with backmixing	20.3	47.9	43.2

[a] Headspace was flushed at 1000 mL/min with air for 2 min before sparging air in water in the fermentor.

[Y] There was statistical difference between flushing the headspace with air and no flush at 95% confidence level ($p < 0.05$).

Utilizing the backmixing effect can be useful in syngas fermentation. Under low syngas conversion, the unutilized gas in the headspace can be entrained back into the medium, thus improving mass transfer and converted into products. However, if the gas conversion was high, the inert gas such as N_2 from producer gas derived from biomass (Ahmed et al., 2006) in the headspace can reduce the k_La/V_L for CO or H_2 at high agitation due to backmixing. Thus, it would be helpful to operate the syngas fermentation at low agitation speed, and high working volume to alleviate the backmixing effect when the syngas conversion efficiency is high.

5.3.3 Predictions of the k_La/V_L values for O_2, CO, H_2 and CO_2

Based on the experimental data, the standard flow rates were converted into the corresponding volumetric flow rates at the various hydraulic heads and headspace pressures used. The predictions of the k_La/V_L for O_2, CO, H_2 and CO_2 were performed at volumetric flow rate range from 40 mL/min to 630 mL/min at 37 ℃, agitation speed range from 150 rpm to 900 rpm, and working volumes 3 L and 5.6 L. The power consumption per unit volume (P_g/V_L) and superficial velocity were calculated at the above range of operating conditions using Eqs. 6 to 10 and 13.

The least square method was applied to determine the constants in Eq. 11. Therefore, the k_La/V_L values for O_2 were estimated using Eq. 14.

$$\frac{k_La}{V_L}\text{for } O_2 = 0.30 \cdot \left(\frac{P_g}{V_L}\right)^{0.39} \cdot v_g{}^{0.79} \cdot 3600 \qquad (14)$$

The experimental and predicted k_La/V_L values for O_2 at the various operating conditions are shown in Fig. 5.4. It was reported that the parameters α and β in Eq. 11 were in the range of 0.3 to 0.7 and 0.0 to 1.0, respectively, and the variance of these parameters was due to measurement error and the configuration of stirred tank reactors (Stenberg and Andersson, 1988; Bredwell et al., 1999). In the present study, the α and β parameters of 0.39 and 0.79, respectively, were within the previously reported range. The experimental data and model predictions of the k_La/V_L values for O_2 were plotted in Fig. 5.5. The model predictions of the k_La/V_L values for O_2 were within 10% of experimental data. The R^2 value for model predictions of the experimental data was 0.97, indicating a good fit.

For syngas fermentation in 7-L Bioflo 415, the overall volumetric mass transfer coefficients for CO, H_2 and CO_2 can be calculated using Eqs. 12 and 14. Therefore, Eq. 14 was modified to predict the k_La/V_L values for CO, H_2 and CO_2 as shown in Eqs. 15 to 17 using the ratios in Table 5.1 based on the penetration theory or surface renewal theory.

$$\left(\frac{k_La}{V_L}\right)_{CO} = 0.31 \cdot \left(\frac{P_g}{V_L}\right)^{0.39} \cdot v_g^{0.79} \cdot 3600 \quad (15)$$

$$\left(\frac{k_La}{V_L}\right)_{H_2} = 0.44 \cdot \left(\frac{P_g}{V_L}\right)^{0.39} \cdot v_g^{0.79} \cdot 3600 \quad (16)$$

$$\left(\frac{k_La}{V_L}\right)_{CO_2} = 0.29 \cdot \left(\frac{P_g}{V_L}\right)^{0.39} \cdot v_g^{0.79} \cdot 3600 \quad (17)$$

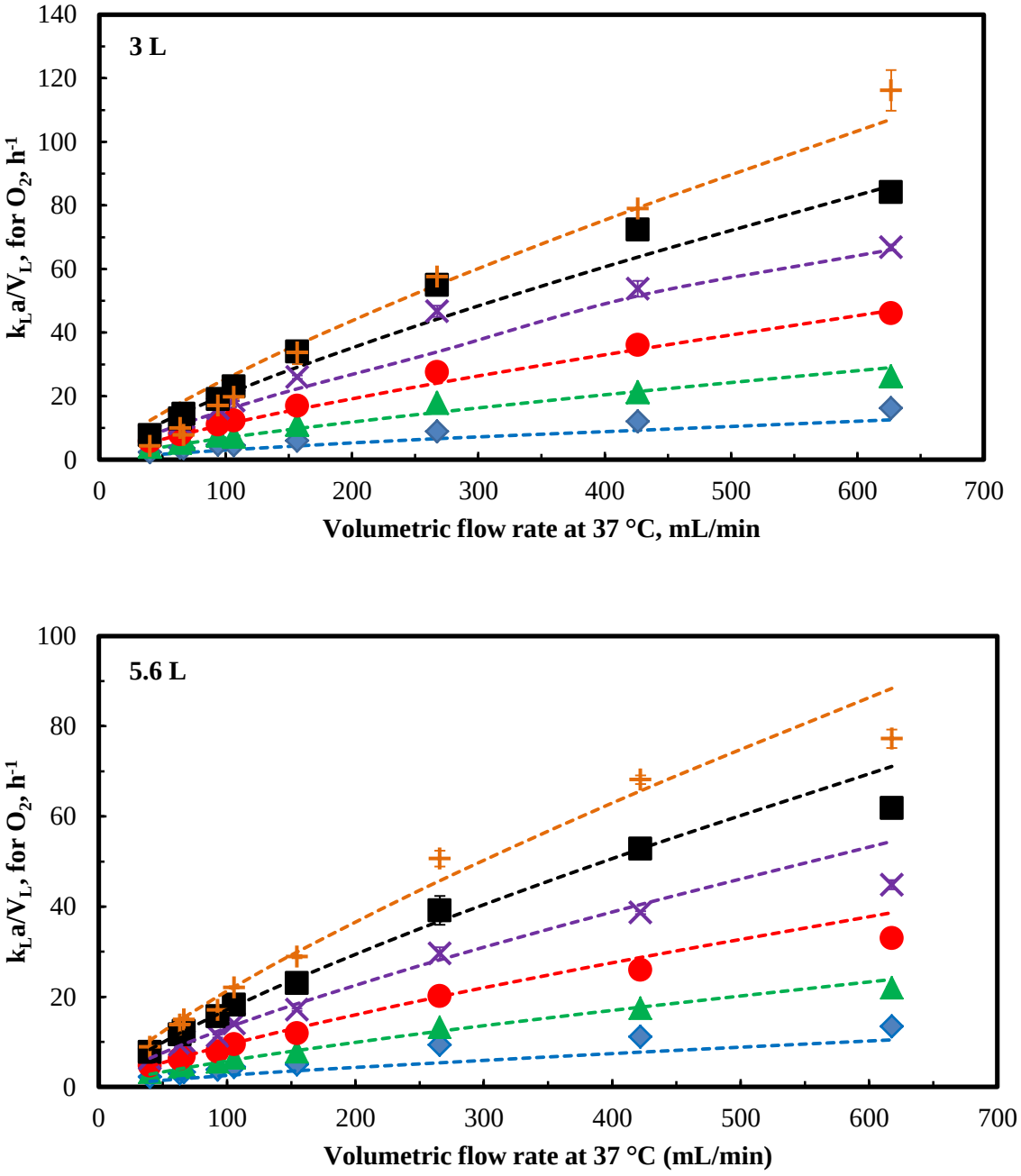

Fig. 5.4 Experimental and predicted kLa/VL values for O_2 with 3 L and 5.6 L working volumes in the 7 L Bioflo 415 fermentor at flow rates between 40 mL/min to 630 mL/min and 37 °C and various agitation speeds: 150 rpm (♦), 300 rpm (▲), 450 rpm (●), 600 rpm (×), 750 rpm (■) and 900 rpm (+); model prediction (dash line); small error bars were not visible.

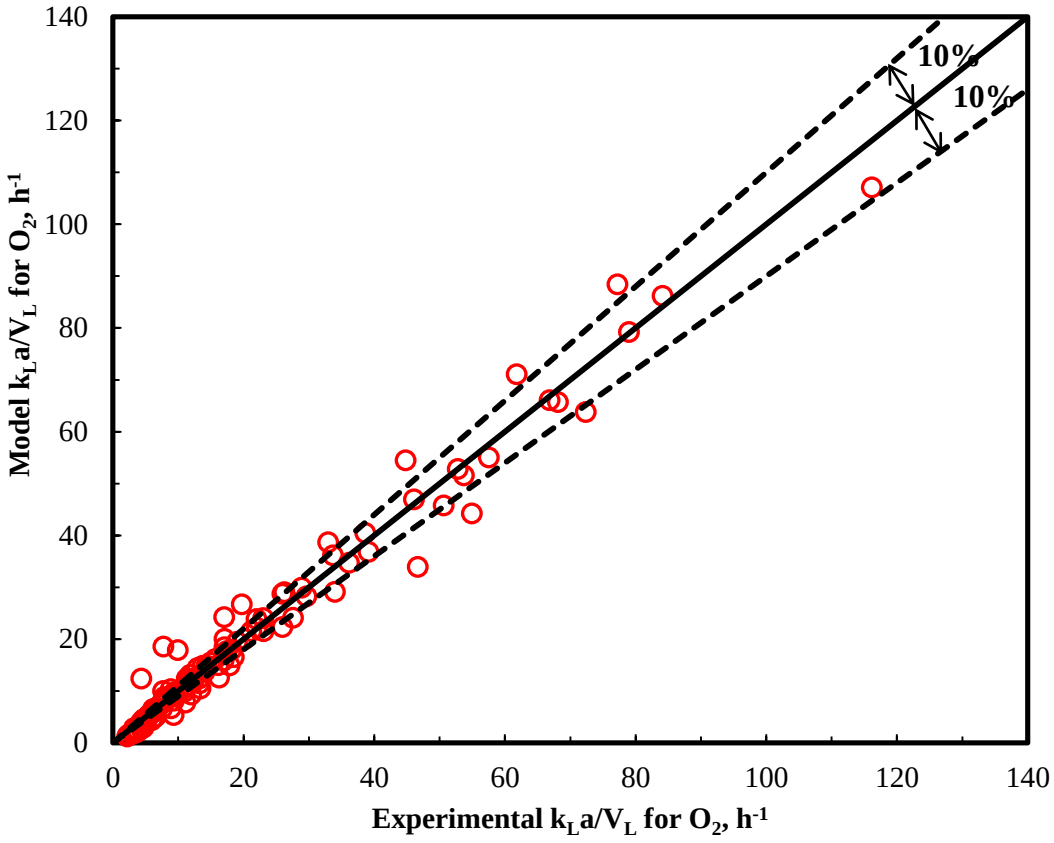

Fig. 5.5 Experimental and predicted k_La/V_L values for O_2 at flow rates between 40 mL/min to 630 mL/min and 37 ℃, agitation speeds range from 150 rpm to 900 rpm in the 3 L and 5.6 L working volumes.

5.4 Conclusions

The k_La/V_L values for O_2 increased by increasing the air flow rates and agitation speeds in the 7-L Bioflo 415 fermentor with the 3 L and 5.6 L working volumes. The increase in headspace pressure decreased the k_La/V_L values for O_2 due to lower volumetric gas flow rate at high pressure. The highest k_La/V_L for O_2 was 116 h^{-1}, which was obtained at 600 sccm, 900 rpm and 101 kPa with the 3 L working volume.

Backmixing effects from the headspace were high at the agitation speed of 900 rpm with the 3 L working volume. The highest k_La/V_L for O_2 due to backmixing was 119 h^{-1}, obtained at headspace pressure of 240 kPa. The mass transfer model predicted the k_La/V_L values for O_2 within 10% of the experimental values. The model was extended to predict the k_La/V_L values for syngas components CO, CO_2 and H_2, which will provide insight in operating the fermentor.

5.5 References

Abubackar, H.N., Veiga, M.C., Kennes, C., 2011. Biological conversion of carbon monoxide: rich syngas or waste gases to bioethanol. Biofuels, Bioprod. Biorefin. 5, 93-114.

Ahmed, A., Cateni, B.G., Huhnke, R.L., Lewis, R.S., 2006. Effects of biomass-generated producer gas constituents on cell growth, product distribution and hydrogenase activity of *Clostridium carboxidivorans* $P7^T$. Biomass Bioenerg. 30, 665-672.

Bakker, A., Smith, J., Myers, K., 1994. How to disperse gases in liquids. Chem. Eng. 101, 98-104.

Blanch, H.W., Clark, d.S., 1997. Biochemcial Engineering. Marcel Dekker, Inc, New York, pp.702.

Bredwell, M.D., Srivastava, P., Worden, R.M., 1999. Reactor design issues for synthesis-gas fermentations. Biotechnol. Prog. 15, 834-844.

Kawase, Y., Halard, B., Moo-Young, M., 1992. Liquid-phase mass transfer coefficients in bioreactors. Biotechnol. Bioeng. 39, 1133-1140.

Klasson, K.T., Ackerson, M.D., Clausen, E.C., Gaddy, J.L., 1993. Biological conversion of coal and coal-derived synthesis gas. Fuel 72, 1673-1678.

Klasson, K.T., Ackerson, M.D., Clausen, E.C., Gaddy, J.L., 1991. Bioreactors for synthesis gas fermentations. Resour. Conserv. Recy. 5, 145-165.

Lee, J.M., 1992. Biochemcial Engineering. Prentice-Hall, Englewood Cliffs, New Jersey, pp.240.

Liew, F.M., Köpke, M., Simpson, S.a.D., 2013. Gas Fermentation for Commercial Biofuels Production. in: Fang, Z. (Eds.), Liquid, Gaseous and Solid Biofuels. InTech, pp. 125-173.

Liu, K., Atiyeh, H.K., Tanner, R.S., Wilkins, M.R., Huhnke, R.L., 2012. Fermentative production of ethanol from syngas using novel moderately alkaliphilic strains of *Alkalibaculum bacchi*. Bioresour. Technol. 104, 336-341.

McCabe, W.L., Smith, J.C., 2005. Unit operations of chemcial engineering. 7 ed. Mcgraw-Hill Inc., pp.1007.

Munasinghe, P.C., Khanal, S.K., 2010. Biomass-derived syngas fermentation into biofuels: Opportunities and challenges. Bioresour. Biotechnol. 101, 5013-5022.

Munson, B.R., Young, D.F., Okiishi, T.H., Huebsch, W.W., 2009. Fundamentals of fluid mechanics. 6th ed. Willey, pp.784.

Orgill, J.J., Atiyeh, H.K., Devarapalli, M., Phillips, J.R., Lewis, R.S., Huhnke, R.L., 2013. A comparison of mass transfer coefficients between trickle-bed, hollow fiber membrane and stirred tank reactors. Bioresour. Technol. 133, 340-346.

Shuler, M.L., Fikret, K., 2002. Bioprocess Engineering: Basic concepts. Second ed. Prentice Hall, Englewood Cliffs, New Jersey, pp.576.

Stenberg, O., Andersson, B., 1988. Gas-liquid mass transfer in agitated vessels—II. Modelling of gas-liquid mass transfer. Chem. Eng. Sci. 43, 725-730.

Vega, J.L., Antorrena, G.M., Clausen, E.C., Gaddy, J.L., 1989. Study of gaseous substrate fermentations: Carbon monoxide conversion to acetate. 2. Continuous culture. Biotechnol. Bioeng. 34, 785-793.

Wilkins, M.R., Atiyeh, H.K., 2011. Microbial production of ethanol from carbon monoxide. Curr. Opin. Biotechnol. 22, 326-330.

Younesi, H., Najafpour, G., Ku Ismail, K.S., Mohamed, A.R., Kamaruddin, A.H., 2008. Biohydrogen production in a continuous stirred tank bioreactor from synthesis gas by anaerobic photosynthetic bacterium: *Rhodopirillum rubrum*. Bioresour. Technol. 99, 2612-2619.

CHAPTER VI

CONTINUOUS SYNGAS FERMENTATION FOR THE PRODUCTION OF ETHANOL, N-PROPANOL AND N-BUTANOL

6.1 Introduction

Syngas fermentation is part of the hybrid thermochemical-biochemical process, also called gasification-syngas fermentation. In this process, feedstocks such as biomass or municipal solid waste are gasified into syngas (CO, H_2 and CO_2), which is then converted into biofuels and chemicals using microbial catalysts (Wilkins and Atiyeh, 2011). Syngas can be converted into ethanol using acetogens such as *Clostridium ljungdahlii*, *Clostridium ragsdalei*, *Clostridium carboxidivorans* and *Clostridium autoethanogenum* (Phillips et al., 1993; Wilkins and Atiyeh, 2011; Ukpong et al., 2012).

Decreasing the medium cost and increasing ethanol titer and productivity are important to improve the economic feasibility of the production of biofuels and chemicals using syngas fermentation technology. Low cost nutrients such as cotton seed extract (CSE) and corn steep liquor (CSL), have been used instead of yeast extract (YE) in

syngas fermentation for ethanol production (Kundiyana et al., 2010; Maddipati et al., 2011). CSL is rich in proteins, vitamins, minerals and amino acids (Lawford and Rousseau, 1997). The industrial cost of CSL was reported to be $0.18/kg, which is about 2% of the industrial price of YE, $9.20/kg (Maddipati et al., 2011). The use of CSL as a replacement of YE, vitamins and minerals in a 7-L fermentor with *C. ragsdalei* resulted in 40% more ethanol production compared to YE medium (Maddipati et al., 2011), indicating the potential of CSL as a low cost nutrient for syngas fermentation.

High ethanol titer and productivity can be achieved through higher cell concentration and improving the mass transfer of the substrate gases CO and H_2 to cells. The highest reported ethanol concentration was 48 g/L, achieved using *C. ljungdahlii* during continuous syngas fermentation with cell recycle and 4 g/L cell mass concentration (Phillips et al., 1993). However, only 6.5 g/L ethanol was produced during continuous syngas fermentation using *C. ljungdahlii* without cell recycle and 2.3 g/L cell mass concentration (Mohammadi et al., 2012). This showed the advantage of cell recycle to obtain high cell and ethanol concentrations during syngas fermentation. When *C. ragsdalei* was used in a two-stage continuous syngas fermentation with cell recycle, a maximum ethanol yield of 15 g ethanol/g cells was obtained (Kundiyana et al., 2011), which was comparable to the yield (12 g ethanol/g cells) with *C. ljungdahlii* (Phillips et al., 1993). The ability to produce high concentrations of ethanol depends on the microorganism, syngas composition and fermentor operating conditions. *Eubacterium limosum* KIST612 only produced 0.3 g/L ethanol in a continuous fermentation using pure CO and cell recycle with a 4 g/L cell mass concentration (Chang et al., 2001).

The H_2:CO ratios in previously reported syngas fermentations were mostly below 0.75, which results in lower carbon conversion efficiency to ethanol or acetic acid as shown in Table 6.1 (Wilkins and Atiyeh, 2011). However, the H_2:CO ratios are affected by the gasification operating conditions and feedstock used. A H_2:CO ratio of 2 can be produced when steam and pure O_2 are used in the gasification process (Turn et al., 1998), which can result in a theoretical carbon to ethanol conversion efficiency of 100%. In addition, an H_2:CO ratio of 2 was reported from gasification of dairy biomass (cow manure) using air (Gordillo and Annamalai, 2010), indicating the potential of dairy biomass for biofuels production.

Table 6.1 Carbon to ethanol and acetic acid conversion efficiencies from syngas with various H_2:CO ratios.

	Stoichiometry	H_2:CO	Carbon conversion efficiency	Product Yield from CO
(1)	$6CO + 3H_2O \rightarrow C_2H_5OH + 4CO_2$	0	33.3%	16.7%
(2)	$3CO + 3H_2 \rightarrow C_2H_5OH + CO_2$	1	66.7%	33.3%
(3)	$2CO + 4H_2 \rightarrow C_2H_5OH + H_2O$	2	100.0%	50.0%
(4)	$4CO + 2H_2O \rightarrow CH_3COOH + 2CO_2$	0	50.0%	25.0%
(5)	$2CO + 2H_2 \rightarrow CH_3COOH$	1	100.0%	50.0%

Recently, *Alkalibaculum bacchi* strains CP11^T, CP13 and CP15 were found to grow at an initial pH 8.0 and convert syngas into ethanol and acetic acid in YE medium (Allen et al., 2010; Liu et al., 2012). In bottle fermentations, strain CP15 was found to be the most promising *A. bacchi* strain for ethanol production because of its higher growth and ethanol production rate and yield compared to CP11^T and CP13 (Liu et al., 2012). However, further process development is required for strain CP15 to increase its potential use in large scale ethanol production. This includes reducing the fermentation medium cost and investigating characteristics of CP15 at larger scale than fermentation bottles. The YE medium cost was relatively expensive at $10.53/L, mostly due to the high cost of the [Tris (hydroxymethyl) methyl]-3-amino propanesulfonic acid (TAPS) buffer. Thus, the first object of the present study was to reduce the cost of CP15 fermentation medium by removal of costly TAPS buffer and replacing YE with CSL. The second objective was to scale up the fermentation from bottle to a 7-L fermentor in continuous mode with cell recycling.

6.2 Materials and methods

6.2.1 Microorganisms

A. bacchi strain CP15 was maintained under anaerobic condition in a standard YE medium at initial pH 8.0 and 37 ℃. The medium preparation and compositions were reported previously (Liu et al., 2012). Strain CP15 inoculum was prepared by sub-culturing twice to reduce the growth lag phase. Inoculum size used was 10% (v/v).

6.2.2 Effect of medium composition

Four fermentation media were formulated without the addition of TAPS buffer with an objective to reduce medium cost (Table 6.2). The composition of the YE medium with 3X minerals was similar to standard YE medium but with threefold more minerals, which was also similar to the amount of minerals added in the YE medium for *C. ragsdalei* in a previous study (Maddipati et al., 2011). In the two CSL media, 20 g/L or 50 g/L CSL replaced YE, vitamins and minerals in the standard YE medium. In addition, all media contained 5 g/L $NaHCO_3$ as a buffer, 2.5 mL/L of 4% cysteine sulfide solution as a reducing agent, and 1 mL/L of 0.1% resazurin solution as a redox indicator. The compositions of the minerals, trace metals and vitamins stock solutions were reported previously (Tanner, 2007) and are also shown in Appendix I. The CSL (Sigma-Aldrich, St. Louis, MO, USA) used in the present study was centrifuged at 16,000 g for 10 min using Accuspin Micro centrifuge (Fisher Scientific, Pittsburgh, PA, USA) to remove the solids before preparing the fermentation medium. The solids were removed to allow measurement of cell mass concentration in the fermentation broth. The fermentation was done in 250-mL serum bottles (Wheaton, NJ, USA) each containing 100 mL of medium. Syngas I was used and the syngas mixture contained 20% CO, 15% CO_2, 5% H_2 and 60% N_2 by volume, which was similar to producer gas generated from the Oklahoma State University gasification facility using switchgrass (Ahmed et al., 2006). The syngas was fed in the fermentation bottles every 24 h at 239 kPa. Fermentation bottles were incubated on an orbital shaker (Innova 2100, New Brunswick Scientific, Edison, NJ, USA) at 150 rpm and 37 ℃. Liquid samples (2 mL) were withdrawn periodically from fermentation bottles under aseptic conditions to measure OD, pH and product

concentrations. Gas samples were withdrawn from the headspace periodically to determine changes in gas composition during fermentation. All fermentations were done in triplicate.

Table 6.2 Compositions of four media formulations used in bottle fermentations.

Medium components (per L)[a]	YE (g/L)	CSL (g/L)	Minerals[b] (mL/L)	Trace metals[b] (mL/L)	Vitamins[b] (mL/L)
Standard YE medium	1	—	10	10	10
YE medium with 3X minerals	1	—	30	10	10
20 g/L CSL medium	—	20	—	10	—
50 g/L CSL medium	—	50	—	10	—

[a] TAPS absent from all media; other components added in all media include 5% $NaHCO_3$, 2.5 mL/L of 4% cysteine sulfide and 1mL/L of 0.1% resazurin.
[b] Compositions of mineral, trace metal and vitamin stock solutions are provided in Tanner (2007).

6.2.3 Continuous syngas fermentation in a 7-L fermentor

Continuous syngas fermentation with cell recycle was operated in a 7-L Bioflo 415 fermentor with an in-place-sterilization system (New Brunswick Scientific Co., Edison, NJ, USA) as shown in Fig. 1. The working volume used was 3.3 L. Two six-blade Rushton impellers were mounted on the fermentor shaft separated by a distance equal to the impeller diameter as suggested by Bakker et al. (1994). Four baffles were used to avoid vortex formation and improve syngas mass transfer. Syngas was sparged

into medium by a microsparger with a pore size of 10-15 μm. Two 0.2 μm filters (New Brunswick Scientific Co.) were place in the inlet and outlet gas lines. Fermentor temperature was controlled at 37 ℃ by a water heating jacket. A pH probe (Mettler Toledo, Columbus, OH, USA) and a dissolved oxygen (DO) probe (Mettler Toledo, Columbus, OH, USA) were used to monitor pH and DO, respectively. The DO probe was used to ensure no O_2 present in the fermentor during syngas fermentation.

Two 5-L Kimble bottles were used to feed fresh fermentation medium to the fermentor and to collect the product permeated from the cell recycle system. The cell recycle system was made of two 0.2 μm pore size hollow fiber membrane cartridges (Model CFP-2-E-5A, GE HealthCare, Piscataway, NJ, USA) and a pressure gauge at the inlet of the membrane cartridge. One membrane cartridge was in standby mode during operation. The flow rates of fresh medium and cell free permeate were controlled using peristaltic pumps (Model 7523-20, Cole-Parmer, Vernon Hills, IL, USA). The retentate from the cell recycle system containing concentrated cells was recycled back into the fermentor at a flow rate of 20 mL/min using a peristaltic pump. The syngas exiting the fermentor was cooled by passing it through a condenser kept at 5 ℃ using a refrigerated recirculator (1156D, VWR International, West Chester, PA, USA).

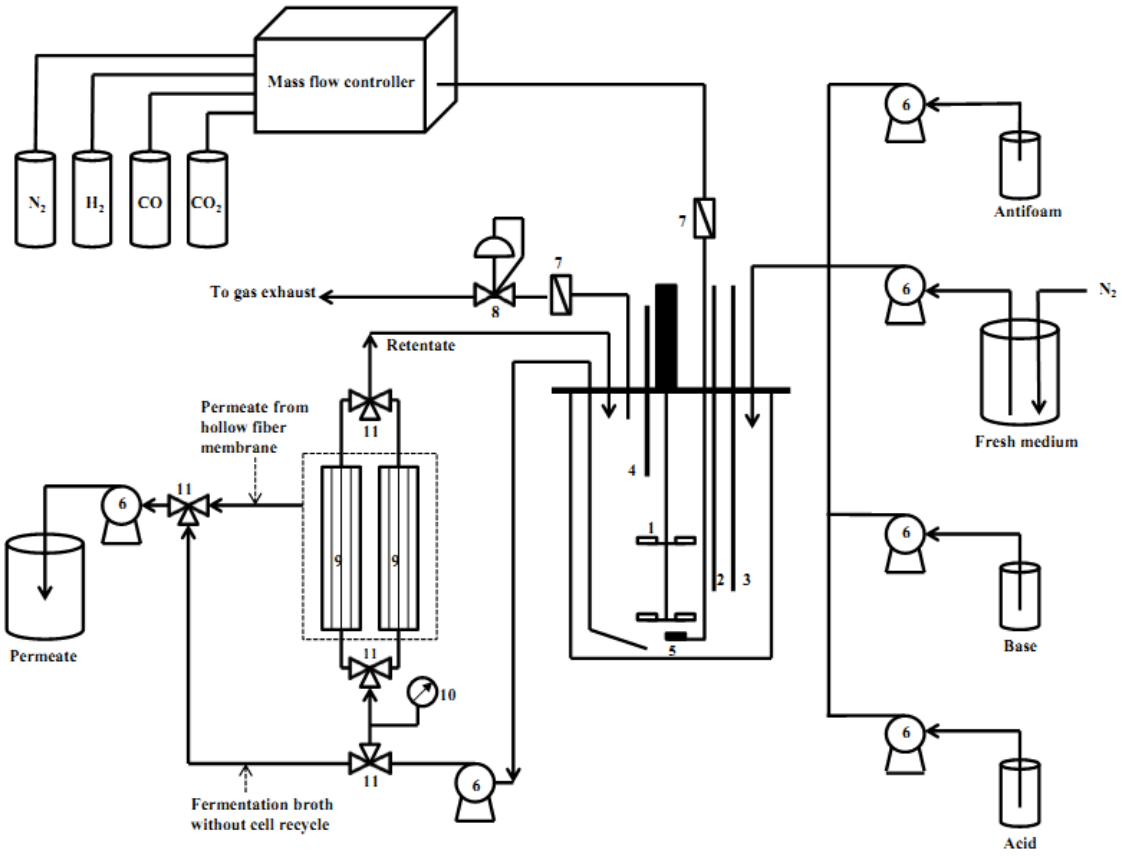

Fig. 6.1 Configuration of continuous fermentation in 7-L Bioflo 415 fermentor; 1. Six-blade Rushton impeller, 2. DO probe, 3. pH probe, 4. Foam probe, 5. Microsparger,6. Peristaltic pumps, 7. 0.2 µm gas filters, 8. Backpressure regulator, 9. Hollow fiber membrane cartridges, 10. Cell recycle system inlet pressure gauge, 11. Two-way valves.

The pH in the medium was controlled using 5 N KOH and 4 N H_2SO_4. The inlet gas flow rate and compositions of CO, CO_2, H_2 and N_2 were controlled using four thermal mass flow controllers (Burkert, Charlotte, NC, USA). Three syngas compositions (Syngas III: 39% CO, 24% CO_2, 27% H_2, 10% N_2, H_2:CO molar ratio ≈ 0.7; Syngas IV: 20% CO, 25% CO_2, 43% H_2, 12% N_2, H_2:CO molar ratio ≈ 2; Syngas V: 28% CO, 60%

H_2, 12% N_2, H_2:CO molar ratio ≈ 2) were studied to evaluate the effect of different H_2:CO ratios on the fermentation process. The syngas flow rate was controlled at 200 sccm (standard cubic centimeter per minute) during the whole fermentation. The headspace pressure in the fermentor was 101 kPa. In addition, three medium formulations (standard YE medium, YE-free medium: no YE in standard YE medium, and 20 g/L CSL medium) were examined (Table 6.2). During fermentation, a foam probe was used to control the foam level not exceed 1.3 cm above the liquid medium level by the addition of 5% antifoam (Antifoam B emulsion, Sigma-Aldrich, St. Louis, MO, USA) with a peristaltic pump.

Before the beginning of the fermentation, the medium was sterilized in place at 121 ℃ for 30 min and cooled by purging 200 sccm N_2 at 150 rpm agitation. Then, the medium was purged for 8 h with Syngas III at 200 sccm. Before inoculation, the medium was reduced by the addition of 2.5 mL/L of 4% cysteine sulfide to scavenge any residual dissolved O_2 in the medium. The pH was adjusted to 8.0 with 5N KOH. The fresh medium in the feeding tank and the hollow fiber membrane cartridge in the cell recycle system were sterilized separately using an autoclave at 121 ℃ for 30 min. Before installation of the cell recycle system, the hollow fiber membrane cartridge was purged with N_2 for 10 min to remove O_2.

6.2.4 16S rRNA analysis for continuous fermentation culture

A cell pellet (40 mL) culture from the 7-L fermentor at the end of the continuous fermentation was used to obtain genomic DNA with the PowerBiofilm™ DNA Isolation Kit (MoBio Laboratories, Carlsbad, CA, USA). After suspending the cell pellet in 350 μL

of solution "BF1", DNA isolation was conducted following the manufacturer's protocol. Cell lysis was achieved by homogenization at full speed for 1 min using a Mini-BeadBeater-8 (BioSpec Products, Bartlesville, OK, USA). Nearly full length bacterial 16S rRNA gene fragments were amplified from 50 ng of DNA in a PCR containing 1x *Taq* buffer with KCl (Fermentas, Waltham, MA, USA), 1.5 mM $MgCl_2$, 0.2 mM each dNTP, 0.2 μM of the forward (27F) and reverse (1391R) primers and 0.5 U of *Taq* DNA Polymerase (Fermentas) in a final volume of 25 μL. Thermal cycling was carried out in a Techne TC-512 thermal cycler (Techne, Burlington, NJ, USA) using the following conditions: initial denaturation for 3 min at 95 ℃; 30 cycles of 30 s at 95 ℃, 30 s at 55 ℃ and 1 min at 72 ℃; and a final extension of 10 min at 72 ℃. Amplified 16S rRNA genes were cloned using the TOPO TA Cloning Kit for Sequencing (Invitrogen Corp., Carlsbad, CA, USA). Vector-specific primers M13F and M13R were used to amplify cloned regions from 96 transformants, purified with ExoSAP-IT® (Affimetrix, Santa Clara, CA, USA) according to the manufacturer's protocol and sequenced on an ABI model 3730 capillary sequencer using the 27F primer. The resulting sequences were trimmed for quality using SeqMan Pro (version 10.1.2; DNAStar, Madison, WI, USA) and aligned with the NAST alignment tool against the Greengenes multiple sequence alignment (DeSantis Jr. et al., 2006). The taxonomic identity for each sequence was determined with the Greengenes (DeSantis et al., 2006) and SILVA (Pruesse et al., 2007) classifiers, as well as pairwise sequence comparison using the EzTaxon Server 2.1 (Chun et al., 2007).

6.2.5 Analytical procedures

6.2.5.1 Cell mass and product concentrations and gas analysis

The cell mass concentration was determined at 660 nm as described previously (Liu et al., 2012). The pH of liquid samples from the 250-mL bottle study was measured using a pH meter. Each liquid sample of 0.7 mL was acidified using 0.7 mL of 0.1 N HCl before solvent analysis. The solvent concentrations were measured using gas chromatography (GC) (Agilent 7890 N GC, Agilent Technologies, Wilmington, DE, USA) with a flame ionization detector (FID) and DB-FFAP capillary column (Agilent Technologies, Wilmington, DE, USA). A modification was done on the method reported in Chapter 4 to shorten the analysis time from 14 min to 8 min. The initial flow rate of carrier gas H_2 was changed from 1.9 mL/min to 2.26 mL/min. The inlet port temperature was changed from 200 ℃ to 225 ℃ and the inlet gas spilt ratio was changed from 50:1 to 20:1. The initial oven temperature was changed from 40 ℃ to 90 ℃ and the final oven temperature was changed from 235 ℃ to 250 ℃. The FID temperature was changed from 250 ℃ to 300 ℃. The new method is as follows: H_2 was used as carrier gas at an initial flow rate of 2.26 mL/min for 10 min. The inlet port temperature was kept at 225 ℃ with a split ratio of 20:1. The initial oven temperature was set at 90 ℃ and held for 2 min. Then it was ramped at a rate of 40 ℃/min to 250 ℃ with 1 min holding time. The FID temperature was set at 300 ℃ with H_2 and air flow rates of 30 mL/min and 400 mL/min, respectively.

A volume of 100 μL of gas from the 250-mL bottle headspace or the 7-L fermentor's exhaust line was injected in an Agilent 6890N GC (Agilent Technologies,

Wilmington, DE, USA) to determine gas composition. A modification was done on the gas analysis method in Chapter 4 to shorten the GC running time from 20 min to 5.5 min. The carrier gas argon holding time was changed from 3.5 min to 2 min. The ramping rate of carrier gas flow was changed from 0.1 mL/min^2 to 2.5 mL/min^2 and the final flow rate of argon was changed from 2.5 mL/min to 4 mL/min. The initial oven temperature was changed from 40 ℃ to 80 ℃ and the initial oven temperature holding time was changed from 3.5 min to 5.5 min. The modified method is as follow: argon was used as carrier gas with an initial gas flow rate of 2 mL/min and holding time of 2 min. The flow rate of carrier gas was then increased to 4 mL/min at a ramping rate of 2.5 mL/min^2. The inlet port temperature was set at 200 ℃ with a split ratio of 30:1. The initial oven temperature was set at 80 ℃ with a holding time of 5.5 min. The TCD temperature was set at 230 ℃.

When CSL medium was used, the sugar contents in the liquid samples were measured using an HPLC (Agilent 1200 series) with a refractive index detector (RID). A Rezex^{TM} RPM-Monosaccharide column (Phenomenex, Torrance, CA, USA) was used and operated at 80 ˚C with deionized water as the mobile phase pumped at 0.6 mL/min for 25 min per sample.

6.2.5.2 Statistical analysis and estimation of kinetic parameters

Duncan's multiple range test was analyzed by GLM procedure using SAS Release 9.3 (Cary, NC, USA) at 95% confidence level to determine pairwise statistical differences of maximum cell concentration, final ethanol concentration, CO and H_2 utilization among four media in the bottle study. The calculations of ethanol yields, CO and H_2 utilization, if applicable, were described previously (Liu et al., 2012). Specific

growth rate, specific gas uptake rate, dilution rate and productivity were calculated below (Shuler and Fikret, 2002):

$$\ln(X/X_o) = \mu \cdot t \quad (1)$$

$$q_x = GUR/(X \cdot V) \quad (2)$$

$$D = F/V \quad (3)$$

$$\text{Productivity} = D \cdot P \quad (4)$$

where X is the cell mass concentration (g/L), X_0 is the initial cell mass concentration (g/L), μ is specific growth rate (h^{-1}), t is time (h), q_x is specific gas uptake rate (mmol gas/g cells·h), GUR is CO or H_2 uptake rate (mmol/h), V is the fermentation working volume (L), D is dilution rate (h^{-1}), F is fresh medium and cell recycle system permeate flow rate via peristaltic pump (L/h) and P is ethanol concentration (g/L).

6.3 Results and discussion

6.3.1 Effect of medium composition

The maximum cell mass concentration, final ethanol concentration, CO and H_2 utilization, and cost of the four media formulations are compared in Table 6.3. The results showed that 20 g/L and 50 g/L CSL media produced about twice as much ethanol as the media with YE ($p < 0.05$). There was no statistical difference between the amounts of ethanol produced in standard YE medium and YE medium with 3X minerals. Also, the difference in ethanol production between the 20 g/L CSL and 50 g/L CSL media was insignificant ($p > 0.05$). Comparable maximum cell mass concentrations were obtained in the standard YE medium and YE medium with 3X minerals. However, 10% more cell

mass was obtained in the 50 g/L CSL medium than in the 20 g/L CSL medium, which could be due to presence of more nutrients in the 50 g/L CSL medium. The detailed product formation and gas consumption profiles are shown in Appendix A.

The maximum cell mass concentration in both YE media was 50% and 38% higher than in the 20 g/L and 50 g/L CSL media, respectively. This could be due to more growth promoting nutrients with the additional minerals, vitamins and trace metals added in the YE medium. Only trace metal solution was added in the CSL medium. Ethanol was produced mostly from the conversion of syngas and not the carbohydrates in the CSL. The theoretical amounts of ethanol that could be produced from consumed monosaccharides in CSL were 0.04 g/L (1.6% of total ethanol produced) and 0.1 g/L (3.6% of total ethanol produced) in 20 g/L and 50 g/L CSL medium, respectively.

The maximum cell mass concentration in both YE media was 50% and 38% higher than in the 20 g/L and 50 g/L CSL media, respectively. This could be due to the additional minerals and vitamins added in the YE medium. Only trace metal solution was added to the CSL medium. Ethanol was produced mostly from the conversion of syngas and not the carbohydrates in the CSL. The theoretical amounts of ethanol that could be produced from consumed monosaccharides in CSL were 0.04 g/L (1.6% of total ethanol produced) and 0.1 g/L (3.6% of total ethanol produced) in 20 g/L and 50 g/L CSL medium, respectively.

Both CO and H_2 utilizations by CP15 were between 42% and 47% in the standard YE medium and the YE medium with 3X minerals ($p > 0.05$) (Table 6.3). There were no significant differences in the gas utilizations by CP15 in the two CSL media ($p > 0.05$).

However, strain CP15 utilized over 45% more H_2 in YE media compared to CSL media.

All media used in the present study did not contain TAPS buffer. Compared to a previous study using standard YE medium with TAPS buffer (Liu et al., 2012), the media cost in the present study decreased by over 94% (i.e., from $10.53/L to below $ 0.61/L) as shown in Table 6.3. The costs of the CSL media were only 3% of the cost of the standard YE medium with TAPS and 73% of the YE medium without TAPS. The results showed that TAPS can be removed from the medium without negative effect on syngas fermentation. In addition, 20 g/L CSL can replace YE as a less expensive medium component in syngas fermentation using strain CP15 with a potential use in large scale ethanol production.

Table 6.3 Maximum cell mass and final ethanol concentrations, CO and H_2 utilization and cost of the four media used during syngas fermentation by *A. bacchi* CP15 in bottle fermentations.

Medium[a]	Standard YE medium	YE medium with 3X minerals	20 g/L CSL medium	50 g/L CSL medium
Max. cell concentration, g/L	0.33 ± 0.00^{A}	0.33 ± 0.00^{A}	0.22 ± 0.00^{C}	0.24 ± 0.02^{B}
Final ethanol, g/L	0.84 ± 0.11^{B}	1.24 ± 0.28^{B}	2.21 ± 0.25^{A}	2.65 ± 0.40^{A}
CO utilization, %	$42.00 \pm 0.53^{B,C}$	$45.59 \pm 0.37^{A,B}$	39.26 ± 0.21^{C}	$43.15 \pm 3.68^{B,C}$
H_2 utilization, %	44.86 ± 1.23^{A}	47.25 ± 1.03^{A}	28.83 ± 0.86^{B}	30.44 ± 2.02^{B}
Medium cost[b], $/L	0.41	0.61	0.30	0.31

[a] TAPS absent from all media.
[b] Based on industrial cost of YE and CSL (Maddipati et al., 2012) and cost of nutrients from Sigma-Aldrich in May, 2013 (St. Louis, MO, USA); Standard YE medium with TAPS cost $10.53/L.
[ABC] The same letter in the same row from Duncan's multiple range test indicates there was no statistical difference at 95% level ($p > 0.05$).

6.3.2 Continuous fermentation in a 7-L fermentor

6.3.2.1 Fermentation in yeast extract medium

The fermentation was started using the standard YE medium without TAPS (Table 6.2) in a liquid batch mode, in which syngas III (39% CO, 24% CO_2, 27% H_2, 10% N_2, H_2:CO molar ratio ≈ 0.7) was fed continuously. Cells started to grow after about 3 h of lag phase. During growth, acetic acid was produced as a growth-associated product (Fig. 6.2 A). The specific CO and H_2 uptake rates increased as cells were growing (Fig. 6.2 B). The agitation speed was set at 150 rpm. When cells were in the exponential growth phase and a cell mass concentration of 0.2 g/L (OD 0.5) was achieved at 13 h, fresh medium was fed continuously in the fermentor at a dilution rate of 0.011 h^{-1} (i.e., 8% of calculated specific growth rate 0.13 h^{-1}) and 100% cell recycle was initiated. During the fermentation period from 13 h to 120 h, the pH of the fermentation medium was controlled at 6.5 because ethanol production started at pH 6.5 with CP15 (Liu et al., 2012) and pH values below 6.5 did not support cell growth (Allen et al., 2010). When the dilution rate was set to 0.011 h^{-1}, there was a gradual increase in cell mass concentration from 0.2 g/L to 0.5 g/L at 72 h. The cell mass concentration did not change from 72 h to 120 h (Fig. 6.2 A). The agitation speed was increased to 300 rpm at 25 h as cell concentration was increasing to supply more syngas. Ethanol production started at 40 h when the pH decreased to 6.5 and ethanol concentration increased to 0.6 g/L at 120 h. Acetic acid production started as cells started to grow and increased to 3.4 g/L at 40 h. Then, acetic acid concentration gradually decreased to 1.5 g/L at 120 h as ethanol was produced. The specific CO and H_2 uptake rates increased to 43 mmol CO/(g cells·h) and 35 mmol H_2/(g cells·h), respectively, in the first 25 h of fermentation (Fig. 6.2 B). Then,

the specific CO and H_2 uptake rates decreased to 27 mmol CO/(g cells·h) and 19 mmol H_2/(g cells·h) at 120 h, respectively, due to the increase in cell mass concentration.

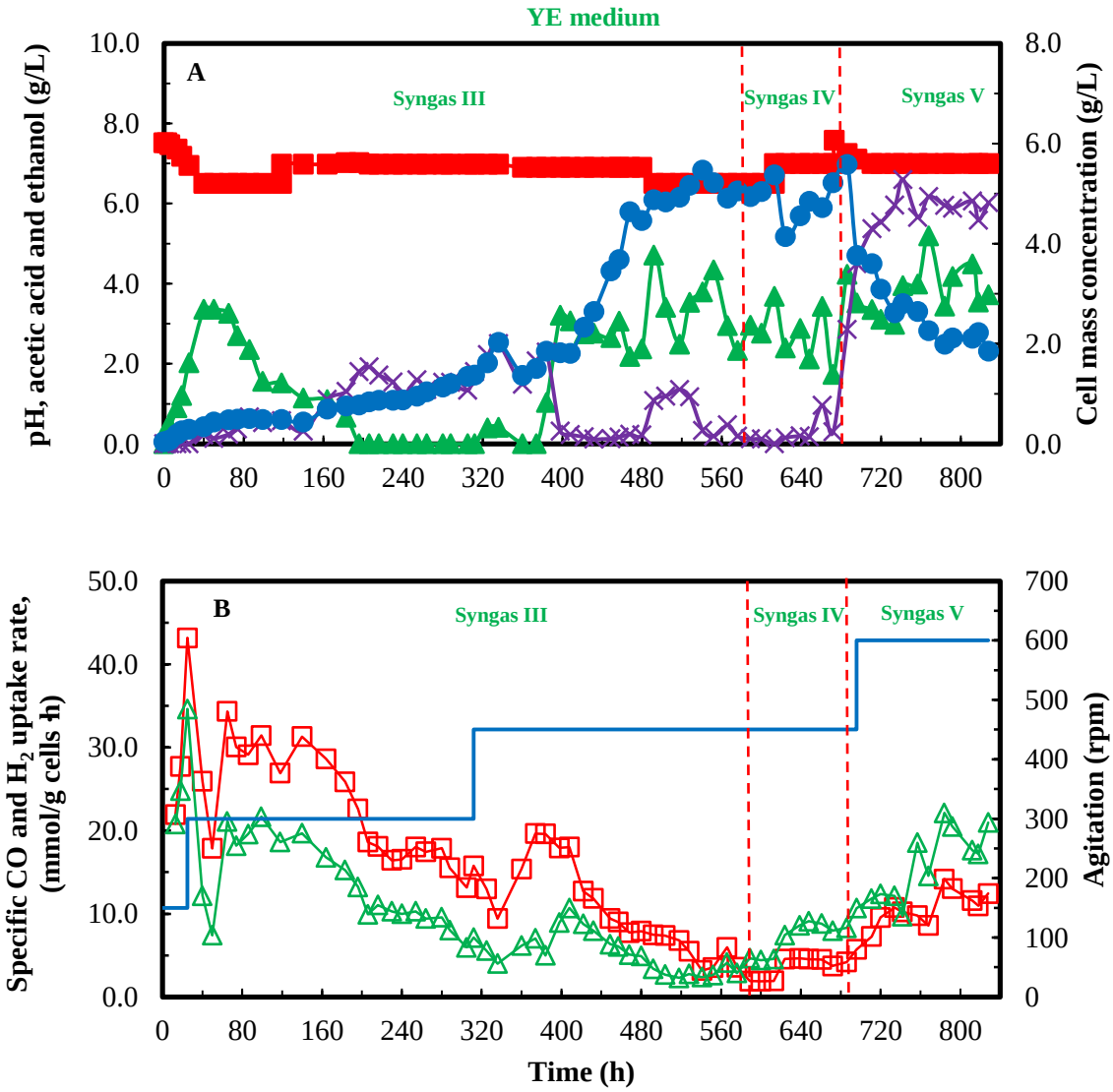

Fig. 6.2 (A) Growth and products profiles (B) Specific gas uptake profiles during continuous syngas fermentation in YE medium with cell recycle; pH (■), cell mass concentration (●), acetic acid (▲), ethanol (×), specific CO uptake rate (□), specific H_2 uptake rate (Δ), and agitation (solid line and no symbol).

Even with 100% cell recycle, the accumulation of cell mass in the fermentor was slow at the dilution rate of 0.011 h^{-1} between 13 h to 120 h, which could be due to low cell growth at pH 6.5, which was reported previously (Allen et al., 2010). Thus, the pH was increased to 7.0 and controlled at this level after 120 h. This resulted in an increase in cell mass concentration from 0.5 g/L to 0.9 g/L between 120 h to 216 h. During the same period, ethanol concentration increased from 0.6 g/L to 1.7 g/L. This showed that ethanol can be produced during cell growth, and pH 7.0 was better than pH 6.5 for both cell growth and ethanol production. The acetic acid concentration dropped to zero at 216 h due to its conversion to ethanol as previously reported (Liu et al., 2012). During the fermentation period from 120 h to 216 h, the specific CO and H_2 uptake rates decreased by 33% and 41%, respectively, due to the increase in cell mass concentration (Fig. 6.2 B).

The dilution rate was increased to 0.017 h^{-1} between 216 h to 288 h to provide more nutrients and grow more cells. The average ethanol concentration between 216 h to 288 h was 1.5 g/L, which was comparable to the ethanol concentration produced at 0.011 h^{-1} (Table 6.4). However, no acetic acid was detected during this period. Cell concentration increased to 1.2 g/L at 288 h. The increase in dilution rate by 50% in this period did not affect ethanol concentration. However, ethanol productivity increased by 60% in the period between 216 h to 288 h compared to the period from 120 h to 216 h. To further increase ethanol productivity, the dilution rate was increased from 0.017 h^{-1} to 0.022 h^{-1} between 288 h to 384 h. This resulted in a further increase in the cell mass concentration by 58%. Ethanol concentration and productivity increased to 2.0 g/L and 42.1 mg/L ħ, respectively. The concentration of acetic acid was only 0.4 g/L. During the fermentation period from 216 h to 288 h, the average specific CO and H_2 uptake rates

were 17 mmol CO/(g cells·h) and 10 mmol H_2/(g cells·h), respectively. The agitation speed was increased from 300 rpm to 450 rpm at 312 h to improve the mass transfer of CO and H_2.There was a slight increase in cell mass, ethanol, acetic acid concentrations and specific CO uptake rate between 288 h to 384 h. However, specific H_2 uptake rate decreased slightly (Fig. 6.2 B).

When the dilution rate was increased to 0.033 h^{-1} between 384 h and 576 h, a rapid increase in the cell mass concentration to 5.5 g/L (equivalent to an optical density, OD, of 14) was measured in the fermentor (Fig. 6.2 A). This was the maximum cell mass concentration achieved. During this rapid cell growth, 5 g/L acetic acid was produced. However, the high cell mass concentration did not improve ethanol production. Instead, ethanol concentration decreased to 0.2 g/L from 384 h to 480 h. This decrease could be due to ethanol utilization by strain CP15 when CO and H_2 mass transfer was limited. In addition, high cell mass concentration required a high amount of carbon for maintenance, requiring ATP through acetic acid production instead of making ethanol. Ethanol was also reported as a substrate for strain CP15 growth (Allen et al., 2010), which explains the decrease of ethanol concentration. Another possible reason for the low ethanol concentration could be due to the increase in dilution rate that washed out ethanol.

Continuous fermentation can wash out cells and products. However, the cells were retained in the fermentor with the cell retention system. Ethanol was not retained in the fermentor as its production rate was lower than its removal rate from the reactor. However, acetic acid accumulated in the fermentor because its production rate was higher than its removal rate. Even though decreasing the pH from 7.0 to 6.5 in the fermentor helped to stimulate ethanol production from 0.2 g/L to 1.4 g/L between 480 h and 518 h,

ethanol concentration then decreased back to 0.2 g/L between 518 h and 576 h with the high cell mass concentration. The specific CO and H_2 molar uptake rates dropped from 20 to 4 mmol CO/(g cells·h) and from 5 to 3 mmol H_2/(g cells·h) between 384 h to 576 h, which was mainly due to the large increase in cell mass concentration from 1.9 to 5.1 g/L. In addition, the increase in cell mass concentration did not result in an improvement in specific CO and H_2 uptake rates (Fig. 6.2 B), which is an indication of CO and H_2 mass transfer limitations. If mass transfer limitations were not present in the fermentor with cell mass concentration increase, the specific CO and H_2 uptake rates should have increased or remained constant.

The syngas fed to the fermentor between 576 h and 672 h was switched from Syngas III (39% CO, 24% CO_2, 27% H_2, 10% N_2, H_2:CO molar ratio ≈ 0.7) to Syngas IV (20% CO, 25% CO_2, 43% H_2, 12% N_2, H_2:CO molar ratio ≈ 2) to investigate if the product profiles change with the higher H_2:CO ratio (Fig. 6.2 A). During this period, the pH was increased to 7.0 at 624 h, which increased cell mass concentration but had only a small effect on ethanol formation. Ethanol concentration was not changed, which could be due to either washout or utilization by strain CP15 as discussed earlier. There was a minor change in the specific CO uptake rate from 3.6 to 3.7 mmol/(g cells·h). The specific H_2 uptake rate increased from 2.9 to 8.0 mmol/(g cells·h) as shown in Fig. 6.2 B. It is important to note that the specific H_2 uptake rate exceeded the specific CO uptake rate when Syngas IV with a H_2:CO ratio of 2 was used due to higher H_2 content. When Syngas III with H_2:CO ratio of 0.7 was used, the specific H_2 uptake rate was lower than the specific CO uptake rate (Fig. 6.2 B).

To examine if the high cell mass concentration in the fermentor caused ethanol

production to drop, cell recycle was stopped from 672 h to 742 h and dilution rate was reduced to 0.011 h^{-1} to prevent a fast cell washout. In addition, Syngas V (28% CO, 60% H_2, 12% N_2, H_2:CO molar ratio ≈ 2) with a similar H_2:CO ratio as in Syngas IV was sparged into the fermentor to provide cells with more CO and H_2. This resulted in a decrease in cell mass concentration in the fermentor from 5.2 g/L to 2.8 g/L at 742 h (Fig. 6.2A). However, ethanol concentration increased to 6.6 g/L. During the same fermentation period, the specific CO and H_2 uptake rates increased from 3.7 to 10.2 mmol CO/(g cells·h) and from 8.0 to 9.7 mmol H_2/(g cells·h), due to the decrease in the cell mass concentration from 5.2 g/L to 2.8 g/L (Fig. 6.2). The agitation speed was increased to 600 rpm at 696 h to provide more gas to cells as their uptake rates were increasing.

The cell recycle system was restarted after 742 h because of the large decrease in cell mass concentration within 70 h of operation and to avoid complete cell washout. From 742 h to 828 h, the cell mass concentration decreased by 34% and acetic acid and ethanol concentrations decreased by 6% and 9%, respectively (Fig. 6.2 A). The specific CO and H_2 uptake rates increased by 22% and 116%, respectively, when the agitation speed was increased from 450 rpm to 600 rpm (Fig. 6.2 B). This indicated that the mass transfer limitation was alleviated by reducing cell mass concentration and increasing agitation. The average molar uptake ratios of H_2:CO using Syngas III, Syngas IV and Syngas V were 0.6, 2.1 and 1.6, respectively. These ratios were close to the H_2:CO ratios supplied in Syngas III (0.7) and in Syngas IV and Syngas IV (2.0). In addition, cells utilized more H_2 than CO when the H_2:CO ratio was above 1. This indicates that the

H_2:CO ratios in syngas affect the cells' preference to uptake H_2 or CO as the electron and carbon source.

6.3.2.2 Fermentation in yeast extract free medium

In the second stage of the continuous fermentation from 840 h to 924 h, YE-free medium was used to evaluate if removing YE would have a positive effect on ethanol production. A previous report showed that eliminating YE from *C. ljungdahlii* syngas fermentation medium increased ethanol concentration (Phillips et al., 1993). However, there was only 13% increase in ethanol production upon removing YE with strain CP15 during the fermentation from 840 h to 924 h (Fig. 6.3 A). In addition, cell mass concentration decreased by 15% and acetic acid concentration decreased by 40% at 924 h. The specific CO uptake rate in YE-free medium with Syngas V (28% CO, 60% H_2, 12% N_2, H_2:CO molar ratio ≈ 2) increased by 3%. However, the specific H_2 uptake rate in YE-free medium with Syngas V decreased by 18% (Fig. 6.3 B).

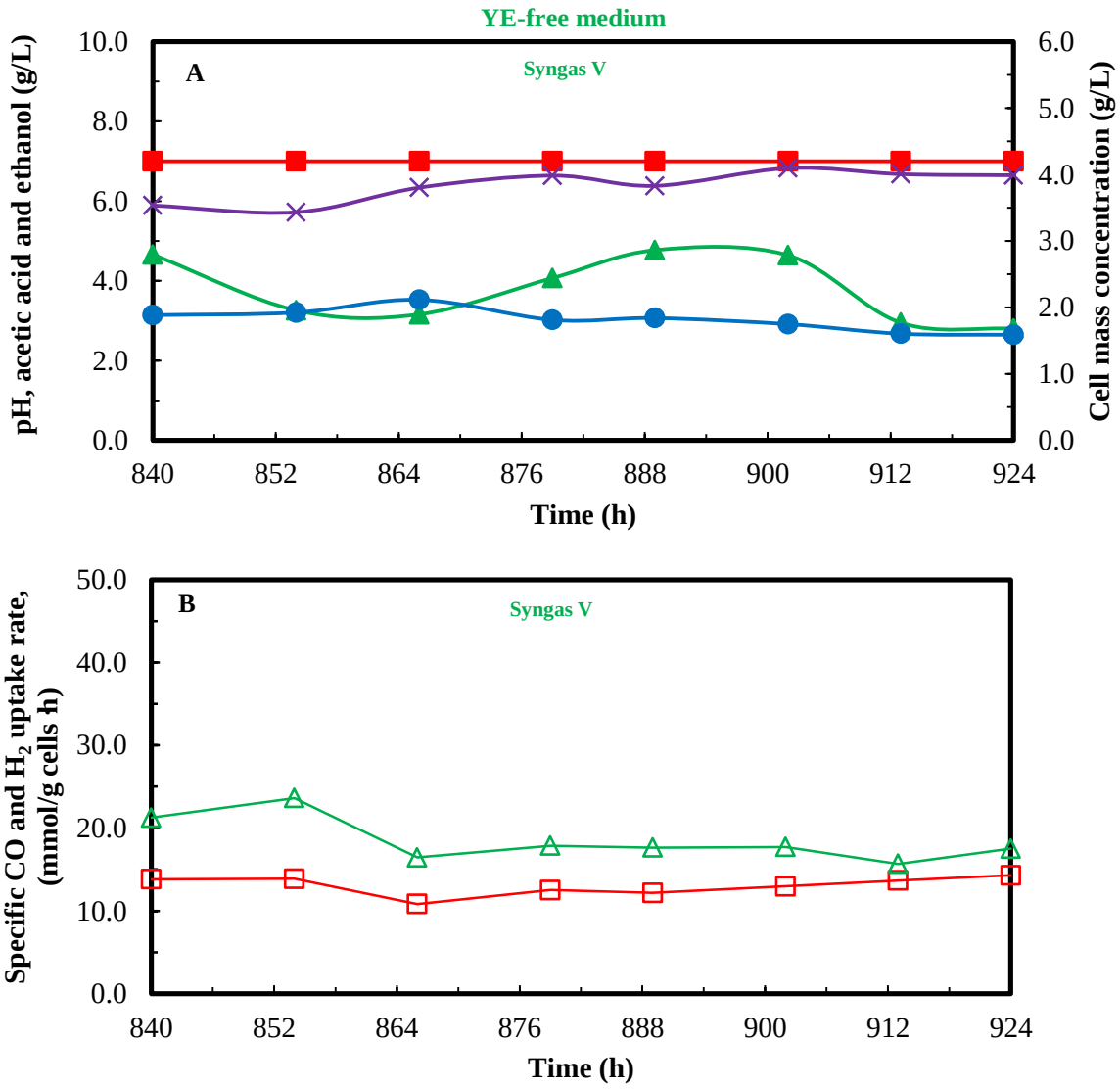

Fig. 6.3 (A) Growth and products profiles (B) Specific gas uptake profiles during continuous syngas fermentation in YE-free medium with cell recycle; pH (■), cell mass concentration (●), acetic acid (▲), ethanol (×), specific CO uptake rate (□), specific H_2 uptake rate (Δ), agitation speed was 600 rpm.

6.3.2.3 Fermentation in CSL medium

In the last stage of the continuous fermentation from 936 h to 1224 h, the medium fed to the fermentor was 20 g/L CSL medium. During this period, there was a slight

increase in ethanol concentration from 6.5 g/L to 7.7 g/L from 936 h to 985 h (Fig. 6.4). However, ethanol concentration quickly decreased to below 2.0 g/L at 1071 h and was stable at a level of 1.7 g/L until the end of fermentation. The specific CO and H_2 uptake rates during this period decreased by 43% and 8%, respectively.

With the CSL medium, n-propanol and n-butanol were produced. The n-propanol and n-butanol concentrations increased to a maximum of 6 g/L and 1 g/L, respectively (Fig. 6.5). In addition, the maximum concentrations of propionic acid and butyric acid were 3.0 g/L and 0.5 g/L, respectively. The decrease in ethanol concentration and production of both n-propanol and n-butanol in CSL medium previously were not observed with strain CP15 during syngas fermentations (Allen et al., 2010; Liu et al., 2012). In addition, strain CP15 was not reported to produce n-propanol or n-butanol. This indicated that the fermentation broth was contaminated with other microorganisms.

Thus, the microbial assemblage in the fermentation broth was characterized by surveying 16S rRNA gene sequences present and determining the identity of contaminants in the fermentor. A total of 61 sequenced clones were analyzed, which indicated that 34 (56%) were from *A. bacchi* strain CP15 and 21 (34%) were classified as *Clostridium propionicum*. The six remaining clones (10%) were characterized as *Clostridium amylolyticum* (2 clones), *Clostridium putrefaciens* (2 clones), *Clostridium carnis* and *Clostridium celerecrescens* (1 clone each). During this continuous fermentation, there was a power failure between 792 h to 812 h, which resulted in no gas and liquid flowing in and out of the fermentor, no agitation and no liquid flowing in the cell recycle system. In addition, n-propanol and n-butanol were first detected between

742 h and 828 h (Table 6.4), which indicates this could be when contamination occurred. However, the exact reason of contamination was unknown.

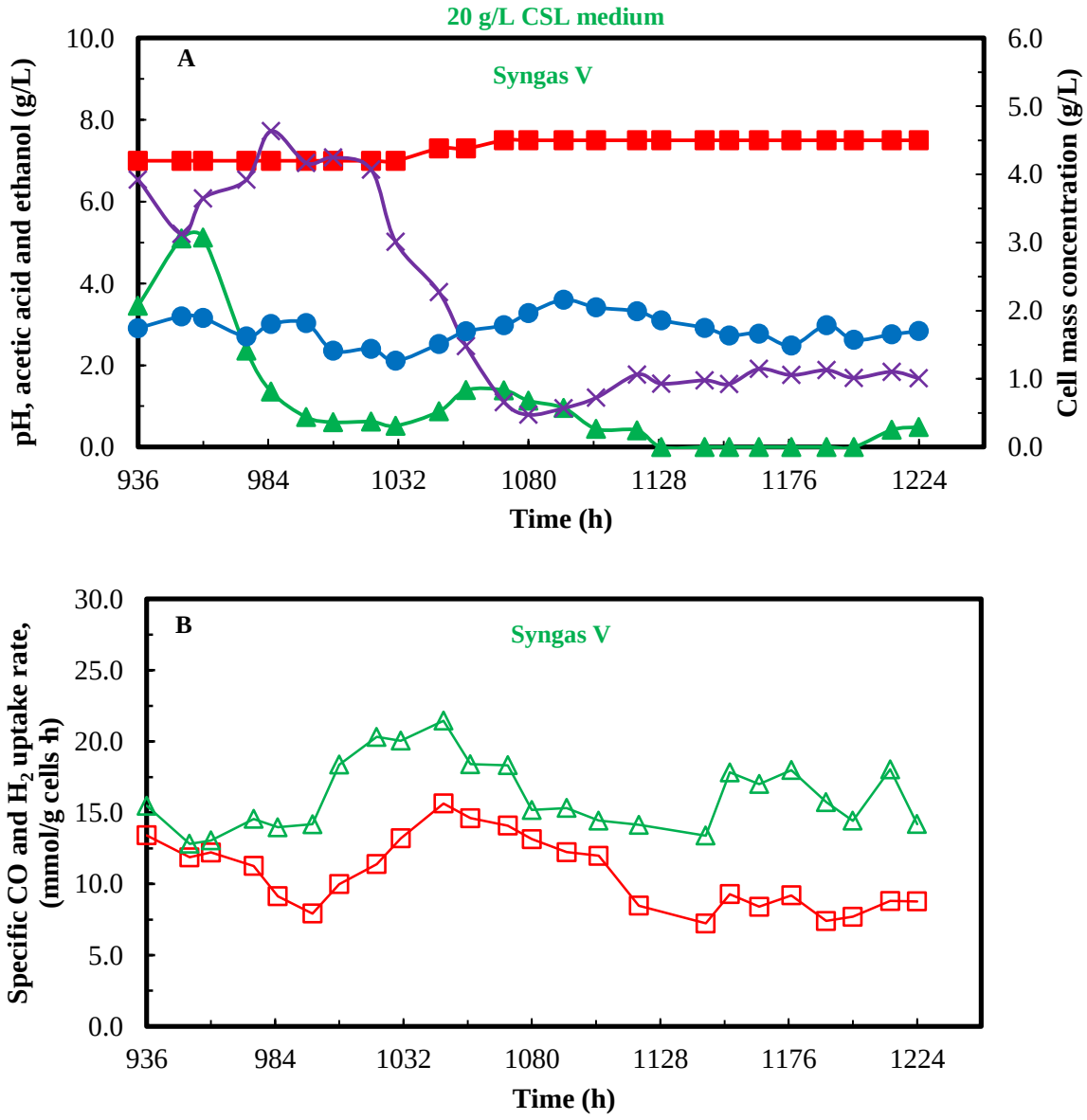

Fig. 6.4 (A) Growth and products profiles (B) Specific gas uptake profiles during continuous syngas fermentation in 20 g/L CSL medium with cell recycle; pH (■), cell mass concentration (●), acetic acid (▲), ethanol (×), specific CO uptake rate (□), specific H_2 uptake rate (Δ); agitation speed was 600.

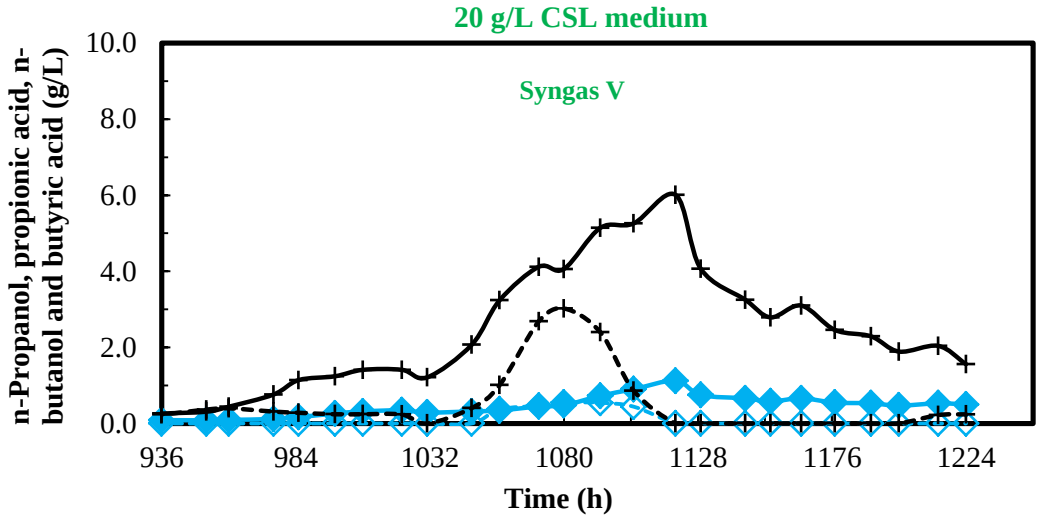

Fig. 6.5 n-propanol, n-butanol, propionic acid and butyric acid profiles during continuous syngas fermentation in 20 g/L CSL medium with cell recycle; n-propanol (+ and solid line), propionic acid (+ and dash line), n-butanol (♦ and solid line), butyric acid (◊ and dash line).

The product profiles at various dilution rates in YE medium with Syngas III and pH 7.0 are shown in Fig. 6.6. Cell mass concentration increased with the increase in dilution rate, which is expected because of the cell recycle system and addition of more nutrients in the fermentor. Acetic acid concentration increased when the dilution rate was above 0.017 h^{-1}. Ethanol production also increased with increasing the dilution rate and reached its highest concentration, 2.1 g/L, at dilution rate 0.022 h^{-1}, at which ethanol productivity was 42 mg/g cells·h (Fig. 6.6 A). However, ethanol concentration and productivity quickly decreased when the dilution rate was increased to 0.033 h^{-1}.

CO and H_2 utilization improved with the increase in the dilution rate due to production of more cells (Fig. 6.6 B). The specific CO uptake rate decreased with the increase of dilution rate. However, H_2 uptake rates decreased until dilution rate was increased to 0.022 h^{-1}, and then it remained constant at dilution rate 0.033 h^{-1}. It was

predicted from the cell growth kinetic model that *Eubacterium limosum* KIST 612 required 5.2 mmol CO/g cells·h for maintenance in fermentation with pure CO (Chang et al., 2001). In the present study, the average specific uptake rates of CO between 480 h and 672 h in the YE medium with Syngas III and Syngas IV at a cell mass concentration of 5 g/L were 5.4 mmol CO/ g cells ħ and 3.5 mmol CO/g cells·h, respectively (Table 6.4). These specific uptake rates of CO by strain CP15 were close to the value reported with *E. limosum* KIST 612. Assuming that strain CP15 has a similar CO maintenance requirement, there was not enough CO transferred to the cells and therefore, cells utilized ethanol for maintenance, which can also explain the low ethanol concentration in the fermentor (Fig. 6.2).

Ethanol concentration in YE medium was at least threefold greater with Syngas V and cell recycle, compared to either Syngas III or Syngas IV (Table 6.4). This was because Syngas V contained more reductants (CO and H_2) compared to either Syngas III or Syngas IV. In addition, the average ethanol yield from CO was the highest with Syngas V in the three media used. About 7% more ethanol was formed in the YE-free medium compared to the YE medium. The use of YE-free medium shifted the conversion of CO and H_2 from more cells to ethanol. Ethanol production in CSL medium was lower than YE and YE-free media. CO utilization in YE medium ranged from 19% to 61% of the supplied gas, while H_2 utilization ranged from 18% to 54% (Table 6.4). The average CO and H_2 utilization in YE-free medium were comparable to YE medium at the same operating conditions with Syngas V. However, CO and H_2 utilization with Syngas V were the lowest in CSL medium (Table 6.4) due to low cell mass concentration.

Table 6.4 Fermentation parameters during continuous syngas fermentation in 7-L fermentor at various operating conditions.

Medium	**YE**								**YE-free**	**CSL**
Time range, h	13-120	120-216	216-288	288-384	384-480	480-576	576-672	742-828	828-924	924-1224
Syngas	III	III	III	III	III	III	IV	V	V	V
Agitation, rpm	150-300	300	300	450	450	450	450	600	600	600
pH	6.5	7.0	7.0	7.0	7.0	6.5	6.5-7.0	7.0	7.0	7.0-7.5
Dilution rate, h^{-1}	0.011	0.011	0.017	0.022	0.033	0.033	0.017-0.033	0.011	0.011	0.011-0.017
Avg. cell mass conc., g/L	0.40	0.73	1.01	1.59	3.10	5.05	4.85	2.25	1.82	1.73
Avg. acetic acid conc. g/L	2.22	0.48	0.00	0.26	2.76	3.44	2.74	4.06	3.73	1.09
Avg. ethanol conc., g/L	0.28	1.36	1.46	1.96	0.20	0.75	0.25	5.99	6.39	3.42
Avg. ethanol productivity, mg/L·h	3.04	15.01	24.13	42.06	6.61	24.73	8.37	65.91	70.30	39.97
Avg. ethanol yield from CO, %	2.98	11.50	18.54	23.78	2.61	10.83	6.01	34.65	39.35	30.57
Avg. CO utilization, %	19.28	28.35	28.47	41.22	59.22	48.57	57.57	61.48	56.97	43.90
Avg. H_2 utilization, %	18.30	23.81	22.81	22.21	53.62	37.18	53.52	44.02	37.88	30.62
Avg. specific CO uptake rate, mmol/g cells·h	28.84	24.18	16.97	15.14	11.82	5.43	3.46	11.35	12.73	10.87
Avg. specific H_2 uptake rate, mmol/g cells·h	19.89	14.32	9.60	5.84	7.35	2.89	6.95	17.65	17.14	16.25
Max. n-propanol, g/L	ND	ND	ND	ND	ND	ND	ND	0.16	0.21	6.01
Max. n-butanol, g/L	ND	ND	ND	ND	ND	ND	ND	0.09	0.09	1.11

ND: Not detectable.

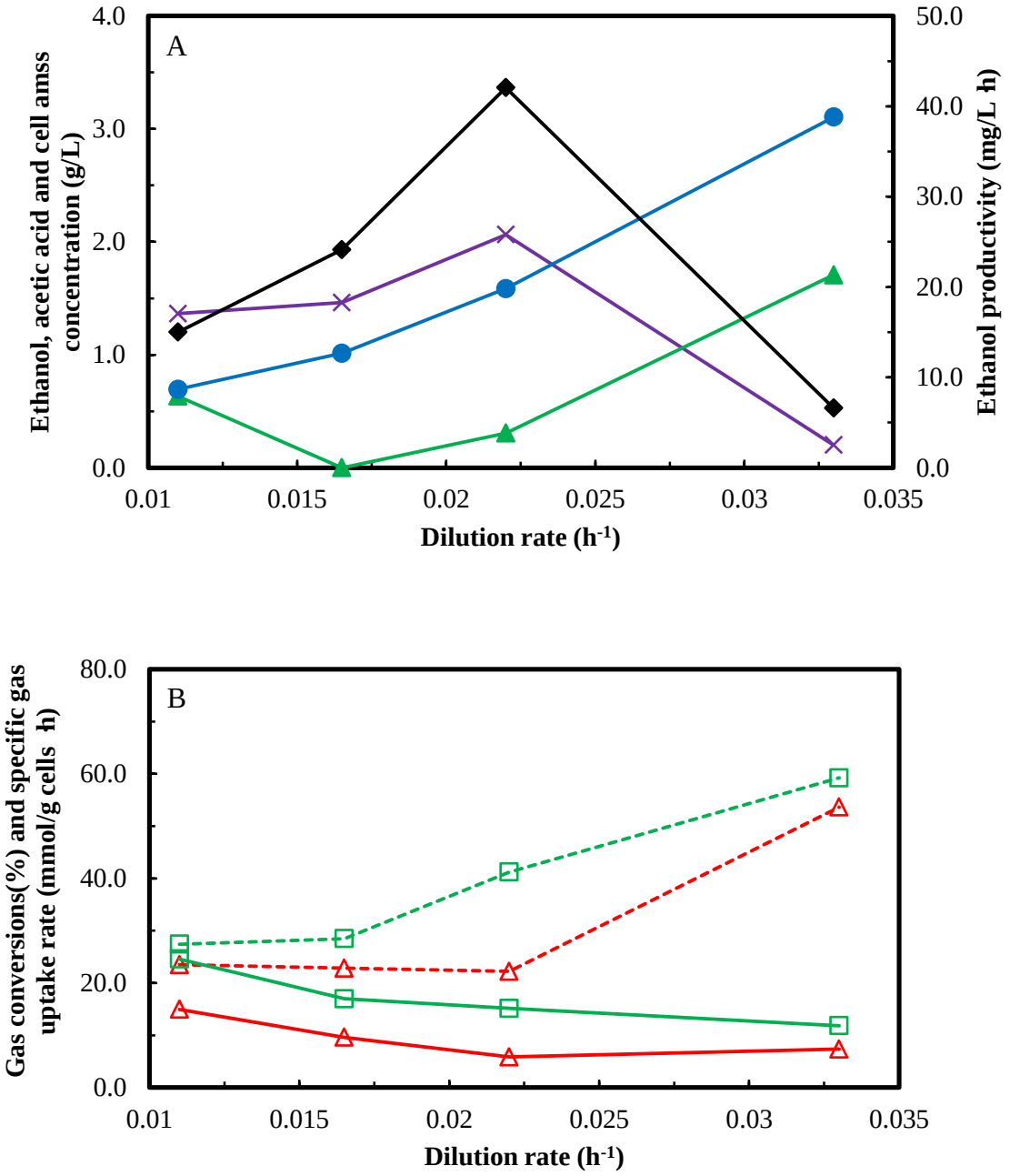

Fig. 6.6 Fermentation profiles in YE medium at various dilution rates at pH 7.0 using Syngas III (A) products profiles, (B) gas uptake profiles; cell mass (●), acetic acid (▲), ethanol (×), ethanol productivity (♦), specific CO uptake rate (□), specific H_2 uptake rate (Δ), CO utilization (□ and dash line), and H_2 utilization (Δ and dash line).

Compared to previous syngas fermentation studies in CSTR, the maximum ethanol productivity of 70 mg/L ħ obtained in the present study with Synags V in YE-free medium (Table 6.4) was close to that reported for *C. ljungdahlii* without cell recycle (78 mg/L ħ) (Mohammadi et al., 2012), but much lower than with cell recycle using *C. ljungdahlii* (1632 mg/L ħ) (Phillips et al., 1993). Coskata, Inc., a company pursing commercialization of syngas fermentation technology, reported an ethanol productivity of 247 mg/L ħ by *Clostridium coskatii* in a continuous fermentation without cell recycle (Zahn and Saxena, 2011). This rate was 3.5 times higher than the rate observed with strain CP15. However, strain CP15 had 4.1 times higher ethanol productivity than *C. ragsdalei* (17 mg/L ħ) in batch fermentation with a continuous gas flow using YE medium (Maddipati et al., 2011).

Although a decrease in ethanol concentration was observed in 20 g/L CSL medium due to contamination, the average ethanol productivity in the present study was 40 mg/L ħ, which was still 48% higher than *C. ragsdalei* in 20 g/L CSL medium (Maddipati et al., 2011). To improve ethanol productivity of strain CP15 in continuous fermentation, mass transfer limitation must be addressed by improving gas transfer rate through increasing gas flow rate, agitation speed or using other reactor configurations such as trickle bed reactor (TBR) or hollow fiber membrane reactor (HFR) (Orgill et al., 2013). In addition, consumption of ethanol by cells should be avoided. This can be done by adjusting reactor conditions and balancing cell mass concentration and the mass transfer rate to provide enough CO and H_2 to meet cells' maintenance requirements and divert CO and H_2 to ethanol formation. The use of lean medium such as YE-free medium can also enhance ethanol production (Table 6.4). The YE-free medium has a low growth

stimulator, which can be a good production medium when a cell recycle system is used.

The simultaneous production of n-propanol and n-butanol with ethanol during the late stages of continuous fermentation with strain CP15 has not been reported previously. The contamination of the fermentor with *C. propionicum* was identified as being probably responsible for n-propanol and n-butanol production at late stages of the fermentation. The culture present in the CSL medium was a mixed culture as confirmed with the 16S rRNA gene sequence. The mixed culture presents a new opportunity for the production of higher alcohols from syngas, which previously has not been reported in the literature.

C. propioncium has been reported to convert lactic acid and the amino acid alanine to propionic acid (Cardon and Barker, 1946; Tholozan et al., 1992). Butyric acid was also produced by *C. propioncium* from the four carbon-amino acid threonine (Cardon and Barker, 1946), which is an amino acid available in YE and CSL. In addition, *Clostridium neopropionicum* was able to convert ethanol into propionic acid and *C. propionicum* displayed a similar metabolic pathway to *C. neopropionicum* (Tholozan et al., 1992). The decreasing ethanol concentration and propionic acid production in CSL medium could have been because of *C. propionicum* or the four other *Clostridium* species in the minority found in the fermentor (Fig. 6.5). In addition, strains *C. ragsdalei* and *C. ljungdahlii* showed the ability to convert propionic acid and butyric acid to corresponding alcohols (Isom et al., 2011; Perez et al., 2012), indicating strain CP15 could have a similar capacity to convert propionic acid or butyric acid produced by *C. propionicum* in the mixed culture into n-propanol and n-butanol. The conversions of these organic acids

to their corresponding alcohols during syngas fermentation using the mixed culture warrant further investigation, which are discussed in Chapter 7.

6.4 Conclusions

Alkalibaculum bacchi CP15 produced 78% more ethanol by replacing yeast extract (YE) with corn steep liquor (CSL) in bottle fermentations. A sustainable ethanol concentration of 6 g/L was achieved in the YE and YE-free media during continuous fermentation with cell recycle. Ethanol production decreased due to high cell mass concentration above 5 g/L and mass transfer limitation. A mixed culture was obtained during continuous fermentation in the CSL medium, which mainly consisted of *A. bacchi* CP15 and *C. propionicum*. The mixed culture produced a maximum of 8 g/L ethanol, 6 g/L n-propanol and 1 g/L n-butanol.

6.5 References

Ahmed, A., Cateni, B.G., Huhnke, R.L., Lewis, R.S., 2006. Effects of biomass-generated producer gas constituents on cell growth, product distribution and hydrogenase activity of *Clostridium carboxidivorans* $P7^T$. Biomass Bioenerg. 30, 665-672.

Allen, T.D., Caldwell, M.E., Lawson, P.A., Huhnke, R.L., Tanner, R.S., 2010. *Alkalibaculum bacchi* gen. nov., sp. nov., a CO-oxidizing, ethanol-producing acetogen isolated from livestock-impacted soil. Int. J. Syst. Evol. Microbiol. 60, 2483-2489.

Bakker, A., Smith, J., Myers, K.J., 1994. How to disperse gases in liquids. Chem. Eng. 101, 98-104.

Cardon, B., Barker, H., 1946. Two new amino-acid-fermenting bacteria, *Clostridium propionicum* and *Diplococcus glycinophilus*. J. Bacteriol. 52, 629-634.

Chang, I.S., Kim, B.H., Lovitt, R.W., Bang, J.S., 2001. Effect of CO partial pressure on cell-recycled continuous CO fermentation by *Eubacterium limosum* KIST612. Process Biochem. 37, 411-421.

Chun, J., Lee, J.H., Jung, Y., Kim, M., Kim, S., Kim, B.K., Lim, Y.W., 2007. EzTaxon: a web-based tool for the identification of prokaryotes based on 16S ribosomal RNA gene sequences. Int. J. Syst. Evol. Microbiol. 57, 2259-2261.

DeSantis Jr., T., Hugenholtz, P., Keller, K., Brodie, E., Larsen, N., Piceno, Y., Phan, R., Andersen, G., 2006. NAST: a multiple sequence alignment server for comparative analysis of 16S rRNA genes. Nucleic Acids Res. 34, W394-W399.

DeSantis, T.Z., Hugenholtz, P., Larsen, N., Rojas, M., Brodie, E.L., Keller, K., Huber, T., Dalevi, D., Hu, P., Andersen, G.L., 2006. Greengenes, a chimera-checked 16S rRNA gene database and workbench compatible with ARB. Appl. Environ. Microbiol. 72, 5069-5072.

Gordillo, G., Annamalai, K., 2010. Adiabatic fixed bed gasification of dairy biomass with air and steam. Fuel 89, 384-391.

Isom, C., Nanny, M., Tanner, R. 2011. Reduction of acids to alcohols by novel acetogens. Annual Meeting of the American Society for Microbiology. Abstract Q-1358.

Kundiyana, D.K., Huhnke, R.L., Maddipati, P., Atiyeh, H.K., Wilkins, M.R., 2010. Feasibility of incorporating cotton seed extract in *Clostridium* strain P11 fermentation medium during synthesis gas fermentation. Bioresour. Technol. 101, 9673-9680.

Kundiyana, D.K., Huhnke, R.L., Wilkins, M.R., 2011. Effect of nutrient limitation and two-stage continuous fermentor design on productivities during "*Clostridium ragsdalei*" syngas fermentation. Bioresour. Technol. 102, 6058-6064.

Lawford, H., Rousseau, J., 1997. Corn steep liquor as a cost-effective nutrition adjunct in high-performance *Zymomonas* ethanol fermentations. Appl. Biochem. Biotechnol. 63-65, 287-304.

Liu, K., Atiyeh, H.K., Tanner, R.S., Wilkins, M.R., Huhnke, R.L., 2012. Fermentative production of ethanol from syngas using novel moderately alkaliphilic strains of *Alkalibaculum bacchi*. Bioresour. Technol.336-341.

Maddipati, P., Atiyeh, H.K., Bellmer, D.D., Huhnke, R.L., 2011. Ethanol production from syngas by *Clostridium* strain P11 using corn steep liquor as a nutrient replacement to yeast extract. Bioresour. Technol. 102, 6494-6501.

Mohammadi, M., Younesi, H., Najafpour, G., Mohamed, A.R., 2012. Sustainable ethanol fermentation from synthesis gas by *Clostridium ljungdahlii* in a continuous stirred tank bioreactor. J. Chem. Technol. Biotechnol. 87, 837-843.

Orgill, J.J., Atiyeh, H.K., Devarapalli, M., Phillips, J.R., Lewis, R.S., Huhnke, R.L., 2013. A comparison of mass transfer coefficients between trickle-bed, hollow

fiber membrane and stirred tank reactors. Bioresour. Technol. 133, 340-346.

Perez, J.M., Richter, H., Loftus, S.E., Angenent, L.T., 2012. Biocatalytic reduction of short-chain carboxylic acids into their corresponding alcohols with syngas fermentation. Biotechnol. Bioeng. 110, 1066-1077.

Phillips, J., Klasson, K., Clausen, E., Gaddy, J., 1993. Biological production of ethanol from coal synthesis gas. Appl. Biochem. Biotechnol. 39, 559-571.

Pruesse, E., Quast, C., Knittel, K., Fuchs, B.M., Ludwig, W., Peplies, J., Glöckner, F.O., 2007. SILVA: a comprehensive online resource for quality checked and aligned ribosomal RNA sequence data compatible with ARB. Nucleic Acids Res. 35, 7188-7196.

Shuler, M.L., Fikret, K. 2002. Bioprocess Engineering: Basic concepts. Second ed. Prentice Hall, Englewood Cliffs, New Jersey, pp.576.

Tanner, R.S., 2007. Cultivation of bacteria and fungi. in: Hurst CJ, Crawford AL, Mills AL, Garland JL, Stetzenbach LD, Lipson DA (Eds.), Manual of Environmental Microbiology. ASM Press, Washington D. C., pp. 69-78.

Tholozan, J., Touzel, J., Samain, E., Grivet, J., Prensier, G., Albagnac, G., 1992. *Clostridium neopropionicum* sp. nov., a strict anaerobic bacterium fermenting ethanol to propionate through acrylate pathway. Arch. Microbiol. 157, 249-257.

Turn, S., Kinoshita, C., Zhang, Z., Ishimura, D., Zhou, J., 1998. An experimental investigation of hydrogen production from biomass gasification. Int. J. Hydrogen Energy 23, 641-648.

Ukpong, M.N., Atiyeh, H.K., De Lorme, M.J.M., Liu, K., Zhu, X., Tanner, R.S., Wilkins, M.R., Stevenson, B.S., 2012. Physiological response of *Clostridium carboxidivorans* during conversion of synthesis gas to solvents in a gas-fed bioreactor. Biotechnol. Bioeng. 109, 2720-2728.

Wilkins, M.R., Atiyeh, H.K., 2011. Microbial production of ethanol from carbon monoxide. Curr. Opin. Biotechnol. 22, 326-330.

Zahn, J.A., Saxena, J. 2011. Novel ethanologenic clostridium species, *Clostridium coskatii*. US patent 2011/0229947.

CHAPTER VII

MIXED CULTURE SYNGAS FERMENTATION AND CONVERSION OF CARBOXYLIC ACIDS INTO ALCOHOLS

7.1 Introduction

Efforts to develop renewable energy are driven by the negative impacts of satiating an ever-increasing global consumption of energy with the burning of fossil fuels (Atsumi et al., 2008). The costs associated with transitioning from fossil to renewable transportation fuels will be minimized if major changes in existing infrastructures can be avoided. Ethanol is a renewable transportation fuel (i.e. biofuel) that can be directly blended with gasoline. Ethanol, however, is hygroscopic and has corrosive characteristics that translate into increased transportation costs because it must be transported mainly by trucks instead of existing gasoline pipelines (Tyner, 2010). Higher alcohols such as n-butanol and n-hexanol are candidates to replace ethanol due to their higher energy density and lower water solubility than ethanol. n-Butanol is less hygroscopic than ethanol and it has a 29% higher volumetric energy density than ethanol (ethanol 21 MJ/L vs n-butanol 27 MJ/L) (Mann et al., 2006; Atsumi and Liao, 2008). n-Propanol is an important

chemical for ink, polymer and pharmaceutical industries (Demirer and Speece, 1998). n-Propanol has also been considered as a candidate for the replacement of gasoline (Simmons, 2011). n-Hexanol has low miscibility with water, less volatility than ethanol and n-butanol and can be blended with biodiesel or gasoline (Yeung and Thomson, 2013). Thus, these higher alcohols have more potential than ethanol as "drop-in" biofuels, and they also can be converted to jet fuels and chemicals (Harvey and Meylemans, 2011).

The hybrid gasification-syngas fermentation technology for the production of fuels and chemicals is on the verge of commercialization. In this process, syngas is produced by gasification of biomass or municipal solid waste followed by conversion of syngas components CO, H_2 and CO_2 to liquid fuels and chemicals (Wilkins and Atiyeh, 2011). Several reports have been published on the production of ethanol and higher alcohols such as n-butanol using syngas fermentation by *Clostridium carboxidivorans*, *Clostridium ragsdalei*, and *Eubacterium limosum* previous known as *Butyribacterium methylotrophicum*(Shen et al., 1999; Tanner, 2008; Maddipati et al., 2011; Ukpong et al., 2012; Ramachandriya et al., 2013). In addition, *C. ragsdalei* is able to convert acetone to isopropanol during syngas fermentation (Ramachandriya et al., 2011).

All previous studies of syngas fermentation for the production of liquid fuels have been focused on the use of monocultures. Mixed cultures of sulfate reducing bacteria, methanogenic archaea and homoacetogenic bacteria using H_2/CO_2 or CO have been reported to produce methane during anaerobic digestion of sludge (Esposito et al., 2003; Sipma et al., 2004). In another study, a mixed culture containing *Rhodospirillum rubrum*, *Methanobacterium formicicum* and *Methanosarcina barkeri* was reported to convert CO,

CO_2 and H_2 to methane via syntrophy among the three bacteria (Klasson et al., 1990).

Alkalibaculum bacchi strain CP15 is capable of producing ethanol at a yield that is 43% higher than *A. bacchi* strains $CP11^T$ and CP13 (Liu et al., 2012). In chapter 6, it was shown that cost of the syngas fermentation medium for strain CP15 can be reduced by 27% by removing costly [N-Tris (hydroxymethyl) methyl]-3-aminopropanesulfonic acid (TAPS buffer) as well as replacing the yeast extract (YE), minerals, and vitamins with the corn steep liquor (CSL). There was 78% more ethanol produced in 20 g/L CSL medium than in the YE medium using strain CP15, indicating the potential of CSL use as a cost-effective nutrient for large scale fermentation. Additionally in Chapter 6, it was shown that strain CP15 can grow to high cell mass concentration during continuous syngas fermentation with cell recycling. During this continuous syngas fermentation in CSL medium, which has not been reported previously for strain CP15 (Allen et al., 2010; Liu et al., 2012). These alcohols were produced from a serendipitous mixed culture formed at the late stages of a continuous fermentation as confirmed by a 16S rRNA gene sequencing. As shown in Chapter 6, the mixed culture consisted largely of *A. bacchi* CP15 (56%) and *Clostridium propionicum* (34%), with the remaining 10% made up of 4 other *Clostridium* species

C. propionicum is known to consume amino acids, and ferments lactate via the acrylate-CoA pathway, converting lactate into propionate and acetate (Cardon and Barker, 1946; Tholozan et al., 1992). *C. propionicum* was reported to not consume carbohydrates (Cardon and Barker, 1946; O'Brien et al., 1990). To our knowledge, there have been no previous reports of n-propanol production during syngas fermentation via mixed culture. This study investigated the production of ethanol, n-propanol and

n-butanol during syngas fermentation using the mixed culture in YE and CSL media in a 3-L fermentor. The ability of a monoculture of *A. bacchi* strain CP15 and a mixed culture of mainly *A. bacchi* CP15 and *C. propionicum* to convert carboxylic acids into their corresponding alcohols was also examined.

7.2 Materials and methods

7.2.1 Microorganisms

The monoculture of *A. bacchi* strain CP15 and mixed culture were maintained on yeast extract (YE) medium with an initial pH 8.0 under anaerobic condition at 37 ℃. The YE medium preparation was previously described (Liu et al., 2012). Inocula of strain CP15 and the mixed culture were prepared by sub-culturing twice to reduce the lag phase of growth. Fermentations with either strain CP15 or the mixed culture were inoculated with 10% (v/v) inocula.

7.2.2 Semi-continuous fermentation in a 3-L fermentor using mixed culture

A 3-L fermentor (Bioflo 110, New Brunswick Scientific Co., Edison, NJ, USA) with 2.5 L working volume was used in a semi-continuous fermentation (i.e., only continuous syngas feed). Two six-blade Rushton impellers separated by a distance equal to the impeller diameter were mounted on an agitator shaft as suggested by Bakker et al. (1994). Four baffles were used to avoid vortices.YE medium and 20 g/L CSL medium without TAPS buffer were used. The YE medium also contained YE, minerals, vitamins and trace metals as descried previously (Liu et al., 2012). The 20 g/L CSL was used to replace YE, vitamins and minerals in the YE medium. All media contained 5 g/L $NaHCO_3$ as a buffer, 2.5 mL/L of 4% cysteine sulfide solution as a reducing agent, and

1 mL/L of 0.1% resazurin solution as a redox indicator. The compositions of the minerals, trace metals and vitamins stock solutions were previously reported (Tanner, 2007). The medium in the fermentor was sterilized at 121 ℃ for 30 min and allowed to cool to room temperature by purging 18 sccm (standard cubic centimeter per minute) N_2 at 150 rpm agitation for 3 h. The medium was then purged for 8 h with 18 sccm Syngas VI (38% CO, 28.5% H_2, 28.5% CO_2 and 5% N_2 by volume, Stillwater Steel Co., Stillwater, OK, USA). Before inoculation, the medium was reduced by adding 2.5 mL/L 4% cysteine sulfide. The fermentor was inoculated with 10% (v/v) of the mixed culture. The inlet gas flow rate was controlled by a thermal mass flow controller (Porter, Hatfield, PA, USA). The pressure in the fermentor headspace was 1 atm (101 kPa). The pH of the medium during the fermentation was controlled above 6.1 via the addition of 7% $NaHCO_3$ because preliminary results showed a substantial decrease in H_2 conversion at pH below 6.1 (Appendix G). When foam in the fermentor was 1.27 cm above the level of liquid, 0.2 mL of 5% antifoam (Antifoam B emulsion, Sigma-Aldrich, St. Louis, MO, USA) was added. The fermentation temperature was controlled at 37 ℃ via a heating jacket (New Brunswick Scientific Co., Edison, NJ, USA). A condenser and a bubbler controlled at 5 ℃ by a refrigerated recirculator (1156D, VWR International, West Chester, PA, USA) were used to condense the vapor leaving the exhaust gas line. Liquid and gas samples were withdrawn from the reactor periodically to measure pH, cell mass and product concentrations, and gas compositions in the exhaust gas line.

7.2.3 Conversion of carboxylic acids into alcohols in bottle fermentations

Fed-batch fermentations in 250-mL bottles (Wheaton, NJ, USA) with 100 mL working volume were used in the conversion of carboxylic acids into alcohols. The

fermentation medium used was the YE medium. The carboxylic acids used included propionic acid, butyric acid, hexanoic acid and lactic acid. Each carboxylic acid was added separately to the medium at the beginning of fermentation to have an initial concentration around 1.5 g/L. A control treatment was used that contained all medium components but no carboxylic acid. The initial pH of the medium was adjusted to pH 7.5 by adding sterilized 2N KOH, and each bottle was inoculated with 10% (v/v) of either strain CP15 or the mixed culture. The Syngas II was used containing 40% CO, 30% CO_2, and 30% H_2 by volume (Stillwater Steel Co., Stillwater, OK, USA). The syngas was fed into all bottles every 24 h at 239 kPa, and the bottles were incubated at 37 ℃ and 150 rpm on an orbital shaker (Innova 2100, New Brunswick Scientific, Edison, NJ, USA). In a related experiment, lactic acid was added to the YE medium, headspace in the bottle was pressurized with 100% N_2 at 121 kPa, and the medium was inoculated with the mixed culture. The purpose of this experiment was to determine if the mixed culture could produce n-propanol from lactic acid under N_2 headspace. Liquid and gas samples were withdrawn to measure pH, cell mass concentration, carboxylic acid and product concentrations, and gas compositions in the headspace. All fermentations were done in triplicate.

7.2.4 Analytical procedures

7.2.4.1 Cell mass, acid and solvent concentrations and gas analysis

Cell mass concentration measurements were made at 660 nm as previously reported (Liu et al., 2012). Each liquid sample (0.7 mL) was acidified using 0.7 mL 0.1 N HCl. Ethanol, n-propanol, n-butanol, n-hexanol, acetic acid, propionic acid, butyric

acid and hexanoic acid concentrations were analyzed using gas chromatography (GC) (Agilent 7890 N GC, Agilent Technologies, Wilmington, DE, USA) with a flame ionization detector (FID) and DB-FFAP capillary column (Agilent Technologies, Wilmington, DE, USA). The detailed GC working conditions for solvents analysis were the same as in Chapter 6.

A volume of 100 µL of gas from 250-mL bottle headspace or the 7-L fermentor's exhaust line was injected in an Agilent 6890N GC (Agilent Technologies, Wilmington, DE, USA) to determine gas composition in the headspace. The detailed GC working conditions for gas analysis were the same as in Chapter 6.

The sugar content of the liquid samples in the CSL medium was measured using high pressure liquid chromatography (HPLC) (Agilent 1200 series, Wilmington, DE, USA) with a refractive index detector (RID). A Rezex^{TM} RPM-Monosaccharide column (Phenomenex, Torrance, CA, USA) was used and operated at 80˚C with deionized water as the mobile phase pumped at 0.6 mL/min for 25 min per sample. Lactic acid concentration in the CSL medium in the 3-L fermentor or in bottle fermentations was determined using HPLC (Agilent 1200 series, Wilmington, DE, USA) with RID and BioRad HPX-87H column (BioRad Corporate, Hercules, CA, USA). The column temperature was 60 ˚C using 0.01 N H_2SO_4 as the mobile phase and pumped at 0.6 mL/min for 40 min per sample.

7.2.4.2 Statistical analysis and kinetic parameters calculation

Duncan's multiple range test was analyzed by GLM procedure using SAS Release 9.3 (Cary, NC, USA) at 95% confidence level to determine pairwise statistical

differences of ethanol concentration, cell mass concentration, gas utilizations and total alcohols production in bottle study among all treatments using either the strain CP15 alone or the mixed culture. Each TTEST was performed using SAS Release 9.3 (Cary, NC, USA) to identify any significant differences (≥95% confidence) in cell growth, carboxylic acid conversion, ethanol production, total alcohol production or gas utilization between strain CP15 and the mixed culture. The estimation of cell mass yield, gas utilization and ethanol yield were reported in previously (Liu et al., 2012).

The percentage conversion of ethanol to n-propanol was calculated using Eq. 1:

Ethanol conversion to n-propanol, % (mol/mol) =

$$\frac{\text{Propanol produced from consumed ethanol, mol}}{\text{Consumed ethanol, mol}} \times 100\% \qquad (1)$$

Carboxylic acids (propionic acid, butyric acid, hexanoic acid or lactic acid) conversions to corresponding alcohols were calculated when the concentration of the alcohol reached a maximum using Eq. 2:

Carboxylic acid conversion, % (mol/mol) =

$$\frac{\text{Maximum moles of produced corresponding alcohol}}{\text{Initial moles of each carboxylic acid}} \times 100\% \qquad (2)$$

The carbon balance was calculated based on the percentage of total carbon produced divided by total carbon consumed. The total produced carbon included that from produced ethanol, n-propanol, n-butanol, acetic acid, propionic acid, butyric acid and CO_2. The total consumed carbon included that from consumed CO, sugars and lactic acid from CSL and the carboxylic acids added into the medium.

7.3 Results and discussion

7.3.1 Semi-continuous fermentation in a 3-L fermentor using mixed culture

7.3.1.1 Cell growth and pH profiles

The maximum cell mass concentrations of the mixed culture were similar in both the YE and CSL media and reached 0.73 g/L (OD 1.9) (Fig. 7.1 A). Cells entered stationary growth phase 48 h after inoculation in both media. Cell mass concentration remained constant in the CSL medium but started to decrease after 84 h in the YE medium, suggesting nutrient limitation. In addition, the growth rate of the mixed culture in the CSL medium was 56% higher than in the YE medium (Table 7.1), which could be due to the consumption of the 1 g/L lactic acid present in the CSL medium in the first 48 h by *C. propionicum* of the mixed culture.

The initial pH of both YE and CSL media before inoculation was 8.0. However, before the addition of reducing agent into the fermentor and inoculation, the medium was purged 8 h with Syngas VI (38% CO, 28.5% H_2, 28.5% CO_2 and 5% N_2 by volume), which resulted in the decrease in pH to 7.1 due to dissolving CO_2 from the syngas in the medium. This value was consistent with the calculated equilibrium medium pH 7.2 using a modified Henderson-Haselbach equation for $NaHCO_3/CO_2$ buffer system (Sowers and Noll, 1995). In the present study, no TAPS buffer was added to the medium. Therefore, the buffer capacity was mainly dependent on the $NaHCO_3/CO_2$ buffer system. During the fermentation, the pH of both media decreased to 6.1 in the first 40 h and remained at this level until 80 h with the pH controlled at above 6.1 by the addition of 7% $NaHCO_3$ (Fig. 7.1 A). The decrease in pH during the first 80 h mainly resulted from acetic acid

production (Fig. 7.1 B). After 80 h, the pH increased to 6.4 in YE medium and 6.3 in CSL medium, which was due to acetic acid conversion to ethanol (Fig. 7.1 B). However, it was observed that the pH of both media decreased to 6.1 after 100 h. This second decrease of pH was associated with a rapid increase in the propionic acid concentration from 0.4 g/L to above 1 g/L in both media (Fig. 7.2 A). This was the first time that propionic acid was produced during syngas fermentation, which was due to the mixed culture.

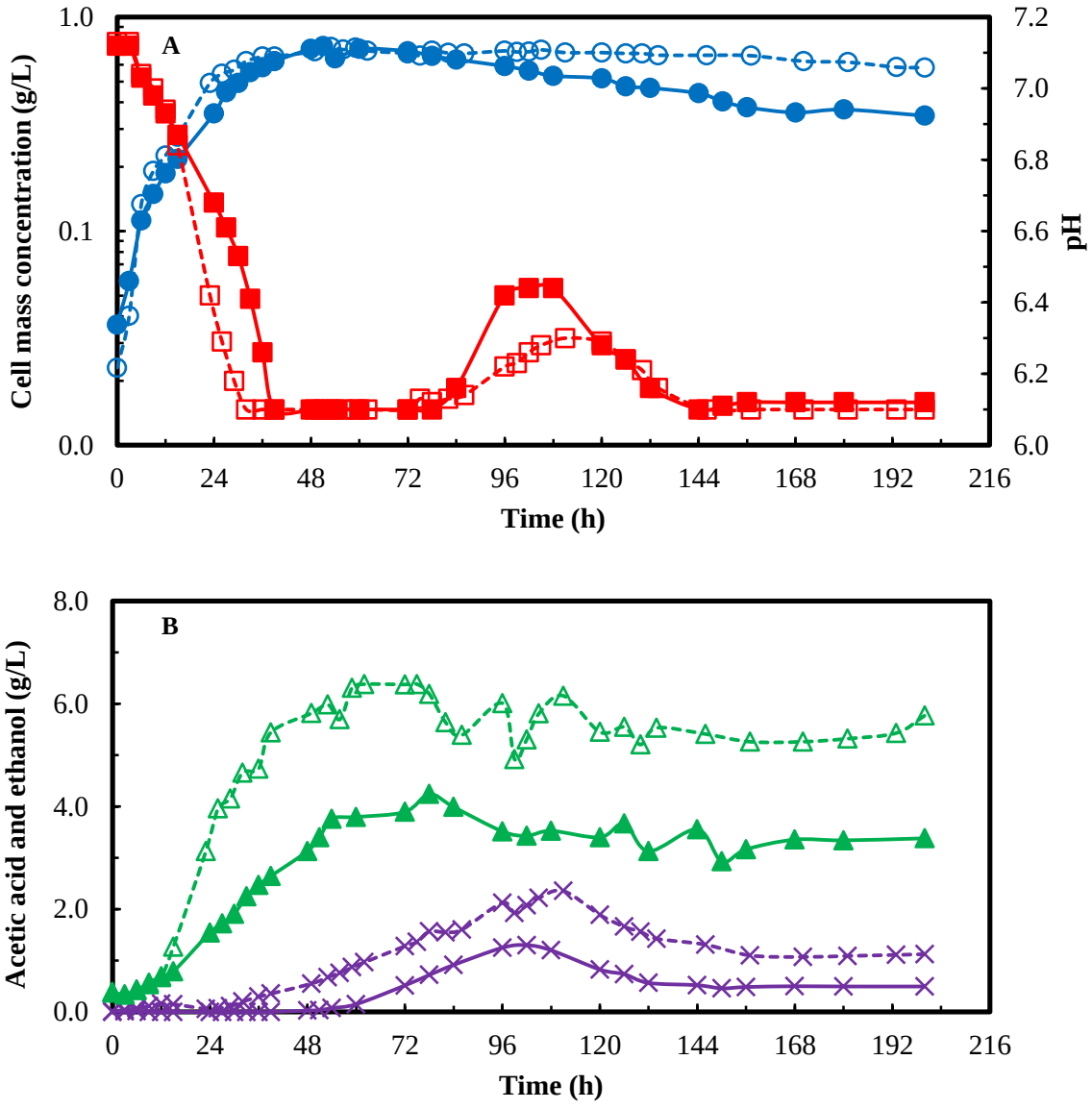

Fig. 7.1 Semi-continuous fermentation profiles in 3-L fermentor using the mixed culture in YE medium (solid line) and CSL medium (dash line); (A) pH (■) and cell mass concentration (●); (B) acetic acid (▲) and ethanol (×).

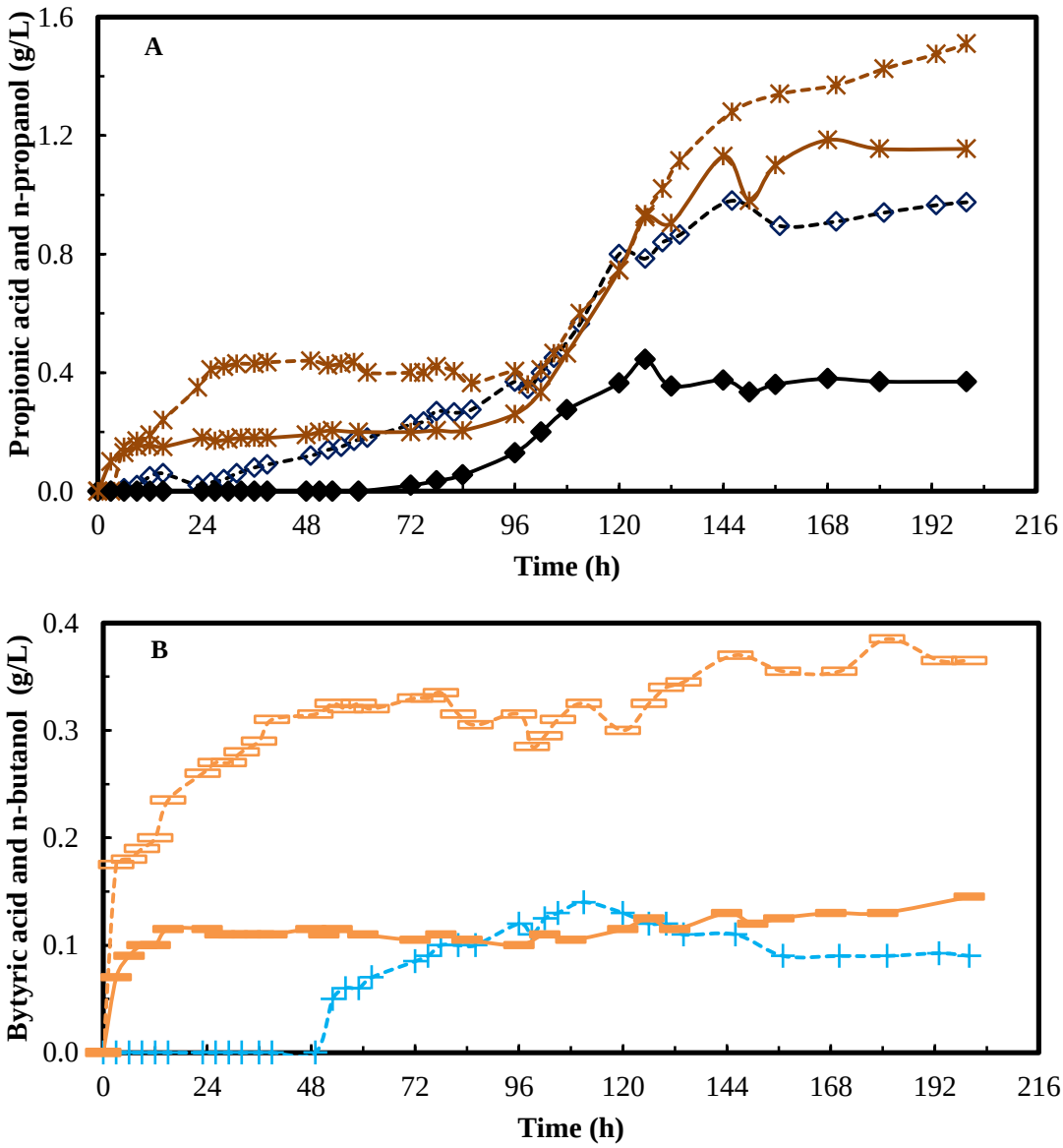

Fig. 7.2 Semi-continuous fermentation profiles in 3-L fermentor using the mixed culture in YE medium (solid line) and CSL medium (dash line); (A) n-propanol (♦) and propionic acid(✳); (B) butanol (+) and butyric acid (▬).

Table 7.1 Kinetic parameters in the YE and CSL media in the 3-L fermentor with the mixed culture.

Kinetic parameters	3-L fermentor study	
Medium	YE medium	CSL medium
Specific growth rate, h^{-1}	0.16	0.25
Cell mass yield, g cells/mol CO	3.68	3.08
Ethanol yield from CO, %[a]	44.72	62.01
Maximum ethanol concentration, g/L[a]	1.30	2.36
Final ethanol concentration, g/L	0.50	1.13
Final n-propanol concentration, g/L	0.37	0.98
Ethanol conversion to n-propanol,% (mol/mol)[b]	15.72	24.52
Final n-butanol concentration, g/L	ND[c]	0.09
Total alcohols concentration, g/L	0.87	2.20
CO utilization, %[a]	40.37	50.32
H_2 utilization, %[a]	28.10	23.93

[a] Cell mass yield was calculated at maximum cell mass concentration; ethanol yield was calculated at maximum ethanol concentration at 102 h and 111 h in YE and CSL medium, respectively. CO and H_2 utilization were calculated at 200 h.
[b] Calculation was based on the time when ethanol started to decrease in YE medium and CSL medium after 102 h and 111 h, respectively, to the end of fermentation using Eq. 1.
[c] ND = Not detectable.

7.3.1.2 Products formation

Acetic acid concentrations in the YE and CSL media reached a maximum of 4.2 g/L and 6.4 g/L at 80 h, respectively (Fig. 7.1 B). After reaching a maximum, acetic acid concentrations in in the YE and CSL media slowly decreased to 3.4 g/L and 4.9 g/L at around 100 h, respectively, due to acetic acid conversion to ethanol. The maximum ethanol concentrations measured in the YE and CSL media were 1.3 g/L at 102 h and 2.4 g/L ethanol at 111 h, respectively (Fig. 7.1 B). Ethanol production in both media was due to the conversion of syngas by the mixed culture, since all of the monosaccharides (glucose, fructose, mannose and galactose) present in the 20 g/L CSL medium at a total concentration of 0.3 g/L were consumed during the first 111 h. Based on the maximum theoretical conversion of sugars to either acetic acid or ethanol however, the sugars could only contribute about 3% to 6% to these products, indicating that syngas mainly contributed to product formation. Moreover, the production of ethanol by the mixed culture was non-growth related, which was observed in a previous study with strain CP15 monoculture (Liu et al., 2012).

The consumption of ethanol after it reached a maximum was observed simultaneously with the production of n-propanol (Fig. 7.1 B and Fig. 7.2 A). The decrease in ethanol concentration was also observed in the continuous syngas fermentation in the 20 g/L CSL medium (Liu et al., Unpublished results). The final concentrations of n-propanol in the YE and CSL media were 0.37 g/L and 0.98 g/L, respectively (Fig. 2 A). The accumulation of n-propanol in the YE medium was associated with the increase in propionic acid concentration after 80 h. Production of n-propanol in the CSL medium started at the beginning of fermentation through the

conversion of lactic acid to propionic acid by *C. propionicum*, followed by reduction of the propionic acid to n-propanol by strain CP15 in the mixed culture. Another source of n-propanol was the conversion of ethanol, whose concentrations decreased by 38.5% and 47.9% from their maxima in the YE and CSL media, respectively. There was 1.6 times more ethanol converted to n-propanol in the CSL medium and total alcohol concentration in the CSL medium was 2.5 times higher than in the YE medium (Table 7.1).

The production of n-propanol and propionic acid from ethanol with the mixed culture could be due to *C. propionicum* by a metabolic pathway similar to *Clostridium neopropionicum*: ethanol→ acetaldehyde → acetyl-CoA→ pyruvate → lactate → lactyl-CoA → propionyl-CoA → propionate (Tholozan et al., 1992). Additionally, strain CP15 could be reducing propionic acid to n-propanol during syngas fermentation, a property shared by *C. ljungdahlii* and *C. ragsdalei* (Perez et al., 2012). In this case, CO and H_2 would serve as reducing equivalents to generate NADH needed by strain CP15 in the mixed culture to reduce the propionic acid likely made by *C. propionicum*.

Thermodynamically, several possible reactions exist for the conversion of ethanol to propionic acid and n-propanol from anaerobic mixed cultures (Wu and Hickey, 1996), which are listed in Table 7.2. Reactions 1 and 2 describe the conversion of ethanol to n-propanol and propionic acid. Reaction 1 may be less likely than reaction 2 as both n-propanol and propionic acid were produced in the present study. Reaction 3 describes the conversion of ethanol to propionic acid, which could due to *C. propionicum*. Reaction 4 describes the direct reduction of propionic acid to n-propanol which could due to *A. bacchi* CP15. Reaction 5 describes the direct conversion of ethanol to n-propanol using CO and H_2 as reactants. Reaction 5 has not been described for any biological system (Wu

and Hickey, 1996), nor have syngas fermenting strains or *C. propionicum* been described as capable of directly converting CO and H_2 to n-propanol.

In addition to n-propanol, n-butanol (0.14 g/L) was produced by the mixed culture in the CSL medium (Fig. 7.2 B). Butyric acid, a growth-associated product, was formed in both YE and CSL media at concentrations of 0.15 g/L and 0.45 g/L, respectively. The production of butyric acid could be due to *C. propionicum* fermenting four carbon amino acids such as threonine into butyric acid (Cardon and Barker, 1946). Given the ability of strain CP15 to convert carboxylic acids to their respective alcohol, it is posited that *C. propionicum* produced butyric acid, which was further reduced to n-butanol by strain CP15 in the mixed culture. Details of this synergy between *C. propionicum* and strain CP15 are discussed in section 7.3.2.

Table 7.2 Possible reactions for ethanol conversion to n-propanol and propionic acid and their standard Gibbs free energy (adapted from Wu and Hickey, 1996).

	Reactions	$\Delta_r G^{0\prime}$, kJ/mol
1	$CH_3CH_2OH + 3H_2 + HCO_3^- + H^+ \rightarrow CH_3CH_2CH_2OH + 3H_2O$	-78.9
2	$CH_3CH_2OH + HCO_3^- + 2H_2 + ½H^+ \rightarrow ½CH_3CH_2CH_2OH + ½ CH_3CH_2COO^- + 2.5\ H_2O$	-72.8
3	$CH_3CH_2OH + HCO_3^- + H_2 \rightarrow CH_3CH_2COO^- + 2H_2O$	-66.7
4	$CH_3CH_2COO^- + 2H_2 + H^+ \rightarrow CH_3CH_2CH_2OH + H_2O$	-51.9
5	$CH_3CH_2OH + CO + 2H_2 \rightarrow CH_3CH_2CH_2OH + H_2O$	-94.2

7.3.1.3 Gas utilization and carbon balance

The cumulative CO and H_2 consumption profiles are shown in Fig. 7.3. Cumulative CO consumption in CSL medium was 27% higher than in YE medium. The cumulative consumption of H_2, however, did not differ considerably between the CSL and YE medium. The percentages of CO and H_2 utilized by the mixed culture in the YE medium at the end of fermentation were 40% and 28%, respectively (Table 7.1). The CO and H_2 utilized by the mixed culture in the CSL medium were 50% and 24%, respectively. The carbon balance in both media showed that there were 86 % and 104 % carbon recovery in the YE and CSL (including the sugars and lactic acid in CSL) media, respectively.

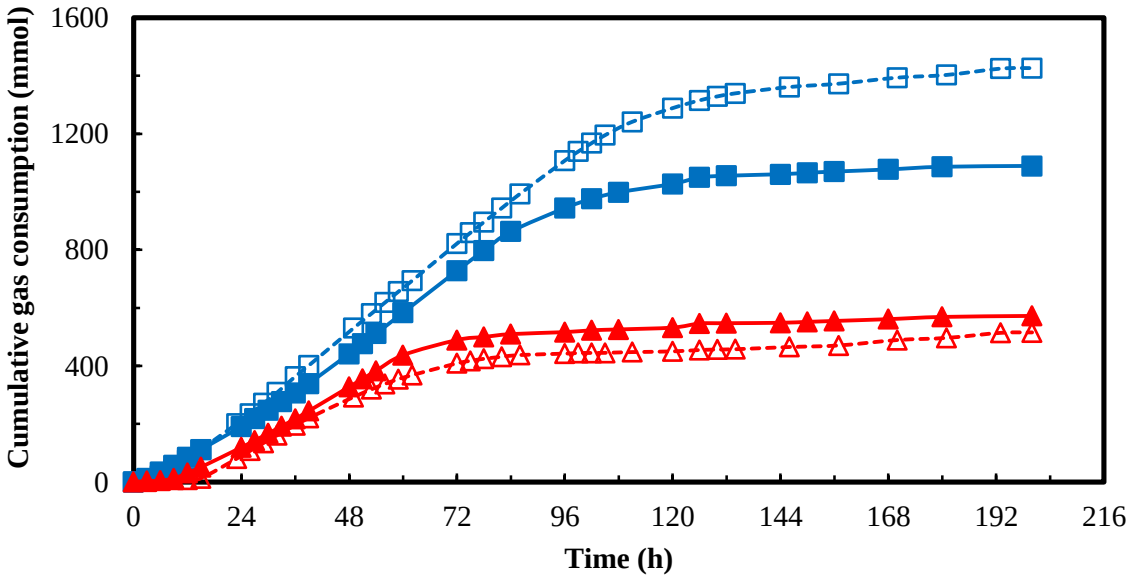

Fig.7.3 Semi-continuous fermentation in 3-L fermentor using the mixed culture in YE medium (solid symbol and solid line) and in CSL medium (open symbol and dash line) cumulative CO (■) and H_2 (▲) consumption.

7.3.2 Conversion of carboxylic acids into alcohols in 250-mL bottles

7.3.2.1 Effect of carboxylic acids on cell growth

Cell growth was observed in all treatments with the carboxylic acids used with either strain CP15 or the mixed culture (Fig. 7.4). However, the maximum cell mass concentration in each treatment varied depending on the individual carboxylic acid added (Table 7.3). The maximum cell mass concentration in each treatment was over 50% higher with the mixed culture than with strain CP15 monoculture ($p < 0.05$).

Growth, measured as maximum cell mass concentration, was inhibited in each treatment with acid compared to cultures with no acid added. Except in the treatment with lactic acid, there were no statistical differences in the percentage of growth inhibition between strain CP15 monoculture and mixed culture with the other acids ($p > 0.05$) (Table 7.3). The order of growth inhibition among the acids used with strain CP15 alone was lactic acid > hexanoic acid > butyric acid ≈ propionic acid > no acid (Table 7.3). The highest inhibition of growth observed was 75% for strain CP15, when lactic acid was added to the medium (Table 7.3). Lactic acid is able to cross bacterial cell membranes in an undissociated form, reducing cell internal pH and disrupting transmembrane proton motive force for ATP formation (Herrero et al., 1985). This inhibition has been observed for other bacteria. For example, growth of *Clostridium thermocellum* was 50% inhibited when grown on cellobiose with an initial lactic acid concentration of 2.7 g/L at pH 7.4 (undissociated concentration of lactic acid equals 7.8×10^{-4} g/L) with N_2 headspace (Herrero et al., 1985). In the present study, the growth cessation of strain CP15 monoculture in the medium with lactic acid was at pH 6.6 with

4.0×10^{-3} g/L undissociated lactic acid, which was fivefold higher than with *C. thermocellum.* This may account for the high level of inhibition for strain CP15 caused by lactic acid.

In the lactic acid treatment under syngas headspace, growth inhibition of the mixed culture was less than half of that for strain CP15. This was because 1.2 g/L of lactic acid was consumed (likely by *C. propionicum*) during the first 24 h of growth, which have reduced the inhibition of strain CP15 in the mixed culture. The inhibition order in the treatments with acid using the mixed culture was hexanoic acid > propionic acid ≈ butyric acid ≈ lactic acid > no acid.

The cell mass concentration of the mixed culture in the lactic acid treatment with N_2 headspace was 38% lower than with syngas headspace (Fig. 4 B). The growth of the mixed culture with a N_2 atmosphere was likely due to the growth of *C. propionicum* that consumed 1.2 g/L lactic acid and produced 0.48 g/L propionic acid and 0.6 g/L acetic acid (carbon recovery in products was 99.1%).Generally, the pH in all treatments using strain CP15 monoculture and the mixed culture was decreasing during acetogenic phase and increasing during the solventogenic phase. The details of pH profiles are described in Appendix B.

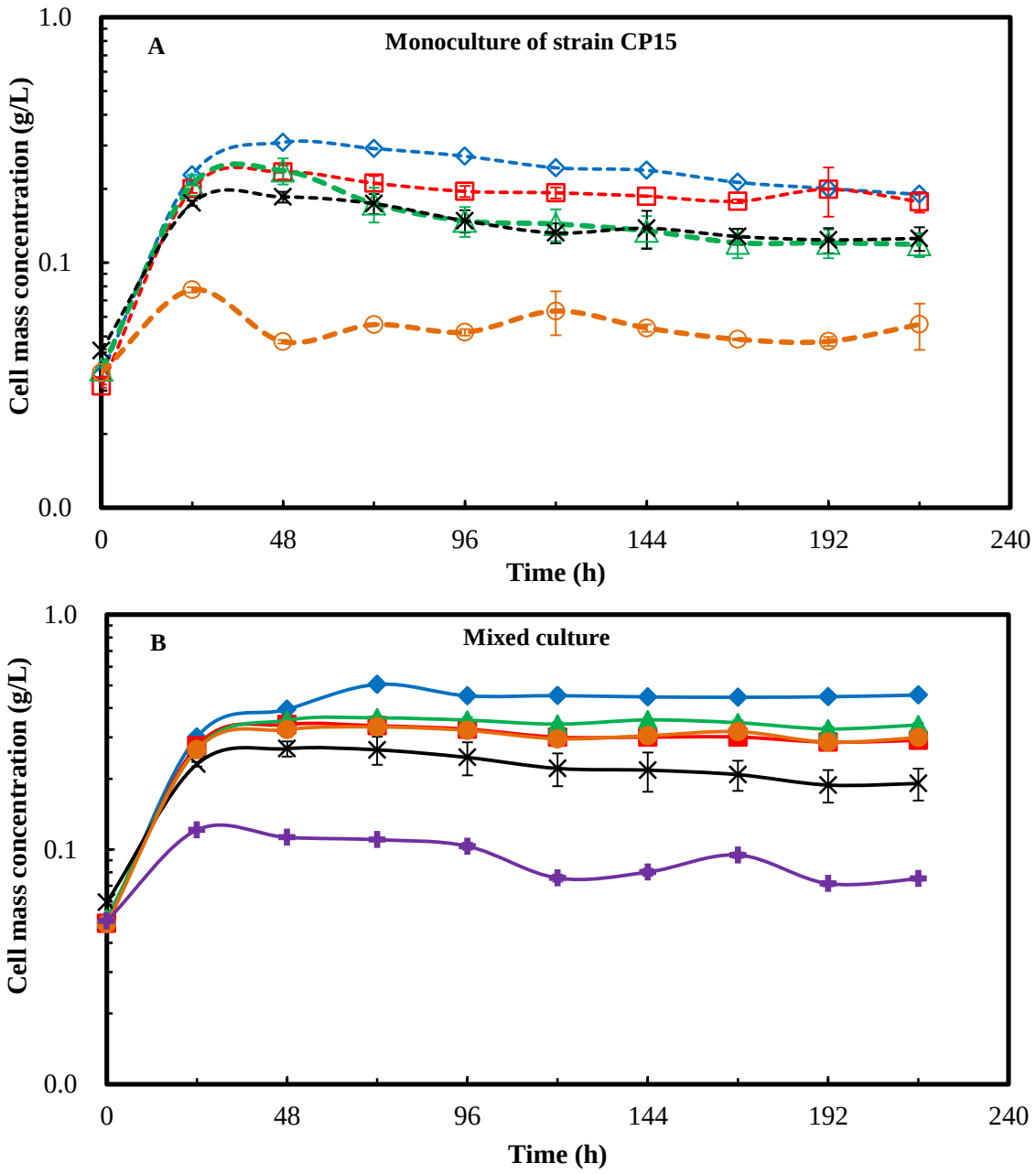

Fig. 7.4 Cell mass concentration profiles during syngas bottle fermentations with the addition of various carboxylic acids (A) monoculture of strain CP15 (open symbol and dash line) and (B) mixed culture (solid symbol and solid line); treatment with no acid (♦), propionic acid (■),butyric acid (▲), hexanoic acid (×), lactic acid (●), lactic acid with N_2 headspace (+).

Table 7.3 Syngas fermentation parameters during the conversion of carboxylic acids into alcohols in 250-mL bottle fermentors.

Treatments [1]	No acid		Propionic acid		Butyric acid		Hexanoic acid		Lactic acid	
	CP15	Mixed culture	CP15	Mixed culture	CP15	Mixed culture	CP15	Mixed culture	CP15	Mixed culture
Max. Cell Conc., g/L	$0.3 \pm 0.0^{A,Y}$	0.5 ± 0.1^{a}	$0.2 \pm 0.0^{B,Y}$	0.3 ± 0.0^{b}	$0.2 \pm 0.0^{B,Y}$	0.4 ± 0.0^{b}	$0.2 \pm 0.0^{C,Y}$	0.3 ± 0.0^{c}	$0.1 \pm 0.0^{D,Y}$	0.3 ± 0.00^{d}
% of growth inhibition[2]	— [3]	—	24.3 ± 4.9^{C}	32.6 ± 2.2^{b}	23.4 ± 9.3^{C}	29.7 ± 0.4^{b}	40.1 ± 3.1^{B}	46.8 ± 4.0^{a}	$75.0 \pm 0.6^{A,Y}$	34.1 ± 1.3^{b}
Final ethanol, g/L	$0.4 \pm 0.0^{A,Y}$	0.2 ± 0.0^{b}	0.2 ± 0.0^{C}	0.2 ± 0.0^{b}	$0.3 \pm 0.0^{B,Y}$	0.6 ± 0.0^{a}	0.3 ± 0.0^{B}	0.5 ± 0.2^{a}	—	$0.2 \pm 0.0^{b,Y}$
Ethanol yield from CO, %	$21.2 \pm 1.1^{A,B,Y}$	10.5 ± 2.1^{c}	$11.8 \pm 0.7^{C,Y}$	8.6 ± 0.7^{c}	19.0 ± 1.7^{B}	20.7 ± 1.2^{b}	$23.1 \pm 2.2^{A,Y}$	34.7 ± 6.1^{a}	—	11.7 ± 1.2^{c}
n-Propanol, g/L	—	—	0.4 ± 0.0^{Y}	1.0 ± 0.2	—	0.9 ± 0.1	—	0.1 ± 0.0	—	0.4 ± 0.0
Propionic acid conv. to propanol,%	—	—	36.8 ± 2.0^{Y}	83.4 ± 2.8	—	—	—	—	—	—
n-Butanol, g/L	—	—	—	—	0.5 ± 0.1^{Y}	0.8 ± 0.0	—	—	—	—
Butyric acid conv. to butanol, %	—	—	—	—	38.6 ± 5.3^{Y}	74.7 ± 5.6	—	—	—	—
Hexanol, g/L	—	—	—	—	—	—	0.8 ± 0.1^{Y}	1.0 ± 0.0	—	—
Hexanoic acid conv. to hexanol, %	—	—	—	—	—	—	63.6 ± 6.0^{Y}	90.7 ± 5.0	—	—
Total alcohols, g/L	$0.4 \pm 0.0^{D,Y}$	0.2 ± 0.0^{e}	$0.6 \pm 0.0^{C,Y}$	1.2 ± 0.1^{c}	$0.8 \pm 0.1^{B,Y}$	2.3 ± 0.1^{a}	$1.0 \pm 0.1^{A,Y}$	1.6 ± 0.2^{b}	—	0.6 ± 0.0^{d}
CO utilization, %	30.6 ± 1.1^{A}	30.5 ± 0.2^{c}	$22.9 \pm 1.0^{B,Y}$	36.4 ± 1.0^{b}	$21.7 \pm 1.2^{B,Y}$	43.5 ± 1.3^{a}	17.2 ± 1.5^{C}	21.5 ± 4.8^{d}	$4.8 \pm 1.0^{D,Y}$	30.5 ± 1.2^{c}
H_2 utilization, %	28.1 ± 3.1^{A}	32.1 ± 1.1^{a}	20.9 ± 3.1^{B}	25.6 ± 1.5^{b}	$16.7 \pm 3.8^{B,Y}$	27.6 ± 2.6^{b}	9.0 ± 3.1^{C}	6.0 ± 1.8^{c}	$4.6 \pm 2.8^{C,Y}$	24.6 ± 1.9^{b}

[1] Product concentrations, yields or gas conversion efficiencies were calculated at the end of experiment of 216 h.
[2] Equal to 1- (maximum cell concentration with added acid /maximum cell mass concentration with no acid) × 100%.
[3] Not applicable or products were not detectable.
[A,B,C,D] Duncan's test group for the monoculture of strain CP15; the same letter in the same row indicates there was no statistical difference among treatments ($p > 0.05$).
[a,b,c,d,e] Duncan's test group for the mixed culture; the same letter in the same row indicates there was no statistical difference among treatments ($p > 0.05$).
[Y] There was statistical difference between the monoculture of strain CP15 and mixed culture using the T-Test ($p < 0.05$).

7.3.2.2 Products formation

Ethanol was produced in all treatments with acids except lactic acid under N_2 headspace (Fig. 7.5). Strain CP15 did not consume ethanol in any of the treatments (Fig. 7.5 A). The mixed culture, however, clearly consumed ethanol after 120 h in the treatments containing propionic acid, butyric acid and lactic acid (Fig. 7.5 B). However, no ethanol was consumed by the mixed culture in the hexanoic acid treatment or the treatment without acid.

Acetic acid was also produced during the syngas fermentation using strain CP15 and the mixed culture (Fig. 7.6), with the greatest amount produced in the treatment without acid. The mixed culture produced a maximum of 4.7 g/L acetic acid, which was 38 % higher than with CP15 alone. In treatment with no acid added to the mixed culture, acetic acid concentration did not decrease after reaching a maximum (Fig. 7.6 B). However, acetic acid concentration decreased from 3.4 g/L to 2.8 g/L in treatments with no acid added to strain CP15 (Fig. 7.6 A). This indicated that the mixed culture generated less NADH to reduce acetic acid to ethanol than strain CP15 alone, resulting in less ethanol production. However, acetic acid conversion to ethanol by the mixed culture was observed in the treatments that contained propionic acid, butyric acid, hexanoic acid or lactic acid (Fig. 7.6 B). The mixed culture was more efficient in the conversion of acetic acid to ethanol compared to strain CP15 alone, suggesting some syntrophic interaction between CP15 and *C. propionicum* in the mixed culture that is not yet understood.

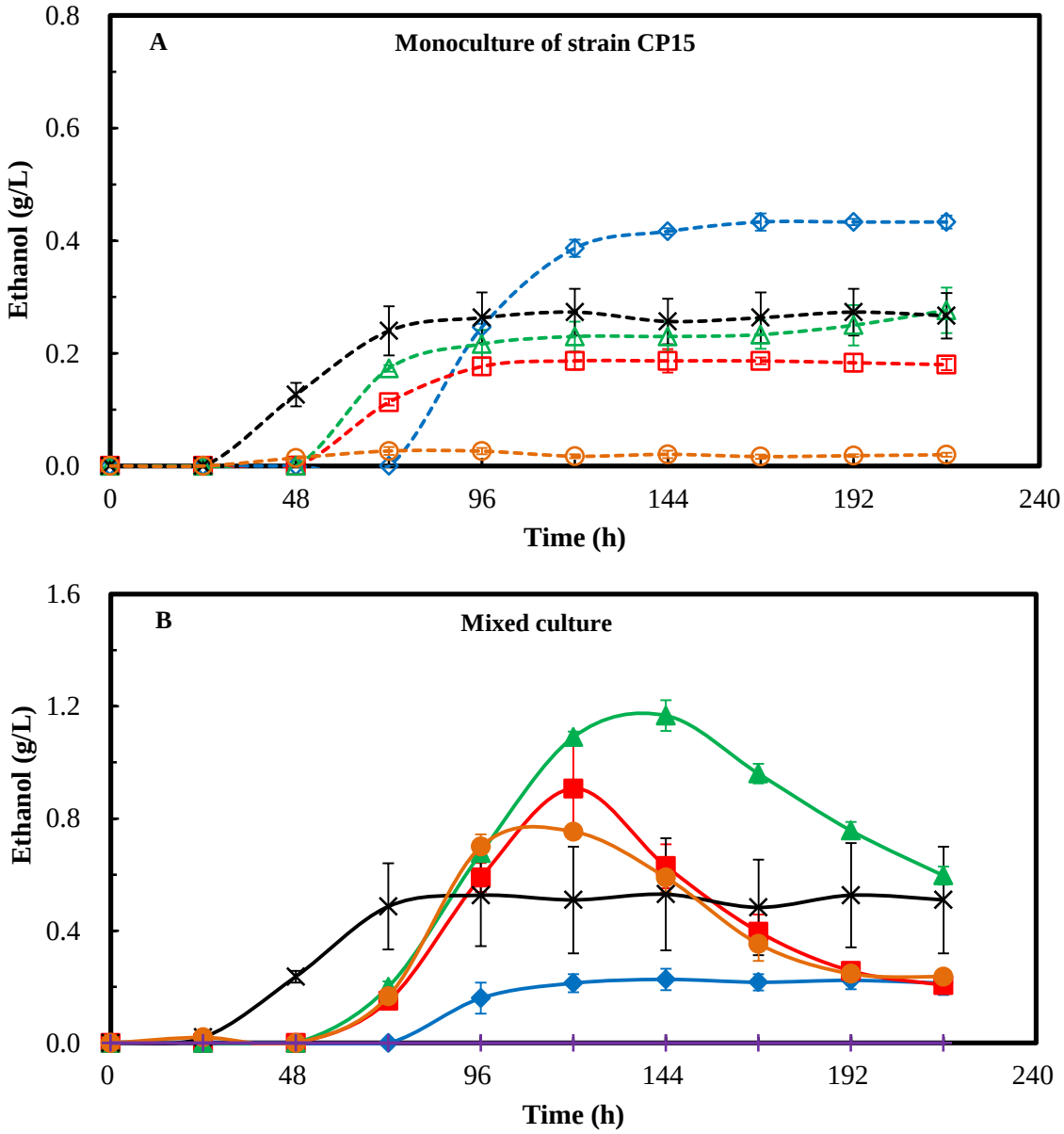

Fig. 7.5 Ethanol profiles during syngas bottle fermentations with the addition of various carboxylic acids (A) monoculture of CP15 (open symbol and dash line) and (B) mixed culture (solid symbol and solid line); treatment with no acid (♦), propionic acid (■),butyric acid (▲), hexanoic acid (×), lactic acid (●), lactic acid with N_2 headspace (+).

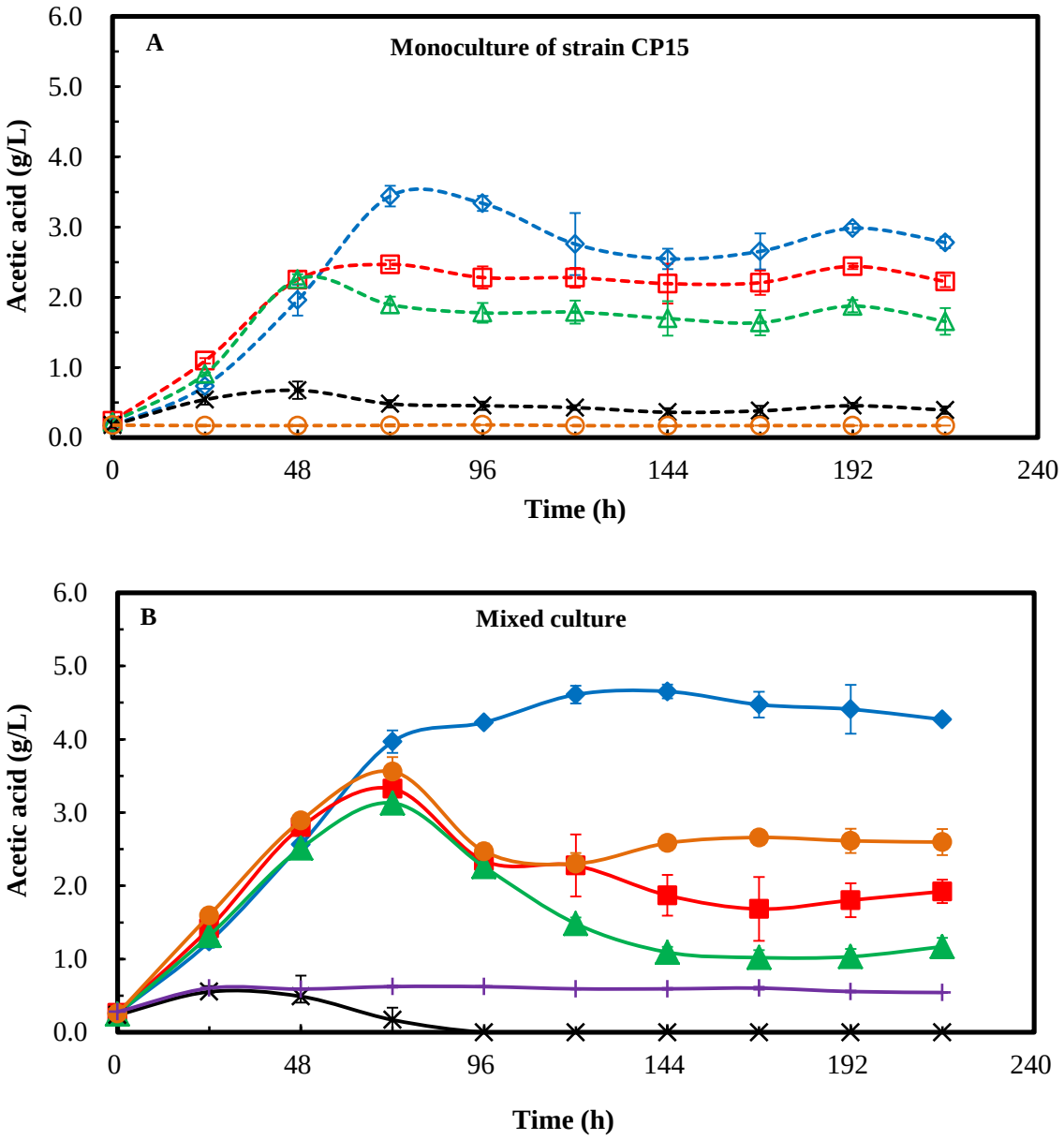

Fig. 7.6 Acetic acid profiles during syngas bottle fermentations with the addition of various carboxylic acids (A) monoculture of CP15 (open symbol and dash line) and (B) mixed culture (solid symbol and solid line); treatment with no acid (♦), propionic acid (■),butyric acid (▲), hexanoic acid (×), lactic acid (●), lactic acid with N_2 headspace (+).

The profiles of carboxylic acid consumption and production of their respective alcohols are shown in Fig. 7.7 and Fig. 7.8 for strain CP15 and the mixed culture. There was a lag phase of 48 h before either strain CP15 alone or the mixed culture began to convert propionic acid to n-propanol. The production of propionic acid after 120 h was observed for the mixed culture (Fig. 7.7 A), which was due to the conversion of ethanol as shown in Fig. 7.5 B. The increase in carboxylic acid concentration was not observed with the butyric acid, hexanoic acid or lactic acid with the mixed culture (Fig. 7.7 and Fig. 7.8). Strain CP15 alone was not able to consume lactic acid (Fig. 7.7 B). The mixed culture, however, directly consumed the lactic acid in the treatments with syngas or N_2 headspace. There was also a lag of about 48 h in the conversion of butyric acid to n-butanol by strain CP15 alone and the mixed culture (Fig. 7.8 A). Both cultures, however, converted hexanoic acid to n-hexanol immediately after inoculation (Fig. 7.8 B).

The mixed culture converted 83.4% of propionic acid to n-propanol (including n-propanol from ethanol), 74.7% of butyric acid to n-butanol and 90.7% of hexanoic acid to n-hexanol, which were 2.3 times, 1.9 times and 1.4 times, respectively, higher than with strain CP15 alone ($p < 0.05$) (Table 7.3). In addition, with similar initial carboxylic acid concentrations in the medium, there were 2.0 times, 2.9 times, and 1.6 times higher total alcohol production from propionic acid, butyric acid, hexanoic acid treatments, respectively, with the mixed culture compared to strain CP15 alone.

The mixed culture completely used the added lactic acid with syngas in the headspace but only utilized 52% of available lactic acid when N_2 was in the headspace (Fig. 7.7 B). Also, it was observed that 23% of lactic acid on a molar basis was converted to n-propanol by the mixed culture when syngas was used in the headspace (Fig. 7.7 B).

These results with the mixed culture conversion of lactic acid to propionic acid supports the results obtained in the CSL medium in the 3-L fermentor, in which lactic acid in the CSL was converted to propionic acid.

In addition, the ability of strain CP15 to convert propionic acid to n-propanol supports the hypothesis that n-propanol produced in the 3-L fermentor was the result of a syntrophic interactions. *C. propionicum* likely converted ethanol to propionic acid, which was converted by strain CP15 to n-propanol. The n-butanol produced in the CSL medium in the 3-L fermentor could be attributed to the conversion of butyric acid by strain CP15. The mixed culture did not produce alcohol in the lactic acid treatment with a N_2 headspace but it did produce n-propanol with a syngas headspace (Fig. 7.7 B). This result, further supports the assertion that n-propanol produced in the 3-L fermentor was mainly because of syntrophic interactions within the mixed culture.

The conversion efficiencies of propionic acid to n-propanol in the present study and published reports for *C. ljungdahlii* ERI-2 and *C. ljungdahlii* (Perez et al., 2012) were as follows: *C. ljungdahlii* ERI-2 (92.7%) > mixed culture (83.4%, present study) > *C. ragsdalei* (72.3%) > strain CP15 monoculture (36.8%, present study). The conversion efficiencies of butyric acid to n-butanol were as follows: mixed culture (74.7%, present study) > *C. ljungdahlii* ERI-2 (68.2%) > strain CP15 monoculture (38.6%, present study) > *C. ragsdalei* (21.0%). For hexanoic acid conversion to n-hexanol, the conversion efficiencies were as follows: mixed culture (90.7%, present study) > strain CP15 monoculture (63.6%, present study) > *C. ljungdahlii* ERI-2 (46.0%).

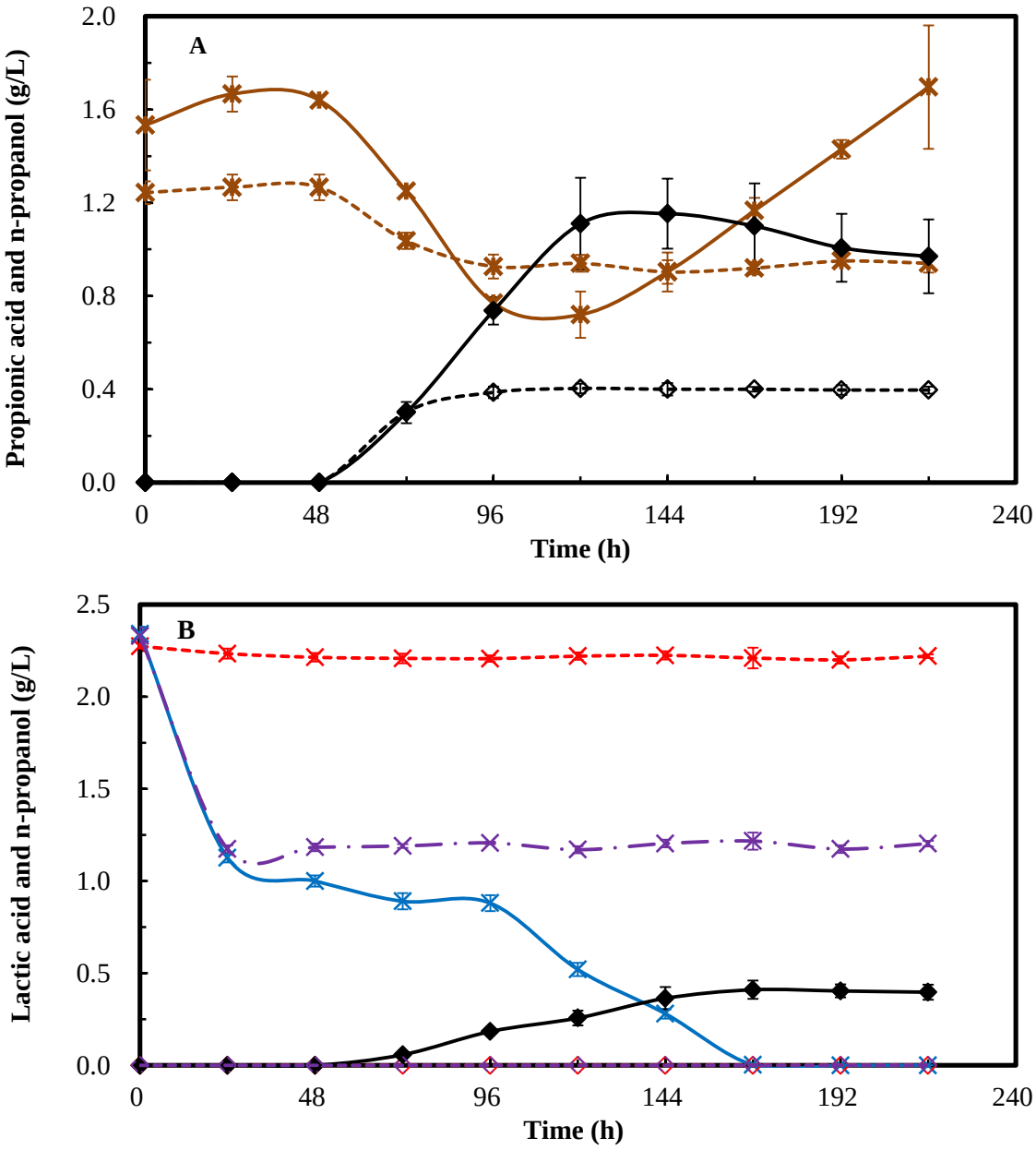

Fig. 7.7 Carboxylic acids and their respective alcohols profiles during syngas bottle fermentations using the monoculture of CP15 (open symbol and dash line) and mixed culture (solid symbol and solid line) for treatments (A) propionic acid (B) lactic acid; n-propanol (♦), propionic acid (✳), lactic acid (×), lactic acid under nitrogen headspace (× and dash dot line).

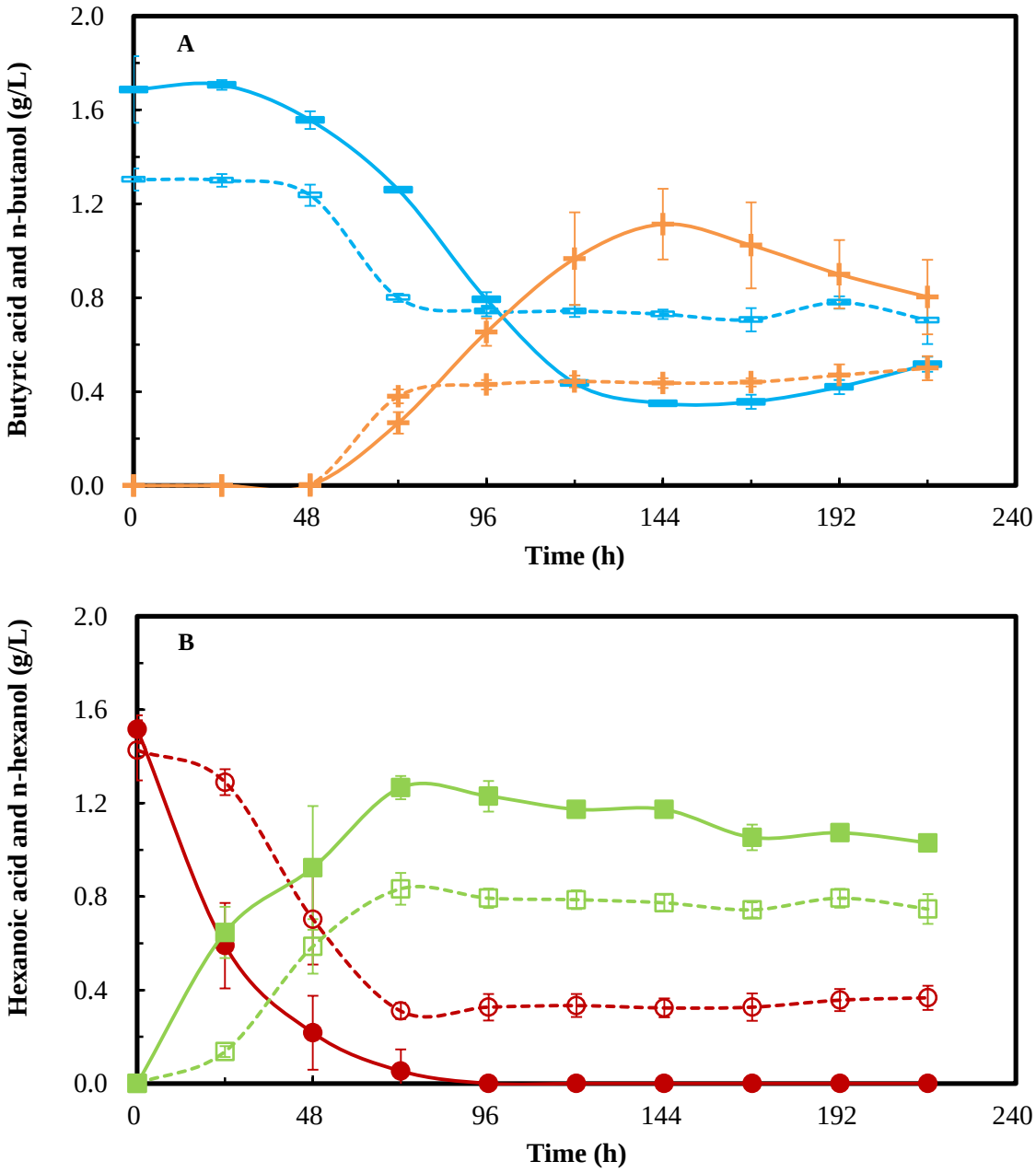

Fig. 7.8 Carboxylic acids and their respective alcohols profiles during syngas bottle fermentations using the monoculture of CP15 (open symbol and dash line) and mixed culture (solid symbol and solid line) for treatments (A) butyric acid (B) hexanoic acid; butanol (+), butyric acid (▬), hexanoic acid (●), hexanol (■).

7.3.2.3 Gas utilization and carbon balance

The mixed culture consumed significantly more CO ($p < 0.05$) in the treatments that contained propionic acid, butyric acid and lactic acid than strain CP15 monoculture (Table 7.3). The mixed culture also utilized more H_2 in the treatments that contained butyric acid and lactic acid. CP15 utilized more CO and H_2 ($p < 0.05$) in the treatments without acid than treatments where acids were added. The carbon recoveries in the products were generally 100% ± 10% for strain CP15 and the mixed culture, indicating that no other major products were generated during the conversion of carboxylic acids to their respective alcohols.

7.4 Conclusions

Over twofold more alcohol was produced in CSL medium than in YE medium during the semi-continuous fermentation in the 3-L fermentor with the mixed culture. Bottle fermentations suggested that n-propanol and n-butanol production were the result of syntrophic interactions between strain CP15 and *C. propionicum*, resulting in over 60% more alcohol production than with strain CP15 alone. In addition, the mixed culture converted 50% more carboxylic acids into their corresponding alcohols than the CP15 monoculture. These results show the advantage of using the mixed culture for higher alcohols production from syngas.

7.5 References

Allen, T.D., Caldwell, M.E., Lawson, P.A., Huhnke, R.L., Tanner, R.S., 2010. *Alkalibaculum bacchi* gen. nov., sp. nov., a CO-oxidizing, ethanol-producing

acetogen isolated from livestock-impacted soil. Int. J. Syst. Evol. Microbiol. 60, 2483-2489.

Atsumi, S., Hanai, T., Liao, J.C., 2008. Non-fermentative pathways for synthesis of branched-chain higher alcohols as biofuels. Nature 451, 86-89.

Atsumi, S., Liao, J.C., 2008. Metabolic engineering for advanced biofuels production from *Escherichia coli*. Curr. Opin. Biotechnol. 19, 414-419.

Bakker, A., Smith, J., Myers, K., 1994. How to disperse gases in liquids. Chem. Eng. 101, 98-104.

Cardon, B., Barker, H., 1946. Two new amino-acid-fermenting bacteria, *Clostridium propionicum* and *Diplococcus glycinophilus*. J. Bacteriol. 52, 629-634.

Demirer, G., Speece, R., 1998. Anaerobic biotransformation of four 3-carbon compounds (acrolein, acrylic acid, allyl alcohol and n-propanol) in UASB reactors. Water Res. 32, 747-759.

Esposito, G., Weijma, J., Pirozzi, F., Lens, P., 2003. Effect of the sludge retention time on H_2 utilization in a sulphate reducing gas-lift reactor. Process Biochem. 39, 491-498.

Harvey, B.G., Meylemans, H.A., 2011. The role of butanol in the development of sustainable fuel technologies. J. Chem. Technol. Biotechnol. 86, 2-9.

Herrero, A.A., Gomez, R.F., Snedecor, B., Tolman, C.J., Roberts, M.F., 1985. Growth inhibition of *Clostridium thermocellum* by carboxylic acids: a mechanism based on uncoupling by weak acids. Appl. Microbiol. Biotechnol. 22, 53-62.

Johns, A., 1952. The mechanism of propionic acid formation by *Clostridium propionicum*. J. Gen. Microbiol. 6, 123-127.

Klasson, K., Cowger, J., Ko, C., Vega, J., Clausen, E., Gaddy, J., 1990. Methane production from synthesis gas using a mixed culture of *R. rubrum , M. barkeri,* and *M. formicicum*. Appl. Biochem. Biotechnol. 24, 317-328.

Liu, K., Atiyeh, H.K., Stevenson, B.S., Tanner, R.S., Wilkins, M.R., Huhnke, R.L., Unpublished results. Continuous sysngas fermentation for the production of ethanol, n-propanol and n-butanol. Bioresour. Technol.

Liu, K., Atiyeh, H.K., Tanner, R.S., Wilkins, M.R., Huhnke, R.L., 2012. Fermentative production of ethanol from syngas using novel moderately alkaliphilic strains of *Alkalibaculum bacchi*. Bioresour. Technol. 104, 336-341.

Maddipati, P., Atiyeh, H.K., Bellmer, D.D., Huhnke, R.L., 2011. Ethanol production from syngas by *Clostridium* strain P11 using corn steep liquor as a nutrient replacement to yeast extract. Bioresour. Technol. 102, 6494-6501.

Mann, J., Yao, N., Bocarsly, A.B., 2006. Characterization and analysis of new catalysts for a direct ethanol fuel cell. Langmuir 22, 10432-10436.

O'Brien, D.J., Panzer, C.C., Eisele, W.P., 1990. Biological production of acrylic acid from cheese whey by resting cells of *Clostridium propionicum*. Biotechnol. Prog. 6, 237-242.

Perez, J.M., Richter, H., Loftus, S.E., Angenent, L.T., 2012. Biocatalytic reduction of short-chain carboxylic acids into their corresponding alcohols with syngas fermentation. Biotechnol. Bioeng. 110, 1066-1077.

Ramachandriya, K.D., Kundiyana, D.K., Wilkins, M.R., Terrill, J.B., Atiyeh, H.K., Huhnke, R.L., 2013. Carbon dioxide conversion to fuels and chemicals using a hybrid green process. Appl. Energy 112, 289-299.

Ramachandriya, K.D., Wilkins, M.R., Delorme, M.J.M., Zhu, X., Kundiyana, D.K., Atiyeh, H.K., Huhnke, R.L., 2011. Reduction of acetone to isopropanol using producer gas fermenting microbes. Biotechnol. Bioeng. 108, 2330-2338.

Shen, G.J., Shieh, J.S., Grethlein, A.J., Jain, M.K., Zeikus, J.G., 1999. Biochemical basis for carbon monoxide tolerance and butanol production by *Butyribacterium methylotrophicum*. Appl. Microbiol. Biotechnol. 51, 827-832.

Simmons, B.A., 2011. Opportunities and challenges in advanced biofuel production: the importance of synthetic biology and combustion science. Biofuels 2, 5-7.

Sipma, J., Meulepas, R., Parshina, S., Stams, A., Lettinga, G., Lens, P., 2004. Effect of carbon monoxide, hydrogen and sulfate on thermophilic (55 C) hydrogenogenic carbon monoxide conversion in two anaerobic bioreactor sludges. Appl. Microbiol. Biotechnol. 64, 421-428.

Sowers, K.R., Noll, K.M., 1995. Techniques for anaerboic growth. in: Robba, F.T., Sowers, K.R., Schreier, H.J. (Eds.), Archaea: a laboratory manual, 1st ed. Cold Spring Harbor Laboratory Press, Cold Spring Harbor, New York, pp. 36.

Tanner, R.S., 2007. Cultivation of bacteria and fungi. in: Hurst CJ, Crawford AL, Mills AL, Garland JL, Stetzenbach LD, Lipson DA (Eds.), Manual of Environmental Microbiology. ASM Press, Washington D. C., pp. 69-78.

Tanner, R.S., 2008. Production of ethanol from synthesis gas. in: J.D. Wall, C.S. Harwood, Demain, A. (Eds.), Bioenergy. ASM Press, Washington D.C., pp. 147-151.

Tholozan, J., Touzel, J., Samain, E., Grivet, J., Prensier, G., Albagnac, G., 1992. *Clostridium neopropionicum* sp. nov., a strict anaerobic bacterium fermenting ethanol to propionate through acrylate pathway. Arch. Microbiol. 157, 249-257.

Tyner, W.E., 2010. Policy Update: Why the push for drop-in biofuels? Biofuels 1, 813-814.

Ukpong, M.N., Atiyeh, H.K., De Lorme, M.J.M., Liu, K., Zhu, X., Tanner, R.S., Wilkins, M.R., Stevenson, B.S., 2012. Physiological response of *Clostridium carboxidivorans* during conversion of synthesis gas to solvents in a gas-fed bioreactor. Biotechnol. Bioeng. 109, 2720-2728.

Wilkins, M.R., Atiyeh, H.K., 2011. Microbial production of ethanol from carbon monoxide. Curr. Opin. Biotechnol. 22, 326-330.

Wu, M.M., Hickey, R.F., 1996. n-Propanol production during ethanol degradation using anaerobic granules. Water Res. 30, 1686-1694.

Yeung, C., Thomson, M., 2013. Experimental and kinetic modeling study of 1-hexanol combustion in an opposed-flow diffusion flame. Proc. Combust. Inst. 34, 795-802.

CHAPTER VIII

CONCLUSIONS AND FUTURE WORK

8.1 Conclusions

The following is a list of conclusions that were reached during the work on this project:

- The moderately alkaliphilic novel strains of *Alkalibaculum bacchi* CP11^T, CP13 and CP15 grew at initial pH between 7.7 and 8.0 and produced ethanol and acetic from Syngas I (20% CO, 15% CO_2, 5% H_2, 60% N_2) and Syngas II (40% CO, 30% CO_2, 30% H_2) in bottle fermentations.
- Ethanol yields from CO by strain CP15 using Syngas I and Syngas II in bottle fermentations were 65% and 76%, respectively, which were 43% higher than using strains CP11^T and CP13.
- The mass transfer analyses using an air-water system in the 7-L Bioflo 415 fermentor at the various operating conditions showed that the overall volumetric mass transfer coefficient, k_La/V_L, increased with the increase in agitation speed and air flow rate with the 3 L and 5.6 L working volumes. The highest k_La/V_L of O_2 was 116 h^{-1}, which was obtained at 600 sccm, 900 rpm and 101 kPa in the 3 L working volume.

The increase in headspace pressure decreased the k_La/V_L of O_2 due to the low volumetric gas flow rate at high pressure.

- The backmixing effects of the headspace on the k_La/V_L of O_2 were due to the entrapment of air from the headspace into water. The k_La/V_L values for O_2 due to backmixing were less than 2 h^{-1} in both the 3 L working volume at 150 rpm and the 5.6 L working volume at 150 rpm and 900 rpm. The k_La/V_L values for O_2 due to backmixing effects in the 3 L working volume at 900 rpm increased from 67 h^{-1} to 119 h^{-1} when the headspace pressure increased from 101 kPa to 240 kPa.
- The mathematical model used in this study predicated the k_La/V_L values for O_2 within 10% of the experimental data. The model was extended to predict the k_La/V_L values for CO, CO_2 and H_2, which would help in operating syngas fermentation reactors.
- *A. bacchi* strain CP15 medium cost was reduced by 27% by removing [N-Tris (hydroxymethyl) methyl]-3-aminopropanesulfonic acid (TAPS buffer) from standard YE medium and replacing YE, minerals, and vitamins with CSL. Over 78% more ethanol was produced in bottle fermentations with CSL medium compared to YE medium.
- Ethanol concentration of 6 g/L was obtained using Syngas V (28% CO, 60% H_2, 12% N_2, H_2:CO molar ratio ≈ 2) during continuous fermentation with cell recycle in YE medium at a dilution rate of 0.011 h^{-1}. A maximum cell mass concentration of 5.5 g/L, equivalent to an optical density of 14, was obtained during fermentation.
- A mixed culture mainly made of *A. bacchi* strain CP15 and *C. propionicum* was able to produce maximum 8 g/L ethanol, 6 g/L n-propanol and 1 g/L n-butanol during continuous syngas fermentation in CSL medium. Production of these alcohols was

attributed to the synergy between strain CP15 and *C. propionicum* in the mixed cuture.

- Semi-continuous syngas fermentation in a 3-L fermentor using Syngas VI with the mixed culture produced over twofold more total alcohols in the CSL medium than in the YE medium, indicating the potential of using CSL as a medium for mixed alcohols production from syngas.
- Bottle fermentations using the mixed culture showed that n-propanol and n-butanol production were based on synergy between strain CP15 and *C. propionicum*. The synergy in the mixed culture resulted in over 60% more total alcohols production than CP15 monoculture.
- The mixed culture converted 50% more carboxylic acids to their corresponding alcohols than CP15 monoculture, which shows the advantage of using the mixed culture in the production of higher alcohols from syngas.

8.2 Future work

The following is a list of future work based on the results obtained in this study:

- Improve the continuous syngas fermentation with the cell recycle system to increase productivity and alcohol concentrations.
- Examine the production of n-propanol from feedstocks that contains lactic acid such as cheese whey by the mixed culture in semi-continuous and continuous syngas fermentation.

- Examine the ability of CP15 monoculture and mixed culture to ferment producer gas made by gasifying agricultural feedstocks such as switchgrass and redcedar.

APPENDICES

APPENDIX A

This appendix contains the detailed product and gas consumption profiles in bottle fermentations with YE and CSL media that were discussed in section 6.3.1. The figures were added in this appendix and not in Chapter 6 due to limitation on the number of figures that can be included in the manuscript submitted for publication.

A Effect of medium composition

A1 Cell growth and pH profiles

Fig. A1 shows that the highest cell mass concentration (0.33 g/L) was obtained in the standard YE medium and YE medium with 3X minerals. There was a slightly decreasing trend in cell mass concentrations in all media once reached maximum. Also, the cell mass concentration in all media decreased when the pH was between 6.1 and 6.5 (Fig. A2).

The pH in all media followed a similar pattern that decreased during acetogenic phase and increased during the solventogenic phase (Fig. A2). The increase of pH was associated with a decreasing trend in acetic acid concentration which was caused by its

conversion to ethanol. Although more acetic acid was produced in both CSL media compared to YE media (Fig. A3), the lowest pH in the media with CSL was above that in YE media (Fig. A2). This can be attributed to the buffering capacity of CSL (Noro et al., 2004).

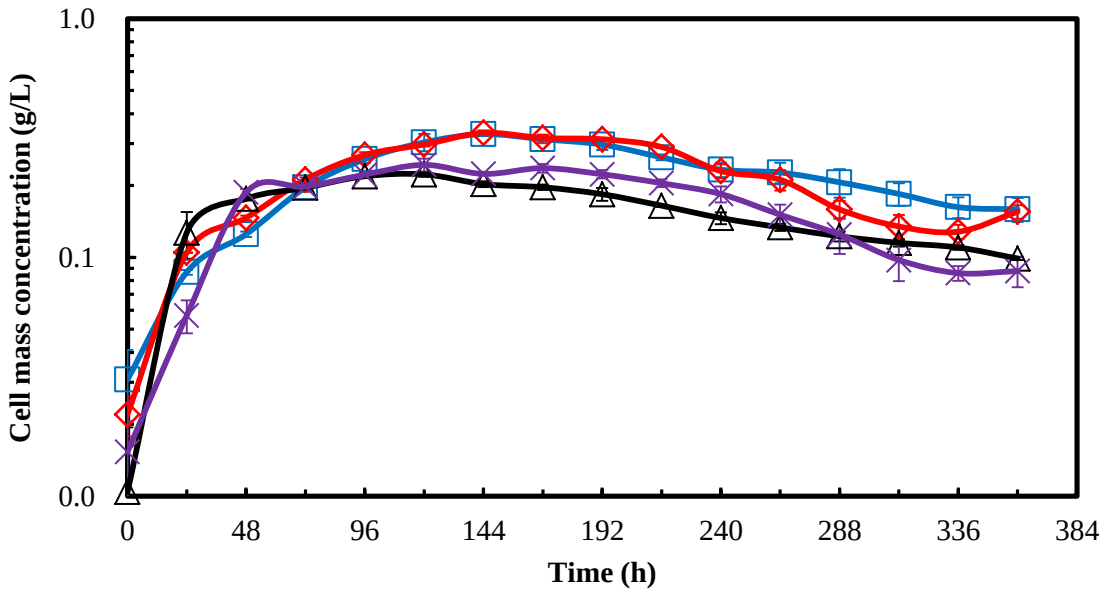

Fig. A1 Cell growth profiles in standard YE medium (□); YE medium with 3X minerals (◊); 20 g/L CSL medium (Δ); 50 g/L CSL medium (x); (n=3).

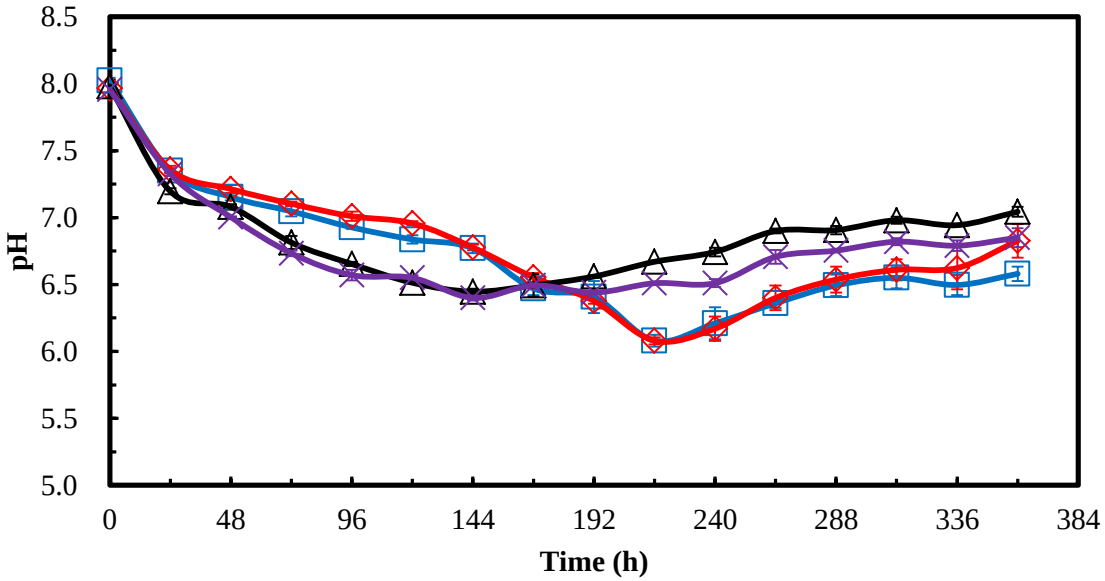

Fig. A2 pH profiles in standard YE medium (□); YE medium with 3X minerals (◊); 20 g/L CSL medium (Δ); 50 g/L CSL medium (x); (n=3).

A2 Products formation

The maximum acetic acid concentrations produced in the standard YE medium and YE medium with 3X minerals without TAPS were 5.3 and 4.4 times (Fig. A3), respectively, higher than the maximum acetic acid concentration (0.9 g/L) produced in the standard YE medium with TAPS described previously (Liu et al., 2012). This was due to 2.8 times more cell mass concentration in the YE medium without TAPS, compared to the YE medium with TAPS. The acetic acid concentration in the 50 g/L CSL medium was the highest (6.4 g/L) ($p < 0.05$) (Fig. A3). In the 50 g/L CSL medium, strain CP15 produced 34% more acetic acid ($p < 0.05$) compared to in the 20 g/L CSL medium. This was due to the presence of more nutrients in the 50 g/L CSL. The results with CP15 were similar to *C. ragsdalei* strain P11 growing in a 50 g/L CSL medium and producing

67% more acetic acid than in the 20 g/L CSL medium (Saxena, 2008). The theoretical amounts of acetic acid produced from consumed monosaccharides were 0.07 g/L (1% of the maximum acetic acid produced) in the 20 g/L CSL medium and 0.19 g/L (3% of the maximum acetic acid produced) in the 50 g/L CSL medium. This showed that acetic acid was mainly produced from syngas by CP15.

Ethanol formation started after 120 h in both CSL media. However, ethanol formation in both YE media occurred after 192 h (Fig. A4). In addition, there was no statistical difference between the ethanol concentrations produced in the standard YE medium and YE medium with 3X minerals. The difference in ethanol concentration between the 20 g/L CSL and 50 g/L CSL media was also insignificant ($p > 0.05$). This was different from *C. ragsdalei* strain P11, which produced lower ethanol concentration in the medium with 50 g/L CSL (Saxena and Tanner, 2011). The results in the present study indicate that a medium with 50 g/L CSL did not inhibit CP15's ability to produce ethanol (Fig. A4).

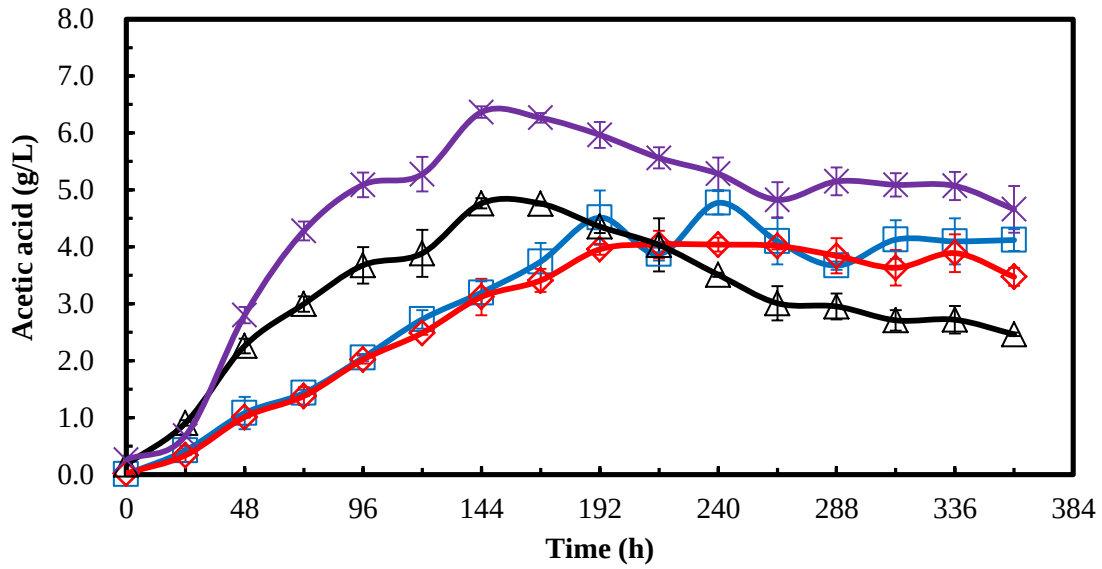

Fig. A3 Acetic acid profiles in standard YE medium (□); YE medium with 3X minerals (◊); 20 g/L CSL (Δ); 50 g/L CSL (x); (n=3).

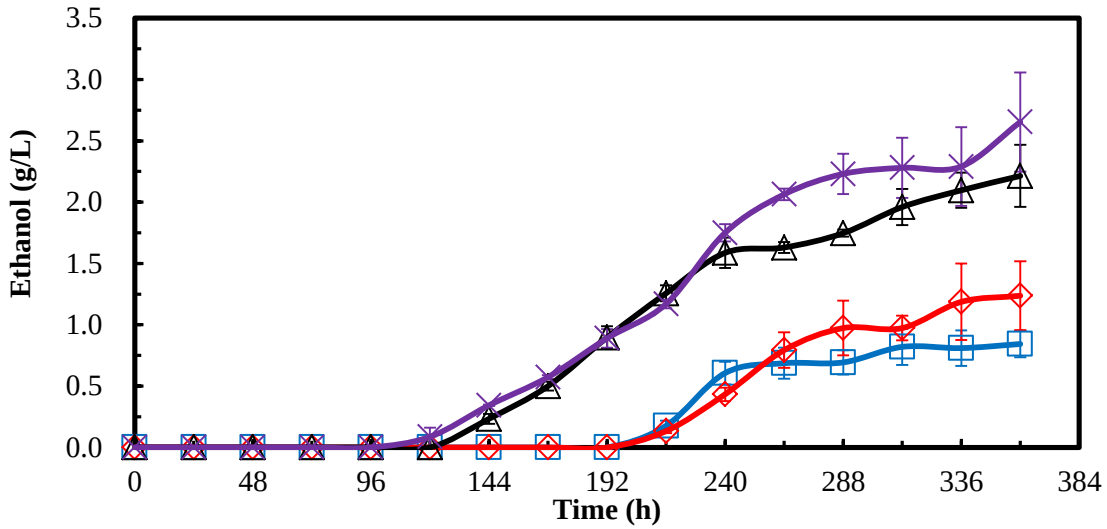

Fig. A4 Ethanol profiles in standard YE medium (□);YE medium with 3X minerals (◊); 20 g/L CSL medium (Δ); 50 g/L CSL medium (x); (n=3).

A3 Gas utilization

Strain CP15 utilized slightly less CO in 20 g/L CSL medium compared to the other media ($p < 0.05$) as shown in Fig. A5. Also, there was 47% more H_2 ($p < 0.05$) consumed in YE media than in the CSL media (Fig. A6). The reduction in H_2 and CO utilization in all media after about 216 h can be due to reduction in pH in the media to the levels caused stress on cell's growth and inhibited H_2ase activity. It was reported that H_2ase activity was increased 4.7 times when the pH in the medium was increased from 6.0 to 7.8 with *C. ragsdalei* strain P11 (Skidmore, 2010; Skidmore et al., 2013). This indicates H_2ase activity favors moderately alkaliphilic conditions.

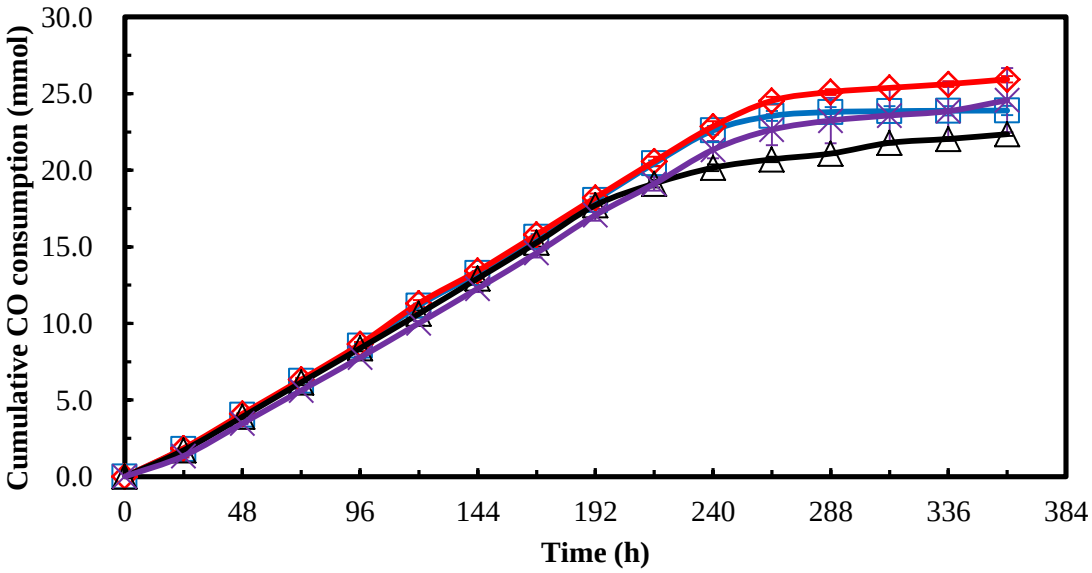

Fig. A5 Cumulative CO consumption profiles in standard YE medium (□); YE medium with 3X minerals (◊); 20 g/L CSL medium (Δ); 50 g/L CSL medium (x); (n=3).

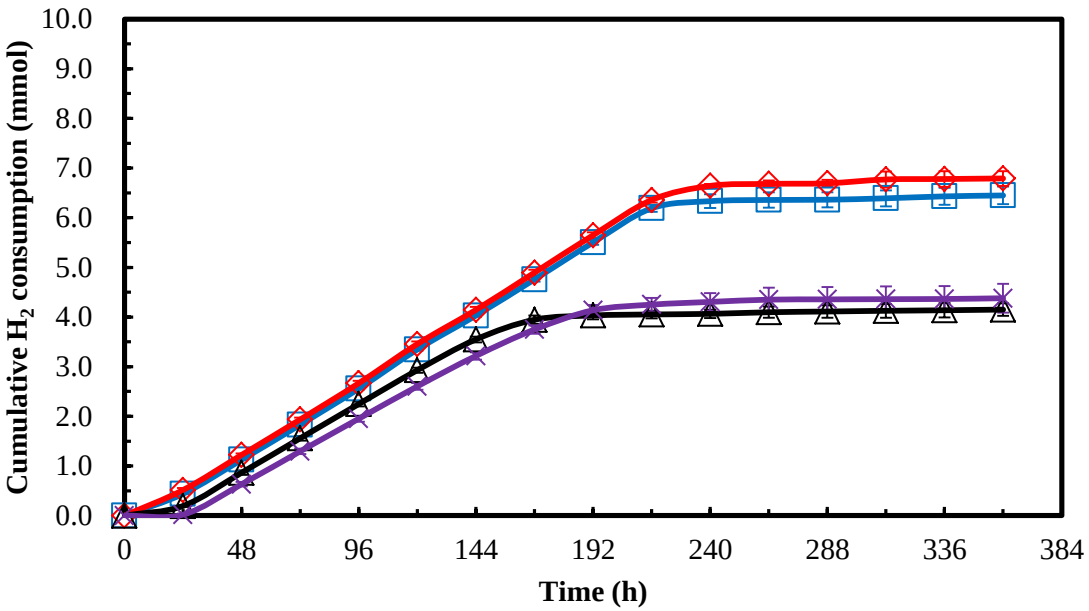

Fig. A6 Cumulative H_2 consumption profiles in standard YE medium (□);YE medium with 3X minerals (◊);20 g/L CSL medium (Δ); 50 g/L CSL medium (x); (n=3).

A4 References

Liu, K., Atiyeh, H.K., Tanner, R.S., Wilkins, M.R., Huhnke, R.L., 2012. Fermentative production of ethanol from syngas using novel moderately alkaliphilic strains of *Alkalibaculum bacchi*. Bioresour. Technol. 104, 336-341.

Noro, N., Sugano, Y., Shoda, M., 2004. Utilization of the buffering capacity of corn steep liquor in bacterial cellulose production by *Acetobacter xylinum*. Appl. Microbiol. Biotechnol. 64, 199-205.

Saxena, J. 2008. Development of an optimized and cost-effective medium for ethanol production by *Clostridium* strain P11. Ph.D. Dissertation. University of Oklahoma, pp. 96.

Saxena, J., Tanner, R.S., 2011. Optimization of a corn steep medium for production of ethanol from synthesis gas fermentation by Clostridium ragsdalei. World J. Microbio. Biotechnol.1-9.

Skidmore, B.E. 2010. Syngas Fermentation: Quantification of assay techniques, reaction kinetics, and pressure dependencies of the *Clostridial* P11 hydrogenase. M.S. Thesis. Brigham Young University, pp. 54.

Skidmore, B.E., Baker, R.A., Banjade, D.R., Bray, J.M., Tree, D.R., Lewis, R.S., 2013. Syngas fermentation to biofuels: Effects of hydrogen partial pressure on hydrogenase efficiency. Biomass Bioenerg. 55, 156-162.

APPENDIX B

This appendix contains the detailed pH and gas consumption profiles in bottle fermentations using strain CP15 monoculture and the mixed culture in the study for the conversion of carboxylic acid to corresponding alcohols discussed in section 7.3.2. The figures were added in this appendix and not in Chapter 7 due to limitation on the number of figures that can be included in the manuscript submitted for publication.

B Conversion of carboxylic acids into alcohols in bottle fermentations

B1 pH profiles

The pH in the media with CP15 monoculture decreased during the acetogenic phase due to acetic acid production (Fig. B1 and Fig. 7.6). The lowest pH values in all treatments were 5.9 observed in no acid, propionic acid and butyric acid treatments. Then, the pH increased due to the conversion of acetic acid to ethanol during the soventogenic phase.

When mixed culture was used, the pH profiles trend was similar to CP15 monoculture. A fast drop in pH was observed during the acetogenic phase with a lowest pH of 5.39 in the no acid treatment (Fig. B1). When ethanol production started, the pH increased due to conversion of acetic acid to ethanol. However, pH profiles in the treatments with propionic acid, butyric acid and lactic acid had slightly decreasing trends when ethanol was consumed by the mixed culture after 120 h (Fig. 7.5). The pH increased in lactic acid treatment under N_2 headspace, which possibly was due to the release of CO_2 from the medium that contained $NaHCO_3$.

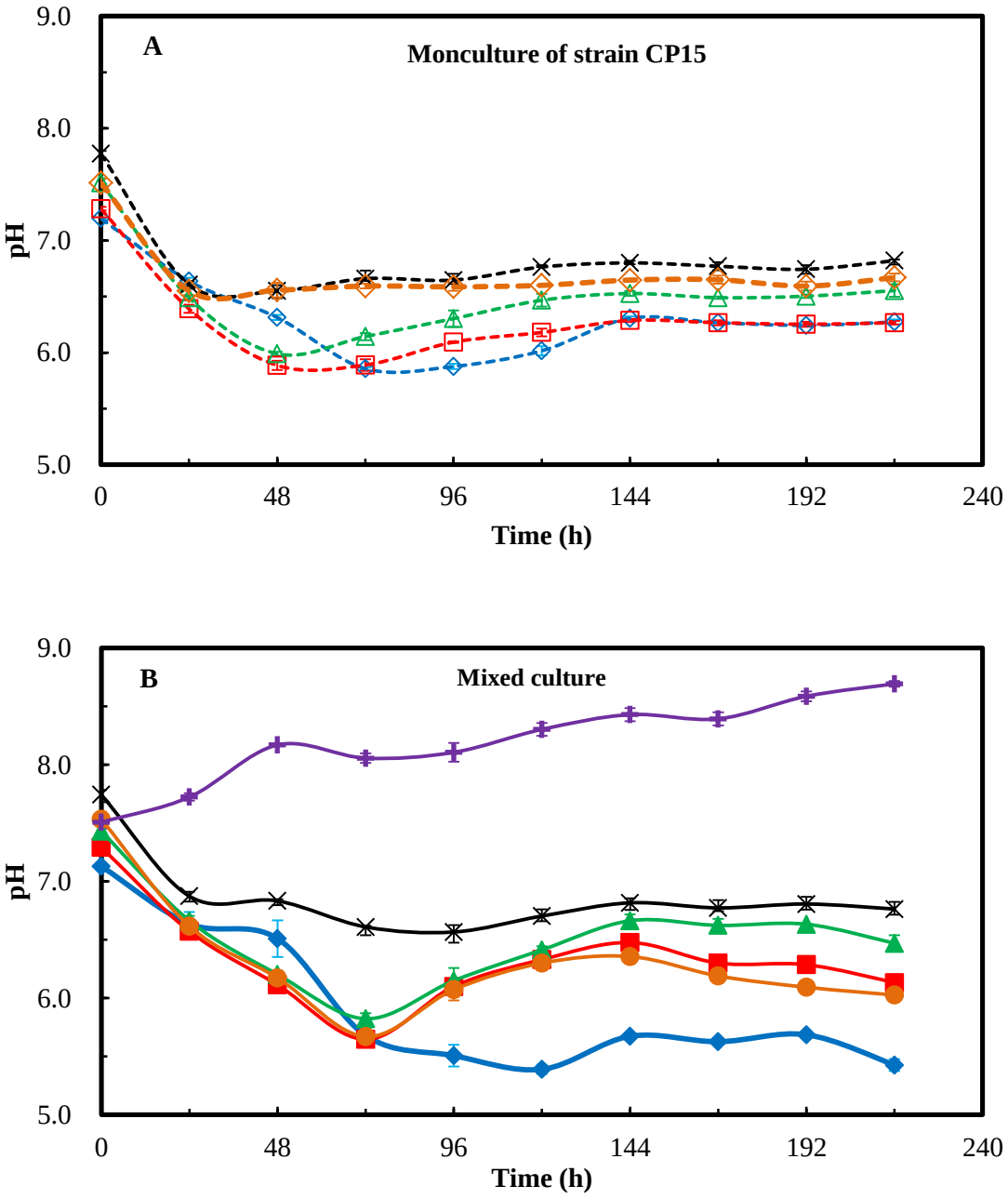

Fig. B1 pH profiles during syngas fermentation in 250-mL bottles with the addition of various carboxylic acids (A) strain CP15 monoculture (open symbol and dash line) (B) mixed culture (solid symbol and solid line); treatment with no acid (♦), propionic acid (■),butyric acid (▲), hexanoic acid (×), lactic acid (●), lactic acid with N_2 headspace (+).

B3 Gas consumption and production profiles

A fast CO and H_2 consumption was observed during cell growth and in early stationary phase using both strain CP15 monoculture and mixed culture (Figs. B2 and B3). In the treatment without addition of acid, strain CP15 monoculture utilized the highest amount of CO than other treatments. However, the highest CO consumption using mixed culture was observed in the treatment with butyric acid.

The highest amount of H_2 consumption was observed in the no acid treatment for both strain CP15 monoculture and mixed culture. The mixed culture utilized significantly more CO in treatments that contained propionic acid, butyric acid and lactic acid than the CP15 monoculture ($p < 0.05$) (Table 7.3). The mixed culture also utilized more H_2 in treatments that contained butyric acid and lactic acid than the CP15 monoculture. The percentages of CO and H_2 utilization in the treatment without acid by CP15 monoculture were significantly higher than in treatments with acids ($p < 0.05$), probably due to presence of more cell mass concentration in the treatment without acid (Fig. 7.4).

The CO_2 production was also observed during the fermentation using both strain CP15 monoculture and mixed culture (Fig. B4). Similar to CO consumption profiles, a fast production of CO_2 was mainly observed during the cell growth phase. The highest CO_2 production was observed in the no acid treatment using CP15 monoculture. However, when the mixed culture was used, the greatest CO_2 production was obtained in the treatment with butyric acid.

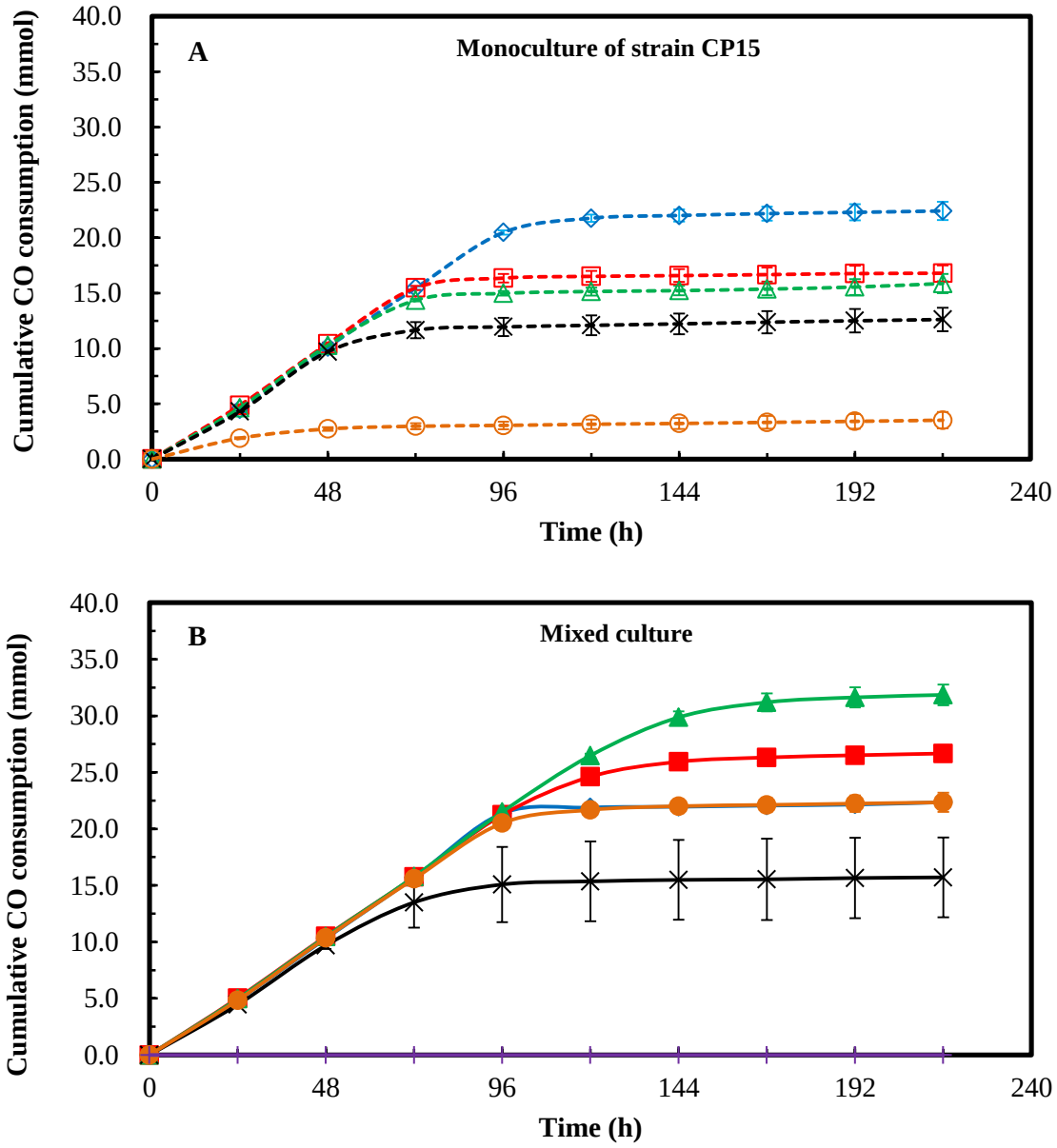

Fig. B2 Cumulative CO consumption profiles during syngas fermentation in 250-mL bottles with the addition of various carboxylic acids (A) strain CP15 monoculture (open symbol and dash line) (B) mixed culture (solid symbol and solid line); treatment with no acid (♦), propionic acid (■),butyric acid (▲), hexanoic acid (×), lactic acid (●), lactic acid with N_2 headspace (+).

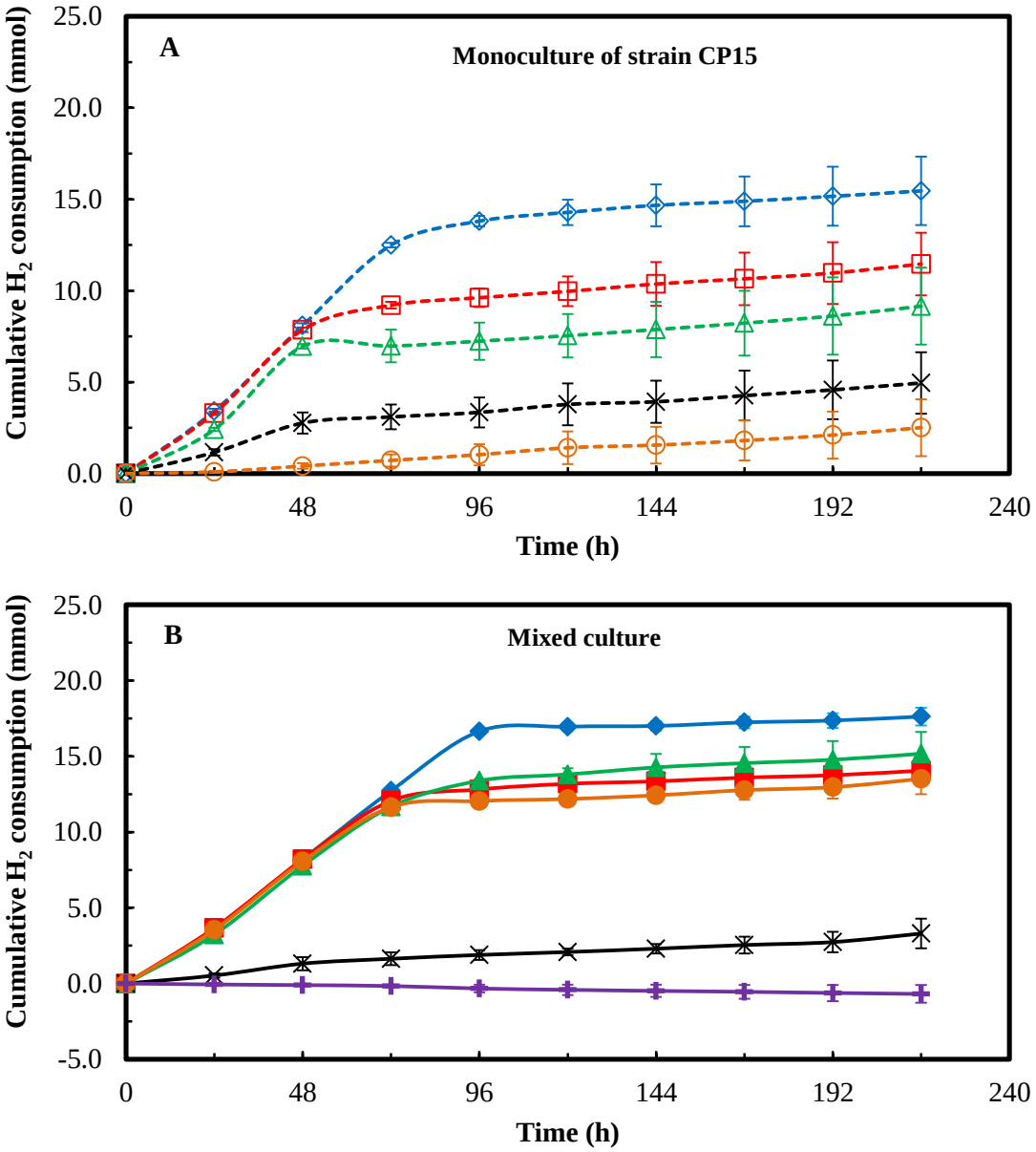

Fig. B3 Cumulative H_2 consumption profiles during syngas fermentation in 250-mL bottles with the addition of various carboxylic acids (A) strain CP15 monoculture (open symbol and dash line) (B) mixed culture (solid symbol and solid line); treatment with no acid (♦), propionic acid (■),butyric acid (▲), hexanoic acid (×), lactic acid (●), lactic acid with N_2 headspace (+).

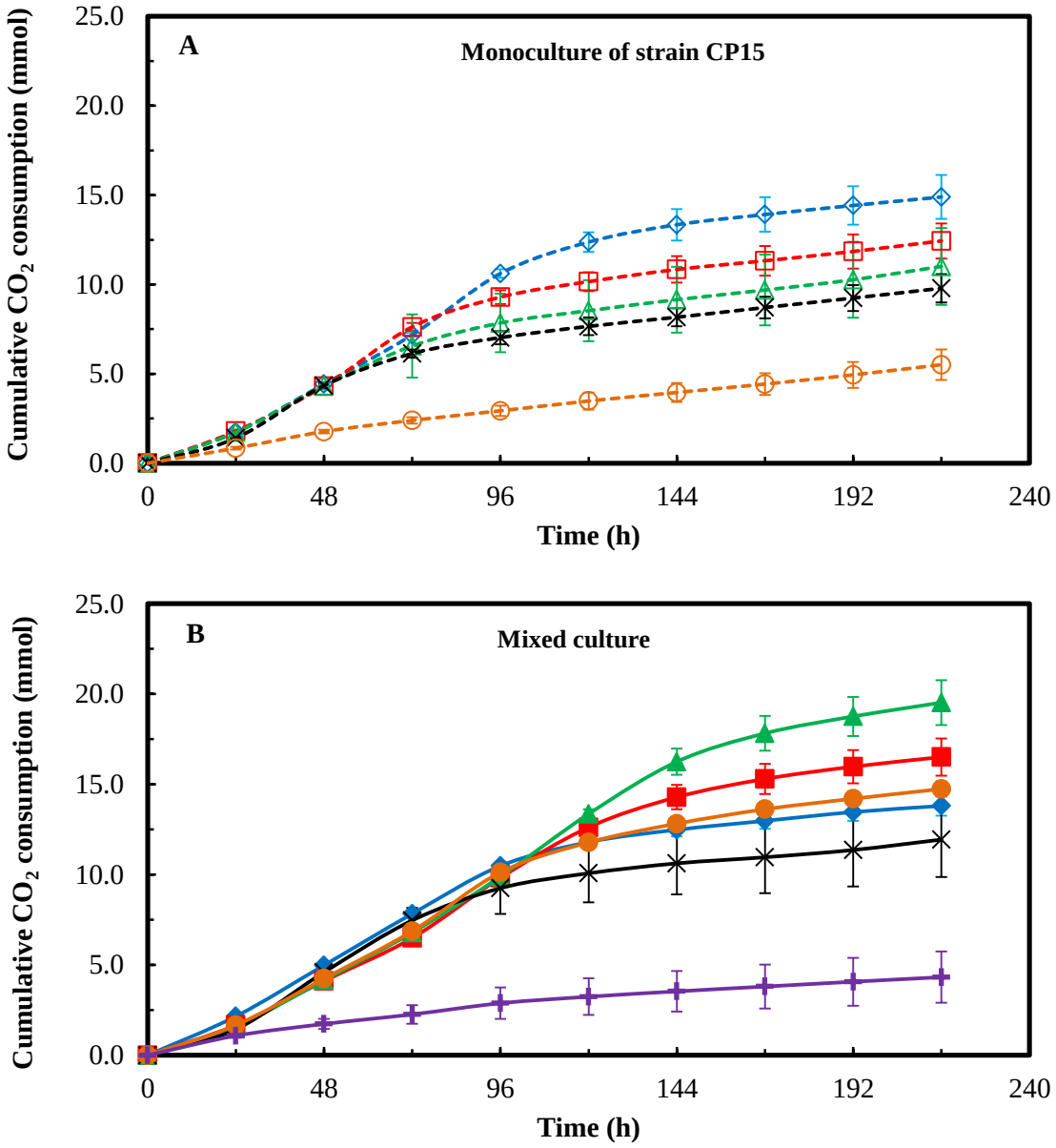

Fig. B4 Cumulative CO_2 production profiles during syngas fermentation in 250-mL bottles with the addition of various carboxylic acids (A) strain CP15 monoculture (open symbol and dash line) (B) mixed culture (solid symbol and solid line); treatment with no acid (♦), propionic acid (■),butyric acid (▲), hexanoic acid (×), lactic acid (●), lactic acid with N_2 headspace (+).

APPENDIX C

C1 Effect of Switchgrass derived producer gas on *Alkalibaculum bacchi* strain $CP11^T$ fermentation

C1.1 Background

Most syngas fermentation research was performed using commercial gas mix to simulate the desired syngas composition studied. Several studies reported the use of producer gas during syngas fermentation (Rajagopalan et al., 2002; Ahmed et al., 2006; Babu et al., 2010; Kundiyana et al., 2010). Producer gas made from gasifying biomass feedstocks contains impurities such as methane, ethane, acetylene, NOx, COS, NH_3, SO_2 and tar (Wilkins and Atiyeh, 2011; Xu et al., 2011). No studies were found on the use of *A. bacchi* strains using real biomass derived syngas.

The objective of the present study is to examine the effect of switchgrass derived producer gas on the ability of *A. bacchi* strain $CP11^T$ to convert the gas to ethanol and acetic acid in bottle fermentations. The producer gas was obtained from the OSU gasification facility, which contained 11.10% H_2, 54.43% N_2, 13.35% CO, 16.38% CO_2, 2.83% CH_4, 0.12% C_2H_2, 0.61% C_2H_4, 0.17% C_2H_6 and 0.42% acetone. The medium used was the standard YE medium with TAPS buffer. The fermentations were performed in 250-mL bottle fermenters. The details of medium preparation and composition, liquid and gas analysis were described in Chapter 4 section 4.2.

C1.2 Growth and product profiles

Strain CP11^T grew to a maximum cell mass concentration of 0.38 g/L using producer gas (Fig. C1). This was comparable to growth profiles obtained with the Syngas I (20% CO, 15% CO_2, 5% H_2 and 60% CO_2) (Liu et al.,2012). The pH dropped to 6.7 and remained at this level. The maximum acetic acid concentration using the producer gas was 4.7 g/L at 288 h and was stable at this level till the end of fermentation. The acetic acid produced from producer gas was 4.3 times higher than with the Syngas I (Liu et al.,2012). The leveling off trend of acetic acid explained the no apparent increase of pH, which usually an indication of acetic acid conversion to ethanol. Only 0.1 g/L ethanol was observed during 360 h of fermentation. There was O_2 contamination in the fermentation bottles after 240 h, which caused the medium color to turn pink. The source of O_2 was from the compressor used in gasification facility to fill producer gas storage tanks, the same producer gas used in this study. The low ethanol (0.1 g/L) production was probably due to the presence of O_2 that deactivated alcohol dehydrogenase responsible for the production of ethanol (Ismaiel et al., 1993). Strain CP11^T produced 0.67 g/L ethanol using Syngas I that did not contain any O_2 or other contaminants as in producer gas (Liu et al., 2012). Syngas fermenting microorganisms are strict anaerobes and their activities will drastically decrease when exposed to O_2.

Isopropanol and acetone were also detected in the fermentation medium. The acetone from the producer gas accumulated in the medium during the fermentation to a final concentration 1.6 g/L. Acetone was used to clean the tars in the producer gas and remained in the producer gas, which explained its accumulation in the medium. Also, no more than 0.05 g/L isopropanol was observed after 360 h of fermentation, which could be

due to the conversion of acetone to isopropanol via a secondary alcohol dehydrogenase as was observed with *C. ragsdalei* (Ramachandriya et al., 2011).

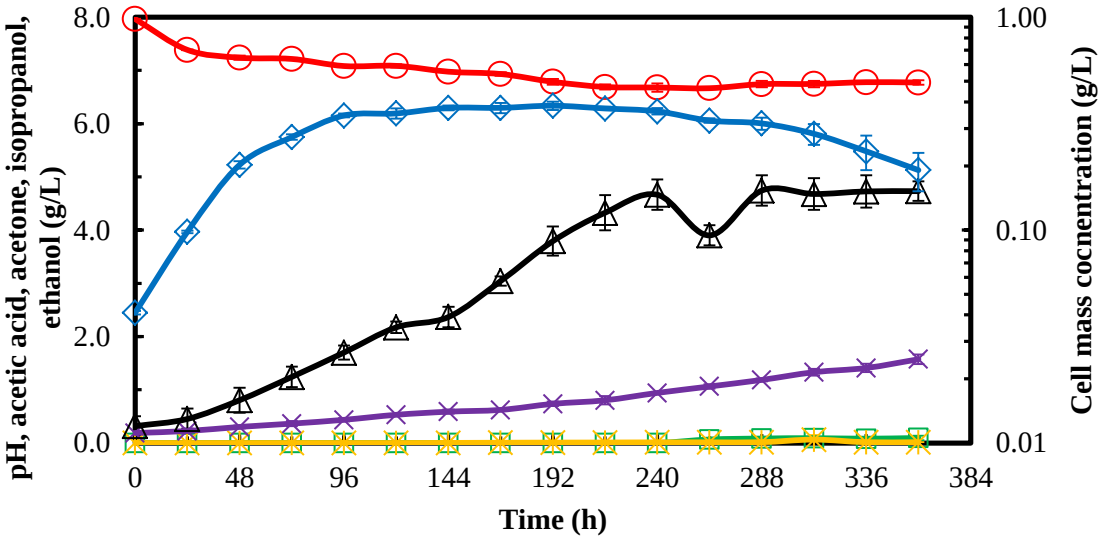

Fig. C1 Growth and products profiles of *A. bacchi* strain CP11^T in producer gas bottle fermentation; cell mass concentration (◊), pH (○), ethanol (□), isopropanol(✳), acetone (×), acetic acid (Δ).

C1.3 Gas consumption profiles

Both CO and H_2 were utilized during the fermentation with strain CP11^T (Fig. C2). More CO was consumed compared to H_2. After 240 h, CO and H_2 consumption started to level off when no more acetic acid was produced (Fig. C1). This showed that both CO and H_2 contributed to acetic acid formation. There was 33.3% less cumulative CO mole consumption by strain CP11^T using the producer gas compared to Syngas I (20% CO, 15% CO_2, 5% H_2 and 60% N_2) reported in Chapter 4. In addition, there was 55% less of cumulative CO_2 production with CP11^T using producer gas than

using Syngas I. However, there was three times more cumulative H_2 mole consumption by strain CP11^T using the producers gas (Fig. C2), compare to Syngas I as in Chapter 4 (Liu et al., 2012). In addition, the percentages of CO and H_2 utilization after 360 h of fermentation were 49.5% and 37.9%, respectively.

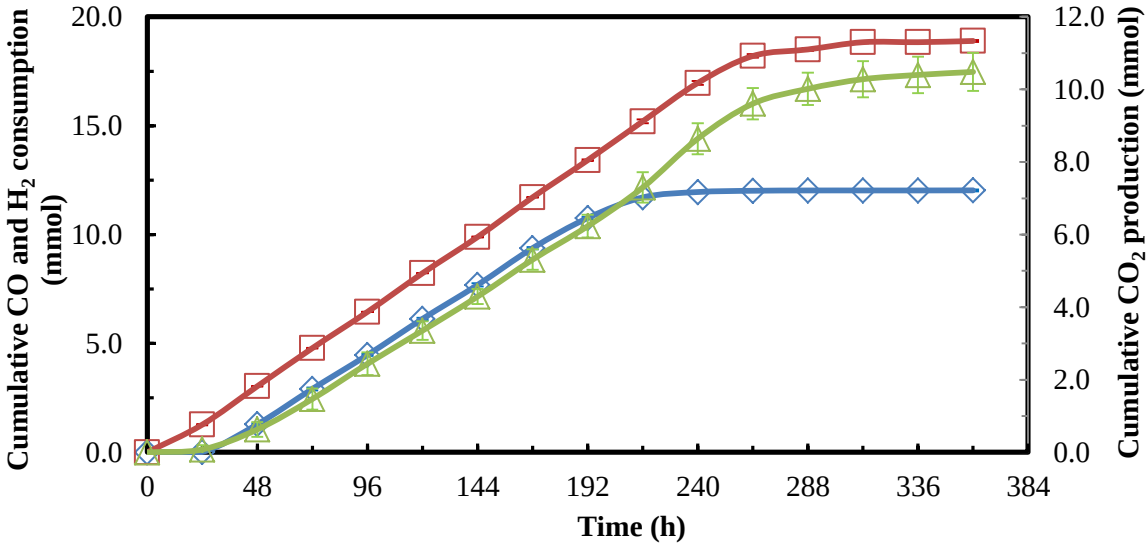

Fig. C2 Gas consumption and production profiles of *A. bacchi* strain CP11^T in producer gas bottle fermentation; CO (□), H_2 (◊), CO_2 (Δ).

C1.4 Conclusions

Acetic acid was the main product from producer gas with only 0.1 g/L ethanol. O_2 contamination possibly caused the low ethanol production. The minute amount of isopropanol produced during the fermentation indicates that strain CP11^T could have a secondary alcohol dehydrogenase responsible for the conversion of acetone into isopropanol.

C1.5 References

Ahmed, A., Cateni, B.G., Huhnke, R.L., Lewis, R.S., 2006. Effects of biomass-generated producer gas constituents on cell growth, product distribution and hydrogenase activity of *Clostridium carboxidivorans* P7^{T}. Biomass Bioenerg. 30, 665-672.

Babu, B.K., Atiyeh, H.K., Wilkins, M.R., Huhnke, R.L., 2010. Effect of the reducing agent dithiothreitol on ethanol and acetic acid production by *Clostridium* strain P11 using simulated biomass-based syngas. Biol. Eng. 3, 19-35.

Ismaiel, A.A., Zhu, C., Colby, G., Chen, J.-S., 1993. Purification and characterization of a primary-secondary alcohol dehydrogenase from two strains of *Clostridium beijerinckii*. J. Bacteriol. 175, 5097-5105.

Kundiyana, D.K., Huhnke, R.L., Wilkins, M.R., 2010. Syngas fermentation in a 100-L pilot scale fermentor: design and process considerations. J. Biosci. Bioeng. 109, 492-498.

Liu, K., Atiyeh, H.K., Tanner, R.S., Wilkins, M.R., Huhnke, R.L., 2012. Fermentative production of ethanol from syngas using novel moderately alkaliphilic strains of *Alkalibaculum bacchi*. Bioresour. Technol. 104, 336-341.

Rajagopalan, S., P. Datar, R., Lewis, R.S., 2002. Formation of ethanol from carbon monoxide via a new microbial catalyst. Biomass Bioenerg. 23, 487-493.

Ramachandriya, K.D., Wilkins, M.R., Delorme, M.J.M., Zhu, X., Kundiyana, D.K., Atiyeh, H.K., Huhnke, R.L., 2011. Reduction of acetone to isopropanol using producer gas fermenting microbes. Biotechnol. Bioeng. 108, 2330-2338.

Wilkins, M.R., Atiyeh, H.K., 2011. Microbial production of ethanol from carbon monoxide. Curr. Opin. Biotechnol. 22, 326-330.

Xu, D., Tree, D.R., Lewis, R.S., 2011. The effects of syngas impurities on syngas fermentation to liquid fuels. Biomass Bioenerg. 35, 2690-2696.

C2 Effect of $NaHCO_3$ on *Alkalibaculum bacchi* strain $CP11^T$ syngas fermentation

C2.1 Background

The mechanisms of making ATP for cell growth and function are mainly discussed in terms of proton pump, sodium pump and Rnf complex (Schmehl et al., 1993; Müller et al., 2008; Köpke et al., 2011). *Moorella thermoacetica* and *Morella thermoautotrophica* and *Clostridium ragsdalei* were proposed to generate ATP from the proton pump, called "H^+-dependent" acetogens (Saxena, 2008). However, Na^+-dependent acetogens ATP production (sodium pump) were found in *Acetobacterium woodii*, *Thermoanaerobacter kivui* and *Ruminococcus productus* (Saxena, 2008). $NaHCO_3$ is used as buffer to avoid fast pH drop during syngas fermentation due to dissolved CO_2 from headspace. Na^+ is an important ion to generate ATP for some alkaliphilic strains based on sodium pump to create transmembrane electrochemical gradient (Pitryuk and Pusheva, 2001; Köpke et al., 2011). Nevertheless, sodium was found to inhibit *C. ragsdalei* growth and ethanol production at a concentration of 171 mM compared to sodium concentration of 34.2 mM in *C. ragsdalei* standard YE medium (Saxena and Tanner, 2012).

No studies were reported on the effect of Na^+ on *A. bacchi* strains syngas fermentation ability. The standard YE medium used for *A. bacchi* contained 60.4 mM Na^+, mainly from $NaHCO_3$. The present study evaluated the effect of $NaHCO_3$ concentrations (0 g/L, 1 g/L and 5 g/L) on strain $CP11^T$ growth and ethanol production in 250-mL bottle fermentation using the standard yeast extract medium with TAPS buffer

and Syngas I (20% CO, 15% CO_2, 5% H_2 and 60% N_2). The composition of the medium and procedures followed are described in Chapter 4 section 4.2.

C2.2 Growth and pH profiles

The difference in the maximum cell concentrations with 0 g/L, 1 g/L and 5 g/L $NaHCO_3$ were not significant ($p > 0.05$) (Fig. C3). However, the lowest pH in the medium with 5 g/L $NaHCO_3$ was above the lowest pH values obtained with 0 g/L and 1 g/L $NaHCO_3$ ($p < 0.05$), indicating a better buffer capacity with 5 g/L $NaHCO_3$. The fast drop in $CP11^T$ cell mass concentration was similar to the previous study (Liu et al., 2012). The reason for cell mass concentration drop could be due to cell lysis because strain $CP11^T$ is sensitive to low pH close to 6.5, which was the lowest pH for growth (Allen et al., 2010). In addition, acetic acid produced during growth stage was reported to diffuse back into the cell cytoplasm in the undissociated form, lowing intracellular pH and decreasing the transmembrane proton gradient (Herrero et al., 1985). *Clostridium coskatii* growth was inhibited when the undissociated acetic acid concentration was 3 g/L (Zahn and Saxena, 2011). In the present study, the calculated lowest undissociated acetic acid level was 0.02 g/L at pH 6.4, indicating the growth inhibition level of undissociated acetic acid for strain $CP11^T$. The results showed that the decrease in the amount of $NaHCO_3$ in the medium had no effect on cell growth.

C2.3 Products formation

Acetic acid was the main product during cell growth (Fig. B4). There was no difference in the maximum acetic acid concentrations with the various $NaHCO_3$ treatments ($p > 0.05$). However, ethanol concentration was highest (0.69 g/L) in the

medium with 5 g/L $NaHCO_3$ ($p < 0.05$) as shown in Fig. B5. Similar amounts of ethanol were produced in the other treatments with 0 g/L and 1 g/L $NaHCO_3$.

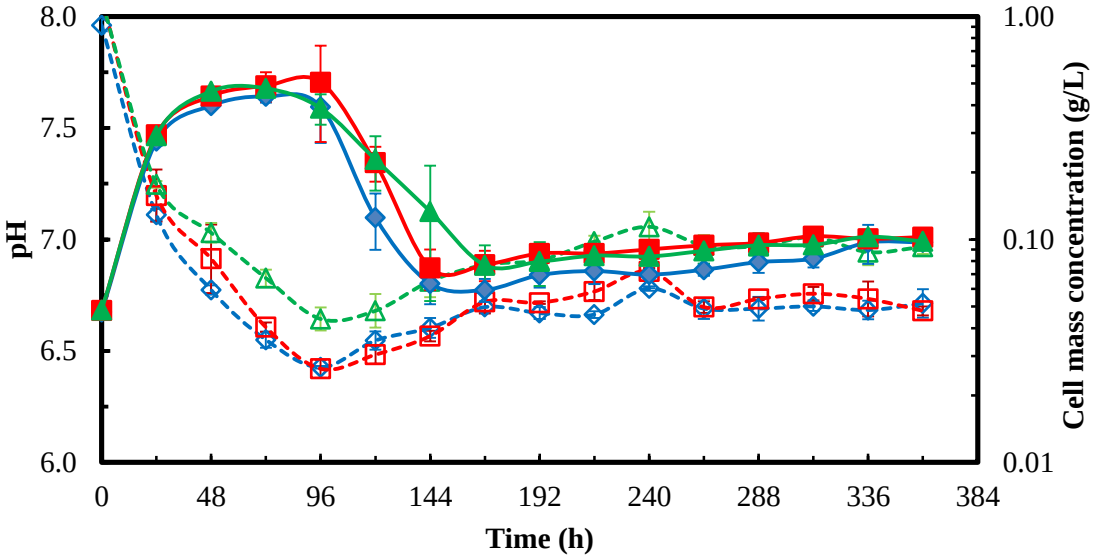

Fig. C3 Growth (solid line and solid symbol) and pH (dash line and open symbol) profiles of *A. bacchi* strain CP11^T at various $NaHCO_3$ concentrations; 0 g/L $NaHCO_3$ (◊), 1 g/L $NaHCO_3$ (□) and 5 g/L $NaHCO_3$ (Δ).

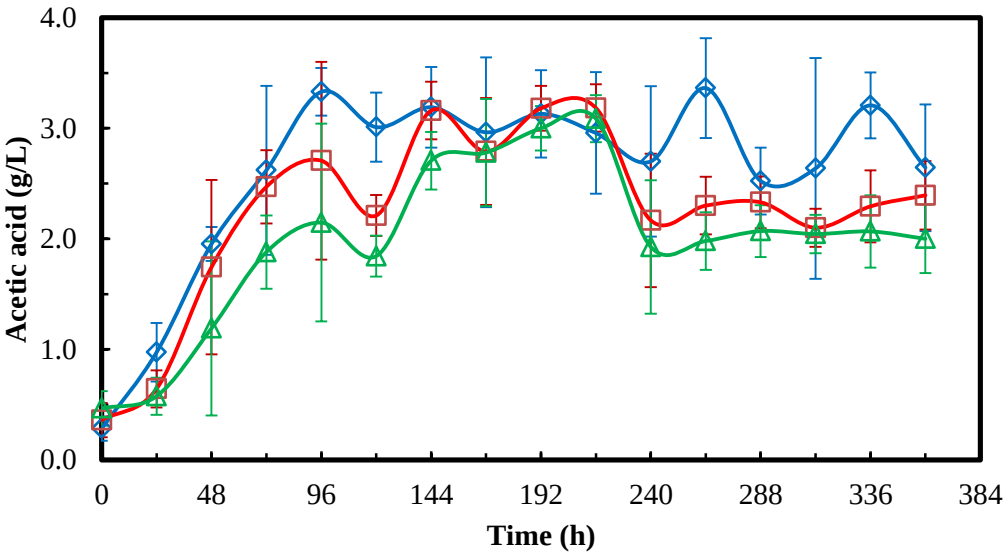

Fig. C4 Acetic acid profiles of *A. bacchi* strain CP11^T at various $NaHCO_3$ concentrations; 0 g/L $NaHCO_3$ (◊), 1 g/L $NaHCO_3$ (□) and 5 g/L $NaHCO_3$ (Δ).

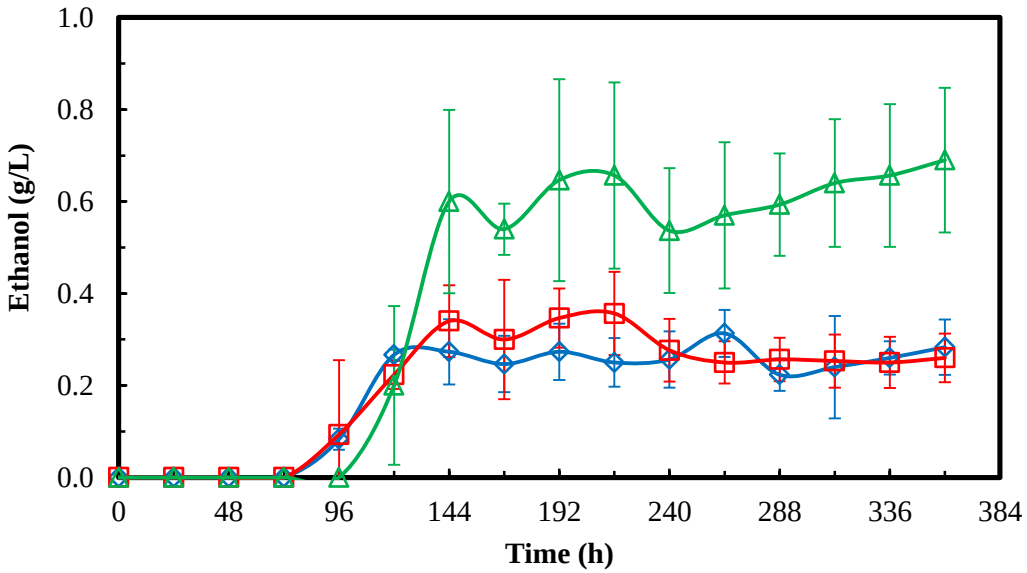

Fig. C5 Ethanol profiles of *A. bacchi* strain CP11^T at various $NaHCO_3$ concentrations; 0 g/L $NaHCO_3$ (◊), 1 g/L $NaHCO_3$ (□) and 5 g/L $NaHCO_3$ (Δ).

C2.4 Conclusions

The decrease or elimination of $NaHCO_3$ from the medium had no effect on CP11^T growth and ability to produce acetic acid. However, ethanol production was significantly decreased when $NaHCO_3$ was reduced below 5 g/L. Thus, 5 g/L $NaHCO_3$ was used in *A. bacchi* strain CP11^T fermentation medium for ethanol production.

C2.5 References

Allen, T.D., Caldwell, M.E., Lawson, P.A., Huhnke, R.L., Tanner, R.S., 2010. *Alkalibaculum bacchi* gen. nov., sp. nov., a CO-oxidizing, ethanol-producing

acetogen isolated from livestock-impacted soil. Int. J. Syst. Evol. Microbiol. 60, 2483-2489.

Herrero, A.A., Gomez, R.F., Snedecor, B., Tolman, C.J., Roberts, M.F., 1985. Growth inhibition of *Clostridium thermocellum* by carboxylic acids: a mechanism based on uncoupling by weak acids. Appl. Microbiol. Biotechnol. 22, 53-62.

Köpke, M., Mihalcea, C., Bromley, J.C., Simpson, S.D., 2011. Fermentative production of ethanol from carbon monoxide. Curr. Opin. Biotechnol. 22, 320-325.

Liu, K., Atiyeh, H.K., Tanner, R.S., Wilkins, M.R., Huhnke, R.L., 2012. Fermentative production of ethanol from syngas using novel moderately alkaliphilic strains of *Alkalibaculum bacchi*. Bioresour. Technol. 104, 336-341.

Müller, V., Imkamp, F., Biegel, E., Schmidt, S., Dilling, S., 2008. Discovery of a Ferredoxin: NAD^+-Oxidoreductase (Rnf) in *Acetobacterium woodii*. Ann. N. Y. Acad. Sci. 1125, 137-146.

Pitryuk, A.V., Pusheva, M.A., 2001. Different ionic specificities of ATP synthesis in extremely alkaliphilic sulfate-reducing and acetogenic bacteria. Microbiology 70, 398-402.

Saxena, J. 2008. Development of an optimized and cost-effective medium for ethanol production by *Clostridium* strain P11. Ph.D. Dissertation. University of Oklahoma, pp. 98.

Saxena, J., Tanner, R., 2012. Optimization of a corn steep medium for production of ethanol from synthesis gas fermentation by *Clostridium ragsdalei*. World J. Microbiol. Biotechnol. 28, 1553-1561.

Schmehl, M., Jahn, A., Meyer zu Vilsendorf, A., Hennecke, S., Masepohl, B., Schuppler, M., Marxer, M., Oelze, J., Klipp, W., 1993. Identification of a new class of nitrogen fixation genes in *Rhodobacter capsalatus*: a putative membrane complex involved in electron transport to nitrogenase. Mol. Gen. Genet. 241, 602-615.

Zahn, J.A., Saxena, J. 2011. Novel ethanologenic clostridium species, *Clostridium coskatii*. US patent 2011/0229947.

APPENDIX D

D Fed-batch fermentation using *A. bacchi* strain CP15 in a 7-L fermentor

D1 Background

A. bacchi strain CP15 was found to be the best ethanol producer compared to strains CP11^T and CP13 in 250-mL bottle fermentations (Liu et al.,2012). The scale up of syngas fermentation using *A. bacchi* strain CP15 in 7-L fermentor is discussed in this section. The objective of this study was to evaluate the ability of *A. bacchi* strain CP15 to convert syngas to ethanol in a 7-L fermentor with intermittent feeding of selected medium nutrients.

A 7-L Bioflo 415 fermentor with 3.3 L working volume was used with syngas continuously fed to strain CP15 and the liquid medium is in a batch mode. The gas flow rate was set to 145 sccm and the headspace pressure to 150 kPa. Syngas II was used containing 40% CO, 30% CO_2 and 30% H_2. No pH control was used. The medium composition was the standard yeast extract medium with TAP buffer as described in Chapter 4 section 4.2. The fermentation was performed in 7 phases.

Phase a was performed with the standard yeast extract medium until 360 h with the agitation speed set at 150 rpm. Phase b, an additional 3 g yeast extract (1g/L), 30 mL minerals solution (10 mL/L), 30 mL vitamins solution (10 mL/L), 30 mL trace metals solution (10 mL/L) and 7.5 mL 4% cysteine sulfide solution (2.5 mL/L) were added to the fermentor that contained 3.3 L. The agitation speed was increased to 300 rpm. The

purpose of phase b was to evaluate if there was a nutrient limitation. The concentrations of nutrients added at the beginning of Phase b were similar to Phase a.

In Phases c and d, 30 mL trace metal solution (10 mL/L) and 30 mL vitamin solution (10 mL/L), respectively, were added to study their effects on fermentation. In Phases e and f, the effects of minerals and pH adjustment on cell growth and products formation were investigated. In Phase e, 30 mL mineral solution (10 mL/L) was added and pH was adjusted to 7 followed by Phase f, in which an additional 30 mL mineral solution (10 mL/L) was added in the fermentor. Finally in Phase g, 3 g yeast extract (1g/L) was added to evaluate if yeast extract can restart cell growth.

D2 Growth, pH and product profiles

D2.1 Phase a, standard yeast extract medium fermentation (0 to 360 h)

After a lag phase of 6 h, cell mass concentration increased to 0.5 g/L (OD 1.3) at 48 h (Fig. D1). When cell mass concentration reached maximum (0.5 g/L), a stationary phase was observed till 360 h. When cell mass concentration began to increase, the pH decreased to 6.75 between 6 h to 33 h, due to the production of acetic acid. Then, the pH increased to 7.0 at 56 h and remained at the same level. Acetic acid concentration reached a maximum concentration of 2.46 g/L at 30 h. Then, it decreased to 0 g/L at 168 h. The decrease in acetic acid concentration was associated with an increase in ethanol concentration and pH (Fig. D1). The conversion of acetic acid to ethanol was also observed in bottle fermentations (Liu et al.,2012). From 192 h to 360 h, acetic acid concentration was 0 g/L. Ethanol formation started at 48 h and reached a maximum of 3.5 g/L at 144 h and was not changed until 360 h.

The CO and H_2 consumption were associated with cell growth (Fig. D2) and began to level off when growth stopped. CP15 consumed 0.9 mol of CO and 0.5 mol of H_2 during 360 h of fermentation.

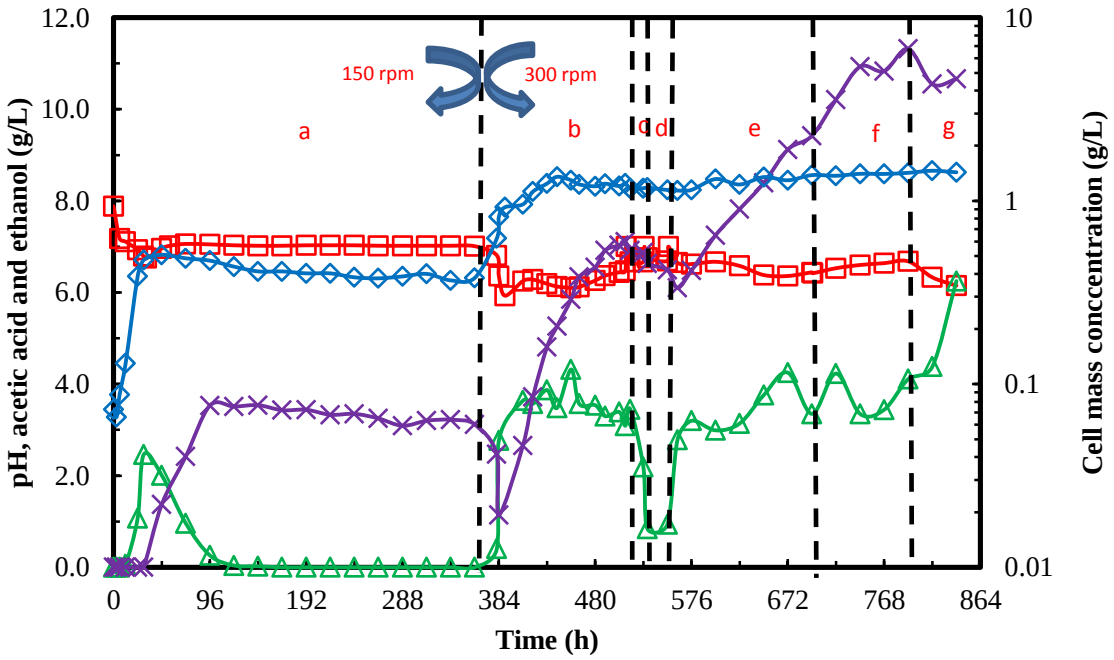

Fig. D1 Growth and products profiles in 7-L Bioflo 415 fermentor with strain CP15; cell mass concentration (◊), pH (□), acetic acid (Δ), ethanol (×); (a) standard YE medium, (b) added vitamins, trace metals, minerals, yeast extract, 7.5 mL 4% cysteine sulfide and adjusted pH to 7, (c) added 30 mL trace metals, (d) added 30 ml vitamin solution and adjusted pH to 7, (e) added 30 mL minerals and adjusted pH to 7, (f) added 30 mL minerals, (g) added 3 g yeast extract.

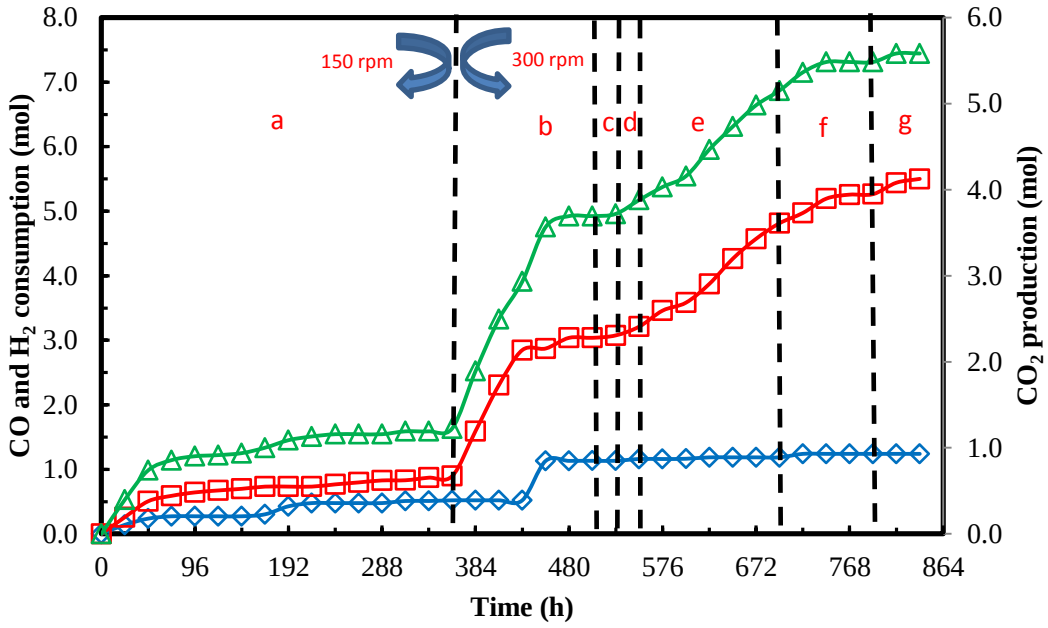

Fig. D2 Cumulative CO and H_2 consumption and CO_2 production profiles in 7-L Bioflo 415 fermentor with strain CP15; H_2 (◊), CO (□), CO_2 (Δ); (a) standard YE medium, (b) added vitamins, trace metals, minerals, yeast extract, 7.5 mL 4% cysteine sulfide and adjusted pH to 7, (c) added 30 mL trace metals, (d) added 30 ml vitamin solution and adjusted pH to 7, (e) added 30 mL minerals and adjusted pH to 7, (f) added 30 mL minerals, (g) added 3 g yeast extract.

D2.2 Phase b (from 360 h to 510 h), added concentrated nutrients and boost agitation from 150 rpm to 300 rpm

As the fermentation profile did not change from 120 h to 360 h, the same concentration of fresh nutrients as in Phase a were added and the agitation speed was increased to 300 rpm to improve the gas to liquid mass transfer. The nutrient added were 10 mL/L vitamins, 10 mL/L trace metals, 10 mL/L minerals, 1 g/L yeast extract and 2.5

mL/L cysteine sulfide. No TAPS or sodium bicarbonate was added. The pH of medium was not adjusted, which started at pH 7.0.

In phase b, cell mass concentration started to increase after adding fresh nutrients, reaching 1.35 g/L (OD 3.4) at 442 h. Compared to the first 360 h of fermentation (phase a), cell mass concentration increased by 3 times. The pH of the culture dropped from 7.0 to 5.9 from 360 h to 390 h, followed by an increase to 6.47 from 390 h to 510 h. Acetic acid concentration increased from 0 g/L to 4.32 g/L during 360 h to 456 h, followed by decreasing to 3.09 g/L from 456 h to 510 h. Ethanol concentration decreased from 3.12 g/L to 1.14 g/L during the cell growth stage. This was also noticed when ethanol was added as a substrate for CP15 at the beginning of the fermentation, which is discussed in Appendix E. After the short decrease in ethanol concentration in Phase b, cells started to produce ethanol to 7.11 g/L from 384 h to 510 h. However, acetic acid concentration did not show clear decreasing trend, which was different from the first 360 h (Phase a). This could be due to more cell mass produced more acetic acid, which made the acetic acid production rate comparable to its conversion rate to ethanol.

Compared to phase a, the amounts of CO and H_2 consumed by CP15 were doubled. This was due to more cells formed with the fresh nutrients and doubling the agitation speed that increased mass transfer rate. In addition, the production of CO_2 was also boosted 2.5 times in Phase b compared to Phase a.

D2.3 Phases c and d (from 510 h to 552 h), added concentrated trace metals and vitamins solution

When trace metals solution (10 mL/L) was added in Phase c and the vitamins solution (10 mL/L) was added in Phase d, the cell mass, ethanol and acetic acid concentrations decreased. This indicates that the addition of trace metals and vitamins into the medium was not helpful in increasing cell mass or product concentrations. But there was a slight increase in CO consumption with no H_2 uptake in Phase d.

D2.4 Phases e and f (from 552 h to 792h), added concentrated minerals solution

In phase e, minerals solution was added and pH was adjusted and then an addition minerals solution was added in Phase f. The cell mass concentration remained constant in phases e and f. However, ethanol concentration increased fast from 6.1 g/L to 11.3 g/L. During the period of 552 h to 672 h, acetic acid concentration increased from 0.9 g/L to 4.3 g/L then was between 3.3 g/L to 4.4 g/L from 672 h to 792 h.

CO consumption and CO_2 production were observed in phases e and f. However H_2 consumption was not observed. The possible reason for improvement in acetic acid and ethanol production in Phases e and f could be the additional minerals such as calcium, magnesium, ammonium and potassium enhanced the enzymes activities in the acetyl-CoA pathway (Table 2.4).

D2.5 Phase g (from 792 h to 840 h), added yeast extract

In phase g, the addition of yeast extract did not boost cell growth but stimulated acetic acid production, which increased from 4.1 g/L to 6.25 g/L. Ethanol concentration did not show a major change and was stable at a level of 11 g/L. There was slight increase of CO consumption in this phase with no clear H_2 consumption.

D3 Conclusions

The results with semi-batch fermentation showed that the cell growth and ethanol production can be largely improved as in Phase b by the addition of fresh nutrients. At the end of Phase a, there were nutrients limitation for growth and function of strain CP15 fermentation. Also, minerals supported ethanol production in Phases e and f. Vitamins and trace metals did not affect the fermentation in Phases c and d. In Phase g, yeast extract was a stimulator for acetic acid production, but it did not resume the cell growth. This preliminary test also showed the potential of CP15 to produce about 11 g/L ethanol with high cell concentration by subsequent addition of nutrients to alleviate nutrients limitations.

D4 References

Gapes, J., Larsen, V., Maddox, I., 1983. A note on procedures for inoculum development for the production of solvents by a strain of Clostridium butylicum. J. Appl. Microbiol. 55, 363-365.

Jones, D.T., Woods, D.R., 1986. Acetone-butanol fermentation revisited. Microbiol. Rev. 50, 484.

Liu, K., Atiyeh, H.K., Tanner, R.S., Wilkins, M.R., Huhnke, R.L., 2012. Fermentative production of ethanol from syngas using novel moderately alkaliphilic strains of *Alkalibaculum bacchi*. Bioresour. Technol. 104, 336-341.

Ljungdahl, L.G., 1986. The autotrophic pathway of acetate synthesis in acetogenic bacteria. Annu. Rev. Microbiol 40, 415-450.

Osman, Y.A., Ingram, L., 1985. Mechanism of ethanol inhibition of fermentation in *Zymomonas mobilis* CP4. J. Bacteriol. 164, 173-180.

APPENDIX E

E Effect of added ethanol on strain CP15 ability to ferment syngas

E1 Background

It is important to examine the ethanol tolerance of the syngas fermenting microorganisms to know their potential for producing the maximum possible concentrations. The decrease in ethanol production rate usually occurs when ethanol accumulates in the medium during bacteria and yeast fermentation. Depending on the microorganisms, ethanol at high concentrations can cause cell membrane leakage and release of the intracellular enzymes, ions or cofactors out of cell cytoplasm (Osman and Ingram, 1985). For example, the syngas fermenting strain *C. ragsdalei* was reported to tolerate 35 g/L ethanol (Huhnke et al., 2010). Although *C. ljungdahlii* has not been tested for ethanol tolerance, the 48 g/L ethanol produced in the medium during continuous fermentation with cell recycle indicates that this strain can at least tolerate 48 g/L ethanol (Phillips et al., 1993). Moreover, ethanol can be used as a substrate to grow syngas fermenting strains such *C. ragsdalei, C. ljungdahlii, A. bacchi, C. carboxidivorans* (Tanner et al., 1993; Liou et al., 2005; Allen et al., 2010; Huhnke et al., 2010). No study has been done on ethanol tolerance of *A. bacchi* strains. The objective of this study is to evaluate if *A. bacchi* strain CP15 can tolerate up to 10 g/L ethanol for growth as well as the potential of ethanol utilization during its growth in standard YE medium with TAPS buffer. The treatments in the present study contained initial ethanol concentrations of 1.2 g/L and 12 g/L with Syngas I (20% CO, 15% CO_2, 5% H_2 and 60% N_2) headspace, and an initial ethanol concentration of 1.2 g/L with 100% N_2 headspace. All fermentation

bottles were pressurized to 239 kPa and flushed with either Syngas I or N_2 every 24 h. The medium compositions and preparation, liquid and gas samples analysis were described in Chapter 4 section 4.2.

E2 Growth and products profiles with N_2 headspace and 1.2 g/L ethanol

When 1.2 g/L ethanol was initially added to the standard YE medium in bottle fermentations with N_2 in the headspace, strain CP15 utilized it completely in 24 h and cell mass concentration increased to 0.1 g/L (OD=0.3) (Fig. E1). The other product from ethanol was acetic acid (2.4 g/L). The theoretical acetic acid from conversion of 1.2 g/L ethanol is 1.6 g/L. However, 0.8 g/L more acetic acid was produced during the fermentation. This could be due to $NaHCO_3$ contributes to the carbon source for acetyl-CoA (Ljungdhal, 1986). Also, ethanol can be used as electron source. Growth of CP15 stopped due to the depletion of ethanol in the medium after 24 h. Then, a fast drop in cell mass concentration was due to substrate depletion and cell lysis. The increasing trend in cumulative CO_2 production after 48 h was probably due to dissolved CO_2 in the medium gradually released to the N_2 headspace when there was no cells' activity (Fig. E1).

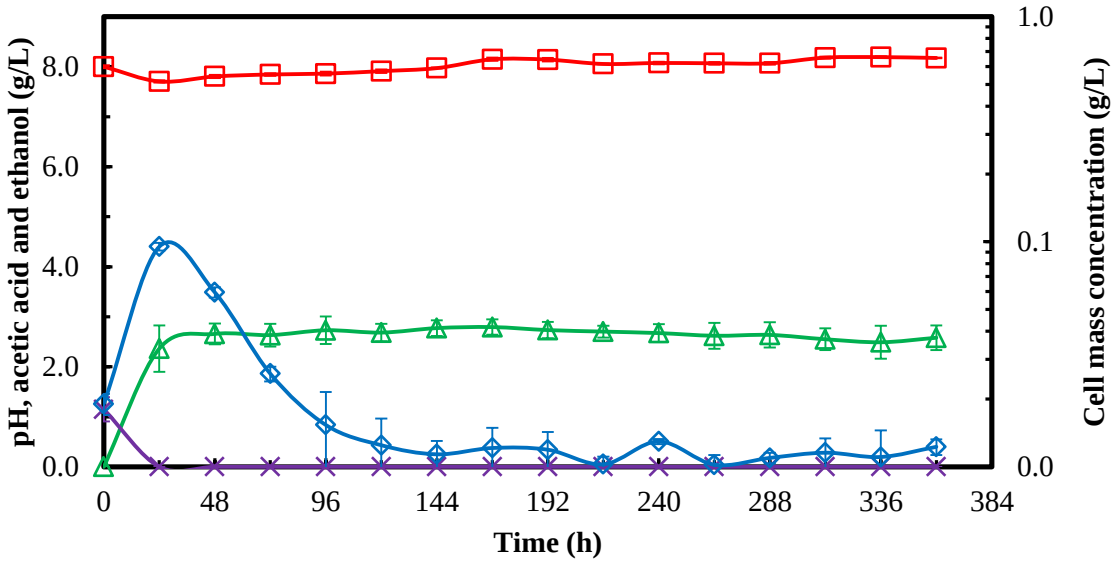

Fig. E1 Growth and products profiles during growth of strain CP15 on 1.2 g/L ethanol with N_2 headspace in bottle fermentation; cell mass concentration (◊), pH (□), acetic acid (Δ), ethanol (×).

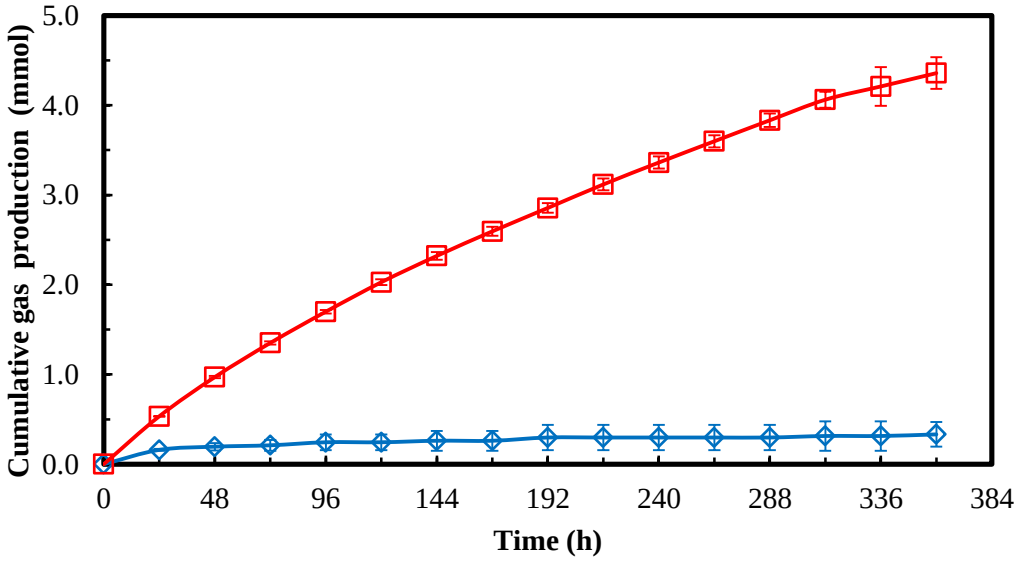

Fig. E2 Gas production profiles during growth of strain CP15 on 1.2 g/L ethanol with N_2 headspace in bottle fermentation; H_2 (◊), CO_2 (□).

E3 Growth and products profiles with syngas headspace and 1.2 g/L ethanol

Similar to N_2 headspace, there was a fast consumption of ethanol with Syngas I (20% CO, 15% CO_2, 5% H_2 and 60% N_2) during the first 24 h and cell mass concentration reached a maximum of 0.28 g/L (Fig. E3), which was 2.8 times higher than in the N_2 headspace (Fig. E1). A maximum acetic acid concentration of 4.7 g/L was produced with Syngas I, which was two times higher than in the N_2 headspace. There was a slight production of ethanol (0.4 g/L) after 192 h and reached, showing the evidence of reversible functionality of alcohol dehydrogenase in *A. bacchi* strain CP15. In addition, there was no H_2 consumption until 24 h due to growth of CP15 was mostly on ethanol. Then, strain CP15 continued growing on CO and H_2. CO consumption in the first 24 h was lower than after 24 h when ethanol was completed utilized by CP15. Also, the carbon from consumed ethanol was 5.2 mmol, which is 3.4 times more than the carbon from consumed CO for the first 24 h. This indicates that ethanol was preferable as substrate for growth than CO or H_2. The final percentages of CO and H_2 utilized by CP15 were 37.1% and 23.2%, respectively. The 2.4 g/L acetic acid could be assumed to be produced from syngas because 2.3 g/L acetic acid was produced with N_2 headspace (Fig. E1). Moreover, ethanol could have contributed to 63% growth during the first 24 h based on the 0.1 g/L cell mass produced in the treatment with N_2 in the headspace.

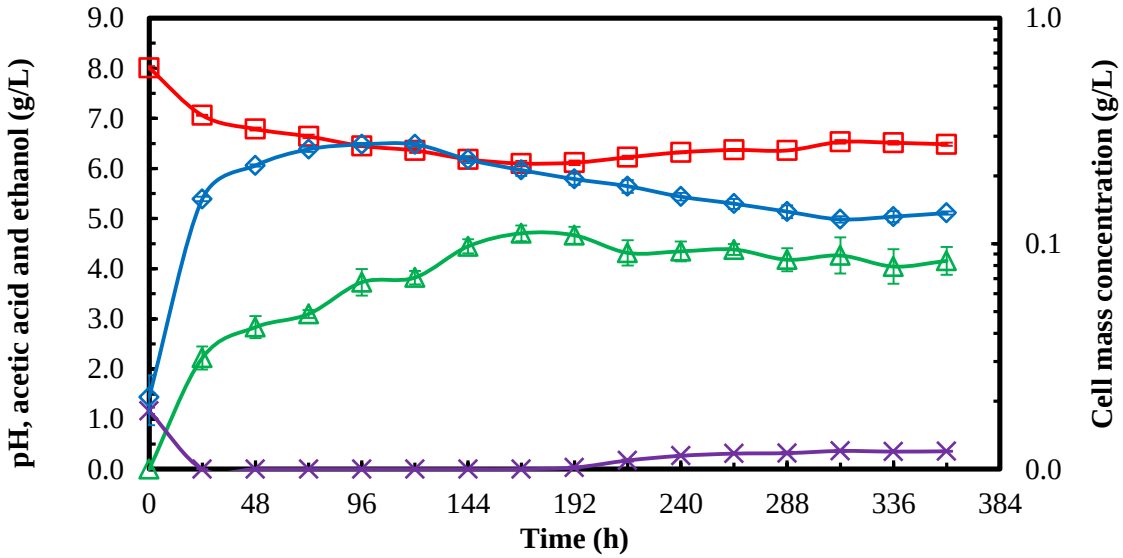

Fig. E3 Growth and products profiles during growth of strain CP15 on 1.2 g/L ethanol with Syngas I in bottle fermentation; cell mass concentration (◊), pH (□), acetic acid (Δ), ethanol (×).

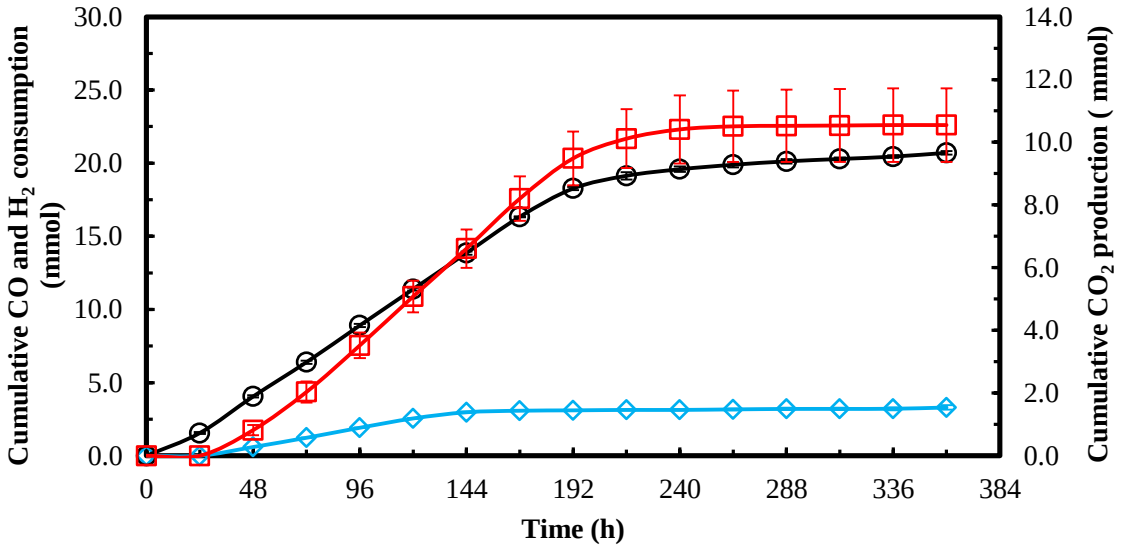

Fig. E4 Gas consumption and production profiles during growth of strain CP15 on 1.2 g/L ethanol with Syngas I in bottle fermentation; CO (○), H_2 (◊), CO_2 (□).

E4 Growth and products profiles with syngas headspace and 12.1 g/L ethanol

There was 24 h growth lag phase when an initial ethanol 12.1 g/L was in the medium with Syngas I (Fig. E5). After 24 h, the cell mass concentration reached 0.16 g/L, which was 37% higher than in the medium with the initial 1.2 g/L ethanol and Syngas I (Fig. E3). Cell mass concentration was stable after 48 h. In the medium with an initial ethanol concentration of 12.1 g/L, only 2.3 g/L ethanol were consumed between 24 h to 48 h. Ethanol concentration then was not changed. A maximum of 4.5 g/L acetic acid was produced in the medium, which was comparable to the amount produced in the medium with the 1.2 g/L ethanol with Syngas I. However, only 7.4 % and 3.2% of supplied CO and H_2 were utilized in the medium with 12.1 g/L ethanol after 360 h (Fig. E6). This was substantially lower than the CO and H_2 consumed in the medium with 1.2 g/L ethanol. The theoretical acetic acid produced from the consumed ethanol was 3 g/L and the other 1.5 g/L acetic acid was assumed to be formed from syngas. The lowest growth pH of strain CP15 was 6.5 (Allen et al., 2010) and the fast drop in medium pH from pH 8.0 to 5.6 after 48 h could be why CP15 growth stopped.

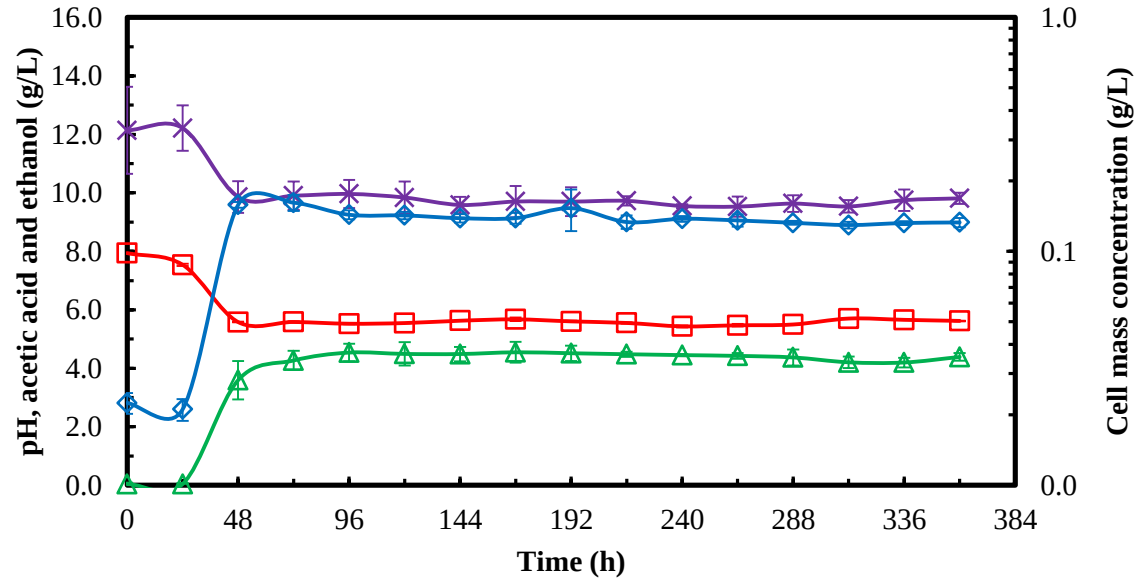

Fig. E5 Growth and products profiles during growth of strain CP15 on 12.1 g/L ethanol with Syngas I in bottle fermentation; cell mass concentration (◊), pH (□), acetic acid (Δ), ethanol (×).

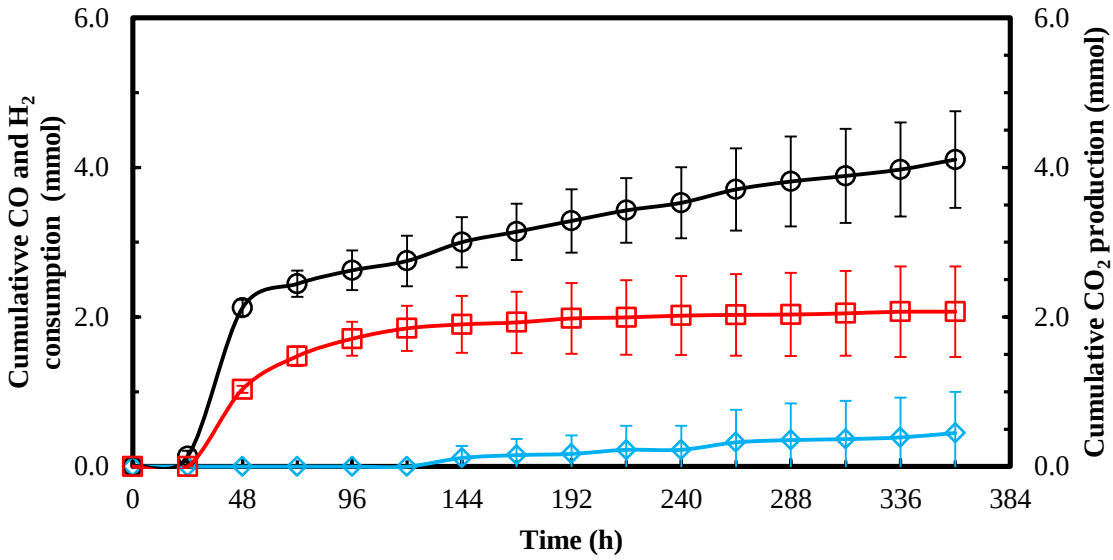

Fig. E6 Gas consumption and production profiles during growth of strain CP15 on 12.1 g/L ethanol with Syngas I in bottle fermentation; CO (○), H_2 (◊), CO_2 (□).

E5 Conclusions

A. bacchi strain CP15 can tolerate 12.1 g/L ethanol. However, this initial ethanol concentration significantly reduced CO and H_2 utilization. Ethanol was preferentially used as a substrate for strain CP15 growth compared to CO and H_2.

E6 References

Allen, T.D., Caldwell, M.E., Lawson, P.A., Huhnke, R.L., Tanner, R.S., 2010. *Alkalibaculum bacchi* gen. nov., sp. nov., a CO-oxidizing, ethanol-producing acetogen isolated from livestock-impacted soil. Int. J. Syst. Evol. Microbiol. 60, 2483-2489.

Huhnke, R.L., Lewis, R.S., Tanner, R.S. 2010. Isolation and characterization of novel clostridial species. US Patent No. 7,704,723.

Liou, J.S.C., Balkwill, D.L., Drake, G.R., Tanner, R.S., 2005. *Clostridium carboxidivorans* sp. nov., a solvent-producing *clostridium* isolated from an agricultural settling lagoon, and reclassification of the acetogen *Clostridium scatologenes* strain SL1 as *Clostridium drakei* sp. nov. Int. J. Syst. Evol. Microbiol. 55, 2085-2091.

Ljungdahl, L.G., 1986. The autotrophic pathway of acetate synthesis in acetogenic bacteria. Annu. Rev. Microbiol 40, 415-450.

Osman, Y.A., Ingram, L., 1985. Mechanism of ethanol inhibition of fermentation in *Zymomonas mobilis* CP4. J. Bacteriol. 164, 173-180.

Phillips, J., Klasson, K., Clausen, E., Gaddy, J., 1993. Biological production of ethanol from coal synthesis gas. Appl. Biochem. Biotechnol. 39, 559-571.

Tanner, R.S., Miller, L.M., Yang, D., 1993. *Clostridium ljungdahlii* sp. nov., an acetogenic species in clostridial rRNA homology group I. Int. J. Syst. Bacteriol. 43, 232-236.

APPENDIX F

F Effect of temperature on strain CP15 ability to ferment syngas

F1 Background

Temperature is an important factor for syngas fermentation due to it affects the microbial growth and substrate utilization. High temperature lowers the solubility of gaseous substrate in the medium (Munasinghe and Khanal, 2010). On the other hand, high temperature can lower the medium viscosity, reduce downstream ethanol distillation and reduce the power input for cooling syngas from gasification process (Munasinghe and Khanal, 2010). *A. bacchi* strain CP15 was observed growth at 45 ℃ (Allen et al., 2010) and this opens an opportunity to study the effects of temperature on strain CP15 ability to ferment syngas.

The objective of the present study was to evaluate the growth and products formation of *A. bacchi* strain CP15 at 45 ℃. The fermentation was conducted in 250-mL bottle fermentors with the standard YE medium with TAPS buffer and two syngas mixtures (Syngas I: 20% CO, 15% CO_2, 5% H_2 and 60% N_2, and Syngas II: 40% CO, 30% CO_2 and 30% H_2). The medium composition and preparation, liquid and gas samples analysis were described in Chapter 4 section 4.2. Two stages of the fermentation were tested. The first stage was performed by growing CP15 at 45 ℃ until no changes in fermentation profiles were observed. Then, the second stage was performed by decreasing the incubation temperature to 37 ℃.

F2 Fermentation with Syngas I

Growth of CP15 was observed to a maximum cell concentration of 0.13 g/L (OD 0.36) during the first stage of fermentation at 45 ℃ with Syngas I (Fig. F1). The maximum acetic acid concentration in the first stage was 0.56 g/L. Ethanol production started at 48 h and reached a maximum of 0.17 g/L at 144 h and then stabilized at this level until 240 h. Compared to CP15 growth and products formation at 37 ℃ in previous study with the same Syngas I (Liu et al.,2012), strain CP15 had comparable cell concentration but produced 39.8% and 88.7% less acetic acid and ethanol at 45 ℃, respectively. The CO and H_2 utilization were also affected by the high temperature at 45 ℃ and only 15.7% CO and 7.0% H_2 of the supplied gases were utilized by 240 h (Fig. F2). This showed the negative effect of high temperature on the substrates uptake.

Due to no change in cell mass concentration, gas consumption and product concentrations at 240 h, the second fermentation stage was studied at 37 ℃ and examine if growth of CP15 would resume at the optimal reported growth temperature. There was a 48 h growth lag phase, after which growth resumed at 312 h and cell mass concentration reached a maximum of 0.27 g/L at 432 h (Fig. F1). Accordingly, acetic acid was also produced during growth and early stationary phase to a maximum concentration of 1.8 g/L at 432 h. The conversion of acetic acid to ethanol was observed staring at 432 h with a final ethanol concentration of 1.6 g/L.

The gas utilization started simultaneously during cell growth at 37 ℃ (Fig. F2). After 240 h, 25.2 % CO and 13.1% H_2 of the supplied gases were utilized. The cell mass,

acetic acid and ethanol concentrations at 37 ℃ improved 2 times, 3.2 times and 9.4 times, respectively, compared to 45 ℃.

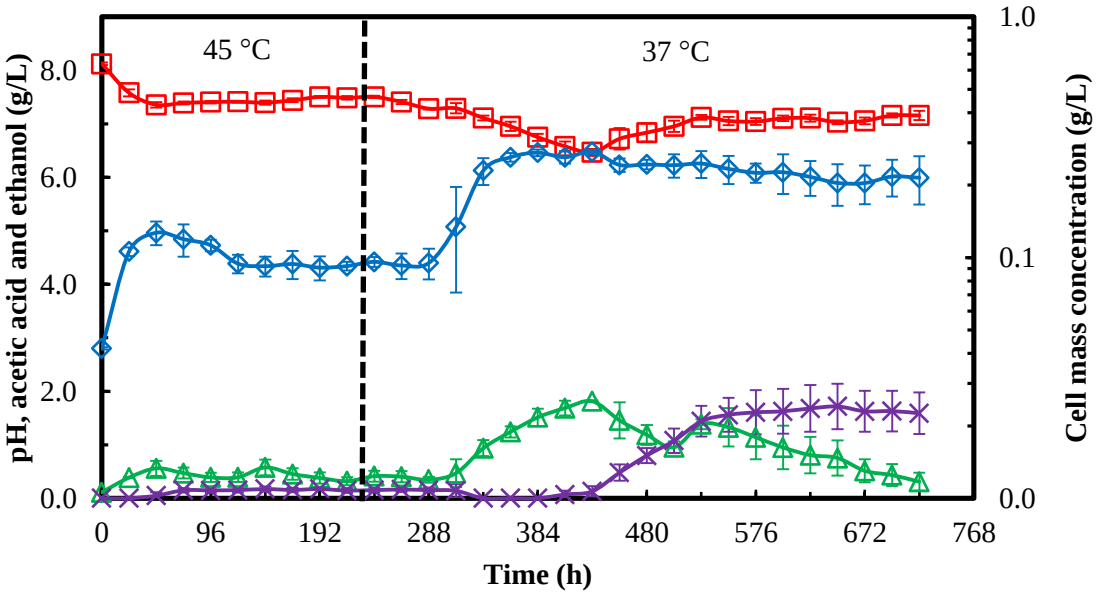

Fig. F1 Growth and products profile of strain CP15 at 45 ℃ followed by 37 ℃ with Syngas I in bottle fermentation; cell mass concentration (◊), pH (□), acetic acid (Δ), ethanol (×).

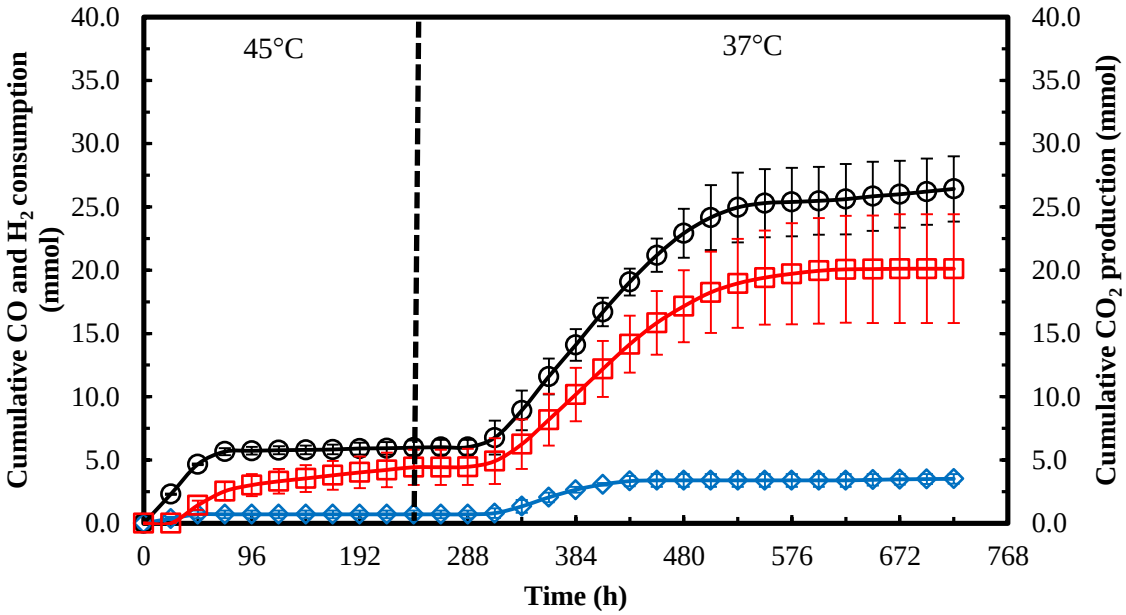

Fig. F2 Gas consumption and production profiles of strain CP15 at 45 ℃ followed by 37 ℃ with Syngas I in bottle fermentation; CO (○), H_2 (◊), CO_2 (□).

F3 Fermentation with Syngas II

Similar fermentation was repeated but Syngas II was used (Fig. F3). The growth of strain CP15 was observed at 45 ℃ to a maximum cell mass concentration of 0.08 g/L, which was 38% less than with Syngas I. In addition, only 0.1 g/L of acetic acid or ethanol were produced. The percentage of gas utilization was fairly low with 4.2% for CO and 0.5% for H_2 (Fig. F4). The decrease in the incubation temperature from 45 ℃ to 37 ℃ after 240 h did not resume growth. This was different from the fermentation with Syngas I. Small amounts of CO and H_2 were consumed after 240 h. The Syngas II with 40% CO has two fold more CO than the 20% CO syngas, which could have negatively inhibited hydrogenase and CODH. But the exact reason is still unknown.

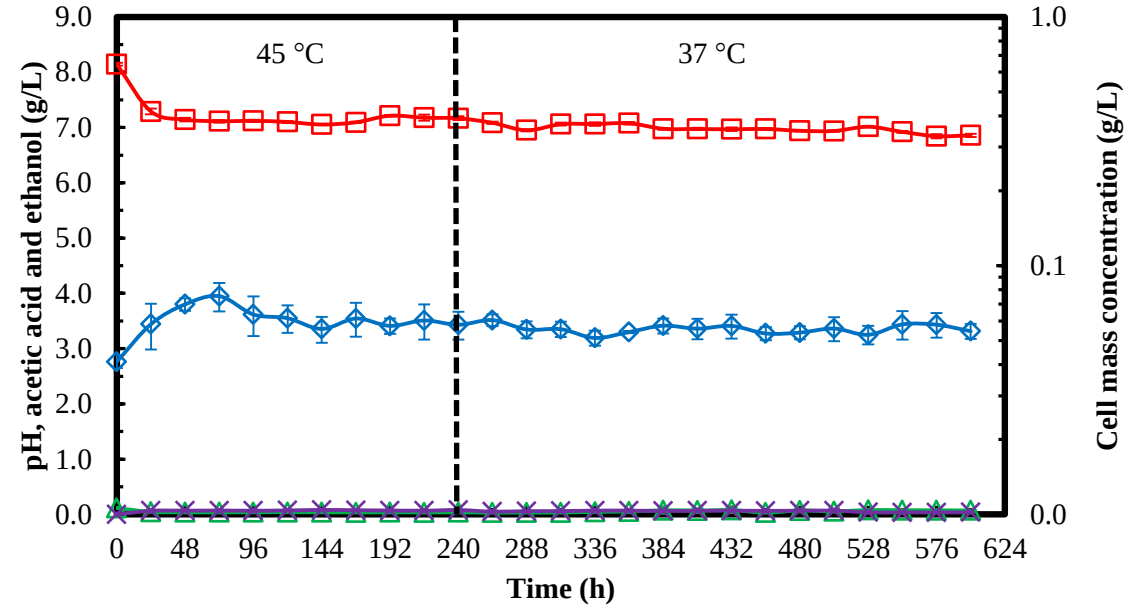

Fig. F3 Growth and products profile of strain CP15 at 45 ℃ followed by 37 ℃ with Syngas II in bottle fermentation; cell mass concentration (◊), pH (□), acetic acid (Δ), ethanol (×).

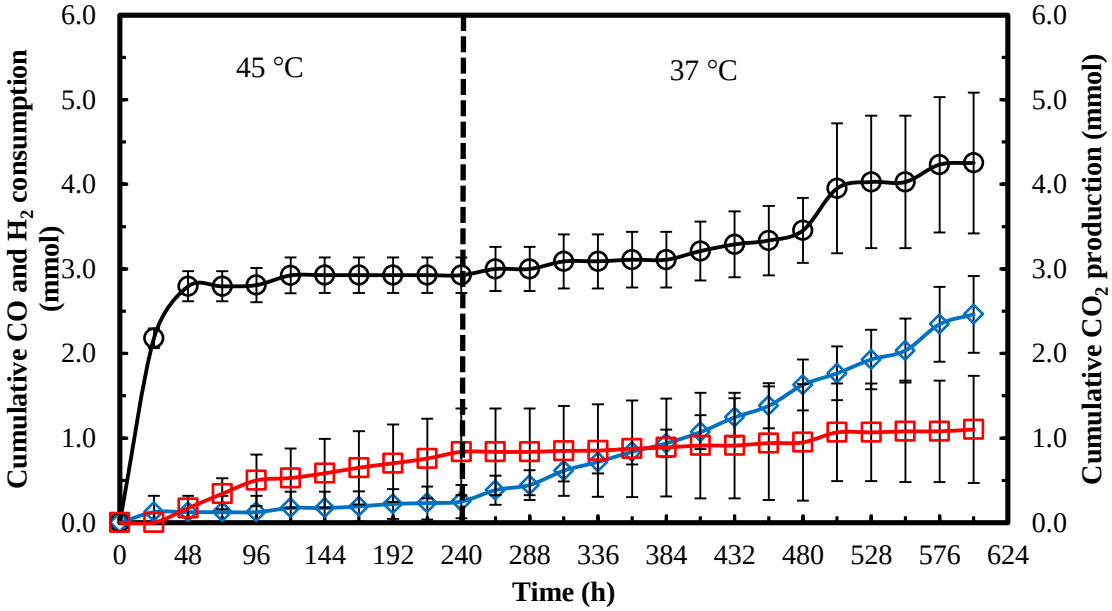

Fig. F4 Gas consumption profile of strain CP15 at 45 ℃ followed by 37 ℃ with Syngas II in bottle fermentation; CO (○), H_2 (◊), CO_2 (□).

F4 Conclusions

Strain CP15 grew at 45 ℃ but at a slower rate than at 37 ℃. In addition, consumption of both H_2 and CO was substantially low at 45 ℃. The switch of the fermentation temperature from 45 ℃ to 37 ℃, resumed CP15 growth only with Syngas I.

F5 References

Allen, T.D., Caldwell, M.E., Lawson, P.A., Huhnke, R.L., Tanner, R.S., 2010. *Alkalibaculum bacchi* gen. nov., sp. nov., a CO-oxidizing, ethanol-producing acetogen isolated from livestock-impacted soil. Int. J. Syst. Evol. Microbiol. 60, 2483-2489.

Liu, K., Atiyeh, H.K., Tanner, R.S., Wilkins, M.R., Huhnke, R.L., 2012. Fermentative production of ethanol from syngas using novel moderately alkaliphilic strains of *Alkalibaculum bacchi*. Bioresour. Technol. 104, 336-341.

Munasinghe, P.C., Khanal, S.K., 2010. Biomass-derived syngas fermentation into biofuels: Opportunities and challenges. Bioresour. Biotechnol. 101, 5013-5022.

APPENDIX G

G Semi-continuous syngas fermentation using a mixed culture of strain CP15 and *Clostridium propionicum* without pH control

G1 Background

During the previous continuous syngas fermentation in a 7-L fermentor discussed in chapter 6, n-propanol and n-butanol were produced in CSL medium by the mixed culture made of mainly strain CP15 and *Clostridium propionicum* as shown in section 6.3. n-Propanol and n-butanol were not produced with CP15 monoculture The objective of this study was to obtain a preliminary data for mixed culture syngas fermentation in a 3-L Bioflo 110 fermentor with 2.5 L working volume under semi-continuous fermentation (i.e., continuous syngas flow and liquid batch). The syngas mixture used was Syngas VI made of 38% CO, 28.5% CO_2, 28.5% H_2 and 5% N_2. Standard yeast extract medium without TAPS was used as described in Chapter 7 section 7.2 and pH was not controlled during the fermentation. The medium preparation, gas and liquid sample analyses were described in Chapter 7 section 7.2. The syngas flow rate was started at 18 sccm and 150 rpm agitation.

G2 Growth and products profiles

The mixed culture cells grew upon inoculation to a maximum of cell mass concentration of 0.57 g/L in 40 h. Then, cell mass concentration was stable at this level until the end of fermentation (Fig. G1). The pH of medium decreased from 7.1 to 5.6 at 48 h and then started to increase to pH 6.0. The decrease of pH was associated with the accumulation of acetic acid in the medium (Fig. G2). The acetic acid production stopped

at 40 h. The maximum acetic acid concentration was 3.3 g/L. After 40 h, there was a clear decrease in acetic acid concentration that corresponded with an increase in ethanol production. Ethanol was a non-growth related product and was produced from the conversion of acetic acid as previously reported (Liu et al.,2012). A maximum ethanol concentration of 1.2 g/L was obtained at 80 h and remained constant until the end of fermentation.

Propionic acid was produced during the fermentation at a maximum concentration of 0.18 g/L (Fig. G3). Then, propionic acid concentration decreased to 0.12 g/L that was corresponding with production of n-propanol of 0.05 g/L. The production of n-propanol was based on the synergy between strain CP15 and *C. propionicum* in the mixed culture as shown in Chapter 7. No butanol was found in this study but 0.16 g/L butyric acid was obtained during the cell growth stage (Fig. G4). The production of propionic acid and butyric acid could be due to *C. propionicum* fermented three carbon amino acid —alanine and four carbon amino acid—threonine found in the yeast extract (Cardon and Barker,1946).

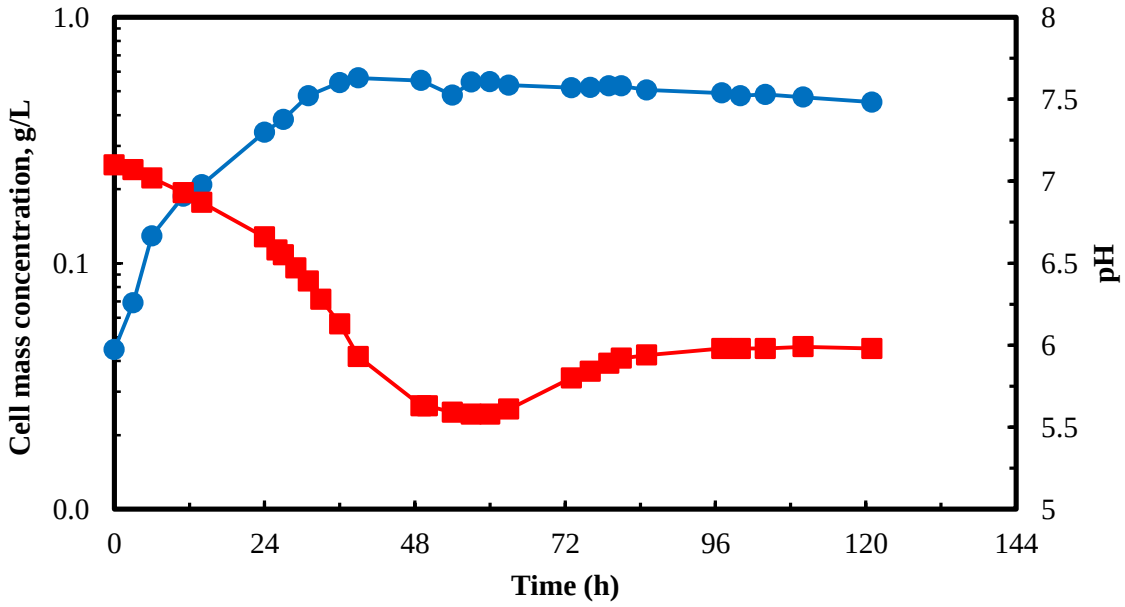

Fig. G1 Growth and pH profiles of the mixed culture in semi-continuous fermentation in 3-L Bioflo 110 fermentor without pH control; cell mass concentration (●), pH (■).

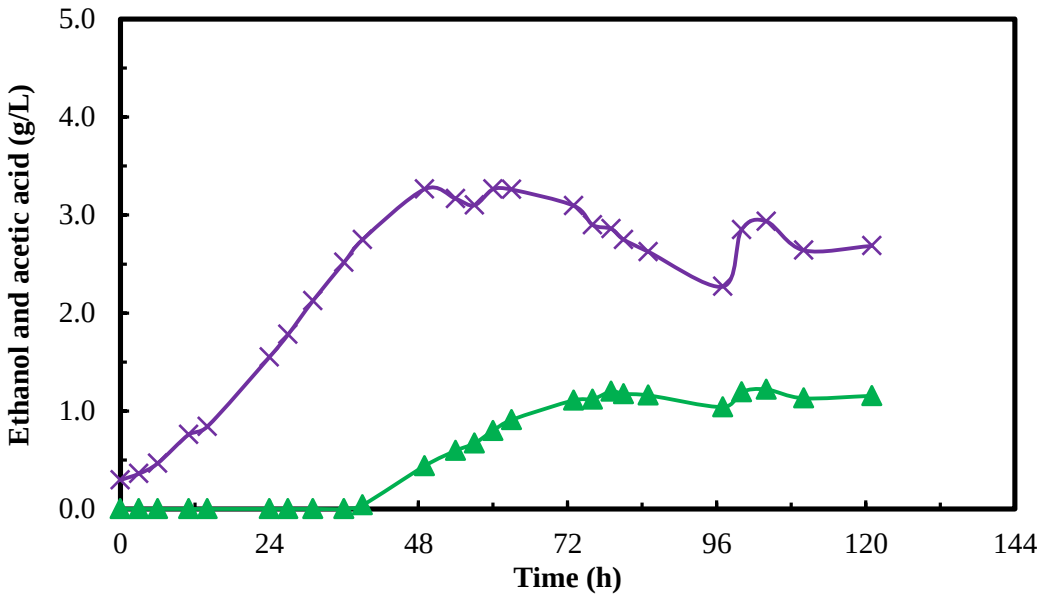

Fig. G2 Ethanol and acetic acid profiles of the mixed culture in semi-continuous fermentation in 3-L Bioflo 110 fermentor without pH control; ethanol (▲), acetic acid (×).

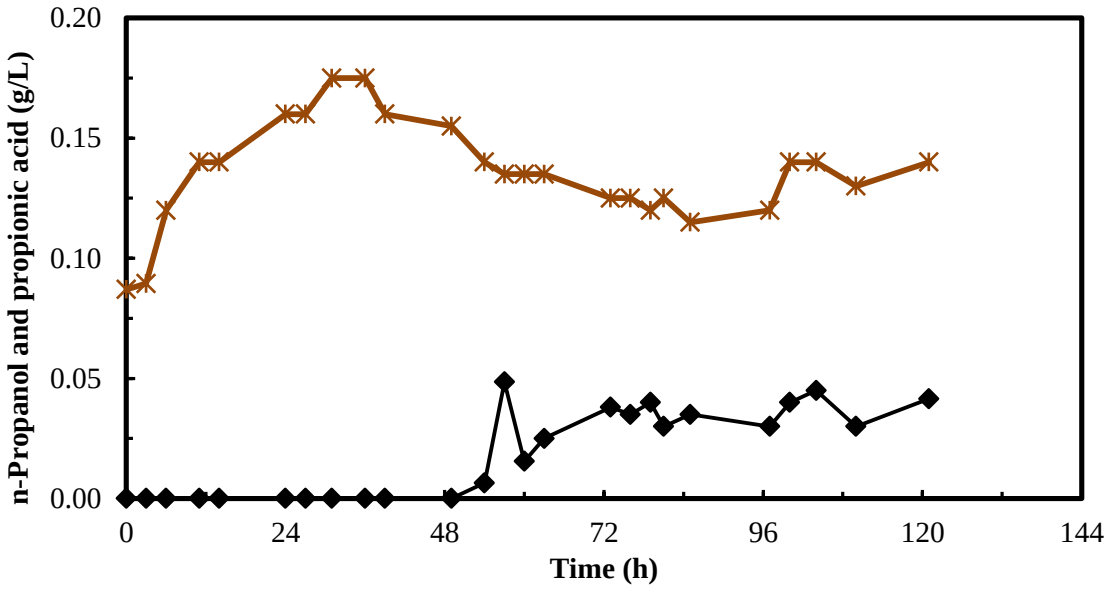

Fig. G3 Propanol and propionic acid profiles of the mixed culture in semi-continuous fermentation in 3-L Bioflo 110 fermentor without pH control; propanol (♦), propionic acid (✳).

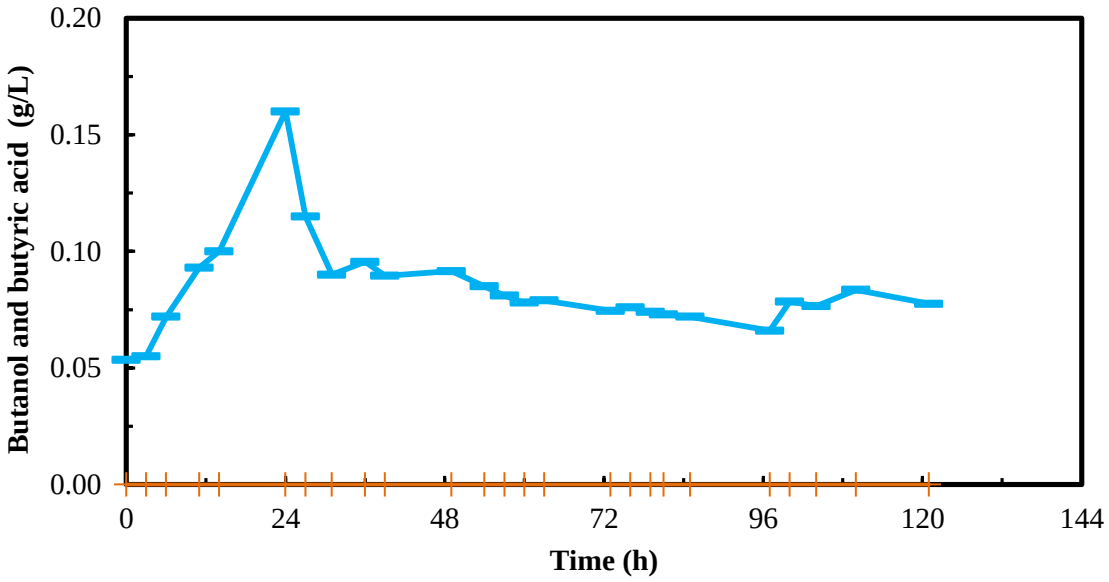

Fig. G4 Butanol and butyric acid profiles of the mixed culture in semi-continuous fermentation in 3-L Bioflo 110 fermentor without pH control; butanol (+), butyric acid (—).

G3 Gas consumption profiles

There were fast consumptions of CO and H_2 during the growth stage till 40 h (Fig. F5). However, there was a fast drop of H_2 utilization after 40 h which was corresponding to pH value below 6 (Fig. G1) that was out of the range reported for strain CP15 of pH 6.5 to 10.5 and for *C. propionicum* growth at pH 5.8-8.6 (Allen et al.,2010; Cardon and Barker,1946). The CO utilization at the end of fermentation was 44.7% and H_2 utilization was 28.8%.

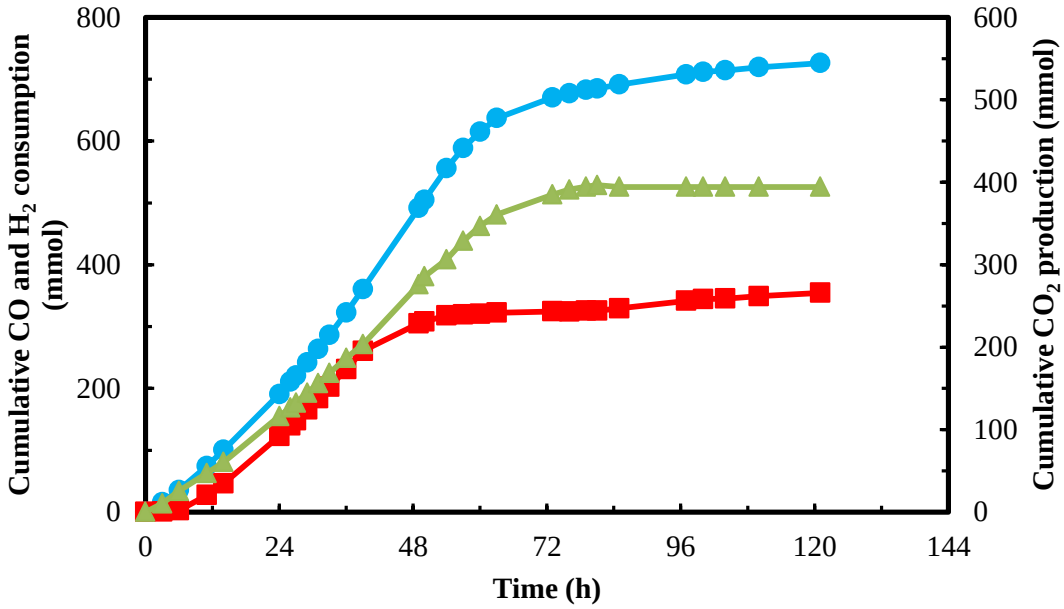

Fig. G5 Cumulative CO and H_2 consumption and CO_2 production profiles using mixed culture in semi-continuous fermentation in 3-L Bioflo 110 fermentation without pH control; CO (●), H_2 (■), CO_2 (▲).

G4 Conclusions

A maximum ethanol and n-propanol concentrations of 1.2 g/L and 0.05 g/L, respectively, were produced in the 3-L Bioflo110 fermentor during mixed culture syngas

fermentation. The pH played an important factor affecting gas utilization. H_2 consumption by the mixed culture was not favorable at pH below 6.0. The pH of the fermentation medium should be controlled above pH 6.0 to boost the conversion of syngas to alcohols by the mixed culture.

G5 References

Allen, T.D., Caldwell, M.E., Lawson, P.A., Huhnke, R.L., Tanner, R.S., 2010. *Alkalibaculum bacchi* gen. nov., sp. nov., a CO-oxidizing, ethanol-producing acetogen isolated from livestock-impacted soil. Int. J. Syst. Evol. Microbiol. 60, 2483-2489.

Cardon, B., Barker, H., 1946. Two new amino-acid-fermenting bacteria, *Clostridium propionicum* and *Diplococcus glycinophilus*. J. Bacteriol. 52, 629-634.

Liu, K., Atiyeh, H.K., Tanner, R.S., Wilkins, M.R., Huhnke, R.L., 2012. Fermentative production of ethanol from syngas using novel moderately alkaliphilic strains of *Alkalibaculum bacchi*. Bioresour. Technol. 104, 336-341.

APPENDIX H

H SAS program used to determine the statistical differences among treatments

H1 SAS code

The following is the SAS program code that was used to determine the statistical differences among treatments based on the Duncan's multiple range tests. The example below is from Chapter 4 that was used to determine the statistical differences of ethanol yields among strains $CP11^T$, CP13 and CP15 with Syngas II 40% CO, 30% CO_2, and 30% H_2.

SAS code:

```
DATA fermentation;

INPUT trt $ yield;

CARDS;

CP11 48.02

CP11 43.19

CP11 44.63

CP13 37.14

CP13 36.87

CP13 25.88
```

CP15 62.15

CP15 58.60

CP15 60.83

RUN;

```
PROC GLM DATA=fermentation;
        CLASS trt;
        MODEL yield = trt;
        MEANS trt /DUNCAN;
Run;
```

H2 Output

The SAS System

Obs	trt	yield
1	CP11	48.02
2	CP11	43.19
3	CP11	44.63
4	CP13	37.14
5	CP13	36.87
6	CP13	25.88
7	CP15	62.15
8	CP15	58.60
9	CP15	60.83

The GLM Procedure

Class Level Information		
Class	**Levels**	**Values**
trt	3	CP11 CP13 CP15

Number of Observations Read	9
Number of Observations Used	9

Dependent Variable: yield

Source	DF	Sum of Squares	Mean Square	F Value	Pr > F
Model	2	1117.534022	558.767011	33.10	0.0006
Error	6	101.284333	16.880722		
Corrected Total	8	1218.818356			

R-Square	Coeff Var	Root MSE	yield Mean
0.916900	8.860928	4.108616	46.36778

Source	DF	Type I SS	Mean Square	F Value	Pr > F
trt	2	1117.534022	558.767011	33.10	0.0006

Source	DF	Type III SS	Mean Square	F Value	Pr > F
trt	2	1117.534022	558.767011	33.10	0.0006

The SAS System

The GLM Procedure

Duncan's Multiple Range Test for yield

Alpha	0.05
Error Degrees of Freedom	6
Error Mean Square	16.88072

Number of Means	**2**	**3**
Critical Range	8.208	8.507

Means with the same letter are not significantly different.			
Duncan Grouping	**Mean**	**N**	**trt**
A	60.527	3	CP15
B	45.280	3	CP11
C	33.297	3	CP13

APPENDIX I

Table I1 Compositions of trace metal, vitamin and mineral stock solutions

Trace metal stock solution	**g/L**
Nitrilotriacetic acid	2
Manganese sulfate monohydrate	1
Ferrous ammonium sulfate hexahydrate	0.8
Cobalt chloride hexahydrate	0.2
Zinc sulfate	1
Nickel chloride hexahydrate	0.2
Sodium molybdate dihydrate	0.02
Sodium selenate	0.1
Sodium tungstate	0.2
Mineral stock solution	**g/L**
Ammonium chloride	100
Calcium chloride	4
Magnesium sulfate	20
Potassium chloride	10
Potassium phosphate monobasic	10
Vitamin stock solution	**mg/L**
p-(4)-Aminobenzoic acid	5
d-Biotin	2
Calcium pantothenate	5
Folic acid	2
Mercaptoethanesulfonic acid (MESNA)	10
Nicotinic acid	5
Pyridoxine	10
Riboflavin	5
Thiamine	5
Thioctic acid	5
Vitamin B12	5

VITA

Kan Liu

Candidate for the Degree of

Doctor of Philosophy

Thesis: PRODUCTION OF ALCOHOLS VIA SYNGAS FERMENTATION USING *ALKALIBACULUM BACCHI* MONOCULTURE AND A MIXED CULTURE

Major Field: Biosystems and Agricultural Engineering

Biographical:

Education:

Completed the requirements for the Doctor of Philosophy in Biosystems and Agricultural Engineering at Oklahoma State University, Stillwater, Oklahoma in December, 2013.

Completed the requirements for the Master of Science in Fermentation Engineering at College of Biological Engineering, Tianjin University of Science and Technology, Tianjin, China in 2009.

Completed the requirements for the Bachelor of Science in Pharmaceutical Engineering at College of Biological Engineering, Tianjin University of Science and Technology, Tianjin, China in 2006.

Experience:
Research Associate, Department of Biosystems and Agricultural Engineering, Oklahoma State University, Stillwater, Oklahoma, USA, 2009 to 2013.

Professional Memberships:
American Society of Agricultural and Biological Engineers (ASABE)